Abstract

In this investigation strength and structural behaviour of prestressed concrete is studied with one full scale test of one flat slab, 16000 mm x 19000 mm, and three slabs on ground each 4000 mm x 4000 mm with thickness 150 mm.

The flat slab was constructed and tested in Aalesund. This slab has nine circular columns as support, each with diameter 450 mm. Thickness of this test slab was 230 mm and there were two spans in each direction, 2 x 9000 mm in x-direction and 2 x 7500 mm in y-direction from centre to centre column. The slab was reinforced with twenty tendons in the middle column strip in y-direction and eight tendons in both outer column strips. In x-direction tendons were distributed with 340 mm distance. There were also ordinary reinforcement bars in the slab. Strain gauges were welded to this reinforcement, which together with the deflection measurements gives a good indication of deformation and strains in the structure.

At a live load of 6.5 kN/m^2 shear failure around the central column occurred: The shear capacity calculated after NS 3473 and EuroCode2 was passed with 58 and 69 %, respectively. Time dependent and non-linear FE analyses were performed with the program system DIANA. Although calculated and measured results partly agree well, the test show that this type of structure is complicated to analyse by non-linear FEM.

Prestressed slabs on ground have no tradition in Norway. In this test one reinforced and two prestressed slabs on ground were tested and compared to give a basis for a better solution for slabs on ground. This test was done in the laboratory at Norwegian University of Science and Technology in Trondheim. The first slab is reinforced with 8 mm bars in both directions distributed at a distance of 150 mm in top and bottom. Slab two and three are prestressed with 100 mm^2 tendons located in the middle of slab thickness, and distributed at a distance of 630 mm in slab two and 930 mm in slab three. Strain gauges were glued to the reinforcement in slab one and at top and bottom surface of all three slabs. In slab two and three there were four load cells on the tendons.

Each slab were loaded with three different load cases, in the centre of slab, at the edge and finally in the corner. This test shows that stiffness of sub-base is one of the most important parameters when calculating slabs on ground. Deflection and crack load level depends of this parameter. Since the finish of slabs on ground is important, it can be more interesting to find the load level when cracks start, than deflection for the slab. It is shown in this test that crack load level was higher in prestressed slabs than in reinforced slab. There was no crack in the top surface with load in the centre, but strain gauges in the bottom surface indicate that crack starts at a load of 28 kN in the reinforced slab, and 45 kN in the prestressed slabs. Load at the edge give a crack load of 30 kN in reinforced slab, 45 kN and 60 kN in prestressed slabs. The last load case gives crack load of 30 kN in reinforced slab, 107 kN and 75 kN in prestressed slabs. As for the flat slab, FE analyses were performed for all of the three slabs on ground, and analyses shows that a good understanding of parameters like stiffness of sub-base and tension softening model, is needed for correct result of the analyses.

URN:NBN:no-2318

URN:NBN:no-2318

Notations

As	reinforcement areas
D	flexural stiffness
E_c	modulus of elasticity in concrete
f	total drape of tendon
f_c'	compressive concrete strength
$f_c'=f_{cc}=f_{cu}$	cylinder strength after 28 days
f_{ck}	characteristic cylinder compressive strength in concrete
f_{cm}	mean compressive concrete strength
f_{ctm}	mean axial tensile strength
f_s	allowable stress in steel
$f_{tkp}=f'_{ct}$	characteristic tensile strength
$f_{tks}=f_{ct,sp}$	characteristic splitting strength
f_{tnp}	tensile strength
k	sub-grade reaction modulus
l	span width, radius of relative stiffness
M	bending moment
m_g	bending moment from dead load
m_p	bending moment from live load
MR	modulus of rupture
m_w	bending moment from prestressing force
n	number of tendons
P	prestressing force
p	distributed load
P_o	tendon force at active ends of tendon
P_x	tendon force in a distance x from stressing point
RH	relative humidity of the ambient air
SR	stress/strength ratio
t	time
u	average coefficient of subgrade resistance
u	coefficient of friction between slab and sub-grade
w	total dead load
w_o	deflection under load for a beam on elastic foundation

$\Delta\alpha$	wobble friction coefficient
ε	strain
γ_{sh}	product of correction factors
μ	friction coefficient
ρ	concrete density
σ	stress
υ	Poisson's ratio

URN:NBN:no-2318

Acknowledgements

The author wishes to express his sincere appreciation and gratitude to the following for their contribution to this research study:

Trygstad Bygg a.s, Brødrene Dyrøy, Vestlandstak a.s, Thyssen Hunnebeck Norge a.s, Bas systemer, Stålgrossisten a.s, Longvas oppmåling and Fabeko sponsored the full-scale test.

Trygstad Bygg a.s, Brødrene Dyrøy, NorBetong Trondheim, tensor contracting b.v, Brødrene Sunde and Fabeko sponsored slabs on ground.

The author is especially grateful to instructor senior lecturer Terje Kanstad for his guidance and encouragement during all phases of the author's dr. ing. degree program, and professor Mahen Mahendran for good support when the author studied at Queensland University of Technology.

The staff at Division of Concrete Structures at the Norwegian University of Science and Technology in Trondheim, especially Jan Øverli for his help with the FEM analysis, the staff in the laboratory with all the instrumentation in the tests, especially thanks to Helge Rødsjø.

Financial support from Trygstad Bygg a.s., Fabeko and Statsbygg are acknowledged.

Also thanks to Anne Marie Stoknes for proofreading this text.

Finally, the author wishes to thank his wife, Merete, and our daughter Veronica for their help and encouragement during all phases of the author's study program, they play a major role in making it possible to complete this study.

Trondheim 2001
Steinar Trygstad

Contents

URN:NBN:no-2318

Chapter 1

Introduction, post-tensioned slabs.

1.1 General Remarks

The use of prestressed concrete in Norway, and in other countries in Europe, has increased over the last years. The most common use of this type of structures has been in USA, (first time tried applied in 1895), England, Singapore and Australia.
Typical applications have been:

- Car parks (50% of all car parks in USA are built with prestressed concrete)
- Shopping centres.
- Office buildings.
- Bridges.

There are two types of systems with tendons, bonded and unbonded tendons. Bonded systems are most commonly used in bridges and other heavy structures, while unbonded tendons are most often used in slabs and beams.

Bonded tendons: multi-strand tendons are placed in a metal duct and the ducts are grouted as soon as possible after stressing the tendons. The grout bonds the tendons to the surrounding concrete.

Unbonded tendons: Plastic sheaths filled with grease containing unbonded monostrands. The unbonded tendon is attached to the concrete only at its end anchors, passive and active ends. The tendons are stressed in the active end about 3 days after casting. Unbonded tendons are cheaper than bonded tendons, grouting is not required. The grease is fire resistant and has low friction coefficient.

1.2 Object and Scope

Some of the main advantages with post-tensioned floors compared to conventional reinforced floors are thinner slabs, increased spans, reduced cracking, water tightness and small deflections. When the spans are increased, the shear force also increases, and if slabs without beams or drop panels are used, there can be a capacity problem near the column.

The main objective of the investigation was to study a flat slab experimentally under static loading increasing from zero until the slab collapsed. The flat slab was constructed in full scale, 19000 mm x 16000 mm. All columns were circular with diameter 450 mm, and length 4500 mm. A full-scale test was desirable instead of several tests in a smaller scale due to well-known size effects in concrete. The objectives of this investigation were to study:

- Shear capacity around the inner column in a situation with realistic reinforcement conditions and bending moments.
- Stress development in the unbonded tendons.
- Minimum reinforcement rules.
- Crack load, crack development, deflections and strains at several locations of the slab.
- The result from the full-scale test compared to the result from FE-analyses.

At the beginning of the project, a literature investigation on flat slab tests revealed that most tests were done in 10 – 33 % of full size. A few single span slabs have been tested in up to 50 % of full size. Furthermore, many series of punching shear tests have been carried out. Typically such tests are done on simply supported slabs in ¼, $^1/_3$ or ½ scale and with an extension of the slab about 1 meters outside the column. These tests are normally done with varying amount of reinforcement and concrete strength. In a test with small extension of the slab from the column, it can be difficult to give the structure a moment representing a longer span. Results from some smaller tests were studied before the final test was done, /57/ Hemakom Roongroj.

In this test a slab in normal size and thickness, calculated after the Norwegian rules, was tested. This eliminates the uncertainty due to the scaling effect of results from a smaller test specimen. This is one of the main problems with tests in smaller scale, since it is difficult to find reliable effects of reinforcement amount, concrete quality, slab thickness, critical sections, and loading around the column. The full-scale test gives also the shear capacity, strain in reinforcement, and deformation in the span from the time loading starts. The full-scale test and results from this test are described in chapter 4.

Based on the result of a full-scale test and an economic evaluation, practical recommendations are made for design of prestressed flat-slabs. The result from the full-scale test is compared with rules from different building codes from Norway (NS 3473), USA (ACI), Europe (Euro Code) and Australia (AS 3600).

Chapter 2

Introduction, slabs on ground.

2.1 General Remarks

Prestressed concrete in floors placed on the ground is not commonly used. In many countries the system is, however, sometimes used in heavily loaded industrial floors and foundation slabs, but in general the advantages by prestressing should imply much more frequent use of it. There are also some airports around the world that are built with prestressed concrete in the runway, and this experience is valuable and can also be applied in floors with heavy loads.

As a part of this study, the author spent three months in Australia, Queensland University of Technology QUT, to study prestressing in slabs on ground. The Australian standard for design of concrete structures, AS3600, has a "different" approach to many topics compared with ACI 318, EuroCode2 and the Norwegian code NS 3473. There will therefore be some comparisons between these standards in the subsequent chapters.

Australia is one of the countries where there has been done some research on prestressed slabs on ground. In Norway an unbonded system will be most common to use, but in Australia bonded systems are most common. This system contains two to four tendons in a flat duct, which is grouted after stressing, and it is used in flat slabs and slabs on ground. For slabs on ground the distance between the distributed ducts with four tendons can be as large as 2000 – 3000 mm.

2.2 Object and Scope

The major advantages with use of prestressed tendons in relation to reinforcement in slabs on ground, are reduced crack development, increased casting area (time-saving), and reduced slab thickness and numbers of joints.

In this part of the dr.ing study "Slabs on no-tension bedding" were studied experimentally under load placed at different locations; in the middle of the slab, at the edge and in the corner. To achieve this, 3 slabs were constructed, each of them was 4000 mm x 4000 mm. The first one was reinforced with ordinary reinforcement, while the other two were prestressed with unbonded tendons in both directions. The distance between the tendons was different in the two slabs. Since the test was done with relatively small and few slabs, it is not possible to give accurate descriptions of moment distribution, loss in prestressing force, friction between slab and sub-base, effect of different concrete qualities and sub grade reactions, generally valid for normal size slabs on ground. However, one of the goals was to investigate whether finite element analysis can be used to describe the test slabs and normal size slabs.

A major objective is due to the hypothesis that one of the main reasons for all the damage on slabs on ground during the last years is the absence of calculation rules in the concrete standards.

The structural behaviour was studied by:

- Strain development in the unbonded tendons.
- Strain development at different locations in the slab.
- Deflection in different points of the slab.
- Crack load and crack development with increasing load.

Before the test was started, a search for literature from earlier tests results was done, but it showed that most tests of these structures are related to airport runways. One of the most interesting tests the author found was from a port / store area in Australia, with large loads, and long casting stages. One important result from this test is a better understanding of the structural behaviour of prestressed slabs on ground. Some of the equations later presented in chapter 7 were also used in this test.

A FE analysis was performed, before the test of slabs started in the laboratory, to indicate the best locations of strain gauges that were glued to the slab. After the tests were finished, one realized that the number of strain gauges should have been increased to give more information from the test.

Since the well-known Westergaard theory is frequently used for design of slabs on ground comparisons of results from this theory and the test were done.

Based on the results from the test and the FE analysis, practical design recommendations are proposed for prestressed floors placed on the ground.

The creep and shrinkage effects were also studied, especially during the hardening period of 2-3 days from casting.

Chapter 3

Design of post-tensioned flat slabs

In the first part of this chapter calculation of deflections and minimum reinforcement rules are subjects shortly described. These subjects will also be further discussed in chapter 4. In the next part shear capacity formulas after different standards are listed. These formulas are used in chapter 4 to compare capacity calculated after different standards with the experimental result. Finally there is a short economy discussion limited to the Norwegian price level.

3.1 Introduction

The maximum span to depth ratio for a flat slab is about 45 increasing to 50 if the slab has drop panels, see table 3-1. If the main goal is to minimise the total price of the slab it can give a good economy to increase the slab thickness to a span to depth ratio of about 35 – 38. In this case drop panels are not necessary (with ordinary loads and column width). If the slab should be as thin as possible, drop panels might be necessary. If the shear capacity is decisive, it can be increased by increasing the column width.

The structural system of flat slabs with tendons distributed in one direction, and concentrated in the other direction, can be described as one way slabs and column strips. The one way slab is not discussed here, but tendons in this direction should be placed after the concentrated tendons, since the tendons in the concentrated direction will be like a beam for the distributed tendons. When calculating the column strip, the first task is to find the width of the column strip. As mentioned above, there are different rules in different standards, but the most common procedure has been to use L/2, see fig 3.1.

If there are column strips in both directions, the width Lx/2 and Ly/2 can be used, alternatively the smallest value Lx/2 can be chosen in both directions if there are long spans in one direction and short spans in the other direction, see fig 3.2.

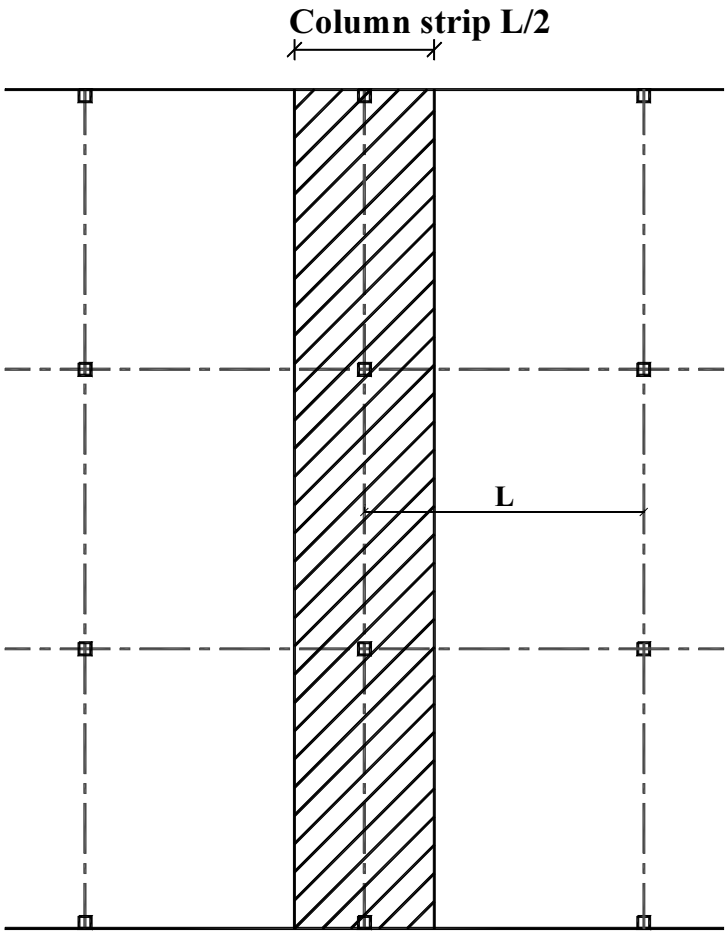

Column strip in a flat slab.
Figure 3.1

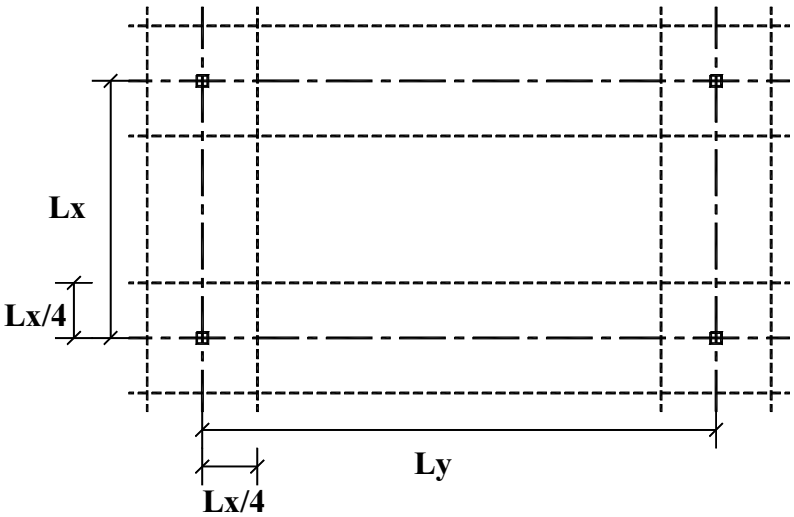

Column strip in both directions in a flat slab.
Figure 3.2

One-way slab	48
Two-way slab	45
Two-way slab with drop panel	50
Two-way slab with two-way beams	55
Waffle (5 x 5 grid)	35
Beams b ≅ h/3	20
Beams b ≅ 3h	30

Maximum span-to-depth ratios for post-tensioned flat slabs suggested by the Post-Tensioning Institute /4/.
Table 3-1

3.2 Calculation of deflection

There are different recommendations for maximum deflection in the standards:

- EuroCode2: "The appearance and general performance of a structure may be impaired when the calculated sag, *f*, of a beam, slab or cantilever exceeds *f* = span/250".
- ACI has limits for deflections varying from l/180 to l/480.
- The total limited deflection in AS3600, is generally l_e/250, where l_e is the effective span of the member.

One of the greatest advantages with prestressed concrete is that with the use of balanced loads there will be small deflections in the slab. This depends of course on how much of the load is balanced, dead load or dead load plus some portion of live load. Since prestressed slabs often are relatively thin, the limit for deflections can be decisive for the slab thickness.

Because the deflection in flat slabs depends on the moment distribution for the two-way system, an accurate calculation will be complicated. Consequently simplified methods often have to be used. In such methods, the deflection depends on choice of column strip width and its bending stiffness.

In a flat slab, the deflections in the middle of the span depend on the support of this strip. In an inner field strip the support often is a column strip, and this strip can have a deflection in the middle, where the field strip is supported. Normally should some of this deflection be added to the calculated deflection in the field strip. The deflection of the column strip can be calculated by means of a frame with load from the ½ span on each side of the column, but with a reduced width for stiffness calculation.

FE-analysis can often give a better indication of deflection than a simplified method.

Calculation of creep and shrinkage after NS 3473, ACI and EuroCode2 are almost the same, but in AS 3600 the shrinkage strain is constant, and after time it is close to shrinkage calculated after NS 3473.
The effects of creep and shrinkage are described in appendix A.

3.3 Minimum reinforcement

The Norwegian standard gives a minimum reinforcement over the column as:

$$As \geq 0.25 \cdot k_w \cdot A_c \cdot f_{tk} / f_{sk} \tag{3.1}$$

where

$$k_w = 1.5 - h / h_1 \geq 1.0 \tag{3.2}$$

h = slab thickness in metre.
h_1 = 1.0 metre
A_c = The concrete cross section area .
f_{tk} = Characteristic tensile strength of concrete.
f_{sk} = Characteristic yield stress of reinforcement.

This reinforcement is distributed over a width equal to the column width plus two times the slab thickness from each side of column. The length of this reinforcement should be 0.15 times the span width in the reinforced direction, to each side measured from centre of column.

The concrete cross section area A_c, is normally 1000 mm width of the slab multiplied with the slab height. But in a flat slab it is the authors opinion that this width should be exchanged with the total width of the column strip and that the total reinforcement must be distributed over the width as described in the previous section. This is not exactly defined in the Norwegian standard, or in any of the other standards that are checked in the present study.

“FIP Recommendations for the design of post-tensioned slabs” /58/ recommend a cross sectional area on at least 0.5% of the concrete cross section. This is about 3 times (depending of slab thickness and concrete tensile strength) the reinforcement amount described in the Norwegian standard, if the cross section width is 1000 mm in both cases.

As the Norwegian standard, ACI 318-89 /11/ says “Bonded reinforcement shall not be required in positive moment areas where the computed tensile stress in the concrete at service load does not exceed $\sqrt{f'_c}/6$ ” for flat plates, defined as solid slabs of uniform thickness.

Prestressed flat slabs can be designed to give compressive stress in the whole slab outside an area around the column. This means that it is possible to skip ordinary reinforcement in span, but if overload occurs, the concrete will crack, and then it is obviously advantageous with a certain amount of reinforcement.

Minimum reinforcement has to be used in spans, perpendicular to the distributed tendons in a one way slab, NS 3473 /9/. The Norwegian standard prescribes also minimum reinforcement in span for a flat slab if cracks can occur.

In a flat slab as described in chapter 4, minimum reinforcement over the column should be carefully evaluated. This because both amount and length of this reinforcement influence shear capacity and deformation in the span. Different length of reinforcement bars might be one way to get a better result without use of more reinforcement.

3.4 Shear capacity

In this chapter, shear capacity formulas from NS 3473, ACI 318-89, EuroCode2 and AS 3600 are listed and shortly commented before the same formulas are used to compare the shear capacity in the full-scale test described in chapter 4. The reason for choice of standards is that NS 3473 is the standard used in Norway where the test was done. EuroCode2 is the new European standard, which also can be used in Norway. ACI is maybe the most known standard, and finally AS 3600 is the standard used in Australia where one part of this study is done.

These standards design shear after different rules, and one factor that was expected to give different capacities is the distance from the column to the critical section, varying from *d/2* to 1.5 *d*.

3.4.1 Capacity formulas

NS 3473 /9/

The critical section is placed in a distance *d* from the column surface after NS 3473, fig 3.3.

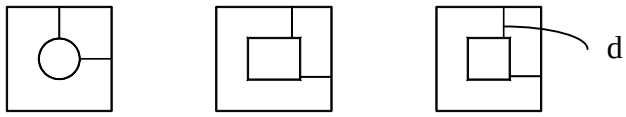

Critical section at the column from /9/.
Figure 3.3

The shear capacity with axial forces in the slab:

$$V_{cd} = V_{co} + 0.8 \cdot \frac{M_o}{M_f} \cdot V_f \leq \left(f_{td} \cdot k_v - \frac{0.25 \cdot N_f}{A_c} \right) b_w \cdot z_1 \qquad (3.3)$$

where

$$V_{co} = 0.30 \cdot \left(f_{td} + \frac{k_A \cdot A_s}{\gamma_c \cdot b_w \cdot d} \right) \cdot b_w \cdot d \cdot k_v \leq 0.6 \cdot f_{td} \cdot b_w \cdot d \cdot k_v \qquad (3.4)$$

f_{td} = Concrete tensile strength.
k_A = 100 N/mm^2
A_s = Reinforcement area crossing the critical section.
γ_c = Material safety factor, concrete.
b_w = Slab width, length of critical section.
d = effective depths of the slab.
k_v = 1.5-d/d_1
d_1 = 1.0 metre.
M_o = $-N_f \cdot W_c / A_c$ $\qquad N_f / A_c \leq |0.4 \cdot f_{cd}|$
N_f =Axial force, positive as tensile.
W_c = Section modulus.
A_c = Cross section area.
f_{cd} = Compressive strength.
M_f = Moment in calculated section.
V_f = Shear force in calculated section.
z_1 = The largest of $0.7 \cdot d$ or I_c / S_c
I_c = Second moment of area.
S_c = First moment of area.

URN:NBN:no-2318

ACI 318-89 /11/

In the ACI 318-89, the critical section is d/2 from the column face. The shear capacity for prestressed concrete, V_c, shall be the lesser of V_{ci} and V_{cw}.

$$V_{ci} = 0.6\sqrt{f'_c} \cdot b_w \cdot d + V_d + \frac{V_i \cdot M_{cr}}{M_{\max}} \qquad (3.5)$$

but V_{ci} can not be taken less than

$$1.7 \cdot \sqrt{f'_c} \cdot b_w \cdot d \qquad M_{cr} = \left(I / y_t\right)\left(6\sqrt{f'_c} + f_{pe} - f_d\right) \qquad (3.6)$$

$$V_{cw} = \left(3.5\sqrt{f'_c} + 0.3 \cdot f_{pc}\right) b_w \cdot d + V_p \qquad (3.7)$$

The shear capacity can alternatively be calculated as:

$$V_c = \left(\frac{\sqrt{f'_c}}{20} + 5\frac{V_u \cdot d}{M_u}\right) b_w \cdot d \qquad (3.8)$$

but V_c need not to be taken less than $\left(\sqrt{f'_c} / 6\right) b_w \cdot d$ (3.9)

nor shall V_c be taken greater than $0.4\sqrt{f'_c} b_w \cdot d$ (3.10)

URN:NBN:no-2318

where

f'_c = specified compressive cylinder strength of concrete.
f_{pe} = compressive stress in concrete due to effective prestress force only, at extreme fibre of section where tensile stress is caused by externally applied loads.
f_{pc} = compressive stress in concrete at centric of cross section resisting externally applied loads
f_d = stress due to unfactored dead load, at extreme fibre of section where tensile stress is caused by externally applied loads
b_w = web width, or diameter of critical section
d = effective depth of the slab
V_d = shear force at section due to unfactored dead load
V_i = factored shear force due to externally applied load
V_p = vertical component of effective prestress force
V_u = factored shear force at section
M_{cr} = moment causing flexural cracking at section due to externally applied loads
M_{max} = maximum factored moment at section due to externally applied loads
M_u = factored moment at the section.

EuroCode2 /16/

EuroCode2 specifies the critical section, d_{crit}, with shear calculation, to be *1.5d* from the loaded area (column), see fig 3.4 /18/.

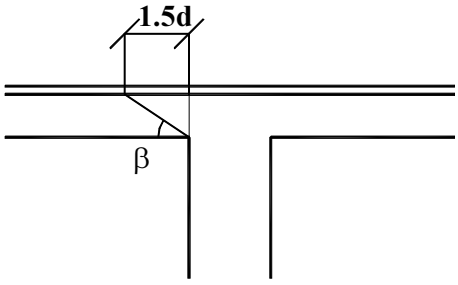

Critical section after EuroCode2.
Figure 3.4

The shear resistance per unit length for slabs without punching shear reinforcement:

$$v_{Rd1} = \tau_{Rd} \cdot k\left(1.2 + 40\rho_l\right)d \tag{3.11}$$

where

$k = \left(1.6 - d\right) \geq 1.0$
τ_{Rd} = Basic shear strength, given in table in /16/
d =(d_x + d_y)/2
d_x and d_y are the effective depths of the slab.

$$\rho_l = \sqrt{\rho_{lx} \cdot \rho_{ly}} \geq 0.015 \tag{3.12}$$

ρ_{lx} and ρ_{ly} relate to the tension steel in x and y direction respectively.

For prestressed elements equation (3.12) applies with

$$\rho_l = \sqrt{\rho_{lx}\rho_{ly}} + \frac{\sigma_{cpo}}{f_{yd}} \geq 0.015 \tag{3.13}$$

$$\sigma_{cpo} = \frac{N_{pd}}{A_c} \tag{3.14}$$

f_{yd} = design yield stress of the reinforcement.
N_{pd} = Prestressing force corresponding to the initial value without losses.

AS 3600 /14/

In the United States and Europe, most of the structures with prestressed concrete slabs are built with unbonded tendons, but in Australia use of bonded prestressed slab structures is made economical by the availability of specially developed flat anchorages and ducts, /13/.

Like ACI the Australian Standard, AS 3600 /14/, has a supplement "Concrete structures-Commentary" /15/ which gives the designer a good digest when designing prestressed concrete. The recommended stress level in tendons is 75 % of f_p. This is about the same level as the Norwegian standard. The concrete is assumed to be uncracked if the tensile stress is less than $0.25 \cdot \sqrt{fc'}$ (MPa) in the extreme fibre. Instead of load and material factors a strength reduction factor varying from 0.6 to 0.8 is used. This safety factor "ϕ", is set to 0.7 for shear. This gives the shear capacity

$$\phi \cdot V_{uo} > V^* \tag{3.15}$$

where the critical section is d/2 from column. Ultimate shear strength of a slab where there is no shear head (drop panel) is

$$V_{uo} = u \cdot d_{om}\left(f_{cv} + 0.3 \cdot \sigma_{cp}\right) \tag{3.16}$$

$$f_{cv} = 0.17\left(1 + \frac{2}{\beta_h}\right)\sqrt{f'_c} \le 0.34\sqrt{f'_c} \tag{3.17}$$

and where there is a shear head:

$$V_{co} = u \cdot d_{om}\left(0.5 \cdot \sqrt{f'_c} + 0.3 \cdot \sigma_{cp}\right) \le 0.2 \cdot u \cdot d_{om} \cdot f'_c \tag{3.18}$$

where

u	= the effective length of the critical shear perimeter.
d_{om}	= the mean value of effective depth around the critical shear perimeter.
f_{cv}	= Concrete shear strength.
σ_{cp}	= the average intensity of effective prestress in concrete.
β_h	= the ratio of the longest overall dimension of the effective loaded area, to the overall dimension. (from figure in AS 3600 /14/)
f'_c	= the characteristic compressive cylinder strength of concrete after 28 days.
V^*	= the shear force at a section, calculated with design load

3.5 Crack width

In a prestressed structure with unbonded tendons and with none, or a minimum of reinforcement, it is important to reduce the possibility of cracks in the concrete. Since there is no contact between tendon and concrete, the cracks which start opening, can be few and wide if there is no reinforcement in the slab to distribute them.

NS 3473 and EuroCode2 give design crack width values in the range 0.2 mm – 0.4 mm, but in a prestressed slab with a minimum of reinforcement it is desired to have compressive stress in the whole section, or design the slab to be uncracked, see appendix A.

3.6 Summary, prestressing in different codes

ACI, EuroCode2 and AS3600 have almost the same description of prestressed concrete. This includes prestressing force, short time losses, minimum reinforcement and reinforcement at the anchorage zone. There are, however, some differences in calculation of long time loss.

Minimum reinforcement over the column is for NS 3473 and ACI approximately equal, while EuroCode2 demands that 1/4 of the maximum moment should be taken by reinforcement and AS 3600 does not have any minimum reinforcement. Recommended reinforcement bar length is nearly the same for the three former standards. In Australia bonded tendons are most often used, and this gives a better control of cracks than unbonded tendons do, if there is no reinforcement parallel to the tendons.

The calculated deflection in a column strip depends of the width of the strip. In the test described in chapter 4, 1/3 of span width between supports were used instead of ½, which is the most common relation. This is done because the spans in prestressed slabs are longer than in reinforced slabs, and the width of the column strip is therefore reduced to 1/3.

EuroCode2 lists only a few points, which have to be controlled. The shear capacity will be compared and discussed in chapter 4, “Full scale test of flat slab”.

3.7 Economical comparison

An economical comparison between structures built in prestressed concrete and steel, reinforced concrete or precast concrete elements is very difficult to carry out. This depends on form cost, concrete available, element transport cost and many other factors. It is also difficult to determine the economical benefit of reduced columns, longer spans and thinner slabs. Prestressed concrete will also be more water tight than ordinary reinforced concrete and precast concrete elements. The author’s experience is that prestressed flat slabs are a good solution if the builder desires short distance between floors, and simple technical installations. This type of structures also gives good fire resistance and small deformations.

It is always interesting to obtain the most economical structure, and since the designer often is familiar with the best economical solution of a reinforced structure, it is also possible to illustrate how to find the best economical solution of a prestressed structure. In figure 3.5, the relations between prestressing force, x-direction, and eccentricity, y-direction, are shown calculated from maximum and minimum stress in top and bottom fibre. This diagram is commonly known as a "Magnel diagram", and the diagram is developed from the equations:

$$\frac{1}{P}\sigma_{t\min} \le \frac{1}{A} + \frac{e}{w_t} \qquad (3.19\ a)$$

$$\frac{1}{A} + \frac{e}{w_t} \le \frac{1}{P}\sigma_{tmax} \qquad (3.19\ b)$$

$$\frac{1}{P}\sigma_{b\min} \le \frac{1}{A} + \frac{e}{w_b} \qquad (3.19\ c)$$

$$\frac{1}{A} + \frac{e}{w_b} \le \frac{1}{P}\sigma_{bmax} \qquad (3.19\ d)$$

where

P = prestressing force.
σ_{tmin} = minimum stress in top fibre.
σ_{tmax} = maximum stress in top fibre.
σ_{bmin} = minimum stress in bottom fibre.
σ_{bmax} = maximum stress in bottom fibre.
w_t = Section modulus for top fibre.
w_b = Section modulus for bottom fibre.
e = Eccentricity.

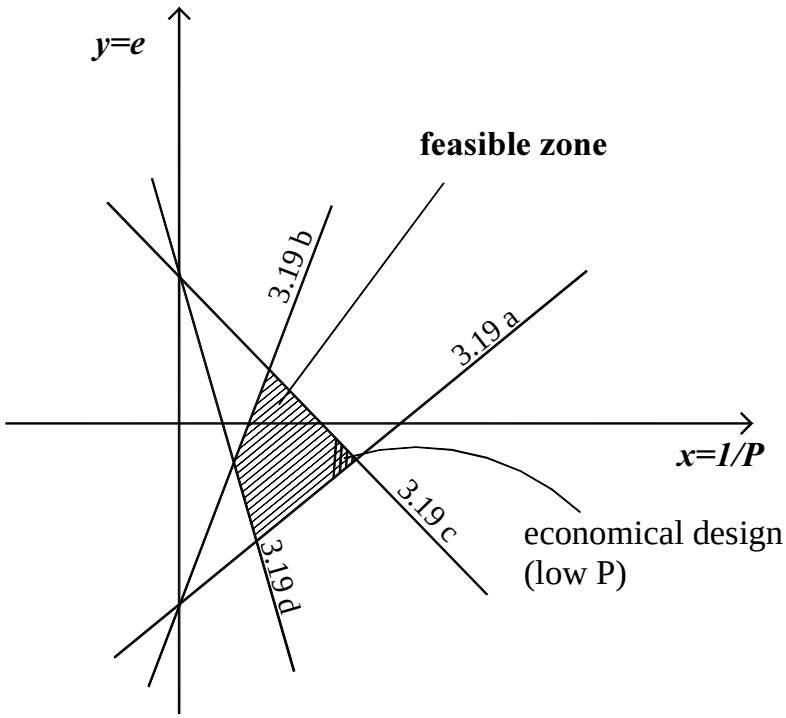

Example to find the best economical structure.
Figure 3.5

The hatched area in figure 3.5 gives the possible relation between prestressing force and eccentricity. It is possible to find the best economical combination from the same figure.

3.8 Design recommendations

There will always be a question of how to get a better structure, and it is also important to work for a better prestressed structure. To achieve this for a prestressed flat slab, some important points can be listed:

- Avoid horizontal restraint of the slab from walls. This can give uncontrolled cracks in the slab.

- In the deflection control it is important to remember that there can be an upward deflection if the total drape of tendons is too large.

- Careful control of the location of reinforcement with prestressing tendons is important. There can be a conflict between tendons and reinforcement, especially over columns with many reinforcement bars.

- Tendons around block-out in the slab must be placed at a safe distance from the edge and with a curvature that does not give cracks from the corner of the holes.

Chapter 4

Full-scale test of flat slab

4.1 Introduction

Many tests with flat slabs in smaller scale have been performed /57/, while there are few tests in full scale reported in the literature. Consequently the main purpose of this investigation is to reduce this shortcoming and to observe the development in stress, strain and deflections with increasing load, and the ultimate failure load of the structure. The test results are compared with results from FE analysis and simplified methods. The layout of the slab is shown in fig 4.1.

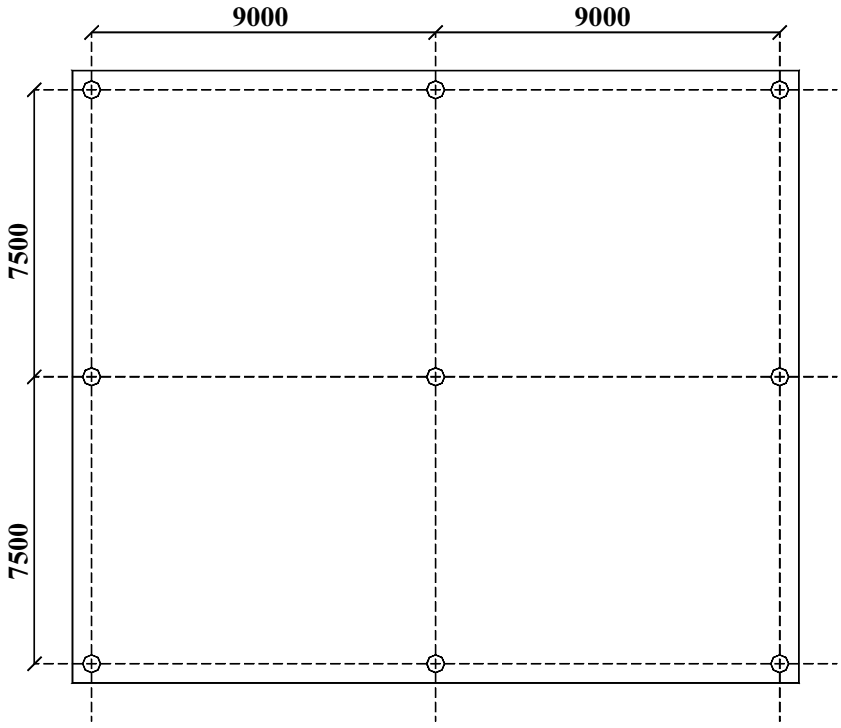

Slab 19000 mm x 16000 mm, thickness 230 mm. Column ϕ 450 mm

Figure 4.1

There are different ways to place the tendons in a flat slab. The most common solution is to place distributed tendons in the longest span and concentrated tendons in a column strip in the shortest span. This is also done here:

The slab is designed as a frame with column strip in the 7500 mm spans, loaded with self-weight and live load from 9000 mm width. In the design the width of the column strip is reduced to 3000 mm. In the other direction the slab is designed as a one way system. Details are shown in appendix A. The live load is 2.5 kN/m^2 uniformly distributed. To obtain this situation in the test, the slab was loaded with water. This gives some deviation from the 100 % uniform load when deflections occur, but since the deflections are small in this type of structures, it was ignored. Since the slab has two spans and is symmetrical in both directions, only one quart of the slab is instrumented, see fig 4.2.

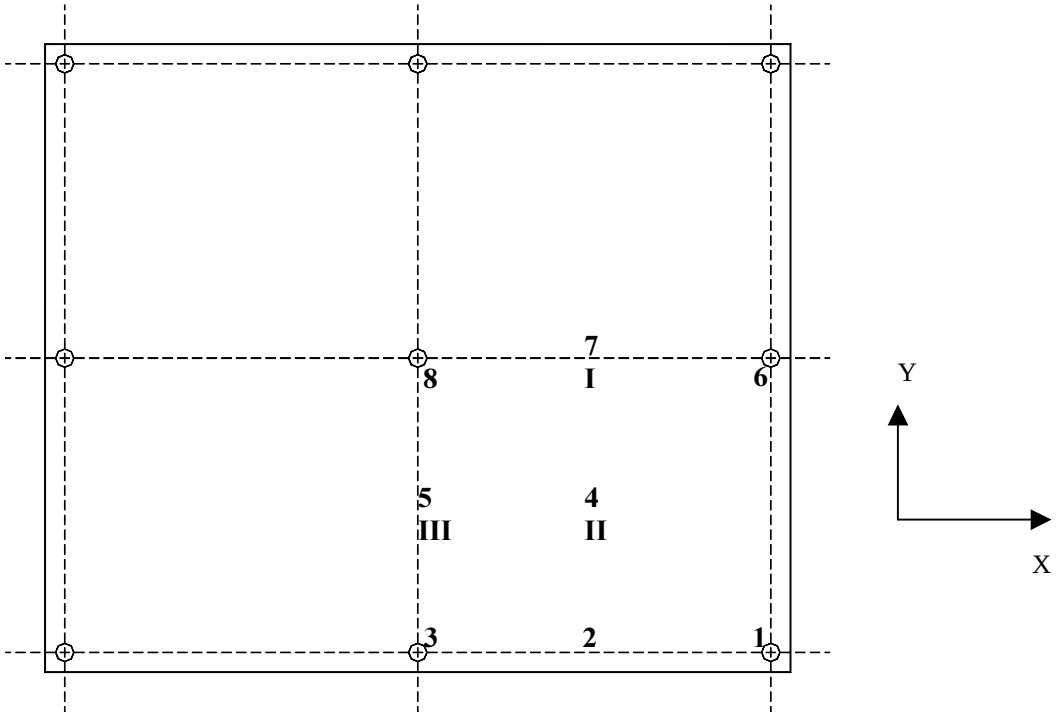

Registration points for deflections I, II, III
Strain gauges in top and bottom of the slab, in both directions in point 1 - 8
Figure 4.2

The slab was supported by nine columns with diameter 450 mm. Under each column there was a foundation that was cast on solid rock, so there should not be any deflections at the column. The columns are neglected when calculating the bending moment in the slab, since the columns are long. This is discussed in chapter 4.9.6 “Discussion of failure results”.

The price of this test was 850000 NKr (120000US$).

4.2 Description of the structure

The slab thickness is 230 mm, which gives a span/depth ratio for the longest span of 40, and for the shortest span about 33. The prestressed tendons give loads upwards in the span, and downwards over the column, and the tendon profiles are designed to balance the load in the span. The number of tendons is calculated to balance the self-weight, equation 4.1.

$$w = \frac{8 \cdot P \cdot f \cdot n}{l^2} \tag{4.1}$$

w = Load from tendon
f = Total drape of tendon
n = Number of tendons
l = Span width
P = Prestressing force (in this case reduced with 15 %)

The concrete slab is prestressed in both directions, in the direction with two spans, each 9000 mm, the distributed tendons have a distance of 340 mm. In the other direction the tendons are concentrated in a column strip, with eight tendons in the 1st, and the 3rd strip, and twenty tendons in the 2nd column strip, see fig 4.3.

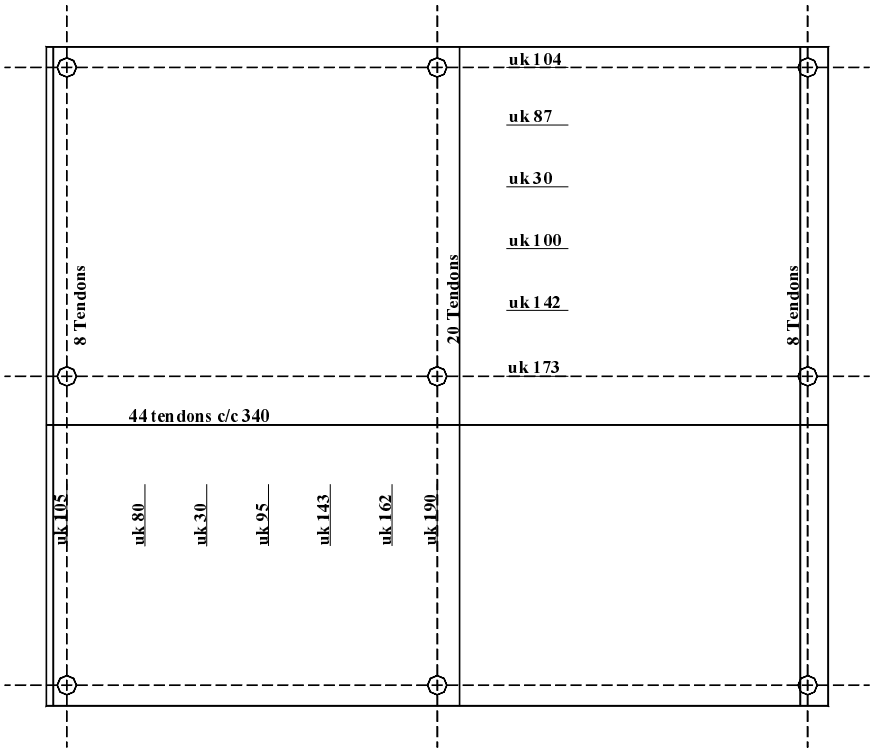

Tendon height in the flat slab.
Figure 4.3

Each column has a diameter of 450 mm, and is 4500 mm long. The slab is designed after the Norwegian building code NS 3473 /9/. The rules in NS 3473 give a possibility to skip reinforcement in spans, if the concrete does not crack. In this test there is placed some reinforcement in the longest span, ø10 c/c 500 mm, since this is normally done in flat slabs, just to distribute possible cracks. The other reinforcement used in the slab is the minimum reinforcement according to the Norwegian building code, see fig 4.4. The reinforcement in spans perpendicular to the distributed tendons is ø10 c/c 300 mm. Over the column the reinforcement should be placed at a length of 15% of the span width from column centre, and distributed over a width equal to the diameter of column and two times the slab thickness to each side of column (/9/ A.18.2.2). The reinforcement cover is 25 mm.

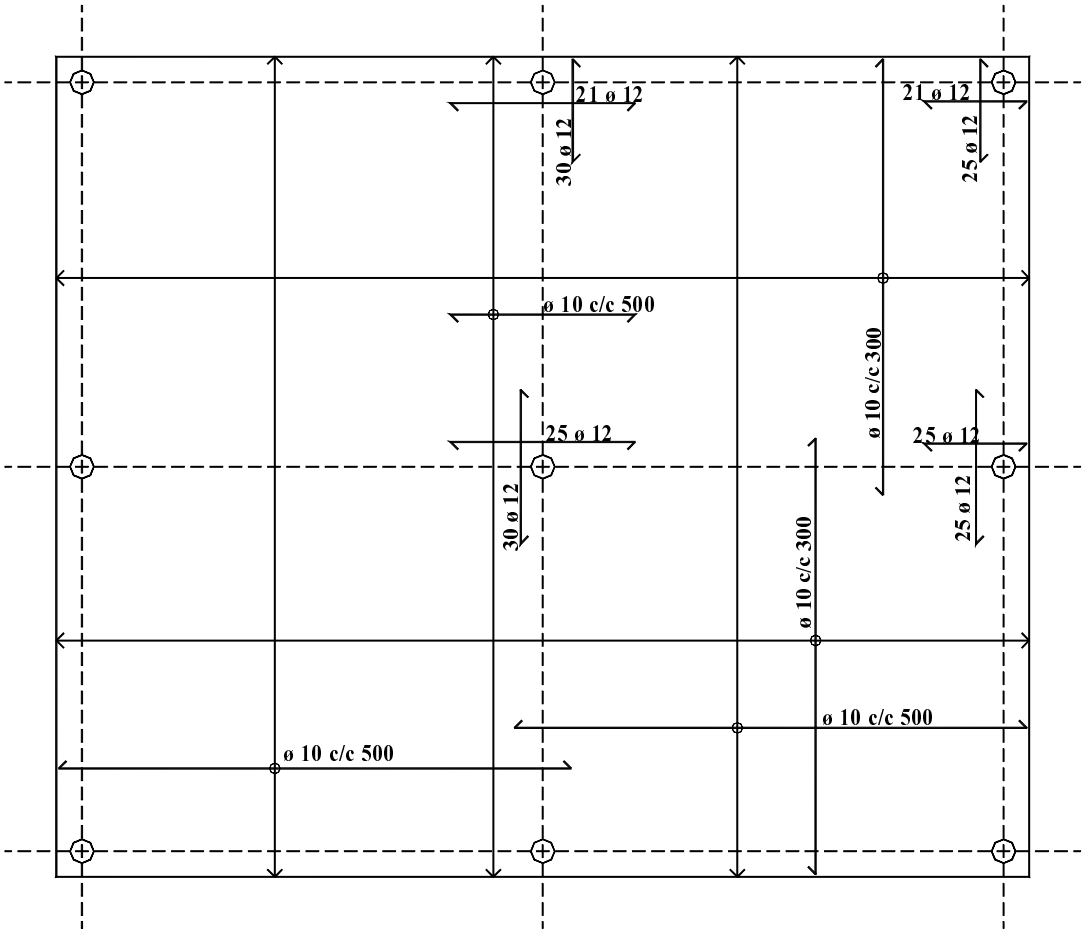

Reinforcement in flat slab
Figure 4.4

A live load of 2.5 kN/m^2, will require some shear reinforcement by the column in the middle of the slab. This reinforcement is omitted, because the slab collapse should be controlled at this column due to safety conditions. Under the slab, and around the middle column, a steel frame is built about 200 mm under the slab. This is done to prevent the slab from falling down to the ground and make damage. When loading with water, a wall is needed around the slab, fig 4.5. A form system with tension wire from side to side is used, and it is covered by a PVC-membrane on top of the slab and to the top of the wall to make it watertight.

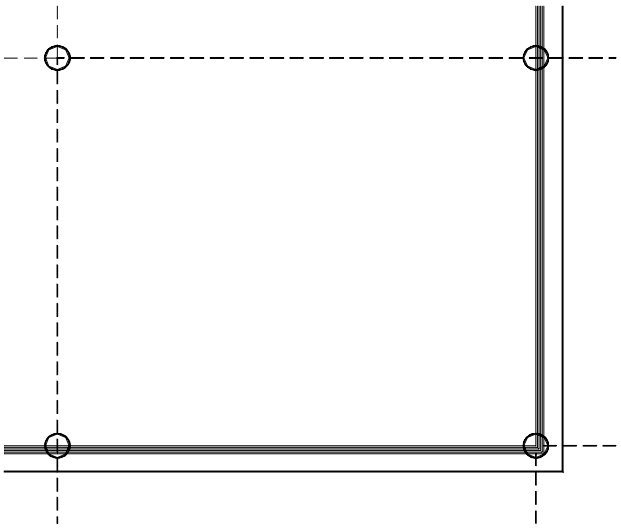

"Pool" walls.
Figure 4.5

In the middle of the slab, a wall around the column point is built, so it is possible to control cracks at the top of slab over an area of 1.2 m x 1.2 m when loading.

4.3 Materials

4.3.1 Form

The slab form is built on aluminium towers, “Alu-Top”, with 200 mm thick wood beams, “Hunnebeck–beam”, on top. Perpendicular to these beams there were the same type of beams at a distance of 550 mm, and on the top of these there was a 21 mm thick plywood form, fig 4.6. The side form was also made from 21 mm thick plywood, with 15 mm thick holes for each tendon. There are many types of slab form systems, but the Alu-Top system was used for the first time in Norway in this test.

Flat slab form.
Figure 4.6

4.3.2 Concrete

The concrete was mixed in a 3 m^3 capacity horizontal rotating type mixer, before it was dropped into a 6 m^3 rotating mixer on a truck. From the truck the concrete is pumped into the form. Concrete C 35 with 22 mm maximum size gravel was used in this test. The concrete receipt is listed in table 4.1.

Cement	P 30 Norcem	302,26	kg/m^3
Plasticizer	Rescon P	2,50	kg/m^3
Water		119,18	kg/m^3
Fine gravel	0-7 mm	1195,43	kg/m^3
Gravel	6-22 mm	775,95	kg/m^3
Total weight		2397,25	kg/m^3
Total water amount		170,83	kg/m^3
Water/Cement ratio		0,56	
Measured slump		169	mm

Average values in concrete prescription.
Table 4.1

Nine cubes were cast for compressive strength testing. The cubes were 100 x 100 x 100 mm. Tests were carried out three times, first when stressing tendons, then after seven days and finally when loading.

4.3.3 Reinforcement, Prestressing strand, Anchorage

Only 10 mm and 12 mm reinforcement bars are used in the slab, with nominal yield stress f_y=500 N/mm^2. A typical stress-strain curve for reinforcing steel is shown in fig 4.7. Young's modulus was 200000 N/mm^2

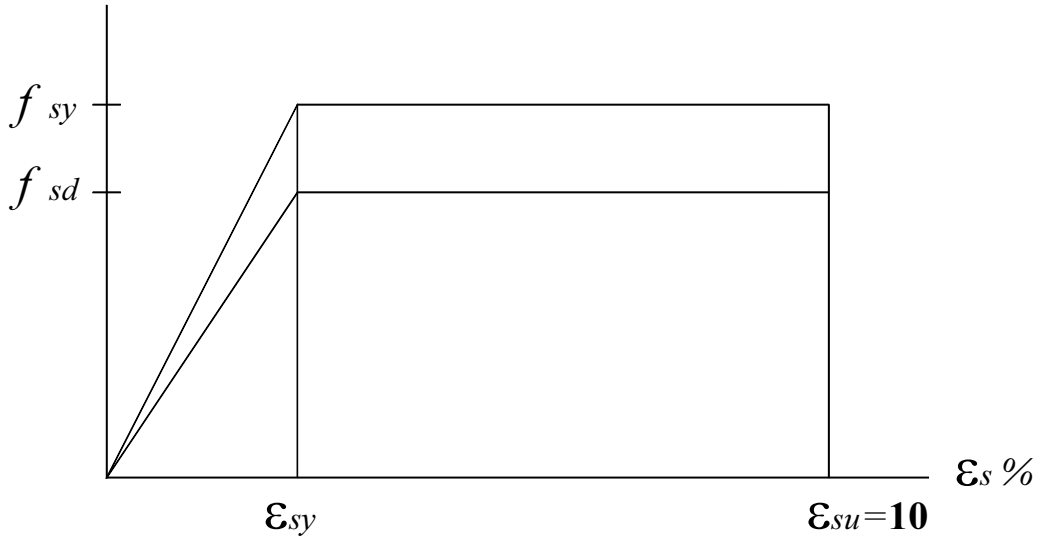

Stress-strain diagram for design, reinforcement, / 9 /.
Figure 4.7

The tendons used in this test were 100 mm^2 (1/2-in) seven wire strands, 1670/1860 unbonded tendons. A typical stress-strain curve for prestressing tendons is shown in fig 4.8. Young's modulus was 196000 N/mm^2

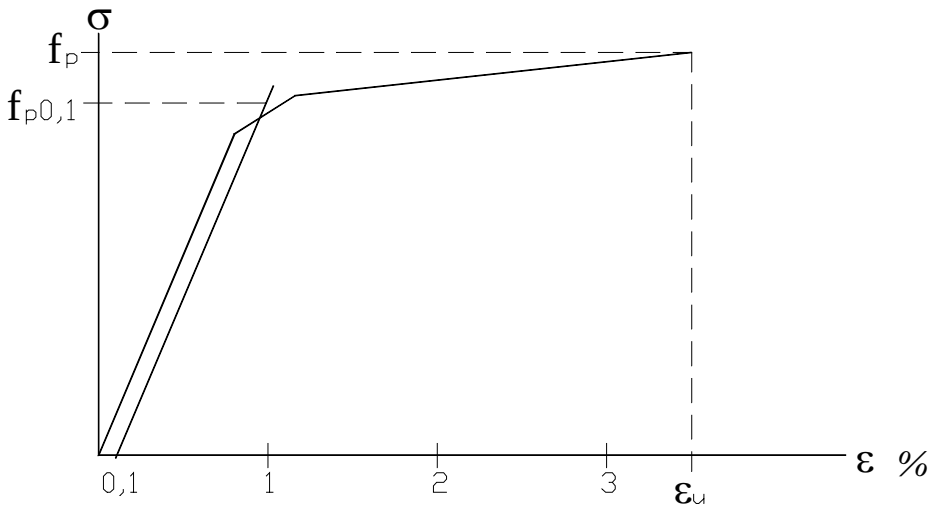

Stress-strain diagram, prestressed tendons.
Figure 4.8

The grease used in this tendon is low friction grease.
After casting, and when the concrete has hardened, the side form is removed, and the anchorage is placed. The anchorage consists of steel plates 60 mm x 100 mm and 15 mm thick. To this a conical cylinder is added where the split cone wedges are placed, see fig 4.9.

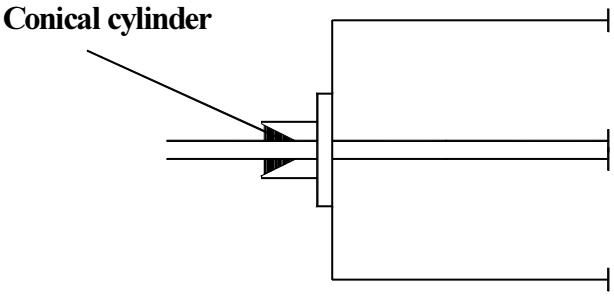

Active anchorage.
Figure 4.9

The slab was post-tensioned after 5 days, providing that the concrete strength was not less than 22 N/mm^2. The tendons were prestressed individually by a hydraulic jack. The prestressing force was measured with a manometer, and for some tendons it was also measured with load cells. The distributed tendons were first tensioned, and then the concentrated tendons were tensioned.

4.4 Fabrication of the flat slab

To prevent the slab from rotating, small concrete walls were built 10 mm from the slab, see fig 4.10.

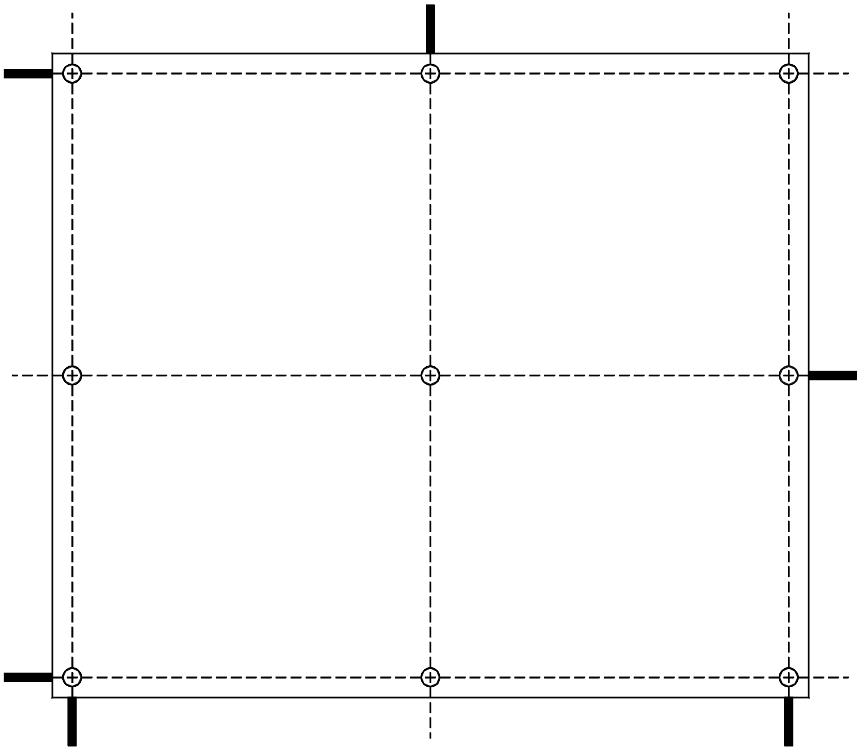

Stabilizing walls.
Figure 4.10

Since the load was distributed, these walls will come into effect only if there should be a large rotation when collapsing.

The longitudinal reinforcement from the column ends in the middle of the slab thickness. Before the tendons were installed, all bottom reinforcement, except the reinforcement in the middle of the 9000 mm span, were placed. First the concentrated tendons were placed, then the distributed tendons. After all tendons were in place, the top reinforcement was placed. In fig 4.2 it is shown where the strain gauges are located. Each of these points has a strain gauge in the top of slab, and in the bottom, and in both directions. Totally 32 gauges were installed in the slab. The strain gauge is fastened to the reinforcement with a soldering iron, see fig 4.11.

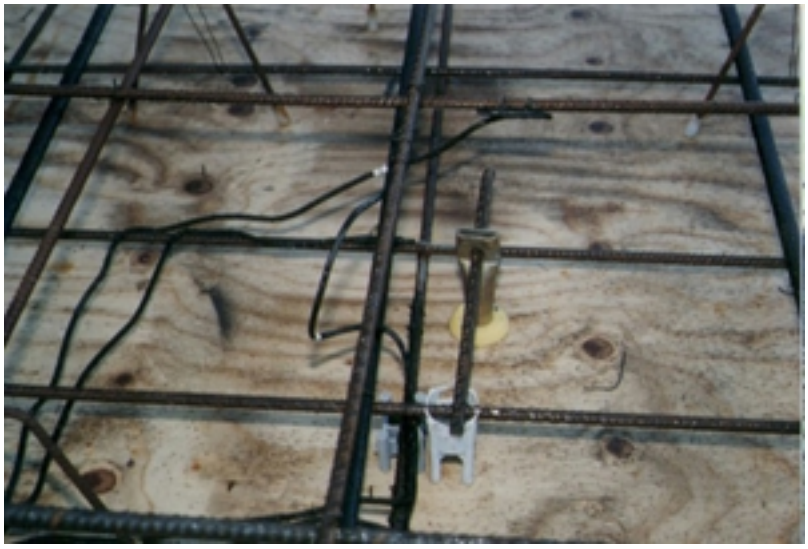

Strain gauges and measure point.
Figure 4.11

There were 3 temperature sensors inside the concrete slab, one at the top of the slab, one in middle and one in the bottom, and one outside for air temperature. In each point where the deflections should be measured, a fastening point for a measuring rod is installed, fig 4.11.

After all instrumentation inside the slab was finished, it was ready for casting. An electronic vibrator was used to consolidate the concrete, and the surface was finished using a helicopter. About 12 hours after the concrete was placed, the slab was moistened. After three days the side form was removed, and the anchorage was placed at the tendons. There were also placed twenty load cells, fig 4.12 and fig 4.13, at the tendons.

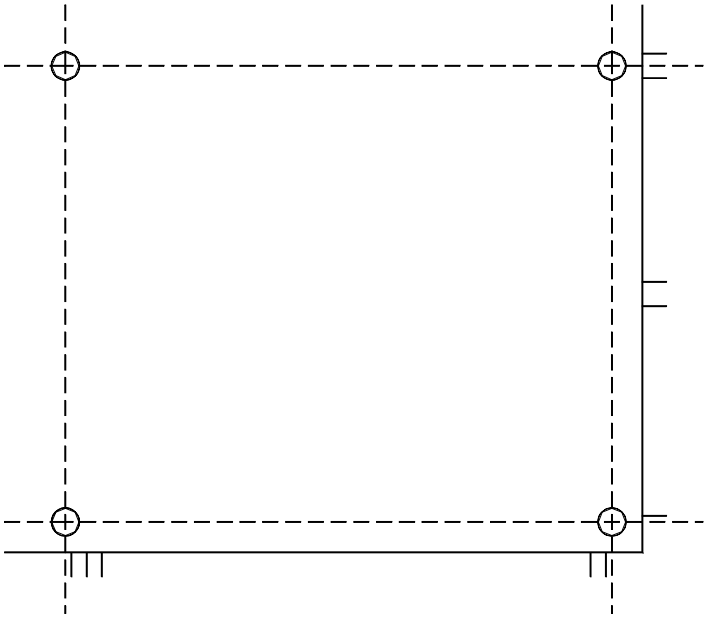

Load cell locations, the other loadcells are symmetrical.
Figure 4.12

Load cell at the anchorage.
Figure 4.13

The elongation of each tendon was measured after tensioning, and the level of the slab was measured before and after form removal.

4.5 Instrumentation

All the measured results of this test are saved in a computer, Schlumberger Solatron 3531D data logger with full bridge repeatability 4μs, limit of error less than 30μs, for quarter bridge repeatability 2μs, limit of error less than 15μs.

For the load cells a 6-wire connection was used, and for the strain gauges a 4-wire connection was used to eliminate any temperature effect on the wires.

The original length of wires for the load cells were 12 and 21 metres and for the strain gauges 12 and 17 metres. This length was extended by 10 metres because the computer had to be moved before the test should start. The load cells were made in the laboratory of the Department of structural engineering at NTNU and consist of steel cylinders with inside diameter 29 mm, outside diameter of 50 mm and length of 65 mm with a conventional full bridge, made by strain gauges of the type WFLA 3. Each load cell was calibrated in a Darteec 500 kN testing machine. The strain gauges used at the reinforcement bars were of the spot weldable type, AWC-8b-3lt with gauge length 8 mm. The strain gauges are produced in Japan, Tokyo Sokki Kenkyujo Co, Ltd.

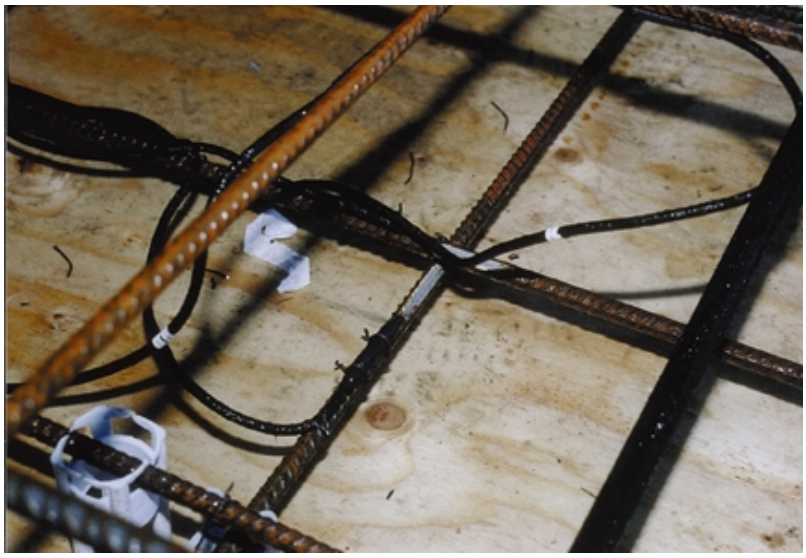

Strain gauge at the reinforcement.
Figure 4.14

Registration of data
Figure 4.15

4.6 Loading

Since the slab was large, and the live load was distributed, water was used as load. With help from the fire department in Aalesund, it was possible to load the slab controlled, with approximately 0.67 m^3/min. The wall that is covered by PVC membrane limits the loaded area. Water was measured by a water gauge and this gives an exact load on the slab. Extra load in the span because of deflection is negligible.

4.7 Test results

4.7.1 General

A great quantity of data from strain gauges, load cells and deflection measurements were recorded. The calculation after NS 3473 had shown that some shear reinforcement by the column in the middle of the slab was necessary, however this reinforcement was skipped so the collapse in the slab should be at this point.

4.7.2 Prestressing force, loss

Each tendon should be stressed to 85 % of f_y, that means for this tendon, 100 mm^2 1670/1860, a force of 141.95 kN. This force was read from a jack manometer and in addition controlled from some tendons with load cells. After short time loss, the force in the tendons is calculated to be 132.6 kN in stressed ends and 136.1 kN in dead ends.

Long time losses from creep and shrinkage in the period from stressing to loading, give an average loss of 3.1 kN in tendons, calculated according to the Norwegian standard /9/. This is shown in chapter 4.8.2. After the loss is calculated, it gives an average force in tendons of 131 kN, 129 kN in stressed ends and 133 kN in dead ends. The concrete strength was at this time 26,1 N/mm^2.

The prestress forces after short time loss give a theoretical elongation of 126 mm for the longest tendons (19000mm). That gives 6.6 mm elongation pr metre of tendon, which is close to the normally used elongation (6 – 6.5 mm) if not an exact calculation is done. The theoretical elongation in the other direction, 16000 mm, is calculated to 106 mm.

Measured elongations are shown in table 4.2. The average elongation (measured) in x-direction is 114 mm, and in y-direction 95 mm. The measured elongation is generally considerably lower than theoretically calculated elongation.

x-direction (19000 mm) 44 tendons	y-direction (16000 mm) 36 tendons
1 tendon with 109 mm elongation	2 tendons with 91 mm elongation
3 tendons with 110 mm elongation	3 tendons with 92 mm elongation
1 tendon with 111 mm elongation	2 tendons with 93 mm elongation
6 tendons with 112 mm elongation	6 tendons with 94 mm elongation
4 tendons with 113 mm elongation	10 tendons with 95 mm elongation
8 tendons with 114 mm elongation	3 tendons with 96 mm elongation
7 tendons with 115 mm elongation	7 tendons with 97 mm elongation
9 tendons with 116 mm elongation	3 tendons with 98 mm elongation
2 tendons with 117 mm elongation	
3 tendons with 118 mm elongation	

Measured elongation.
Table 4.2

With elongation as described above, the average force can be calculated as:

$$P = E \cdot A \cdot \frac{\Delta L}{L} \tag{4.2}$$

This gives an average force of 117.6 kN in x-direction, and 116.4 kN in y-direction. The average observed force from load cells is 119 kN in x-direction, and 112 kN in y-direction after stressing, 115 kN and 108 kN just before loading starts. That means 4 kN loss in both directions in a period of 18 days (calculated 3.1 kN, without calculated loss from relaxation). The results are compared in figure 4.16.

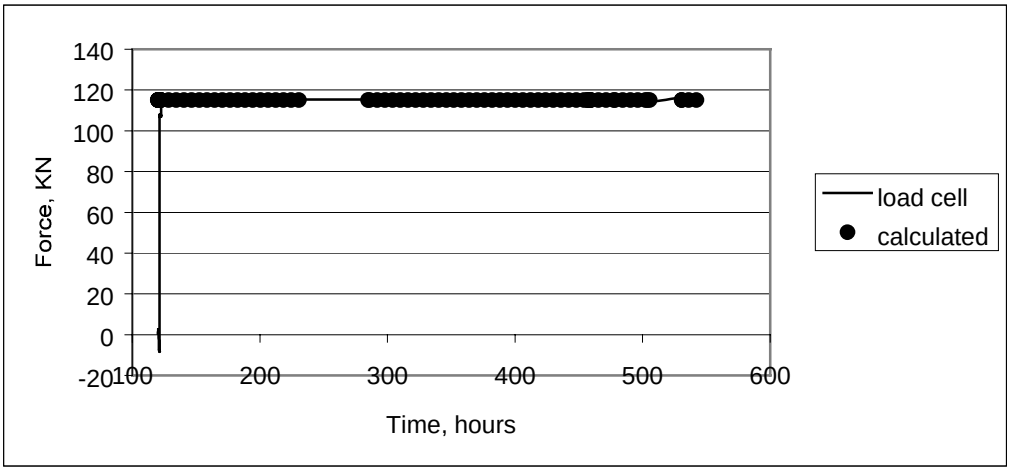

Tendon force in point 1(fig 4.2) from load cell and calculated from measured elongation, x-direction, after jacking stressed end, channel 101.
Figure 4.16a

The measured prestressing forces are approximately 10 percent lower than the theoretical forces. The reason for this might be larger anchorage set, too low manometer pressure when stressing the tendons or other practical circumstances.

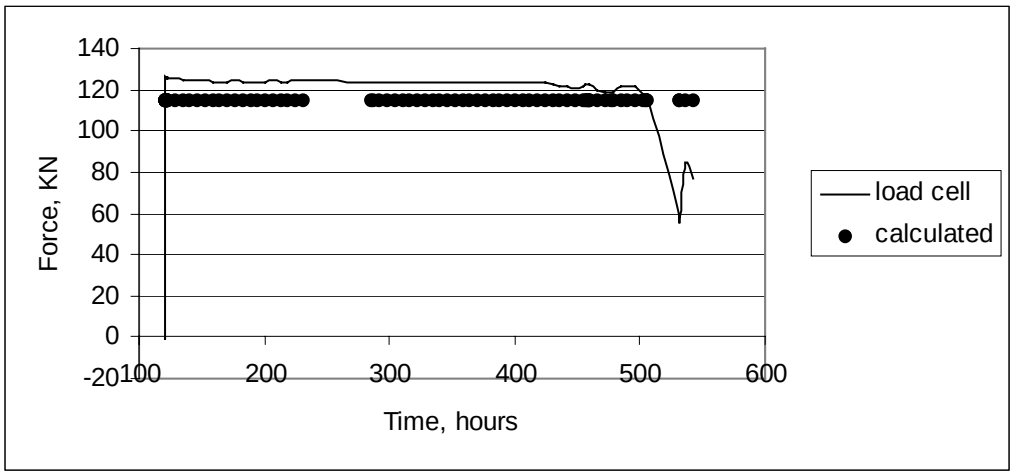

Tendon force opposite of point 1(fig 4.2) from load cell and calculated from measured elongation, x-direction, after jacking dead end, channel 103.
Figure 4.16 b

Until just before failure the tendons have only a small increase of forces, about 1 % increase from the start of loading until the failure occurs. This can be seen from fig 4.17. In this figure it is shown that the forces in the tendons do not increase continuously. The reason for this irregularity can be the variation in force when cracks occur and also an effect of friction between tendons and the plastic sheet.

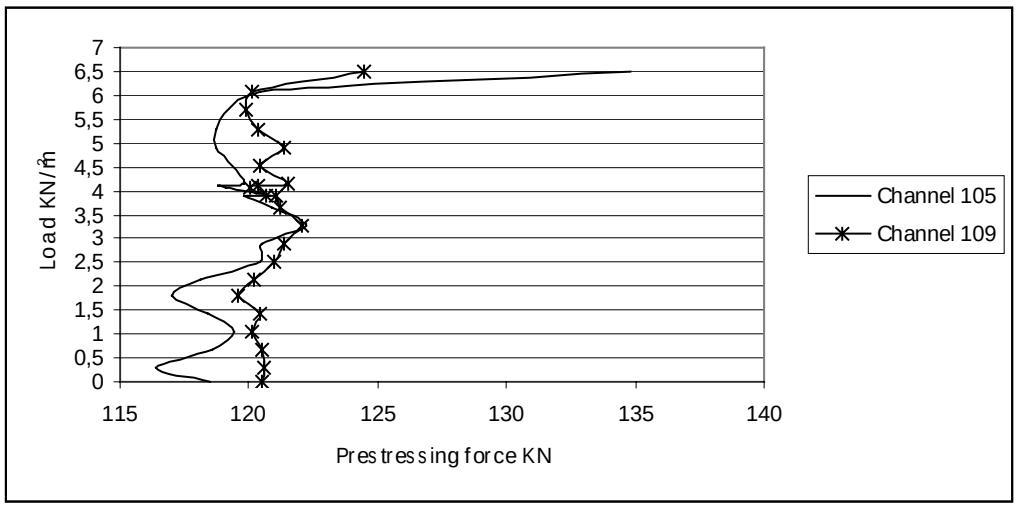

Force in tendons from the start of loading until failure occurs.
Figure 4.17

The force in the tendons in the distributed direction, channel 105 and 109, in the middle column strip, has approximately 120 kN in both ends before loading. This force increases until load of 3.25 kN/m^2 and then it decreases until load of 5.5 kN/m^2. The average force in the tendons at this time was 120.8 kN. At this time the reinforcement over the column started yielding, and the prestressing forces increased considerably.

4.7.3 Deflections

One of the greatest advantages with prestressed concrete is that by use of balanced loads, there will only be small deflections in the slab. In this test the balanced load is equal to the dead load. The level of the slab top was measured before and after the form was removed, 6-7 days after casting. There was no measurable difference in level when removing the form. Deflections were measured in three points, fig 4.2, when loading the slab. The measured deflections are later presented in figure 4.26.

4.7.4 Temperature and strain before prestressing

The temperature sensors in the slab should give an indication of the hardening temperature in relation to air temperature. As seen from fig 4.18, the temperature in the concrete has a maximum of 23 ^{o}C in the bottom of the slab, 18.8 ^{o}C at the top and 22,2 ^{o}C in the middle. This difference can be explained by the form in the bottom that functions like an insulation or membrane for the slab, and the air temperature will not reduce the concrete temperature so quickly.

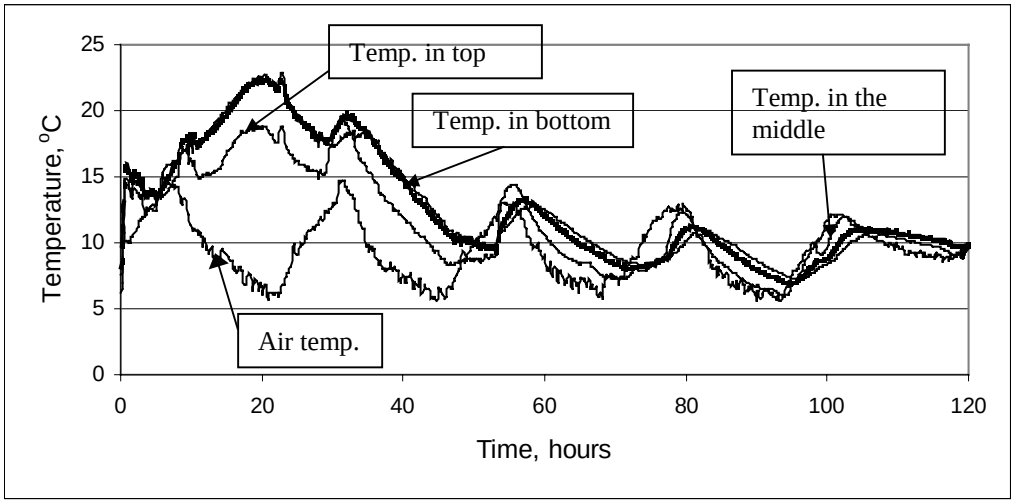

Temperature in the concrete and air from casting.
Figure 4.18

After five days (120 hours) the concrete temperature and the air temperature are approximately equal. The maximum temperature in the concrete is reached 23 hours after casting. From fig 4.19 it can be seen that the temperature has an effect of strain in the steel. Maximum strain in steel from temperature is 0.08 $^{o}/_{oo}$.

The strain gauges are temperature compensated which means that the true (total) strain can be calculated from the equation:

$$\varepsilon_{true} = \varepsilon_{reg} + \alpha_T \cdot \Delta T \qquad (4.3)$$

ε_{reg} = measured strain
α_T = thermal dilation coefficient
ΔT = temperature change

The strain gauges were attached to the reinforcement in eight points, fig 4.2, in both directions in top and bottom of the slab, totally 32 strain gauges.

Strains in reinforcement, measured from start of casting, in point 4 top and bottom, x- and y- direction are shown in figure 4.19.

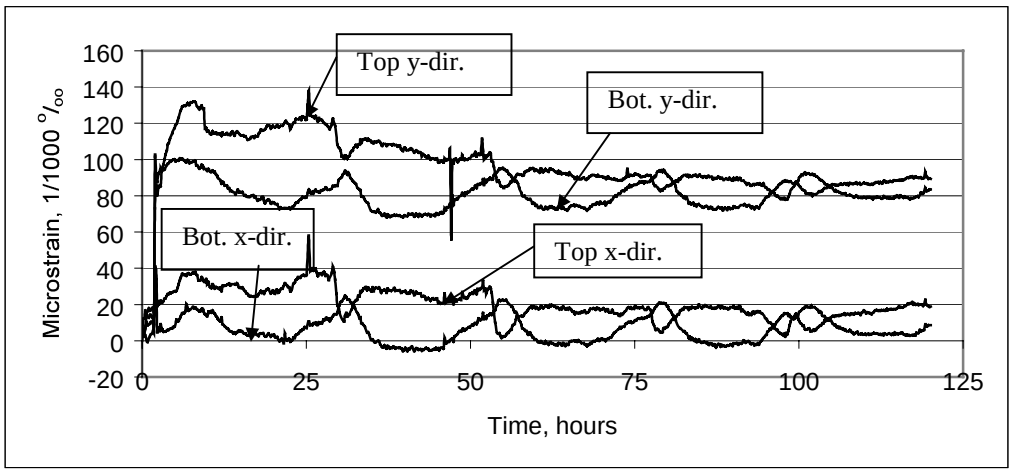

Strain in reinforcement before prestressing.
Figure 4.19

4.7.5 Strain development in the period after prestressing

About 121 hours after casting, the prestressing starts. All the strains are then set equal to zero and the increase of strain in the reinforcement parallel to the concentrated tendons are shown in figure 4.20 a, b, c and d.

After stressing of tendons, the concrete has an axial stress of about 1,5 N/mm^2 from distributed tendons, and somewhat higher in the perpendicular direction from the concentrated tendons.

Perfect balance between prestressing force and dead load, and with centric prestressing force in stressed ends, will give the same compressive strain in top and bottom.

As shown in the figures below, there are deviations from this perfect load situation, and this can partly be explained by:

- The load is not perfectly balanced since there are concentrated tendons in one direction and distributed tendons in the other direction
- Development of crack above the middle column
- Upward load in the span and downward load over column from tendons
- Temperature variation from maximum day temperature of 14 ^{o}C to minimum night temperature, 6 ^{o}C.

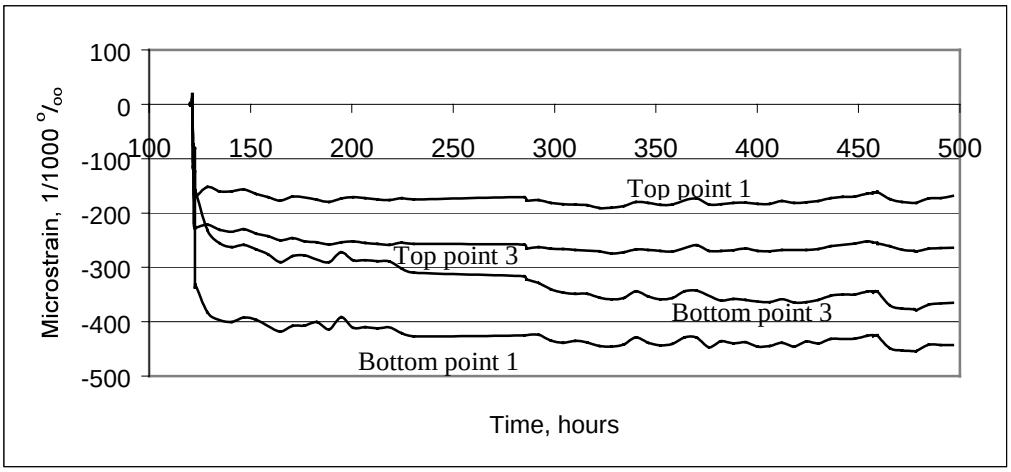

Strain gauge in y-direction point 1 and 3.
Figure 4.20 a

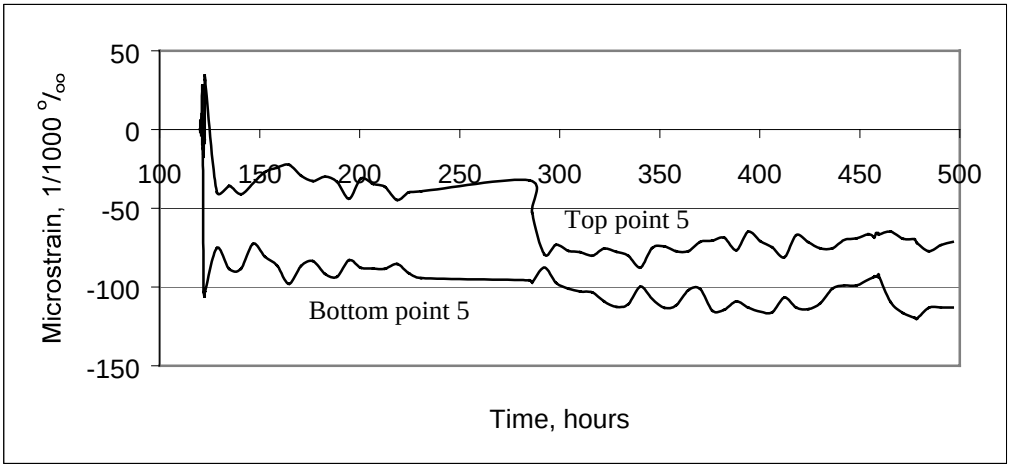

Strain gauge in y-direction point 5.
Figure 4.20 b

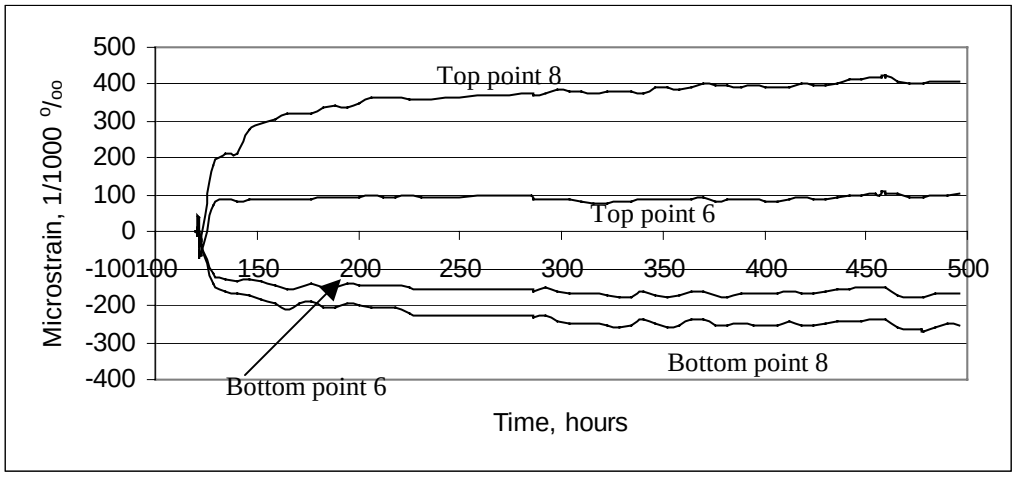

Strain gauge in y-direction point 6 and 8.
Figure 4.20 c

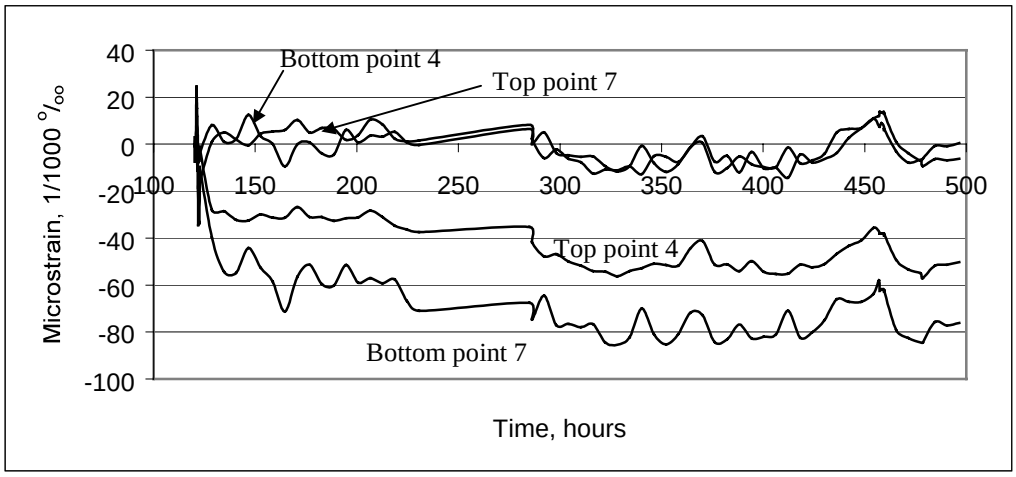

Strain gauge in y-direction point 4 and 7.
Figure 4.20 d

Strain gauges in reinforcement point 1 and 3 (from figure 4.2), figure 4.20 a, close to the stressing point of concentrated tendons and parallel to this, show that in point 1 there is larger difference in strain between top and bottom reinforcement than in point 3.

The effect of the bending moment from the columns can partly explain the differences between strains in top and bottom.

Strain plot in point 5, figure 4.20 b, shows a higher compressive strain in bottom than in top of slab. That means that the load is not exactly balanced in this point.

Perfect balance will give a compressive strain in top and bottom close to 80 microstrain.

In figure 4.20 c it can be seen that the gauge parallel to concentrated tendons in top of slab in point 8, has higher strain than the other gauges. The reason for this is the large bending moment in this area. This also holds for point 6, but since this is an outer support, the moment is less.

In point 4 and 7, figure 4.20 d, there are only small strains since these strain gauges are placed between and parallel to the column strip, but it is interesting to notice that reinforcement in point 7 in the bottom, has some compressive strain.

In the other direction, parallel to the distributed tendons, the development of strain is shown in point 1 and 6 in figure 4.21 a, point 2 and 7 in figure 4.21 b, point 3 and 8 in figure 4.21 c and finally point 4 and 5 in figure 4.21 d. The last two points are located in the middle of the span in the column strip direction, see figure 4.2. In general these results confirm the results from the y-direction.

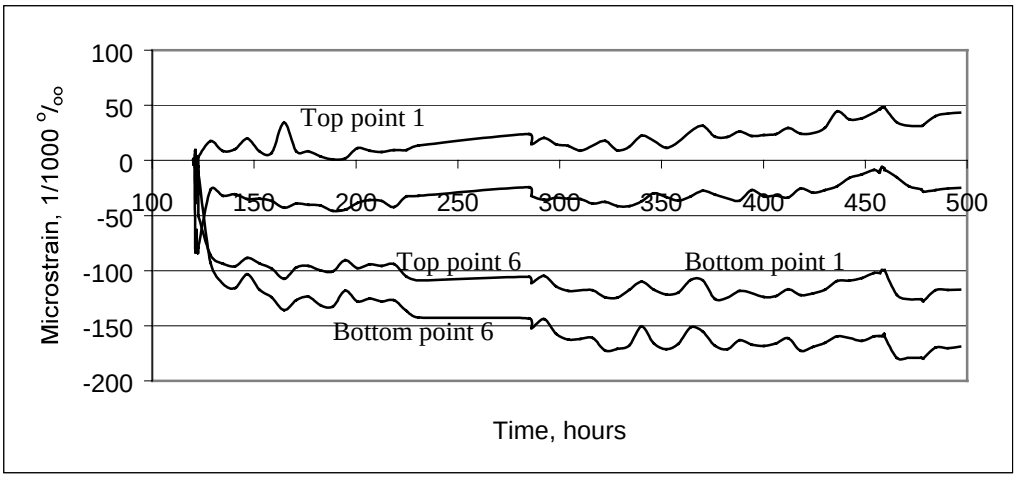

Strain gauge in x-direction point 1 and 6
Figure 4.21 a

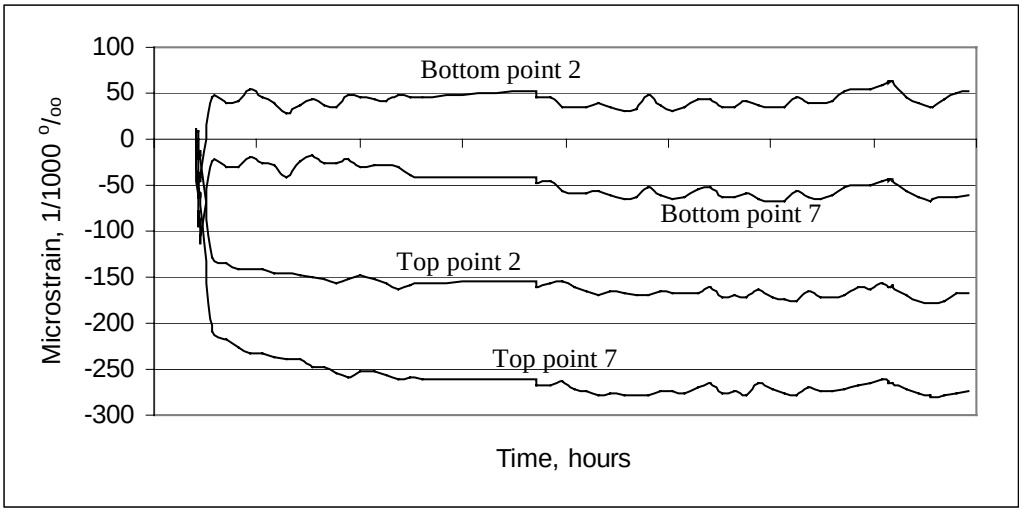

Strain gauge in x-direction point 2 and 7.
Figure 4.21 b

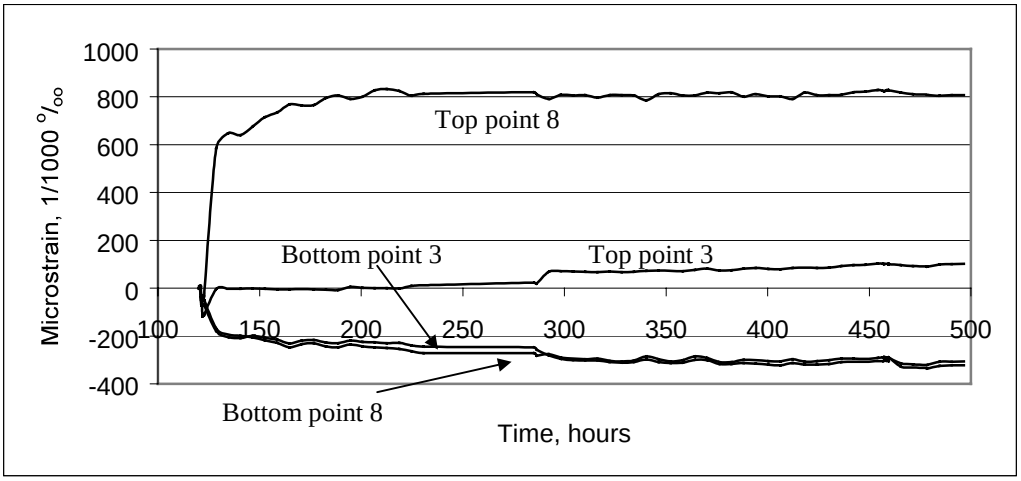

Strain gauge in x-direction point 3 and 8.
Figure 4.21 c

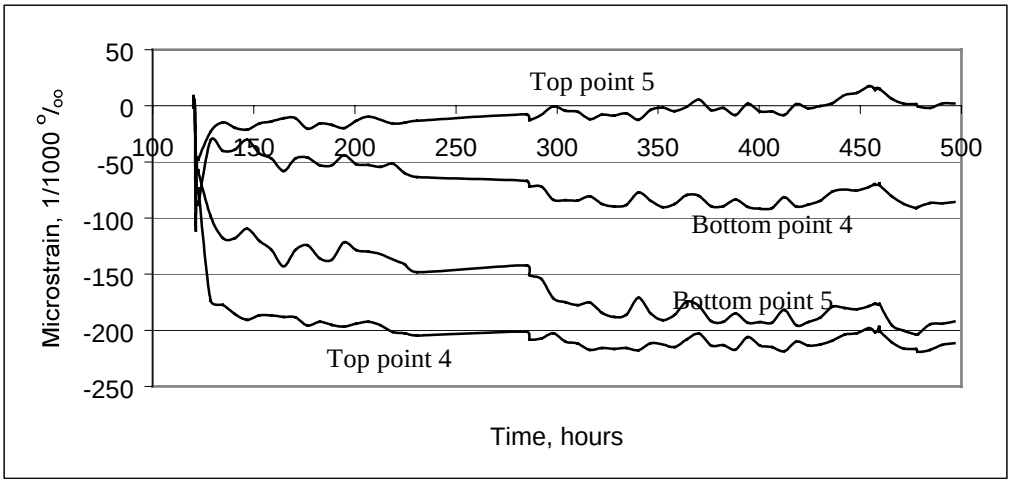

Strain gauge in x-direction point 4 and 5.
Figure 4.21 d

4.7.6 Strain development in the failure test

Development of strain in reinforcement, y-direction, from the start of loading until failure is shown in figure 4.22 a, point 1 and 3, figure 4.22 b, point 6 and 8, and figure 4.22 c, point 4 and 7. The results are also presented in appendix A.

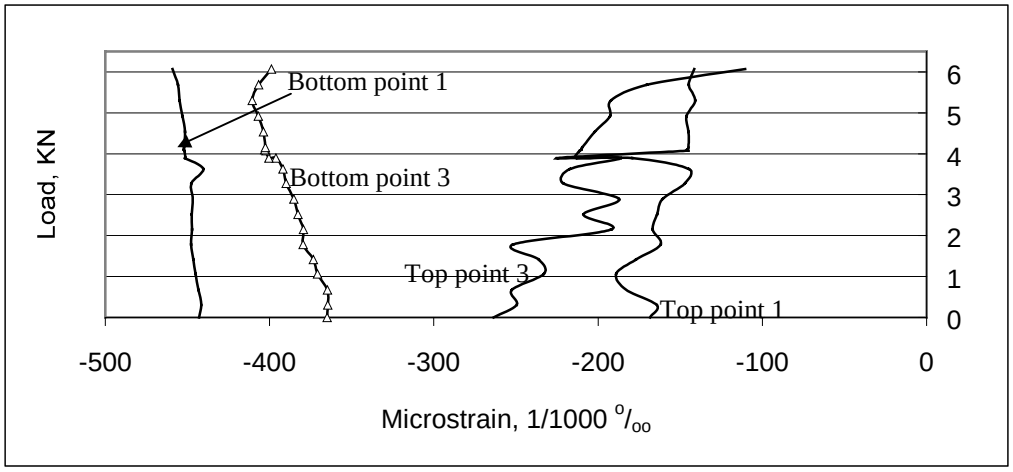

Strain gauge in y-direction point 1 and 3.
Figure 4.22 a

From figure 4.22 a, it can be seen that strain in bottom and top in point 1 and 3 shows only small changes. This is because these strain gauges are placed close to the support where moments are small.

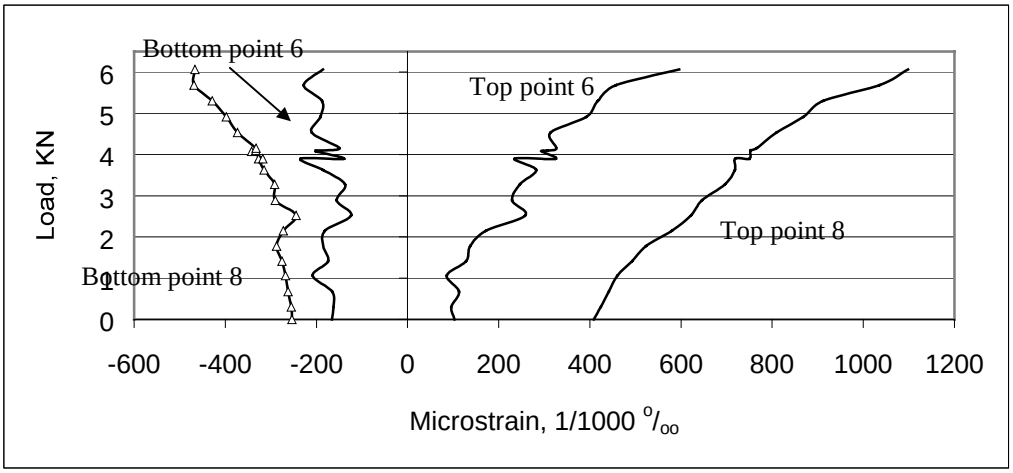

Strain gauge in y-direction point 6 and 8.
Figure 4.22 b

Figure 4.22 b shows that there are large tensile strains in points 6 and 8 at the top, and compressive strains in bottom. The strains in point 6 have a maximum of 0.6 $^{o}/_{oo}$ with a load of 6.0 kN/m^2 before failure at 6.5 kN/m^2. By the middle column, point 8, there was a maximum of 1.1 $^{o}/_{oo}$ at the same time. There were only small compressive forces in the bottom in this point.

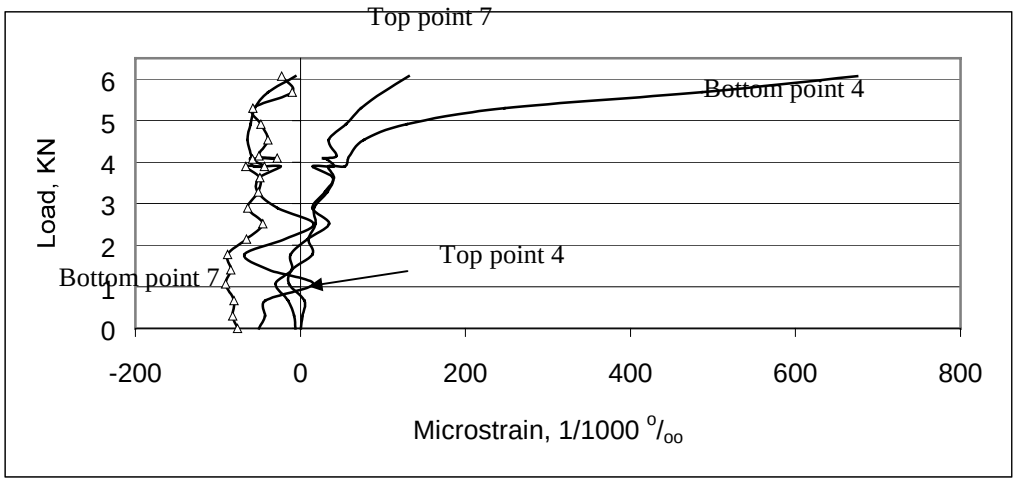

Strain gauge in y-direction point 4 and 7.
Figure 4.22 c

Strains in point 7 and top point 4 are relative small, but in bottom point 4 the tensile strain start increasing when the load pass 4 kN/m^2. This might be a result of a two-way effect.

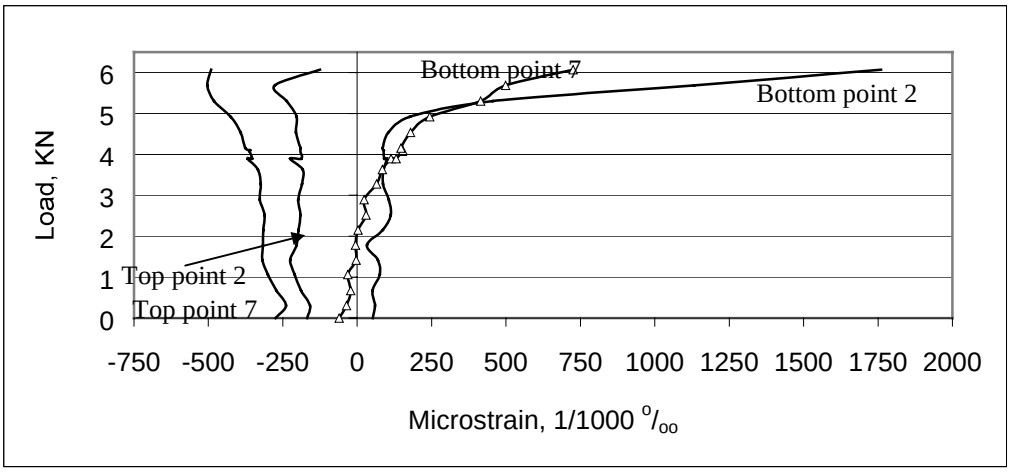

Strain gauge in x-direction point 2 and 7.
Figure 4.23 a

The compressive strains in top of point 2 and 7 are approximately constant when loading the slab, figure 4.23 a. At the bottom the strains are close for these two points until load of 5.25 kN/m^2, and then the strain increases more in point 2 than in point 7. This might be because the crack development is faster near a free edge than in the middle of the slab.

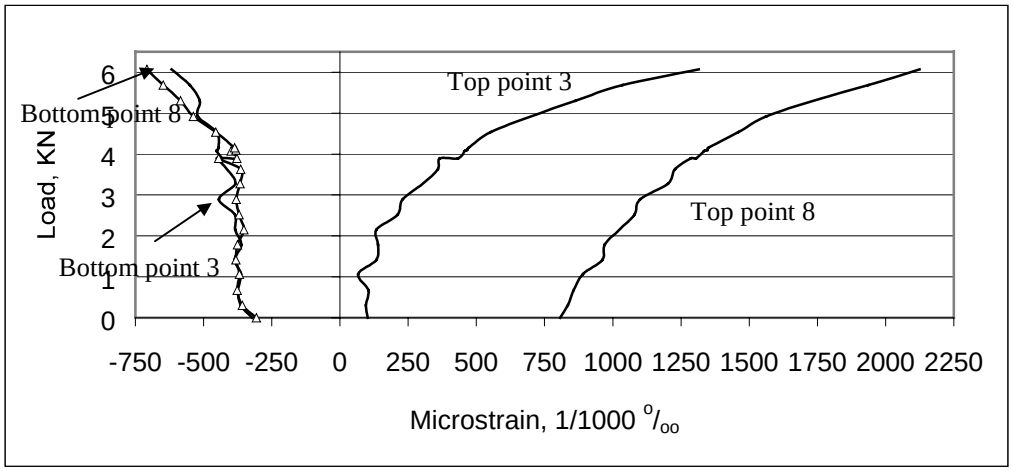

Strain gauge in x-direction point 3 and 8.
Figure 4.23 b

Strain in the bottom of point 3 and 8 increases from 0.3 °/oo until 0.6 °/oo up to a load of 6.0 kN/m^2, figure 4.23 b. In the top the maximum strain occurs in point 8 at the same load stage. The reinforcement yields in this point with a load of 6.5 kN/m^2.

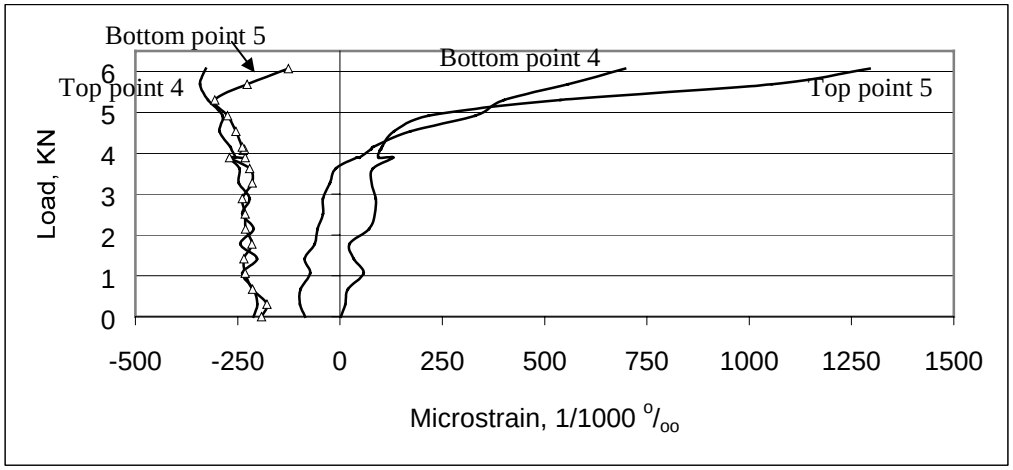

Strain gauge in x-direction point 4 and 5.
Figure 4.23 c

Figure 4.23 c, related to point 4 and 5, shows a strain development similar to a continuous one way slab. There are tensile strains in top over support, point 5, and in the bottom of the span, point 4. As seen from the figure, there is a higher strain over support than in the span. The results confirm the support effect of the column strip.

4.7.7 Summary of the test results

A flat slab, 19000 mm x 16000 mm with thickness 230 mm was loaded with water until the slab collapsed by shear failure around the middle column. The slab has two spans in each direction, 2 x 9000 mm in x-direction and 2 x 7500 mm in y-direction from centre to centre of columns. Each column has a diameter of 450 mm. There were a total of nine columns to support the slab. Prestressed tendons and minimum reinforcement were used in this test slab.

Tendons are distributed at a distance of 340 mm in x-direction and concentrated in the column strips in y-direction with twenty tendons in the middle column strip, and eight tendons in each of the end column strips.

The concrete quality is C 35 with prescribed twenty-eight days cube compressive strength of 35 N/mm^2. The maximum allowable prestressing force in the tendons is 85 % of f_y, i.e. 140 kN for a 100 mm^2 tendon, before loss.

The average observed force from load cells is 119 kN in x-direction, and 112 kN in y-direction after stressing, 115 kN and 108 kN just before loading starts. There is only a minor increase of prestressing forces in tendons when loading the slab, about 1 %.

Maximum temperature in concrete was 23 ^{o}C, which occurred 23 hours after casting. Deflection with the design load, 2.5 kN/m^2 was 4.5 mm in the middle of span, and maximum deflection before failure, at 6.5 kN/m^2, was 30 mm.

Only the reinforcement in top of slab over the middle column yields when failure occurs. Strain in reinforcement in column strip, top point 5 x-direction, increases until maximum 1.3 $^o/_{oo}$, and in the middle of spans, bottom point 4 x-direction, until 0.7 $^o/_{oo}$.

After the failure there were distributed cracks in the bottom of the slab, see figure 4.24, and concentrated cracks over the middle column in top of slab, see figure 4.25.

Crack in the bottom of the slab after failure.
Figure 4.24

Crack in the top of the slab over the middle column.
Figure 4.25

4.8 Test results compared to simplified methods

4.8.1 General

Before this test was done, the slab had to be calculated to find the best economical and practical structure. Recommended span to depth relation for a slab like this is about 40, which gives a chosen slab thickness of 230 mm. Loss in prestressing is about 15 %, and that gives distribution of tendons as shown in chapter 4.2.

4.8.2 Prestress loss

Losses in prestressing force are calculated only after short time and equations to calculate loss are given in appendix A. The friction loss in tendons is calculated as:

$$P_x = P_o \cdot e^{-\mu(\alpha+\Delta\alpha\cdot x)} \tag{4.4}$$

For distributed tendons this gives:

P_o = 141 kN
μ = 0.05
$\Delta\alpha$ = 0.02 rad/m
α = $\left(\frac{105-25}{3604}+\frac{190-25}{5496}\right)\cdot 2 = 0.104$ (from figure 4.3)
x = 19 m

=> Px =<u>137.6 kN</u>

This gives a loss in passive end of distributed tendon of 3.4 kN.

Loss from anchorage set in active ends is calculated as:

$$\Delta P = \frac{s \cdot E_p \cdot A_p}{l} + a \cdot l \tag{4.5}$$

since the reaction length of the anchorage set is larger than the total length of tendon. And the reaction length of the anchorage set is calculated as:

$$l_{set} = \sqrt{\frac{s \cdot E_p \cdot A_p}{a}} \tag{4.6}$$

Loss in passive ends from anchorage set is calculated as:

$$\Delta P = \frac{s \cdot E_p \cdot A_p}{l} - a \cdot l \tag{4.7}$$

With anchor set s = 4 mm, and gradient from friction loss:

$$a = {3.4kN}/{19m} = 0.179kN/m$$

the length l_{set} (=20931 mm) is longer than tendons (19000mm).

This means there are losses in both ends of tendons from anchorage set.

This gives a loss in active ends of 7.5 kN and in passive ends 0.7 kN.

The last short time loss is from elastic shortening. This loss is calculated as:

$$\Delta P = \varepsilon_{cs} \cdot E_p \cdot A_p \tag{4.8}$$

and $$\varepsilon_{cs} = \frac{\sigma_c}{2 \cdot E_c} \tag{4.9}$$

E_c is estimated to be 20000 N/mm^2.

σ_c is average stress in concrete before this loss (1.73 N/mm^2)

This gives a loss in active and passive ends of 0.85 kN.

Total short time loss in active ends is then 7.5 kN + 0.85 kN = 8.35 kN
and 3.4 kN + 0.7 kN + 0.85 kN = 4.95 kN in passive ends.

This gives an average compressive stress in concrete of 1.7 N/mm^2.

Long time losses from creep and shrinkage in the period from stressing to loading are calculated after the Norwegian Standard /9/. This gives a long time loss until 18 days after stressing of 3.1 kN.

From chapter 4.7.2, the average observed force (from load cells) in tendons is 119 kN in x-direction after stressing, and 115 kN after 18 days. Calculated short time loss and long time loss (until day 18) in active ends, is 8.35 kN + 3.1 kN = 11.45 kN. With a stressing force of 141 kN, this gives a force in tendons at start of loading of 129.55 kN. That means theoretical force is 12 % higher than observed force when loading starts. Loss from relaxation of tendons is not included in this.

This indicate that the average jacking force is about 126.5 kN (115 kN + 11.45 kN). One possible reason for the low prestressing force is that when the jacking force was reached, the wedge was set at the same time. If the force had been held constant for a short time, the friction loss would decrease, and the total force in tendons would be higher.

4.8.3 Shear

Dead load, 2.5 kN/m^2 live load, and load from prestressed tendons give a shear force in the critical section after NS 3473 /9/ of 164.8 kN/m at the column in the middle, designed as the support reaction divided to the length of critical section, d from the column. This shear force is without factors. The shear capacity after /9/ is calculated to 154.3 kN/m. This means shear reinforcement is needed, but since the failure in the slab should be in this point, shear reinforcement is skipped. The shear force calculated in the frame program, middle column strip, is 317 kN at the middle column, and moment at the same location is 216 kNm. If these forces are distributed over a section length equal to two times the width of critical section, b_w, (1672 mm after NS 3473 /9/) the shear force is 190 kN/m and the moment is 129 kNm/m. This shear force includes the load inside the critical section, i.e. it can be reduced, and be close to the shear force calculated from NS 3473 /9/. Shear capacity formula is given in chapter 3.4.1.

NS 3473 /9/ also gives possibility to include increased shear capacity due to the axial load from the prestressing. This gives an increase of shear capacity of 6 kN, with an axial force inside the critical snit from 20 tendons after short lime losses, distributed in an area of a total width of 9000 mm.

Shear capacities according to Norwegian standard, EuroCode2, ACI and AS 3600 for the tested slab calculated with live load 2.5 kN/m^2, are given in table 4-3. The shear force is calculated with dead load, 2.5 kN/m^2, and 6.5 kN/m^2 live load in an area of 9.0 x 7.5 m^2 minus an area inside the critical section. Shear force and length of critical section are also given in table 4-3.

The area of prestressed tendons is not included in the reinforcement area in equations for shear capacity.

	Length of critical section in mm.	Shear force N/mm (2.5 kN/m^2)	Shear force N/mm (6.5 kN/m^2)	Shear capacity N/mm
NS 3473	3344	164.8	244.7	154.3
EuroCode2	3232	170.3	252.8	150.0
ACI	2020	274.5	407.5	282.6
As 3600	2020	274.5	407.5	413.4

Table 4.3

It is difficult to calculate the exact shear force around the column because some of the load from tendons goes directly in to the column. If shear force is calculated as in table 4-3, it is on the safe side since the shear capacity from tendons is not included in this. The slab failure happened with a live load of 6.5 kN/m^2, and from table 4-3 it can be seen that the capacity from NS 3473 is passed with 58 percent. The capacity after AS 3600 is not passed, in EuroCode2 the capacity is passed with 68 percent and in ACI with 44 percent.

4.8.4 Deflections

It is a large problem when calculating deflection in a flat slab, to determine a representative width and stiffness of the column strip. The column width in this calculation was chosen to 1/3 of the span width. That means a 3000 mm wide column strip, including dead load and live load from 9000 mm.

The stiffness was determined under the assumption of uncracked concrete. The contribution from reinforcement and prestressing steel was neglected.

Before this test was done, a frame program was used to calculate deflection in the middle of the span in both directions and then the deflection in point II, from figure 4.2, was calculated like the sum of deflection in point I and III.

Since this slab was prestressed with distributed tendons in one direction and concentrated tendons in the other direction, a first approximation is to say that deflections in point I and point II should be equal. But point I has columns as support in both ends, and point II has spans with concentrated tendons as support in both ends.

The deflections in point II should therefore be larger than deflection in point I. The theoretical deflections for point I and III are calculated with a distributed live load of 2.5 kN/m^2.

The theoretical deflection in point I was calculated to 4.2 mm while the corresponding observed deflection was 5 mm. The theoretical deflection in point III was calculated to 4.3 mm, and the observed deflection was also here 5 mm.

The deviations can be explained by the fact that some cracking took place over the middle column, which have an influence on deflection in the middle of span.

Since the deflection in point II was set to 4.2 mm + 4.3 mm = 8.5 mm, it gives a difference of 4 mm from observed deflections, 4.5 mm.

The conclusion is that the theoretical and observed deflections seem to be in good accordance in point I and III. It is also surprising to observe that deflection in point II is equal to deflection in point I. The main reason for this is the two-way effect in the slab at the edge. The results are presented in figure 4.26.

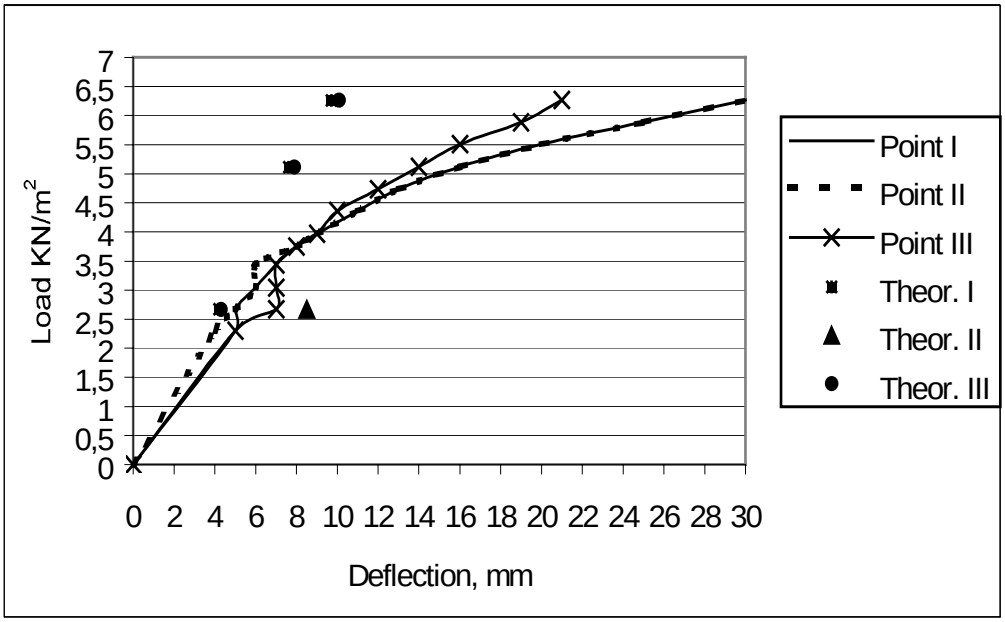

Deflection.
Figure 4.26

The theoretical deflection with a distributed load of 5 kN/m^2 is in point I 7.6 mm and with a load of 6.5 kN/m^2, 9.7 mm. In point III the theoretical deflection was calculated to 7.9 mm and 10.1 mm.

The theoretical deflections are not so close to the observed deflections as for 2.5 kN/m^2. The main reason for the large deviation, is the stiffness reduction due to of cracking.

4.9 FE analysis of prestressed flat slab

4.9.1 General

The finite element method is an advanced tool which makes it possible to find stress and strain in every point in a structure, but since there are many parameters and effects to be considered, relatively large deviations between calculated results and the test results might occur. In this test of full-scale concrete flat slab, measured values for strains and deflections are compared with results from non-linear analysis done with FEM program “Diana” release 6.1. TNO Building and Construction Research developed this program in Delft, Netherlands. The tested slab was first studied with linear analysis, non-linear analysis and finally a non-linear time dependent analysis. It has to be added that it was necessary with additional computer runs after the test was done, to bring the calculated results closer to measured results. This was done by a parameter study with realistic parameter variation.

The slab is symmetric in both directions, so only one quart of the slab has to be analysed, see fig 4.27.

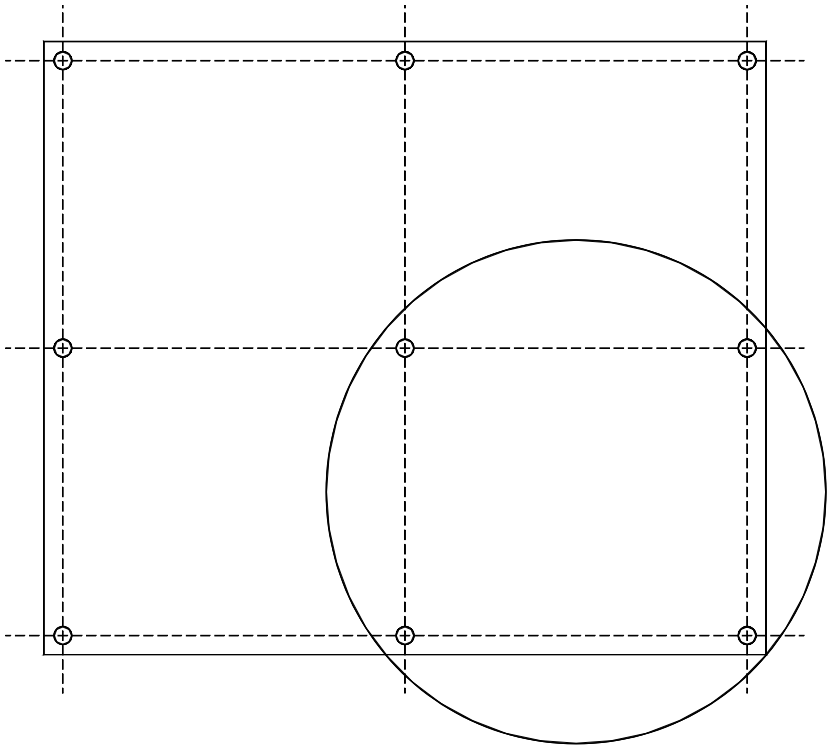

Analysed part of slab.
Figure 4.27

4.9.2 Element model and material parameters

Since prestressed concrete slabs are subjected to both bending and membrane forces, a rectangular shell element Q20SH /52/ was selected to model the concrete. This is a four-node quadrilateral isoparametric curved shell element based on linear interpolation and Gauss integration over the element area. Number of integration points over the element area is 2 x 2, and 7 points in slab thickness.

The Cauchy stress in the integration points is given as:

$$\sigma = \begin{Bmatrix} \sigma_{xx} \\ \sigma_{yy} \\ \sigma_{zz} = 0 \\ \sigma_{xy} = \sigma_{yx} \\ \sigma_{yz} = \sigma_{zy} \\ \sigma_{zx} = \sigma_{xz} \end{Bmatrix} \tag{4.10}$$

Figure 4.28 shows these stresses on a unit cube in their positive direction.

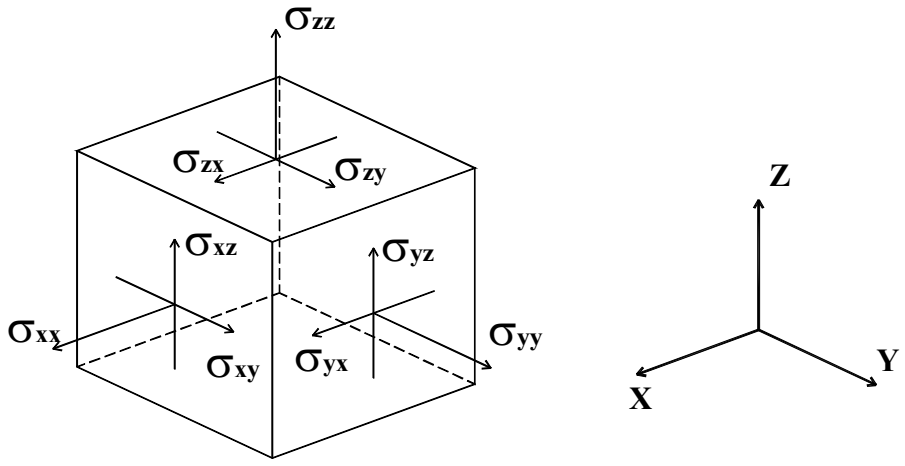

Cauchy stresses.
Figure 4.28

From the basic stresses DIANA can derive the bending moments ***m*** and forces ***f*** as:

$$m = \begin{Bmatrix} m_{xx} \\ m_{yy} \\ m_{xy} = m_{yx} \end{Bmatrix} \qquad f = \begin{Bmatrix} n_{xx} \\ n_{yy} \\ n_{xy} = n_{yx} \\ q_{xz} \\ q_{yz} \end{Bmatrix} \tag{4.11}$$

Figure 4.29 shows these moments and forces on the infinitesimal part dx dy in their positive direction.

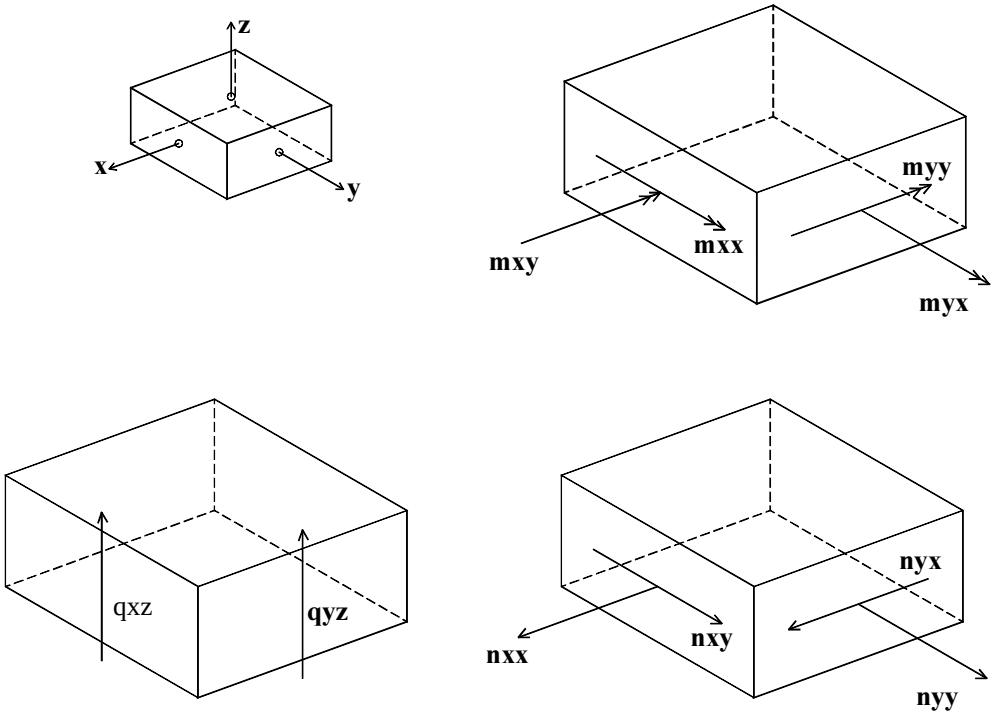

Moments and forces.
Figure 4.29

Typical for the rectangular Q20SH element is that the strain ε_{xx}, the curvature κ_{xx}, the moment m_{xx}, the membrane force n_{xx}, and the shear force q_{xz} are constant in x-direction and vary linearly in y-direction. The strain ε_{yy}, the curvature κ_{yy}, the moment m_{yy}, the membrane force n_{yy}, and the shear force q_{yz} are constant in y-direction and vary linearly in x-direction.

The reinforcement is modelled as a grid. Prestressed tendons are also given in a grid, as illustrated in figure 4.30.

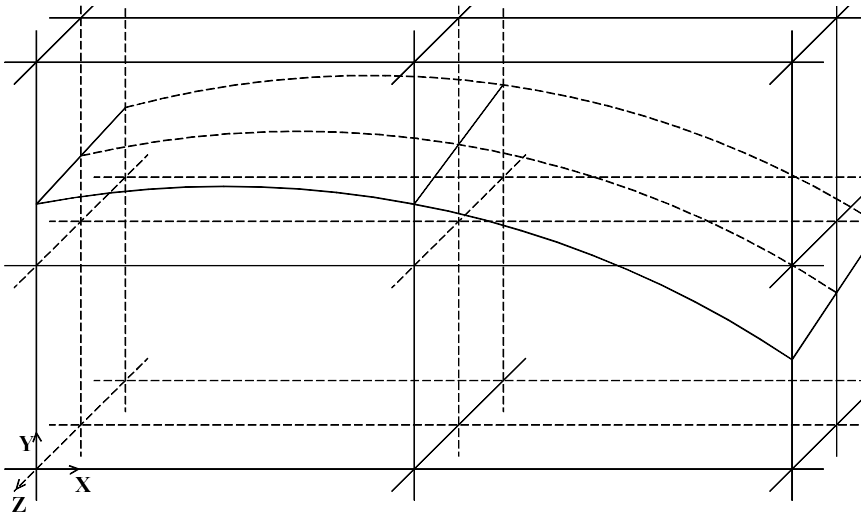

Grid from prestressed tendons in an element.
Figure 4.30

Small elements in the areas around the supports and larger elements in the other areas have been selected to improve the accuracy of the solution in the critical region with reasonable computational effort, see figure 4.31. The smallest element is 250 mm x 250 mm, and the largest element is 1500 mm x 1250 mm.

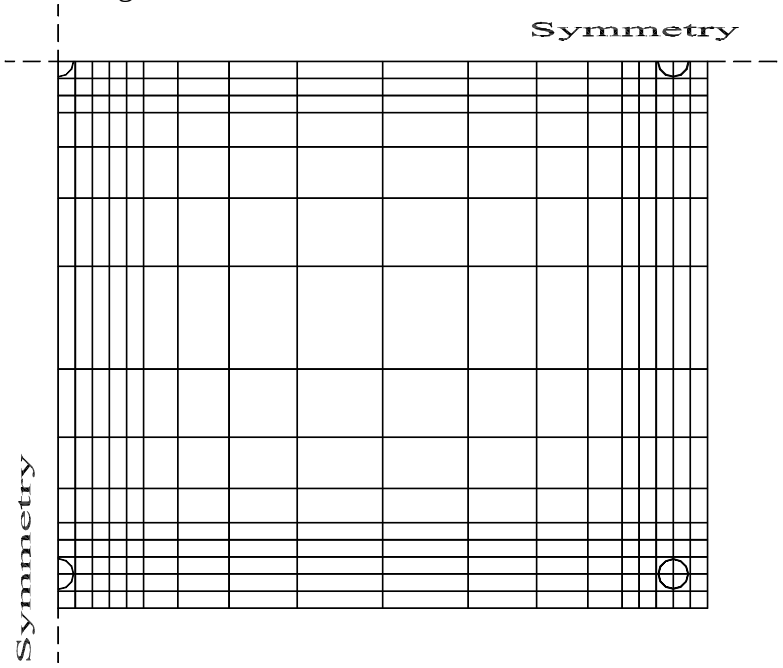

Mesh in finite element analysis from ¼ of the slab.
Figure 4.31

The loads are self-weight, prestressing force and distributed load. Prestressing force is defined as a distributed force along the outer edge of the slab, where the tendons are located. The command “nobond” is used to indicate that the reinforcement is not bonded to the mother element. The input syntax of prestress depend on the reinforcement type, bar or grid, and it is specified explicitly as initial stress. Start point, inflection points and end point of grid, has to be specified.

If only one value for each stress component is given, the stress distribution is uniform, constant (stress along the tendon) if not, it is necessary to specify stress for each stress component in each element node.

Two separate types of analyses were carried out, long time analysis from casting until loading and short time analysis from loading to failure.
In the long time analysis the creep and shrinkage model for the European CEB-FIP Model Code 1990 is used. The solution method is based on linear viscoelasticity with aging effects and this method is equivalent to the principle of linear superposition.

The most important material parameters are presented in table 4.4.

The modulus of elasticity calculated after NS 3473 /9/ is 25800 N/mm^2 after 28 days, but since this test were done earlier than 28 days after casting, it was reduced to 23600 N/mm^2. To model cracking, constant stress cut off was chosen, a crack arises if the major principal tensile stress exceeds f_t. This value was set equal 2.4 N/mm^2 in the first analysis. One of the tension softening models in this analysis, is shown in figure 4.32 a. This is a model with a linear descending branch where ε_u is the ultimate strain in the x-direction of the diagram and f_t is the tensile strength in y-direction for reinforced concrete. The DIANA manual recommends /52/:

$$\varepsilon_u = \sigma_{y,steel} / E_{steel} \qquad (4.12)$$

In the analysis done after the failure test, the bilinear tension softening model was used in an area outside 2500 x 2500 mm^2 around the column in the middle.

This is done because there is large concentration of reinforcement around the column in the middle, and this gives different stiffness and crack distribution than in other part of the slab.

To describe the yield surface for reinforcement and prestressed tendons Von Mises' model was chosen. The yield stress in reinforcement was set to 500 N/mm^2 and in tendons 1670 N/mm^2. It is possible to include calculation of prestressing loss in this FE program, but in this case the prestressing force was reduced to 120 kN, which means losses in prestressing are 15%. This reduction of prestressing force is a normal estimate, and in this test the measured average prestressing force was 119 kN after stressing, and 115 kN when loading starts.

Material parameters and geometry are completely described in appendix A.

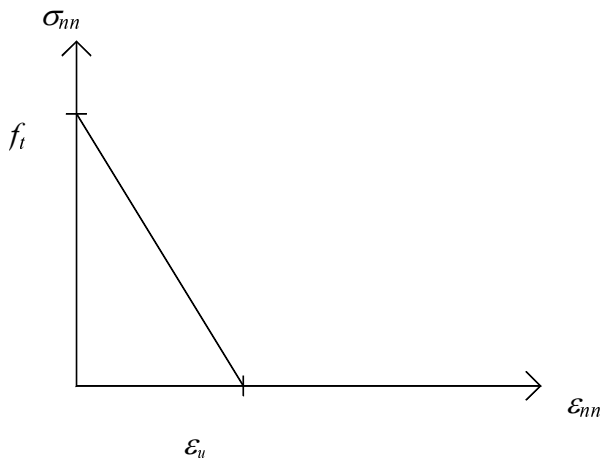

Tension softening- smeared cracks, linear relation.
Figure 4.32 a

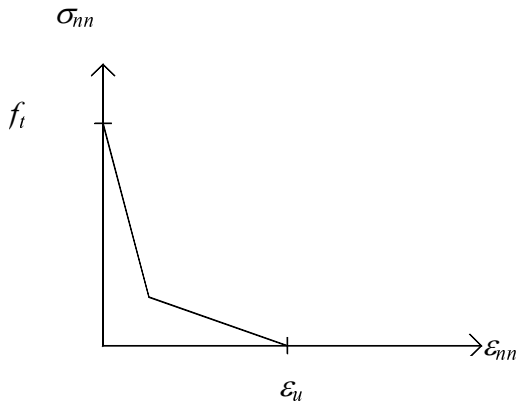

Tension softening- smeared cracks, bilinear relation.
Figure 4.32 b

Some of the input data used in FE analysis are shown in table 4.4 and in appendix A.

Modulus of elasticity concrete	23600 N/mm^2
Modulus of elasticity reinforcement	200000 N/mm^2
Modulus of elasticity prestressed tendons	196000 N/mm^2
Poisons ratio	0.2 (concrete, reinforcement, tendons)
Yield value reinforcement	500 N/mm^2
Yield value tendons	1670 N/mm^2
Prestr 1200.0 0.0	Prestressing force after loss. 1200 N/mm^2 in x-direction and 0 N/mm^2 in y-direction.
Prestr 0.0 1200.0	Prestressing force after loss. 0 N/mm^2 in y-direction and 1200 N/mm^2 in x-direction.

Some material parameters used in analysis.
Table 4.4

4.9.3 Long time analysis

Observed strains and strains from the finite element analysis are plotted in figure 4.33-4.39 for point 2, 3, 4, 5, 6, 7 and 8. The start for this plot is 120 hours after casting, which means before prestressing start. Two sets of analyses are carried out “FEM-1” where cracking is neglected, and «FEM-2 where the linear tension softening model is used to describe the post cracking behaviour.

In measured points outside the middle column, observed strain and strain calculated with FE analysis are in good accordance, but around the middle column there are some deviations between measured and calculated strains as shown in the figures under. This can partly be explained by:
In the finite element analysis the self-weight of the slab is loaded in steps, but in “real life” it is loaded faster, and in this test there are strain gauges only at one side of the reinforcement. If strain gauges were glued to both sides of reinforcement, an average strain will possibly give a more correct result.

Figure 4.40 a-e shows measured and calculated (FEM-2) strains distribution across the slab thickness before loading. These figures show that deviations in strain in point 2, 4, 5 and 7 are relatively small, and that the largest deviations are in point 8. The reasons for the deviations are further discussed in the subsequent chapter 4.9.4.

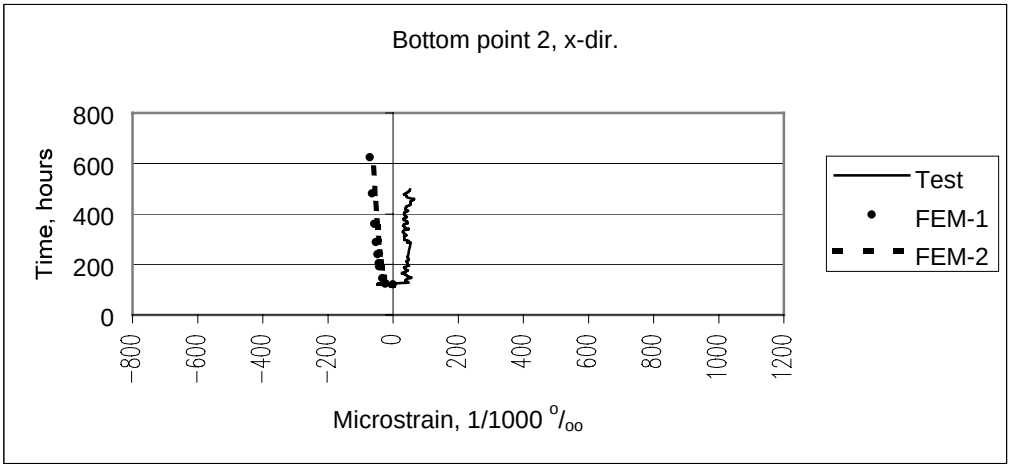

Strain from FE analysis and observed strain in point 2.
Figure 4.33

Point 2 is located in the middle of span in x-direction and close to the edge in the other direction. Strains from test and analysis are close until the form is removed. After that there is a small tensile strain in this point.

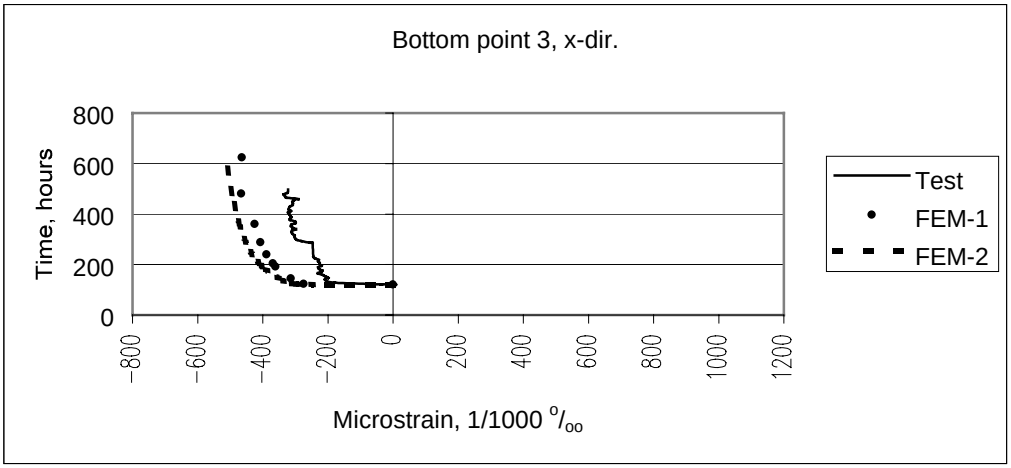

Strain from FE analysis and observed strain in point 3
Figure 4.34a

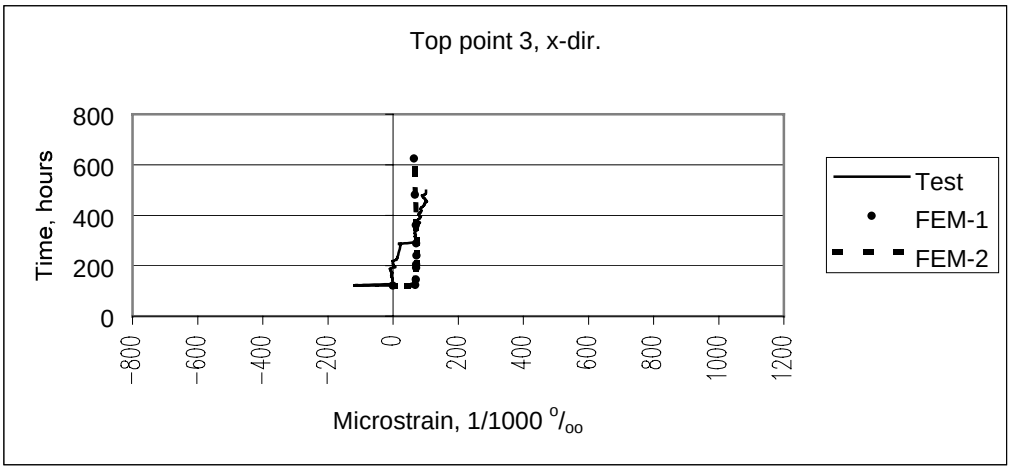

Strain from FE analysis and observed strain in point 3.
Figure 4.34 b

Strain in x-direction in point 3, located over the middle column in x-direction and end column in y-direction, is shown in figure 4.34 a and b. There is some higher compressive strain in the bottom from FE analysis than in test. But in top of the slab, strains are close.

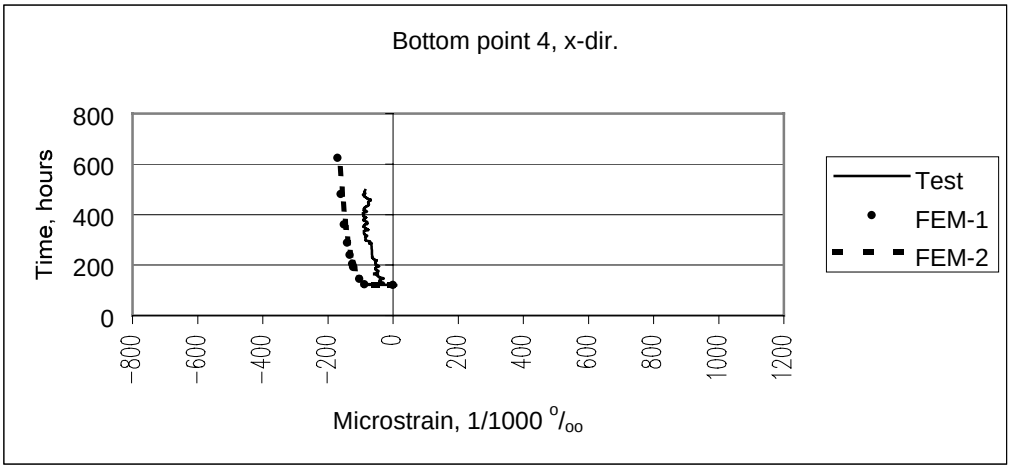

Strain from FE analysis and observed strain in point 4.
Figure 4.35 a

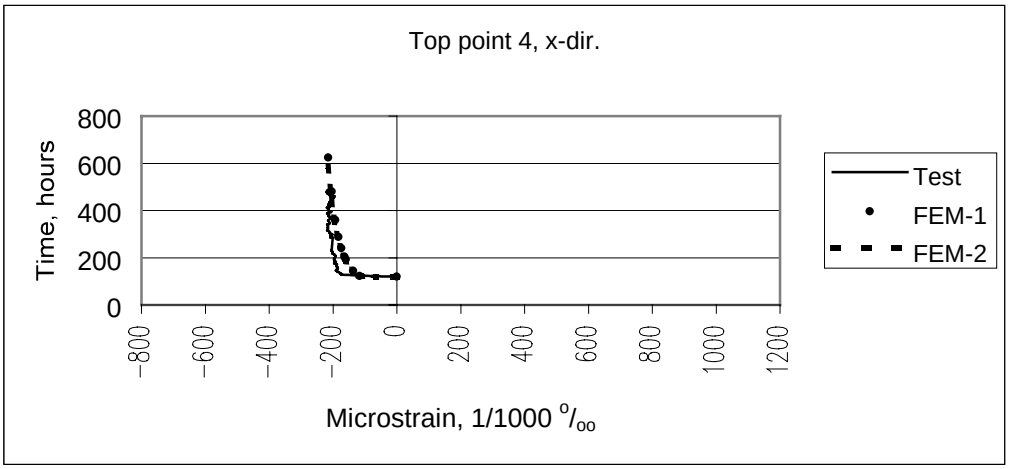

Strain from FE analysis and observed strain in point 4.
Figure 4.35 b

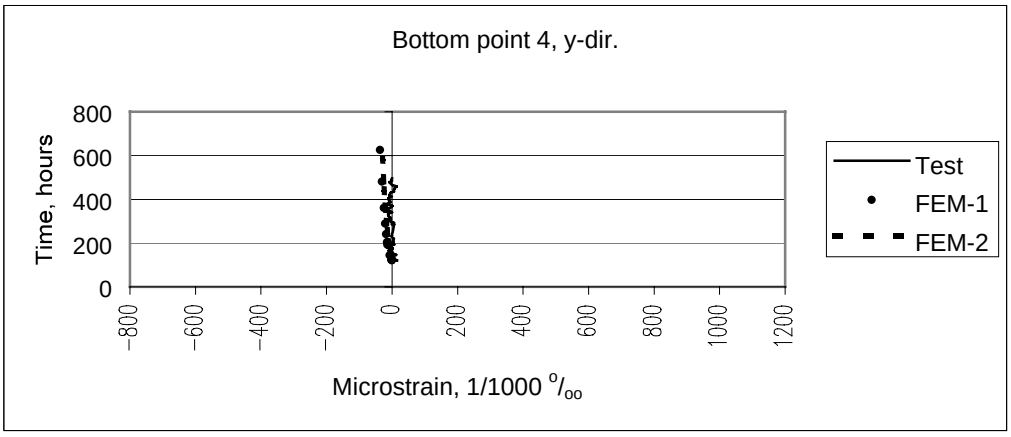

Strain from FE analysis and observed strain in point 4.
Figure 4.35 c

Point 4 is located in the middle of span in x- and y-direction, and the measured strain is plotted in figure 4.35 a and b. In figure 4.35 c, strain in the bottom in y-direction is plotted.
In figure 4.35 a it can be seen that observed strain and strain from FE analysis are very close from start at 120 hours and until the first time step at 122.4 hours. After this time the observed strain increases from –85 microstrain to –30 microstrain. After this time the development of observed strain is about the same as strain from FE analysis.

In figure 4.35 b it can be seen that observed strain and strain calculated with FE analysis are in good accordance. Figure 4.35 c shows that in this point there are only small strains in y-direction.

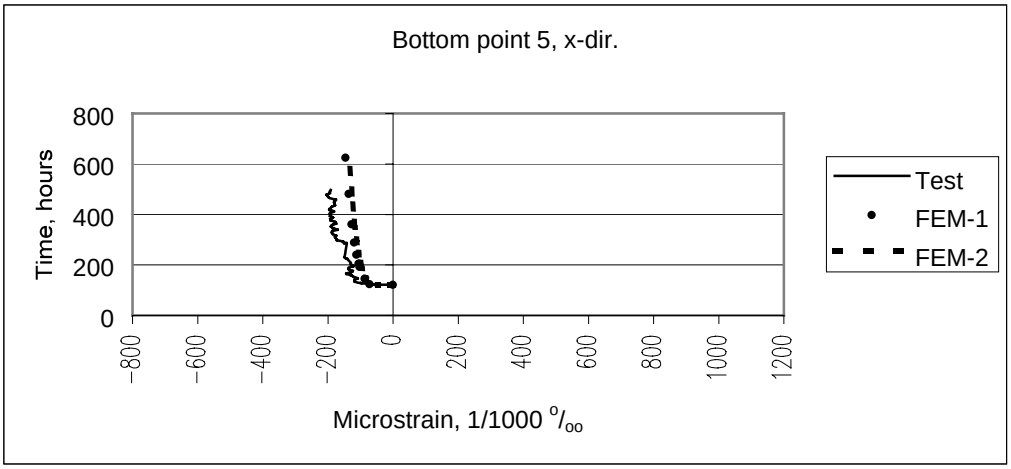

Strain from FE analysis and observed strain in point 5.
Figure 4.36 a

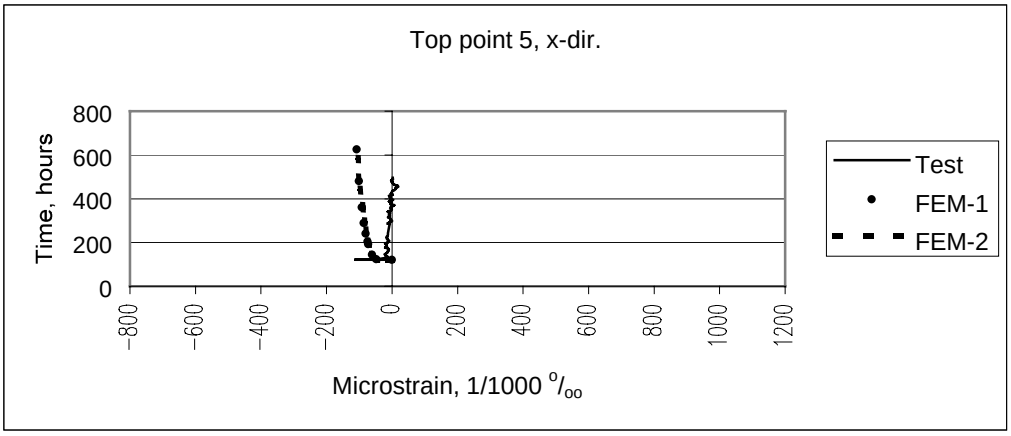

Strain from FE analysis and observed strain in point 5.
Figure 4.36 b

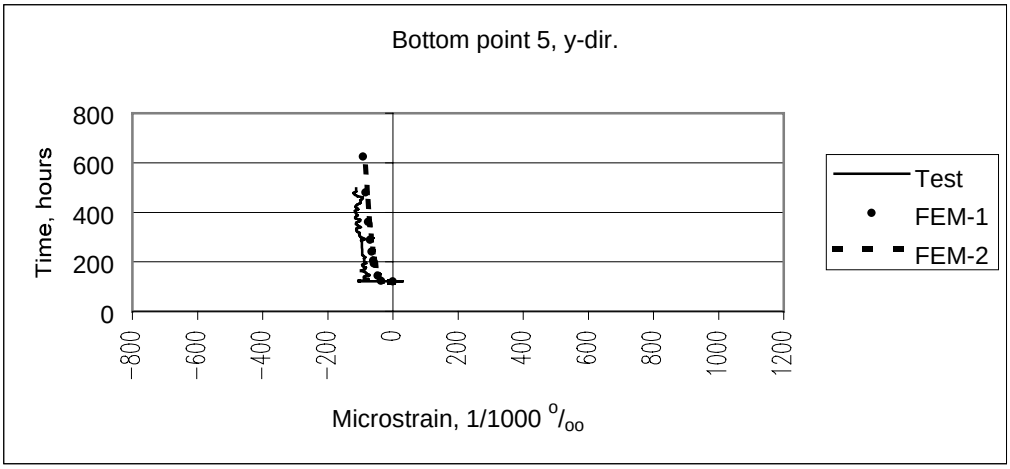

Strain from FE analysis and observed strain in point 5.
Figure 4.36 c

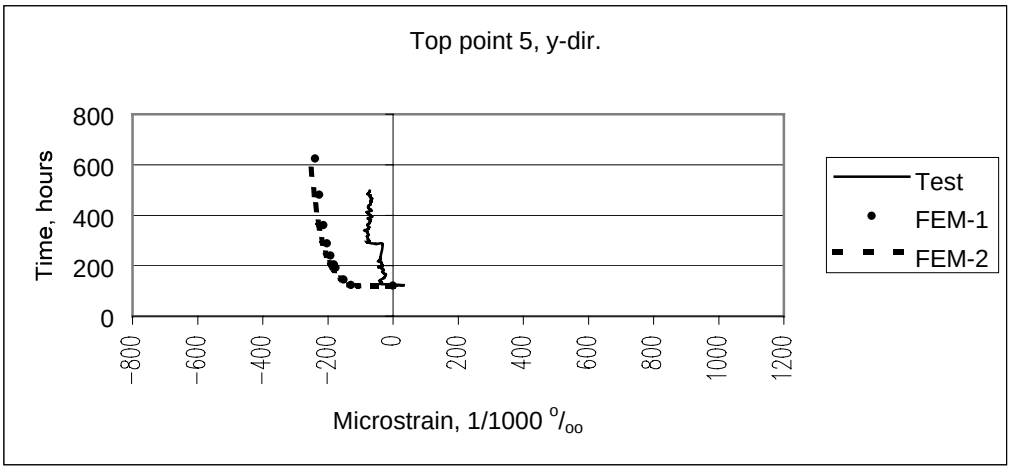

Strain from FE analysis and observed strain in point 5.
Figure 4.36 d

Point 5 is located in the middle of the span in y-direction in the middle column strip. Figure 4.36 a and b show strains parallel to the distributed tendons and figure 4.36 c and d show strains parallel to the concentrated tendons. Development of observed and calculated strain in the bottom of slab in x- and y-direction are almost equal in this point, but in the top in x-direction, the observed strain decreases from start of the prestressing, and then it increases when the form is removed. Figure 4.36 d shows a larger deviation between results from test and analysis.

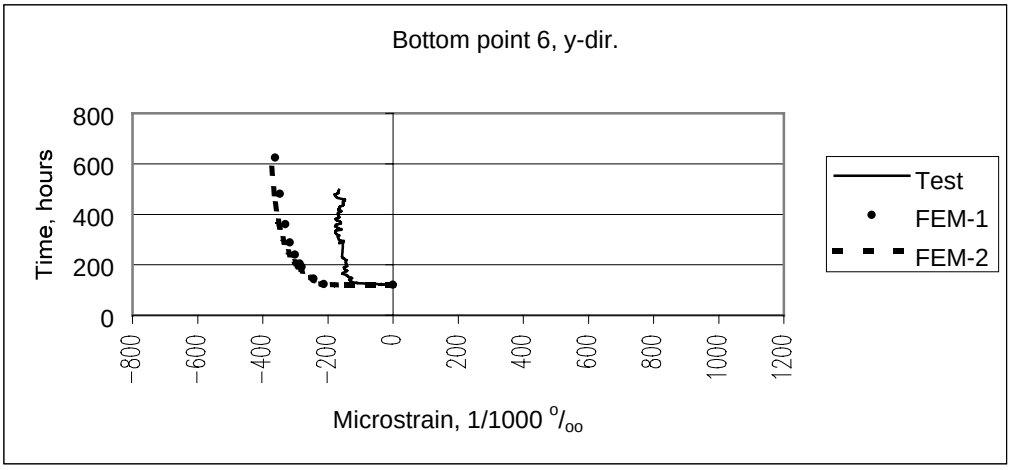

Strain from FE analysis and observed strain in point 6.
Figure 4.37 a

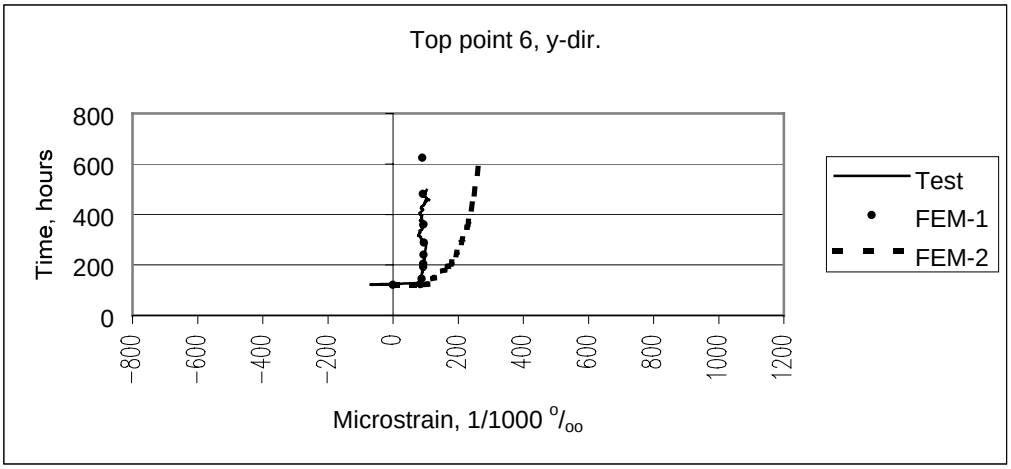

Strain from FE analysis and observed strain in point 6.
Figure 4.37 b

Point 6 is located over the middle column in y-direction and end column in x-direction. Figure 4.37 a and b show strain in y-direction in this point, and figure a shows that analysis gives a higher compressive strain than observed in the bottom. Observed strain and results from the first analysis are close in the top of the slab, in this point. Strain in the last analysis is higher in this point.

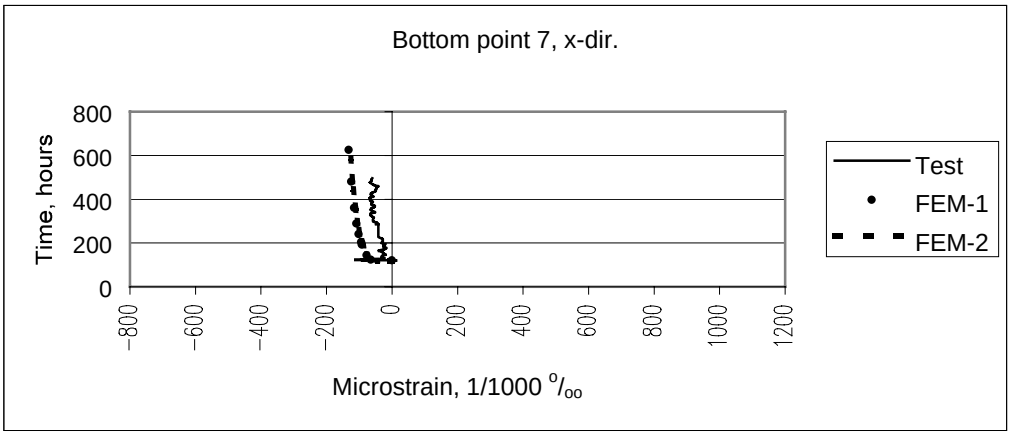

Strain from FE analysis and observed strain in point 7.
Figure 4.38 a

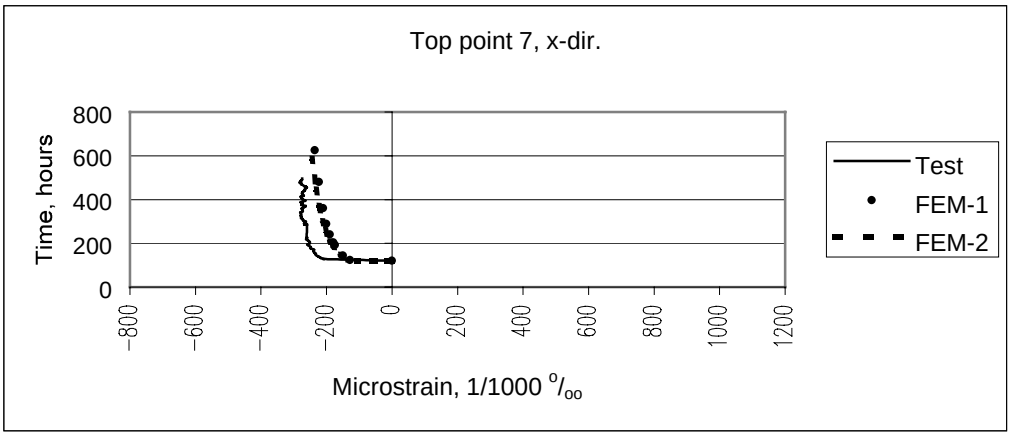

Strain from FE analysis and observed strain in point 7.
Figure 4.38 b

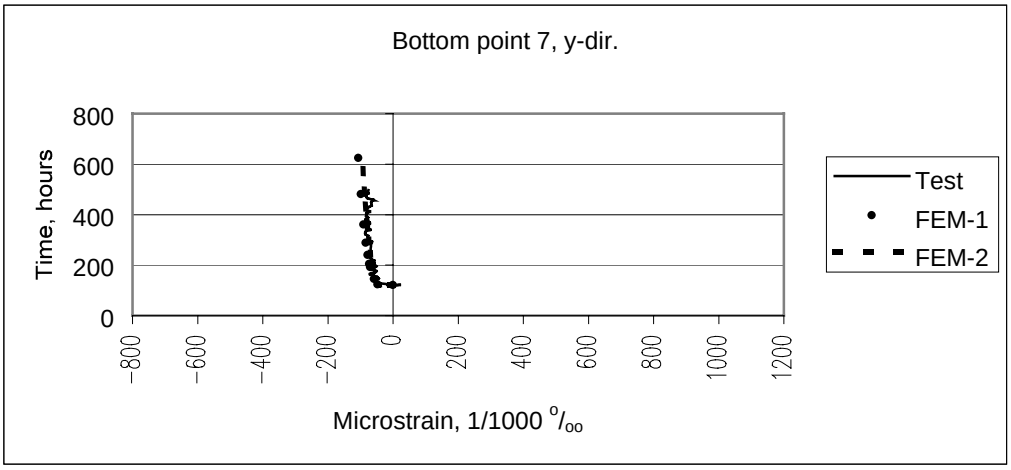

Strain from FE analysis and observed strain in point 7.
Figure 4.38 c

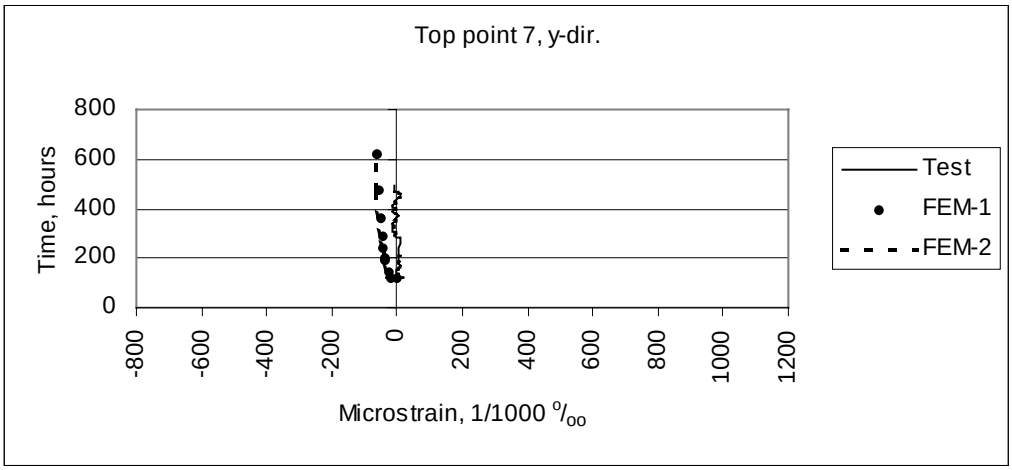

Strain from FE analysis and observed strain in point 7.
Figure 4.38 d

Point 7 is located in the middle of span in x-direction ("column strip"). Observed strain in the bottom has the same development as in point 4 with an increase of strain after removing the form. This shows that development of strains in a flat slab are approximately equal in the span, independent of "column strip" in x-direction as long as the tendons are distributed in this direction.
After this, the observed strain and strain calculated with FEM have the same development, but strain from analysis is somewhat lower than observed strain. Observed strain and strain from FE analysis in the top of point 7, x-direction, develop similarly, but observed strain is lower than strain from analysis.
In figure 4.38 c it can be seen that strain from analysis and test are close, and figure 4.38 d shows that strain in y-direction at the top of the slab, is negligible.

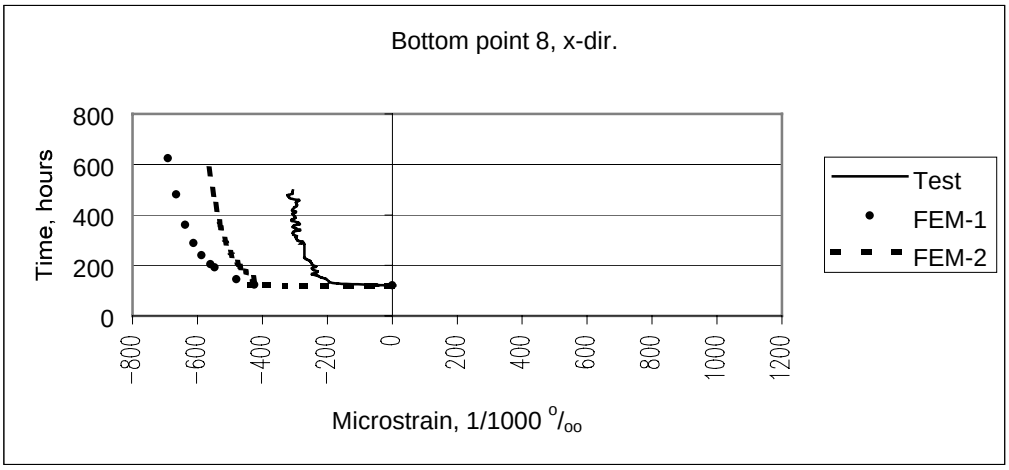

Strain from FE analysis and observed strain in point 8.
Figure 4.39 a

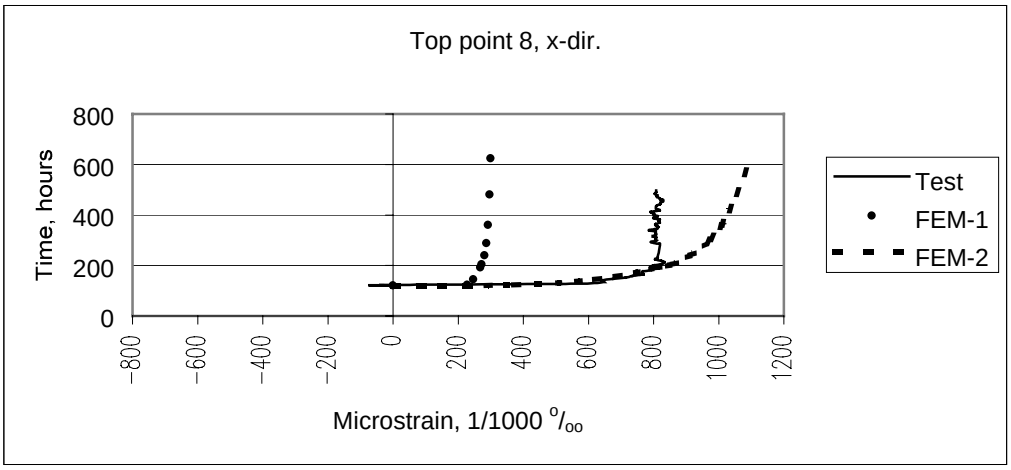

Strain from FE analysis and observed strain in point 8.
Figure 4.39 b

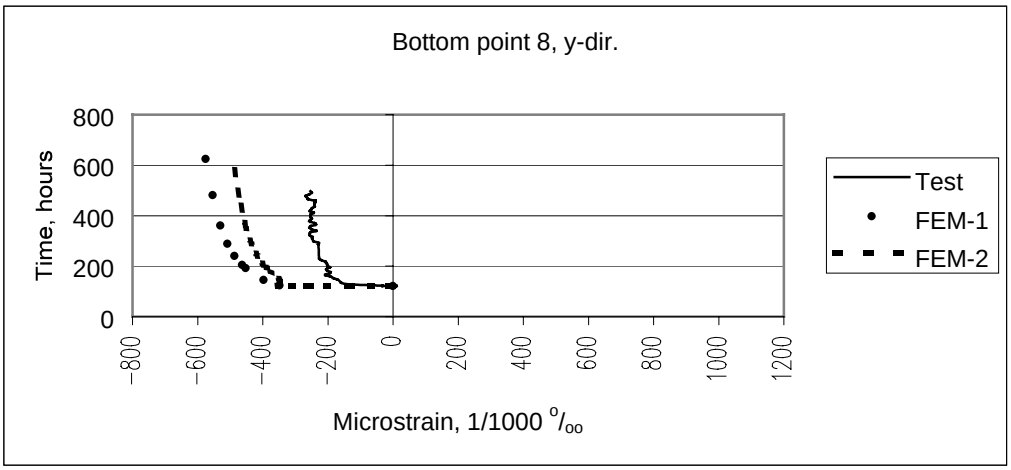

Strain from FE analysis and observed strain in point 8.
Figure 4.39 c

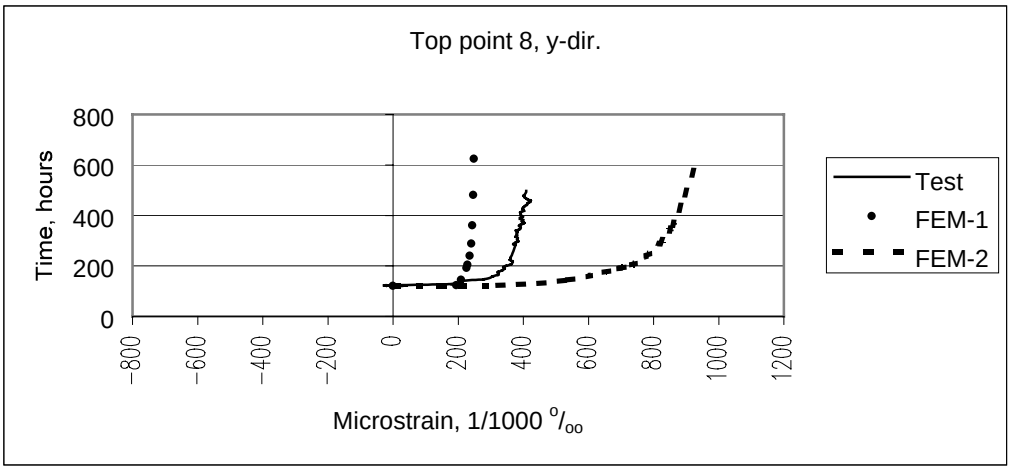

Strain from FE analysis and observed strain in point 8.
Figure 4.39 d

Point 8 is located in the middle of the slab, over the middle column. The highest strains were expected in this area. Since cracking starts around the middle column, deviation between the two analyses was expected. The largest deviations are in the top, figure 4.39 b and d, but also in the bottom in the analysis that takes care of crack, it is closer to the observed strain. From figure 4.39 b and d it can be seen that the observed tensile strain is somewhat higher than calculated strain from the first FE analysis and lower than the last FE analysis.
The amount of reinforcement in this point can have an effect of the result.

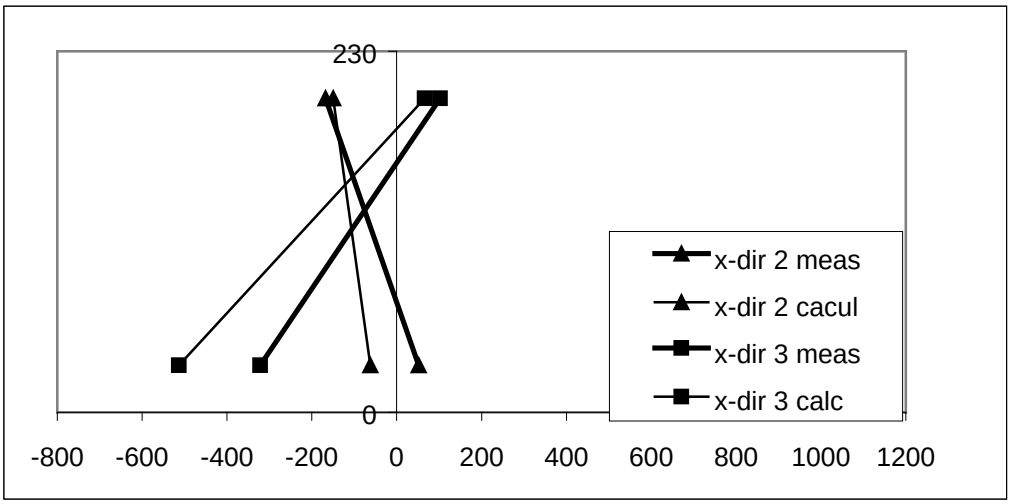

Measured and calculated strain distribution across the slab thickness,
x-direction point 2 and 3.
Figure 4.40 a

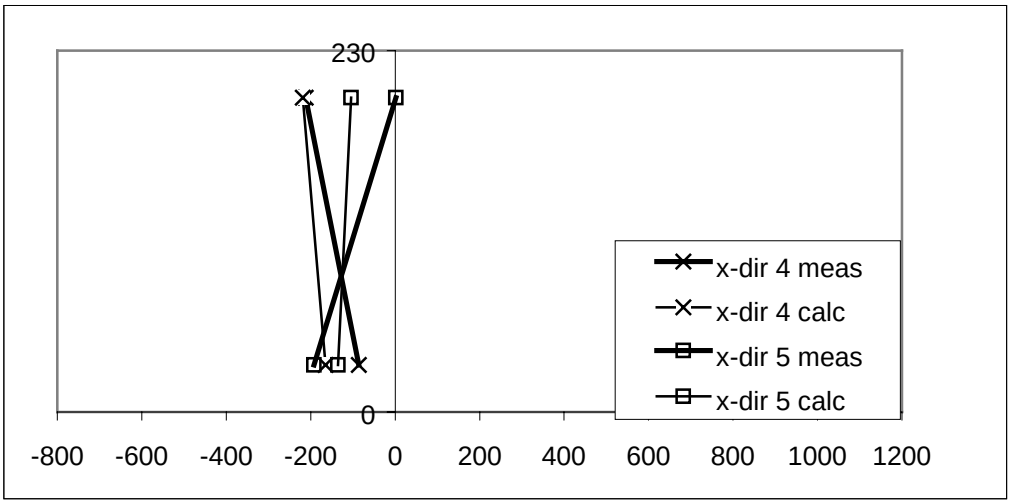

Measured and calculated strain distribution across the slab thickness,
x-direction point 4 and 5.
Figure 4.40 b

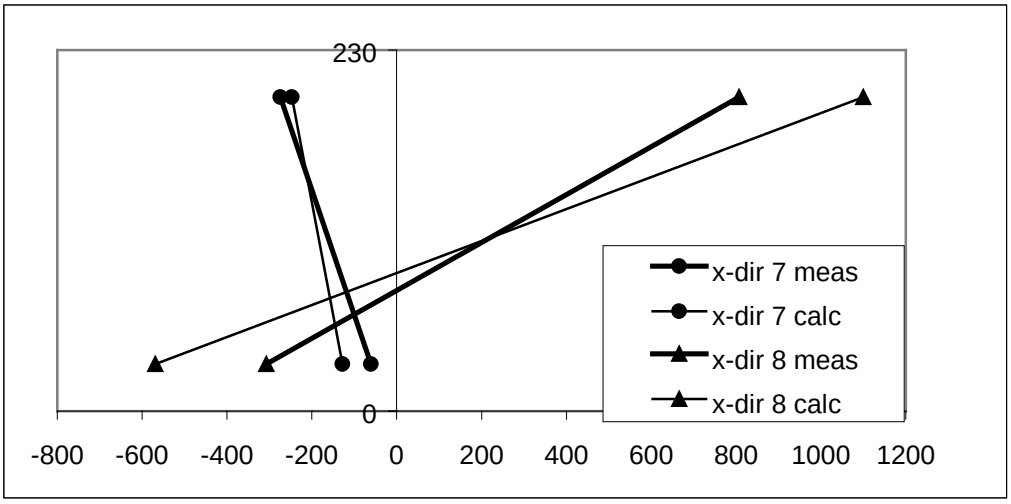

Measured and calculated strain distribution across the slab thickness,
x-direction point 7 and 8.
Figure 4.40 c

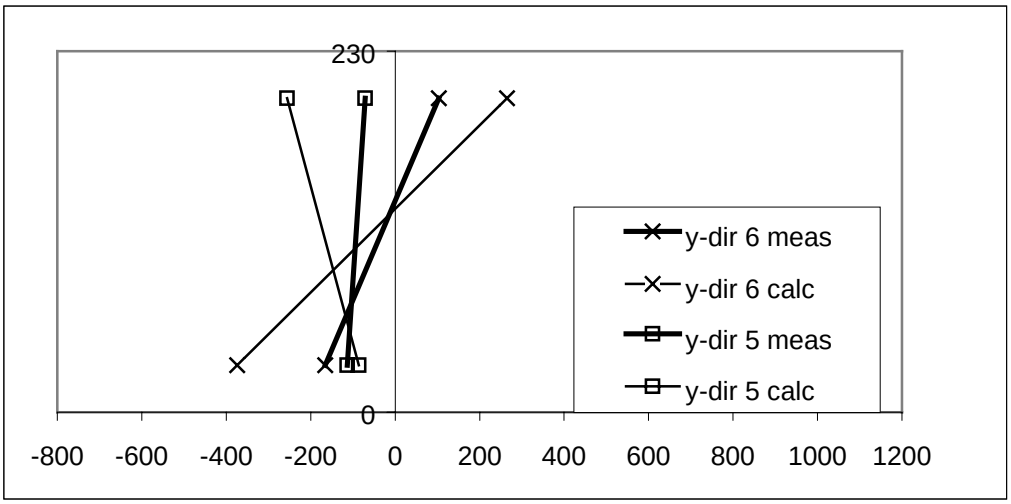

Measured and calculated strain distribution across the slab thickness,
y-direction point 5 and 6.
Figure 4.40 d

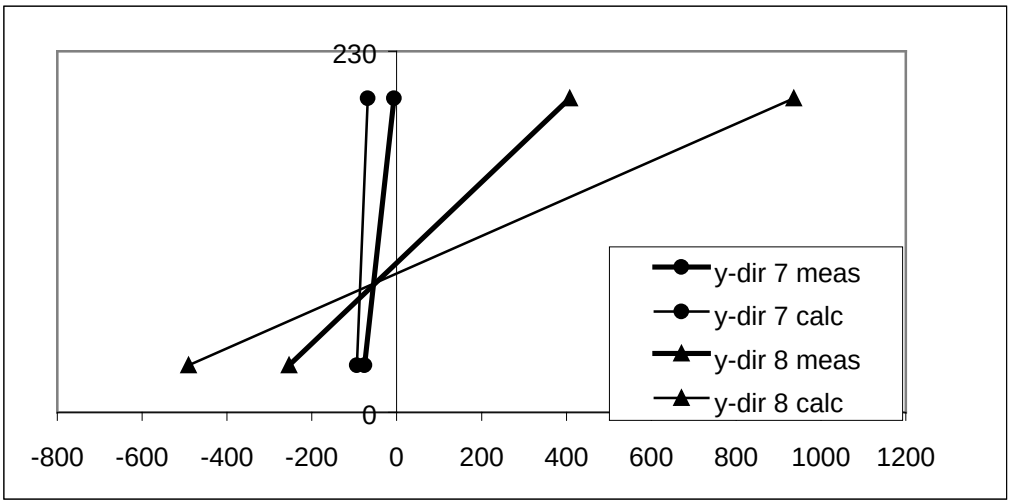

Measured and calculated strain distribution across the slab thickness,
y-direction point 7 and 8.
Figure 4.40 e

4.9.4 Discussions of long time results

In the long time analysis load from self-weight and prestressing are included.

Figures 4.33-4.39 show that development of the theoretical strain in the slab deviates somewhat from observed strain. The strains are relatively small since balanced load is pursued. Some cracks can have occurred when the tendons are stressed, see for instance the strains in point 3, 6 and 8.

Some reasons for the deviation between theoretical and observed stress can be:

- The loading from the tendons is not applied proportionally since all the distributed tendons are stressed 100 % before the tendons in the other direction. It is possible that stressing in two operations, all tendons stressed to 40-50 % of total prestressing force, and then 100 % stressing, give better results with more distributed prestressing force.
- Figures 4.33-4.39 show that some strain plots from test have a jump when the form is removed. This jump is not in the analysis, and the reason for this might be that self weight in analysis is loaded gradually together with the prestressing until all load is active. In practice the load from self-weight will be loaded step by step when the form is removed, and results in a local jump in strain.
- A general comparison between observed strain and strain from analyses shows that measured strain and strain from analysis are close, except over the middle column, see figure 4.40. In this point analysis gives a higher tensile strain in top and lower compressive strain in bottom than measured strains, with largest deviation in y-direction (column strip).
- Only one element type was used in this analysis. Other element types, mesh size or crack models can be used, with maybe some closer results, but certainly it does not fully explain the deviations.

- Deviation from theoretical jacking force and parabola of tendon, has also an effect on strain in the slab. To see the result of this, the jacking force is reduced to 115 kN (indicated in chapter 4.8.2) and a new analysis is done. Figure 4.46a shows strain in point 4, bottom in x-direction, and figure 4.46 b shows strain in point 8, y-direction in top of the slab. Reduced jacking force (115 kN) and 5 mm "wrong" tendon profile in the bottom give results as shown in the same figure. "Test" is observed strain, "115-kN" is strain with reduced prestressing force to 115 kN and "tendon" is strain with reduced prestressing force and 5 mm higher tendon in the bottom of slab than described.
- When the slab is calculated, it is assumed no crack from self-weight and prestressed tendons. From the strain gauges, it is possible to see that crack occur before the slab is loaded by live load. That means that moment over the middle column is higher than calculated, and minimum reinforcement can be more important than first assumed.

In a test like this, there will always be a question about accuracy in the observed results. A possible improvement is to use strain gauges on both sides of reinforcement to get an average strain.

4.9.5 Failure test

In figure 4.41 – 4.45 calculated and observed load/deflection and load/strain-curves are plotted. After the failure test was done, some additional analyses were done to improve the agreement between theory and experiment as explained previously in chapter 4.9.2.

As shown in the load/strain-curves, there are some deviations between FE analysis and observed strains. Some of this effect can be explained by the FE analysis' disregarding of the time-dependent effect in the concrete. Strains in point 7 in x-direction are almost equal to strains in point 4, x-direction. This indicates that a slab-direction develops similarly in the whole length, independent of "column" strip in this direction. Observed strain in the bottom compared with strains from the finite element analysis shows that use of two different tension softening models give closer agreement to the observed strains than one model for the whole slab.

As in x-direction observed strains in y-direction are somewhat lower than strain from FE analysis in the top. The reason for this can be as in the other direction: strain depends on location of measure point in test slab and measure point in FE model. Two different tension softening models (fem3-1) give results closer to the observed strain than one model does in point 4, 5 and 7.

Deflection from the first FE analysis and observed deflection from tests are plotted in figure 4.41 a, b and c.

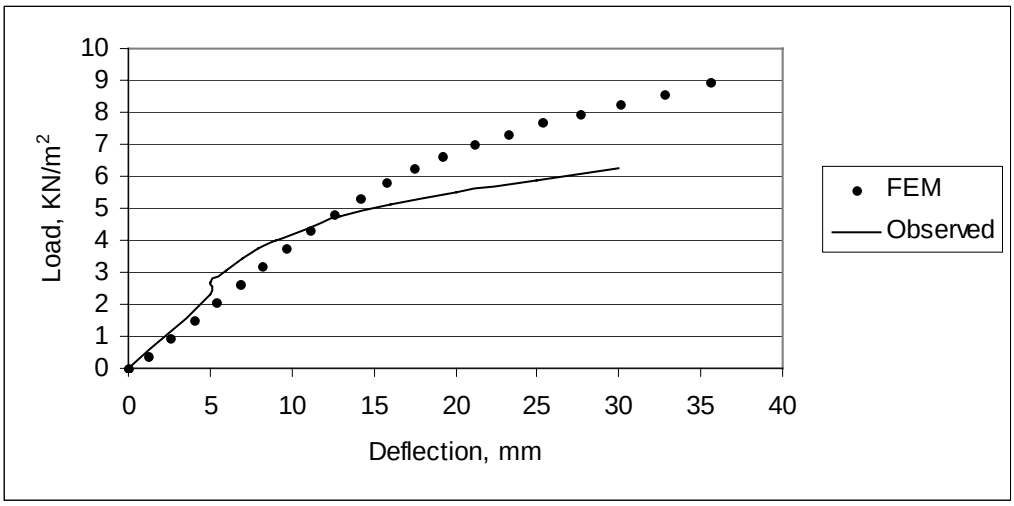

Deflections in point I.
Figure 4.41 a

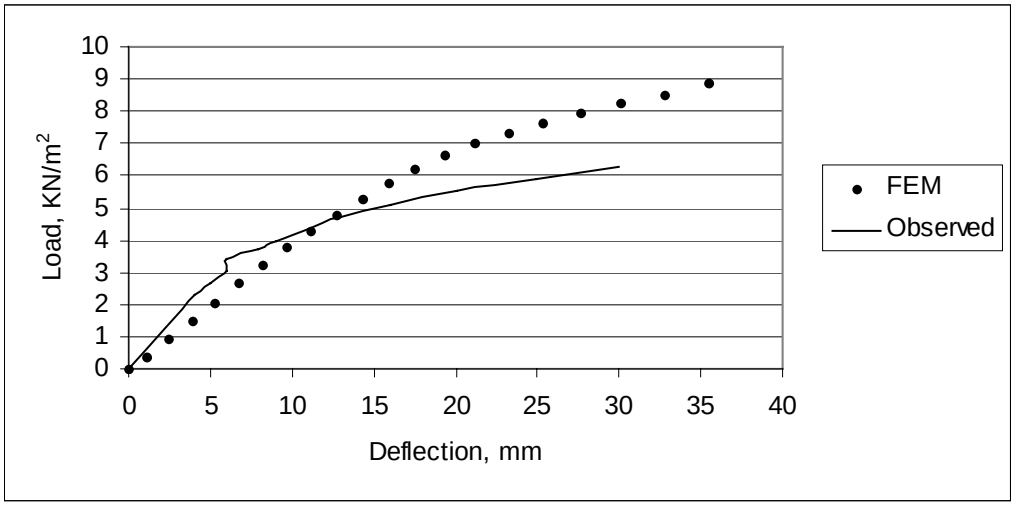

Deflections in point II.
Figure 4.41 b

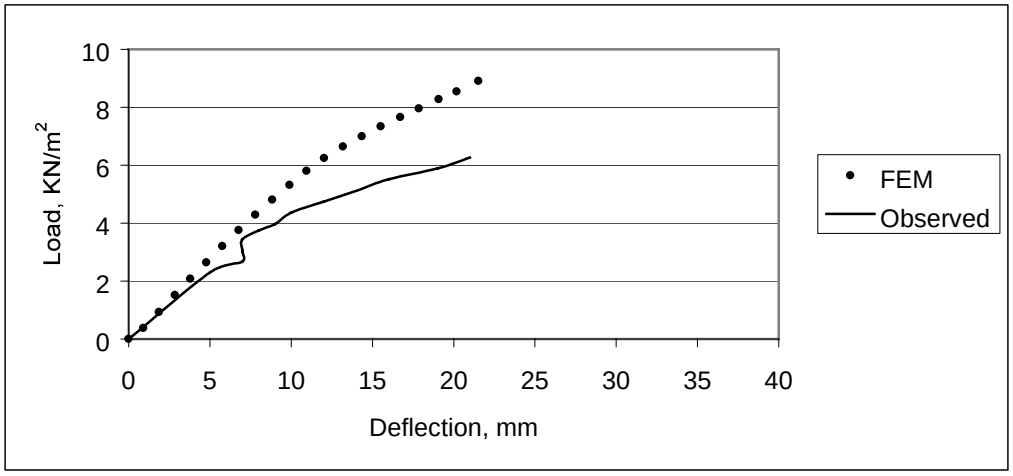

Deflections in point III.
Figure 4.41 c

Load-deflection curves are good indicators of the ability of the numerical simulations to describe the global response of a structure. The calculated deflections are in close agreement with the observed deflections until a load of 4.5-5 kN/m^2. At this time the observed deflections increase compared to the deflections calculated with FE analysis. The reason for this can be that cracks developed around the middle column and in point 4, 5 and 7, at this stage, and these cracks also have an influence on deflections in the span.

Figures 4.42-4.45 show comparisons between measured and calculated reinforcement strains in point 4, 5, 7 and 8 from figure 4.2. These four points are the most interesting locations to control in the slab, and since the other points have less strains, they are not commented any more here. Strains in these points are given in appendix A.

In figures 4.42-4.45 strains from the finite element analysis done before the failure test, are marked with “FEM”. After the failure test was done, some new analyses were done and the results from two of these are marked with fem3-1 and fem2-2. In fem3-1 the concrete tensile strength “CRKVAL” is 1.0 N/mm^2 outside an area of 2500 x 2500 mm^2 around the middle column, and inside this area the tensile strength is 3.0 N/mm^2. In fem2-2 the concrete tensile strength is constant throughout the slab, and equal to 2.0 N/mm^2. In the analysis done before test, a linear stress-strain relation was used after cracking, and in the two last analyses a bilinear relation was used, see figure 4.32 a and b. The other parameters are equal for these two analyses and they are given in appendix A.

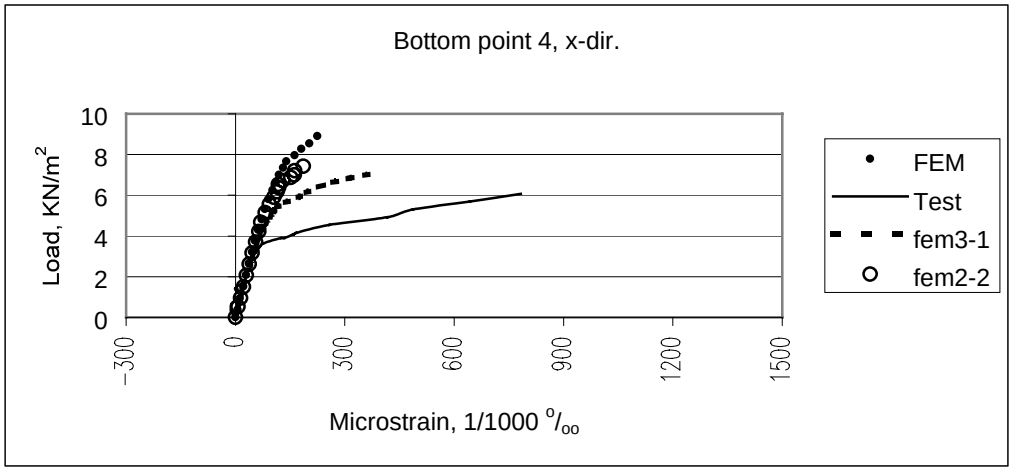

Strain from FE analysis and observed strain in point 4.
Figure 4.42 a

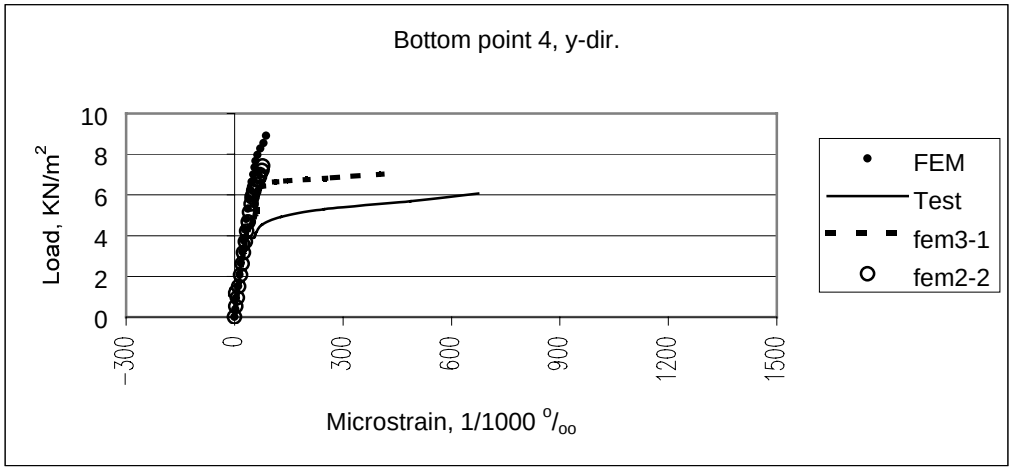

Strain from FE analysis and observed strain in point 4.
Figure 4.42 b

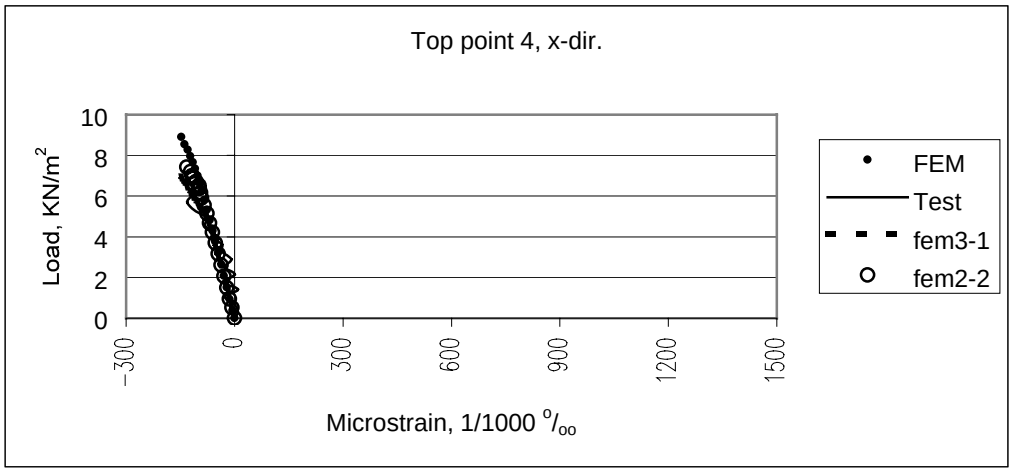

Strain from FE analysis and observed strain in point 4.
Figure 4.42 c

As for the deflection, the calculated strains in point 4 are in close agreement with the observed strain until a load of about 4.0 kN/m^2. From the time the concrete starts

cracking, the observed strain in reinforcement increases more than the strain from analysis.

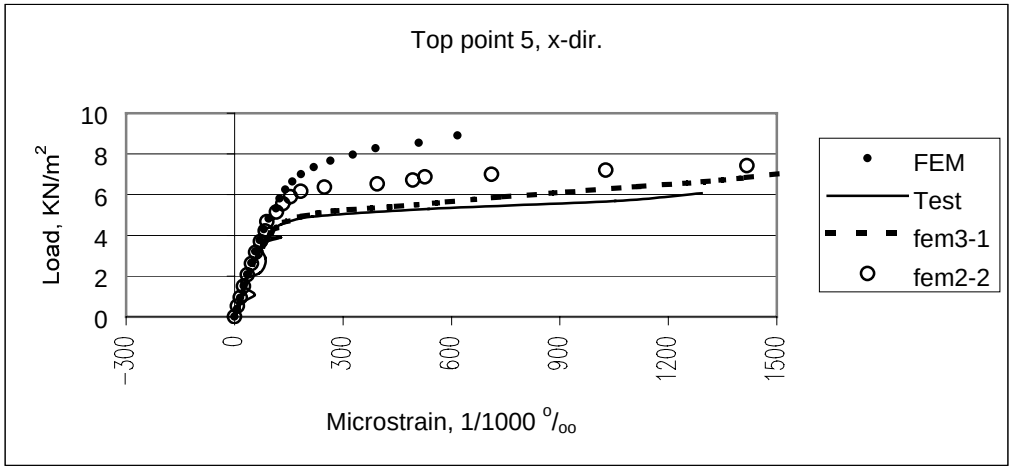

Strain from FE analysis and observed strain in point 5.
Figure 4.43 a

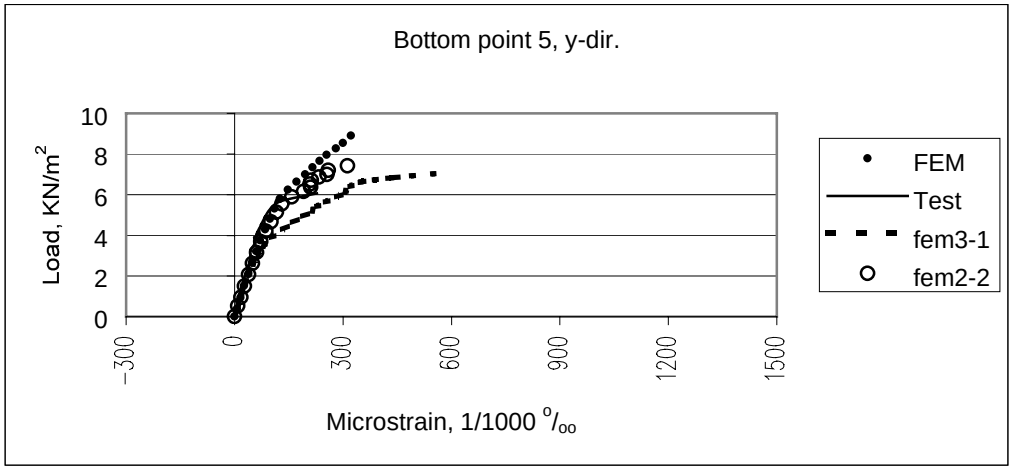

Strain from FE analysis and observed strain in point 5.
Figure 4.43 b

Figure 4.43 a and b show strains in point 5, in the middle of column strip.
The observed strain in the top of the slab, perpendicular to the column strip, is close to strain calculated with FE analysis until a load of 4.0 kN/m^2. In the column strip direction in the bottom of the slab, the observed strain and strain from FE analysis are close until a load of 6.0 kN/m^2. The reason for this can be the effect of the concentrated tendons, high axial force.

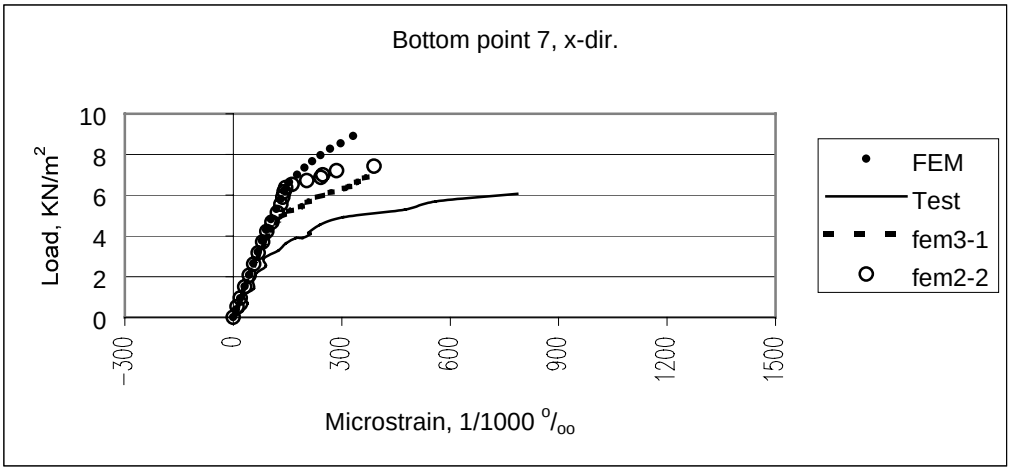

Strain from FE analysis and observed strain in point 7.
Figure 4.44 a

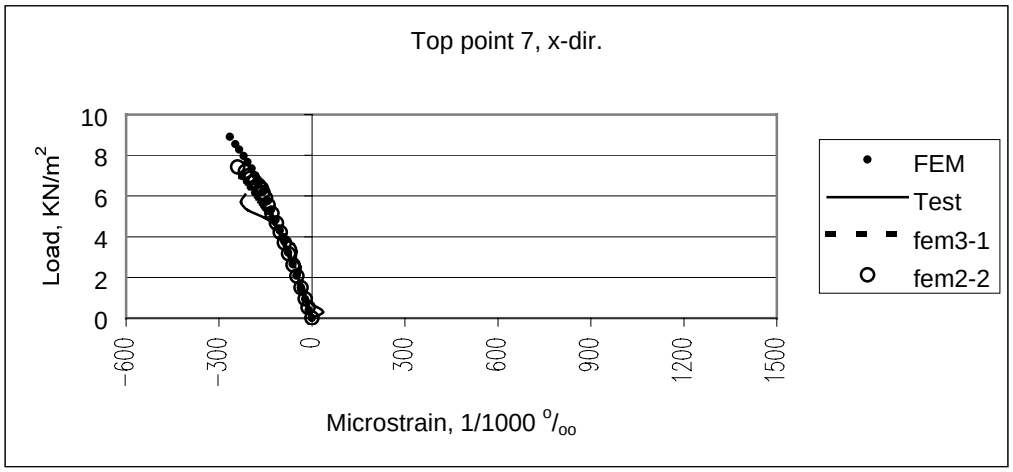

Strain from FE analysis and observed strain in point 7.
Figure 4.44 b

Figure 4.44 a and b show strains in point 7. Observed strain and strain from FE analyses are both small and close to each other in top point in x-direction. In the bottom the strain from FE analysis is somewhat lower than observed strain with a load from 3.0 kN/m^2 and higher.

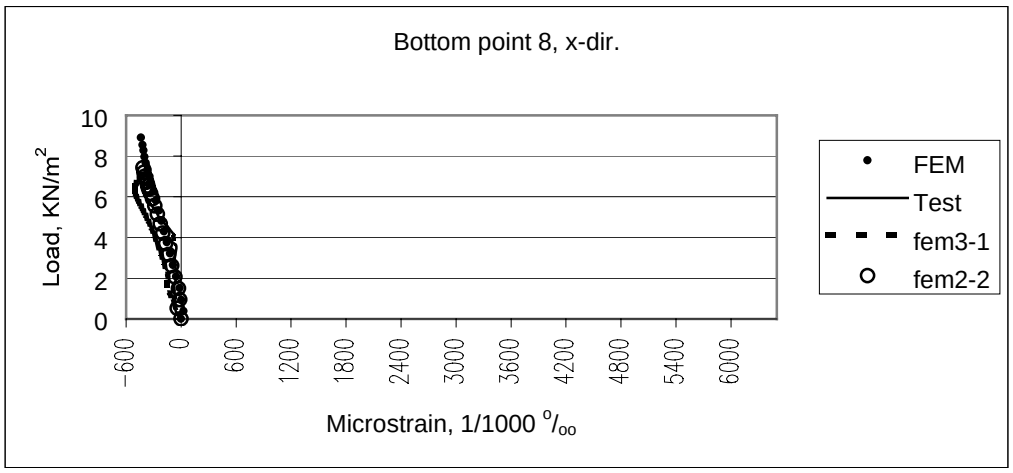

Strain from FE analysis and observed strain in point 8.
Figure 4.45 a

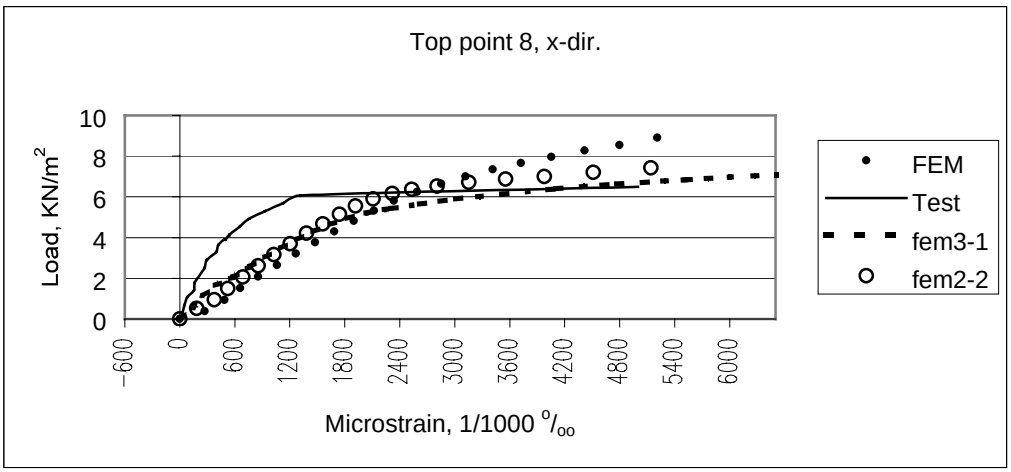

Strain from FE analysis and observed strain in point 8.
Figure 4.45 b

The strains at the middle column in x-direction are shown in figure 4.45 a and b. At the bottom the observed strain and strain from FE analysis are close until a load of 5.5 kN/m^2. On the top the observed strain are lower than strain from FE analysis from the start of loading. Since this point is the most critical one in the slab, the chosen model of prestressed tendons can have an influence on the results in FE analysis. And if the strain gauge in the test slab is not placed exactly at the same place as where strain is measured in the FE model, it might also cause a difference. This because variations in strain decrease fast from maximal strain with increasing distance from this point.

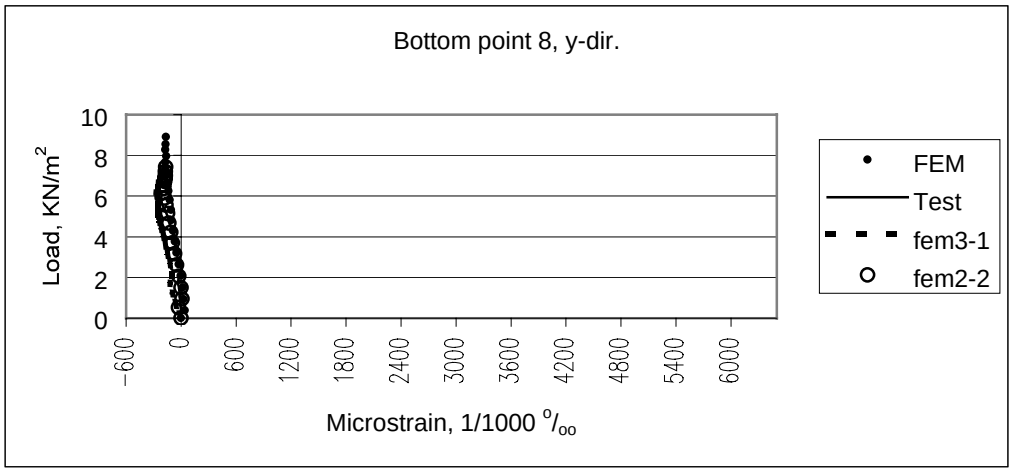

Strain from FE analysis and observed strain in point 8.
Figure 4.45 c

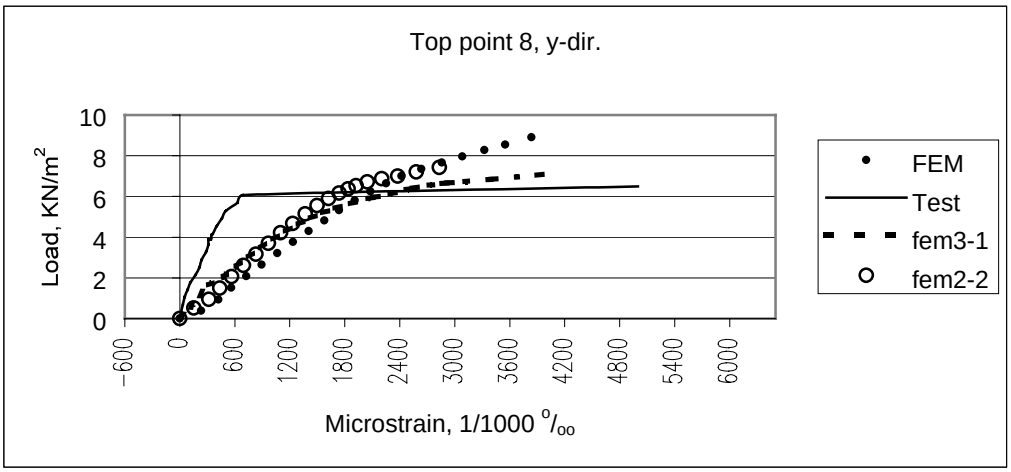

Strain from FE analysis and observed strain in point 8.
Figure 4.45 d

Strains in y-direction in point 8 are shown in figure 4.45 c and d. As in x-direction, the observed strain in the bottom and strain from FE analysis are close from the start of loading.

4.9.6 Discussion of failure test results

In this test failure was assumed to occur around the column in the middle as a shear failure. The shear capacity was calculated after the Norwegian standard, NS 3473 /9/, with a load of 2.5 kN/m^2. To get enough capacity to this load, shear reinforcement was necessary around the column in the middle of the slab. This shear reinforcement was skipped, to be sure that the failure starts in this point. With a load of 6.5 kN/m^2, the failure occurred as a shear failure around the middle column.

Results from the full-scale test are compared with results from the finite element analysis done with the FE-program, "Diana". Some results are listed and discussed here:

- Development, location and increasing of crack width in concrete are complex and difficult three-dimensional problems. FE analysis can be one way to go to get better understanding of this problem.
  Analysis of this slab does not give exactly the same result as observed after the first run. After the observed strain was available and plotted together with strain from FE analysis, a new analysis was done with new parameters in the data file. The modulus of elasticity and the tensile strength were changed. Results from this analysis were somewhat closer to the observed results than the first analysis.
- There is a good correspondence between theoretical and observed deflections until a load of 5 kN/m^2. This can be seen in figure 4.41. After this, the observed deflection increases more than deflections in the analysis. There is relatively good correspondence between strain from analyses and observed strain until a load of 4 kN/m^2, except in point 8 over the middle column. The deviation between observed strain and strain from analysis in this point, and deflection in the span, is due to the development of cracks near the column in the middle. This cracking starts earlier in the test than in the analysis. Strain in reinforcement in the middle of span and in column strip span was low before failure. After failure the strain increased until about 50 % of yield strain. Reinforcement strain in top over column, increased continuously until yielding with a load of 6 kN/m^2. With shear reinforcement by the column, the capacity will increase.
- The finite element program DIANA, can also include loss in prestressing from relaxation and anchorage slip, but in this analysis the prestressing force was reduced with the theoretical calculated loss from these. This test also shows that results from finite element analysis done with two different tension softening models, are closer to the observed strain than for one model for the whole slab. The area around column in the middle (2.5 x 2.5 m^2) was modelled with tension softening model 1, and the other with model 2, see figure 4.32. This gives a different and a more correct relation between stiffness for these two areas, since the area around the column in the middle has more reinforcement than the other parts of the slab. Since the strain gauge is glued to the reinforcement at only one side, this might have an influence on measured strain, and with strain gauge glued to the reinforcement on both sides, top and bottom, the result will give a better description of the real strain in reinforcement.

- It is assumed that the moment distributions from the slab to column are small and therefore neglected. With few and small span widths, the contraction in the length direction of the slab is small, and the effect on the bending moments can be neglected.
- From the “observed strain” plot, it is possible to indicate when cracks occur in top of the slab over the column in the middle, and from figure 4.20 c and 4.21 c it is possible to see that point 8 has crack in both direction before loading starts. Most probably there were also cracks in point 3 and 6 before loading.
- The measured values from the strain gauges include strain from temperature variation, cracks, creep and shrinkage until loading. This is not included in the FE analysis, and this can explain some of the deviation between measured and calculated strains.
- The results from analysis show that this type of structure is complex to calculate: long-time effects, two-ways effects and change in moment when cracks occur, are some of the problems in a flat slab.
- Since the shear capacity is decisive in this test, capacities after NS 3473 /9/, ACI /11/, AS 3600 /14/ and EuroCode2 /16/ are calculated and compared with the observed results. This is given in table 4-3 above. The critical section is equal when calculating after ACI and AS 3600. That means that shear force is equal for these two standards. NS 3473 and EuroCode2 calculates critical section with another distance from column than the two other standards do, and they give close shear forces.

4.10 Conclusions

The following conclusions are made on the basis of the reported test results and analysis of the full-scale test of prestressed flat slab.

1. The critical type of failure for this flat slab is shear failure around the column. Installing shear reinforcement might be difficult because of tendons, top slab reinforcement, and column reinforcement. The problem can be avoided by widening the column, since this gives longer critical section and consequently higher shear capacity.

2. The slab was loaded until failure with a load of 6.5 kN/m^2. This gives a shear force in the critical section of 245 N/mm calculated after the Norwegian standard, NS 3473 /9/. Shear capacity calculated after the same standard is 154 N/mm. That means that the capacity is passed with 58 percent. Relations between shear force, when failure occurs, and capacity calculated after ACI /11/, EuroCode2 /16/ and AS 3600 /14/ are 408/283 (+44 %), 253/150 (+69 %) and 408/413 (-1%), respectively.

3. Observed and calculated prestressing force after losses (included 18 days of long time loss) is 115 kN and 129 kN. If the maximum jacking force had been held constant for a short time before the wedge was set, some of this difference (12 %) might be reduced. Total calculated short time loss in active ends is 8.4 kN, and in passive ends it is 5.0 kN. The long time loss is calculated to 3.1 kN. Average compressive stress in concrete from prestressing is 1.7 N/mm^2. There was negligible increase of prestressing force when the slab was loaded. Development of strain in analysis and test are relatively close in most points, but some deviation occurs in point 8, over the middle column. Strain plots have a “jump” when the form is removed, which is not found in analysis since here the loading is done continuously until all load is active. One way to go to obtain a more correct prestressing force, is to stress all tendons two times, first 50 % of prestressing force in all tendons, and then until 100 %, and hold this force for a short time before the wedges are locked.

4. The calculated deflection depends on chosen structural system and slab stiffness. The total width of the column strip was chosen as 1/3 of span width perpendicular to the direction where concentrated tendons were placed. An alternative method is to use a diagonal strip. This is more complicated and does not always give more correct results. The author’s recommendation is to calculate deflection for the two directions as independent one-way-systems. For the point in the middle of the spans (point II) this approach overestimated the deflections by 89 %. The main reason for the deviation is the two-way reaction from the edges.

5. From the long time analysis it can be seen that observed strains are close to calculated strains, except over the middle column. The deviation between measured and calculated strains can partly be explained and reduced by: stressing the tendons in two operations, control of moment distribution between slab and column, strain gauges should be glued to both sides of the reinforcement and deviation between location of strain gauges in test and analysis.

6. FE analysis gives strain in good correspondence to the observed strain until a load of 4 kN/m^2, except over the middle column. Deviation between observed and calculated strain in this point can partly be explained by development of crack in the slab around the column. Since the analysis does not include strain from temperature, cracks, creep and shrinkage, some of the deviation can be explained by these values too.

7. It is possible to skip the reinforcement in spans if there is a compressive stress in the slab. This test shows that some reinforcement in the span give a good distribution of crack when they occur. NS 3473 /9/ gives a minimum reinforcement over column, but it is a discussion of this reinforcement amount should be distributed per metre or total reinforcement in span width should be distributed over a length equal to the column width plus two times the slab thickness from each side of column. In this test total reinforcement were distributed in a distance from each side of column, and this gives a good distribution of crack over the column.

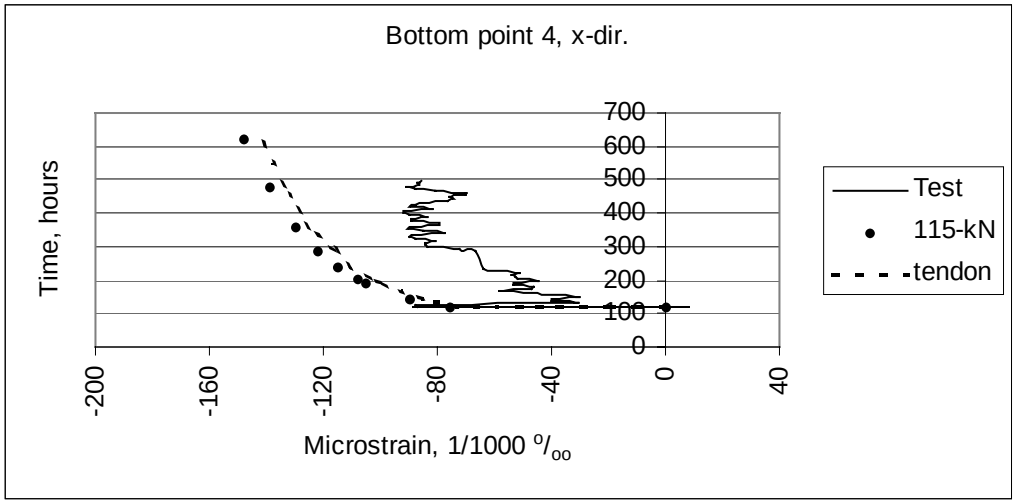

Strain from test “Test”, FE analysis with reduced jacking force “115-kN” and wrong tendon profile, ”tendon”.
Figure 4.46 a

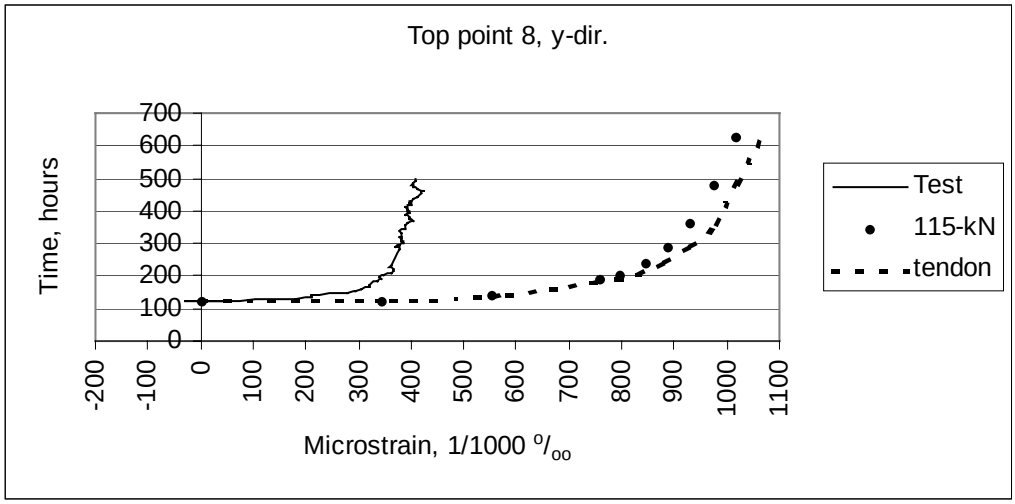

Strain from test "Test", FE analysis with reduced jacking force "115-kN" and wrong tendon profile, "tendon".
Figure 4.46 b

The effect of reduced prestressing force and changed tendon profile in point 4, middle of span in both directions, is shown in figure 4.46 a. This shows that there is only a small difference between the two plots, and from the last analysis in figure 4.35 a, the strain increases with 16 %, which is closer to the observed strain.

Over the middle column, point 8, the strain also increases with 8% and 14% compared to the last analysis from figure 4.39 d. That means strain from analysis in figure 4.39 d is closer to the observed strain. This is normal since reduced prestressing force and higher tendon profile in span, gives a higher moment over column.

It is important to note that strain from analysis plotted in figures above, is an average strain, for example the final strain in analysis with reduced prestressing force is plotted with a value of 1017 microstrain in point 8. Strains in element (four nodes) are 569, 1464, 569 and 1464 microstrain. Last observed strain in the same point is 410 microstrain. This shows that in heavily loaded points like point 8, the location of the strain gauge has a large influence on the observed results.

Chapter 5

Materials and structural properties of slabs on ground

5.1 Introduction

Designers and contractors do often not give concrete slabs on ground the same attention as other structural elements like columns, walls, beams and slabs. Slabs on ground are also given small attention in standards and structural codes and in the concrete courses taught at the universities. The reason for this can be that it is not so dramatic if a floor should fail. The common practice where description of this type of structure depends only on the previous work the designer has done is unsatisfactory and leads to a large number of damaged floors. Since one of the largest problems with floors is drying shrinkage cracking, it is surprising that so few floors for industrial buildings have been designed as prestressed slabs. This type of slab has obvious advantages related to elimination of cracks from drying shrinkage, and reduced slab thickness. Floors without prestressing need joints at a distance of maximum 5000 - 6000 mm to control cracking from drying shrinkage. The joints can be prepared before casting, or made by sawing the day after casting. Both possibilities, however, slow the construction process, and can be expensive for the builder.

Slab on ground design has over the last years benefited from development of concrete pavement on airports and roads. Calculations of slabs are often done with tables and influence diagrams, but this does not give accurate results. An alternative method is to apply FE analysis, but there is also here some difficulties due to choice of structural system and model parameters.

5.2 Subgrade

5.2.1 General

The capacity and displacement of slabs on ground depend on the material below the slab. If the original subgrade does not have enough bearing capacity it is necessary to replace it with fill of good quality, fig 5.1.

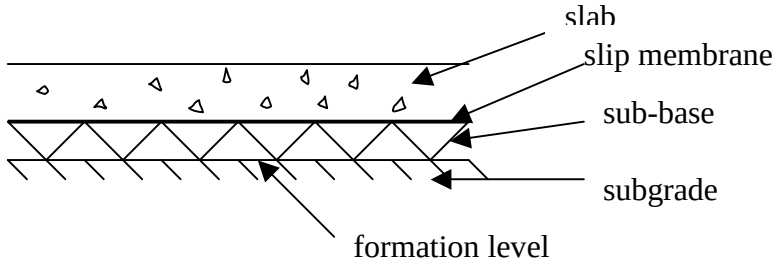

The elements of a floor.
Figure 5.1

For highest performance, fill should be laid in 150 mm layers, each well compacted /34/. The sub-base modifies the local elastic behaviour of the ground and influences the stress development in the concrete slab. A minimum depth of 150 mm is generally considered essential for this purpose. Some apply the rule that the thickness of sub-base should have the same thickness as the concrete placed over it. It is important that the top surface of sub-base is compacted and blended with fine crushed material. The maximum particle size in sub-base is usually recommended to about 75 mm. This makes it easier to lay a sub-base with necessary tolerance of plainness.

With accurately levelled sub-base the friction between concrete and the material below is reduced. In some structures a membrane between concrete and sub-base might be necessary to stop transport of humidity from ground to concrete. A membrane is also advantageous since it reduces the friction between concrete and sub-base.

5.2.2 Modulus of subgrade reaction (k-value)

The sub-base stiffness depends on the modulus of elasticity and thickness of sub-base. The modulus of elasticity is not always known for this type of materials, and the k-value must be taken from tables. Table 5.1 is a typical example /34/.

Description	Unit dry weight kg/m^3	Modulus of subgrade reaction, k N/mm^3
Coarse-grained gravely soils	1900-2300	0.054-0.082
Coarse-grained sand and sandy soils	1600-2100	0.054-0.082
Fine-grained soils – silt and clay	1450-2000	0.027-0.054
Fine-grained soils – silt and clay	1250-1700	0.014-0.050

k values for subgrades, from "Concrete industrial ground floors" /34/
Table 5.1

In an ideal situation where the modulus of elasticity is known and the subgrade is very stiff, the modulus of subgrade reaction can be calculated from:

$$k = E/h \qquad (5.1)$$

E = Sub-base modulus of elasticity
h = Thickness of sub-base.

Measurement of k-value can also be done by a plate-loading test on top of the compacted subgrade or, if sub-base is used, on top of sub-base /35/.
In the most common test setup a 30-in. (762-mm) diameter plate is loaded with a constant load (normally 0.07 N/mm^2). The k-value is calculated by dividing the load by the measured deflection:

$$k = p / \delta \text{ in } N/mm^3 \qquad (5.2)$$

Before calculating the k-value, it can be desirable to estimate a thickness of sub-base. In table 5.2 /30/ there are some proposed values.

Theoretical studies and full-scale road experiments /30/ have shown that uniformity of support is more important than actual bearing strength.

Classification of subgrade	Typical soil types	Recommended thickness of sub-base in mm
Weak	Clay	150
	Silt	
	Sandy, silty, clay with water-level within 60 mm of formation level	
Normal	Well graded and drained sand	80
	Sandy gravel	

Recommendations for thickness of sub-base, from R. Colin Deacon ”Concrete ground floors” /30/

Table 5.2

5.3 Concrete

5.3.1 General

When casting slabs on ground the contractor often desires to have a “self levelling” concrete. This is nearly possible by the use of superplasticizers, but it ought to be done under a specialist’s directions. Slabs on ground are normally reinforced with bar mats.

Measurement of compressive strength is the conventional method for concrete quality specification. The most important strength parameter for slabs on ground is however the tensile strength, since crushing of concrete is normally not a problem in this type of structure.

The selection of concrete quality must also consider durability requirements, and ACI recommends a 28-days compressive strength of 4000 psi (27 N/mm^2) for class 4 floors (light industrial/commercial buildings) and 4500 psi (31 N/mm^2) for class 5 (single-course industrial buildings). There is no recommendation for concrete strength in the Norwegian standard for slabs on ground.

5.3.2 Tensile strength

There are at least three different ways to determine the tensile strength of concrete, the splitting strength test, bending test and the uniaxial tensile strength test. In general the splitting strength test and the bending test are simpler to perform and therefore more commonly used.

The splitting tensile strength can be calculated as:

$$f_{ct,sp} = \frac{2 \cdot F_u}{\pi \cdot l \cdot d} \tag{5.3}$$

where

$f_{ct,sp}$ = tensile splitting strength
F_u = Total line load at failure
d = diameter of cylinder
l = length of cylinder.

Flexural strength, or theoretical extreme fibre stress at the failure load, is often denoted the modulus of rupture, MR. It can be predicted from the compressive cylinder strength as /35/:

$$MR = K\sqrt{f_c'} \tag{5.4}$$

MR = Modulus of rupture
K = constant with normal range 8 - 10 (normally used 9.0) (Unit: psi)
= 0.66 – 0.83 (normal 0.747) (Unit: N/mm^2)
f_c' = Compressive strength

Compressive strength after 90 days can also be used, and this is equivalent to about 110 to 114 per cent of 28-day strength /38/. The American Concrete Institute Building Code uses a default value:

$$MR = 7.5\sqrt{f_c'}, \qquad \text{in psi} \tag{5.5}$$

Coefficient in the range 9-11 are commonly obtained by testing /41/.

Alternatively the modulus of rupture, MR, can be determined from the tensile strength. The relation between these two values depends on thickness of test specimen, and the Norwegian standard NS 3473 /9/ gives a range from 1.0 to 1.5 with 1.0 for specimen thicker than 500 mm.

The design tensile strength may be derived from EuroCode2 /16/ after the following equation:

$$f_{ctm} = 0.30 \cdot f_{ck}^{2/3} \tag{5.6}$$

where

f_{ck} = characteristic cylinder compressive strength of the concrete.

CEB-FIP Model Code 1990, /33/: If only the tensile splitting strength of the concrete is known, the mean axial tensile strength may be estimated as:

$$f_{ctm} = 0.9 \cdot f_{tks} \tag{5.7}$$

After Norwegian standard /9/ the characteristic tensile strength is calculated from the splitting strength as:

$$f_{tkp} = \frac{2}{3} \cdot f_{tks} \tag{5.8}$$

where

f_{tks} is characteristic splitting strength from testing.

Design tensile strength, after Norwegian standard, can then be calculated as:

$$f_{tnp} = \frac{f_{tn}}{f_{tk}} \cdot f_{tkp} \tag{5.9}$$

f_{tn} and f_{tk} are taken from the table in the Norwegian standard.

After the Australian standard the characteristic tensile strength is:

$$f'_{ct} = 0.4 \cdot \sqrt{f'_c} \qquad (5.10)$$

where

$f'_c = f_{ck}$ = characteristic cylinder compressive strength of the concrete.

Since EuroCode, ACI and AS 3600 use cylinder compressive strength, and Norwegian standards use cube compressive strength to predict the tensile strength, a relation between cylinder and cube compressive strength must be used if the different formulas shall be compared. The relation used in NS 3473 are /46/:

$$f_{cube} < 55N/mm^2 \qquad f_c' = 0.80 \cdot f_{cube} \qquad (5.11\ a)$$

$$f_{cube} > 55N/mm^2 \qquad f_c' = f_{cube} - 11N/mm^2 \qquad (5.11\ b)$$

The moment capacity depends on the quality of concrete, but it is not easy to recommend a concrete strength in slabs on ground. One possible solution for calculating the total reaction in a slab is to use the modulus of rupture, MR, around the load, since MR describes extreme fibre stress in this area, and design tensile strength from EuroCode in other stress calculation.

5.3.3 Shrinkage

One of the most important factors when designing the concrete mixes for slabs on ground is to get concrete with a minimum of shrinkage. There are many factors that influence the size of shrinkage strain, since shrinkage depends on percent of fine aggregate in concrete, relative humidity, thickness of slab, amount and type of cement, slump and air in concrete and the type of aggregate. But two of the main factors to reduce this, are to increase the aggregate content in concrete to a maximum, and reduce water in concrete to a slump of 50 - 70 mm. Water - cement ratio of maximum 0.50 should be desired. To increase the aggregate size can be a problem with very thin slabs, but normally the slab is thick enough to use 22- 25 mm as maximum particle size.

5.4 Reinforcement

In slabs on ground, the designer has the choice between plain, reinforced, fibre reinforced and prestressed concrete. Prestressed slabs are discussed in chapter 7. When the slab thickness is 150 mm and larger, many designers use double reinforcement in the slab. With a good sub-base, this has limited value since the normal function of reinforcement is to control cracking, not to prevent it. If the slab is designed as supported by ground beams or piles, traditional concrete theory is used, and this also gives bottom reinforcement in the slab. With a single bar mat, this reinforcement should be placed in the upper 1/3 of the slab. This gives the best crack control of the top surface. By the use of steel or polypropylene fibre reinforced concrete in ground slabs, the flexural strength is increased, and the cracks reduced

One load case in slabs on ground is “load” from friction between the sub grade and structure. In a slab with long distance between the movement joints, a careful consideration of sub grade friction is necessary to prevent crack. It is important to note that in a slab of 100 m length, the friction can reduce the effect of prestressing force with one third (or more).

In a test done by D. Pettersson /60/, friction between concrete and sub grade was measured. The friction tests were performed on concrete slab on ground materials such as sand, sand covered by plastic sheet, crushed aggregate and crushed aggregate covered by plastic sheet. The slab was loaded by different load level. Test results show that the maximum friction increases with increasing size of the particles and is reduced by plastic sheeting between the structure and the ground. Crushed aggregate give the largest coefficient of friction, about 2.75. The friction can be reduced to 0.75-1.0 if a plastic sheet is installed between the ground material (sand) and the structure. The coefficient of friction has a peak value and then decreases with increasing displacement to an almost constant value.

The simplest way to estimate the friction force is to assume linear variation along the slab /39/:

$$F_F = w \cdot u \cdot x \tag{5.12}$$

where x is the distance from the end of the slab, with a maximum of $L/2$. From maximum friction force estimated reinforcement can be given by:

$$A_s = \frac{w \cdot L \cdot u}{2 \cdot f_s} \tag{5.13}$$

Friction force:

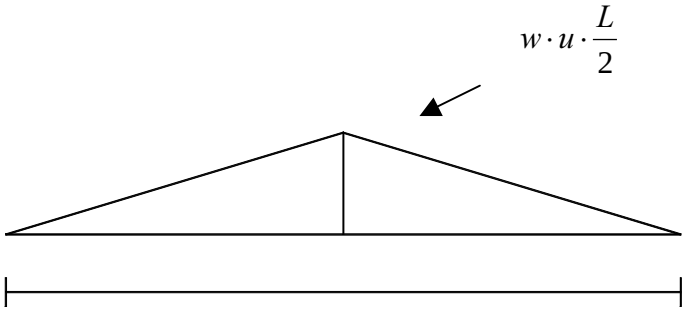

Development of friction force in a distance from edge.
Figure 5.2

where

A_s = Area of steel in mm^2/mm
w = Weight of slab N/mm^2
L = Length of slab between joints, mm
u = Coefficient of friction between slab and subgrade, (1.5 - 2.0)
f_s = Allowable working stress in steel, N/mm^2

It is seen from this equation and figure 5.2 that the amount of reinforcement varies directly with the length of the slab.

For axially loaded concrete structures, the following well-known equation should be used to calculate the minimum reinforcement:

$$p_s = \frac{A_s}{A_c} \cdot 100 = \frac{f_t}{f_s} \cdot 100 \qquad (5.14)$$

where

p_s = Reinforcement in percent
A_s = Reinforcement, mm^2
A_c = Concrete area, mm^2
f_t = tensile strength, N/mm^2
f_s = allowable stress in steel, N/mm^2

This equation is deduced from the principle that after the concrete cracks, the reinforcement should be able to carry the crack load at the working stress level. The equation should be used to control cracking in slabs on ground where axially restrained shrinkage and temperature effects are the major sources to stress development. Equation 5.13 is most used, and gives a smaller reinforcement amount than equation 5.14.

5.5 Prestressed tendons

Forces from drying shrinkage alone can reach ultimate tensile strength. By bringing in an axial force into the slab, tensile failure cannot occur until the internal tensile stresses exceed the residual compression plus ultimate tensile strength. Axial forces can be brought into the slab by using prestressed tendons in one or two directions. The effect of prestressed concrete is to produce slabs that have no movement joints over areas up 100 x 100 m, and at the same time reduce or prevent cracks from drying shrinkage.

5.6 Joints

Joints may often cause large problems in industrial floors, since the edges are vulnerable to damage. Wide joints and the use of small hard wheels increase the risk of damage. If distributed cracks can be tolerated the number of joints can be reduced. Cracks and joints are two problems in industrial floors that are related to each other. This will not be discussed further here, but joints and their layout are discussed in /34/ and /39/.

Chapter 6

Test of slabs on ground

6.1 Introduction

Several problems with concrete floors are related to cracking. Cracks in concrete can be classified in two categories, cracks occurring while the concrete still is in the plastic stage and cracks in hardened concrete /31/. Plastic shrinkage most often occurs in the top surface of slabs before hardening starts. ACI 224 /32/ describes settlement crack as a crack that occurs after vibration and finishing, because the concrete has a tendency to continue the consolidation. This crack occurs if there is a thin concrete cover. The best way to reduce this type of cracks is to decrease the concrete slump, increase concrete cover and use thin reinforcement. The crack problem in hardened concrete is amongst others due to drying shrinkage and temperature variations in addition to external loads.

With prestressed slabs on ground, there are axial forces in one or both directions, and this causes some compression in the slab. The friction between concrete and sub-base caused by the compression, gives unwanted forces in the structure, and it is necessary to reduce it as much as possible. One method to do this is to use a plastic membrane between concrete and the sub-base.

The purpose of this investigation was to simulate floors on ground, loaded with concentrated load in different places, and then follow the strain development in concrete, reinforcement and in the prestressed tendons. It was expected that development of cracks in prestressed slabs, stressed at an early age of the concrete, is reduced in relation to reinforced slab. A final objective is, as described in chapter 2, to contribute towards better understanding of the structural behaviour and improved design methods.

6.2 Description of slabs

The slabs were 4000 mm x 4000 mm which should give values also valid for larger slabs. The slab configuration is chosen because the loading rig does not have more free space than 4000 mm. Three slabs were produced, each 150 mm thick. This thickness is normally used as minimum thickness for slabs on ground. The slabs will be referred to as S1, S2 and S3, fig 6.1 a, b, c. S1 was reinforced with a K335 (335 mm^2/m) reinforcement net in top and bottom. The concrete cover for S1 was 25 mm in bottom and top. S2 was prestressed with unbonded tendons at a distance of 630 mm in both directions. In S3 the spacing between the tendons was 930 mm.

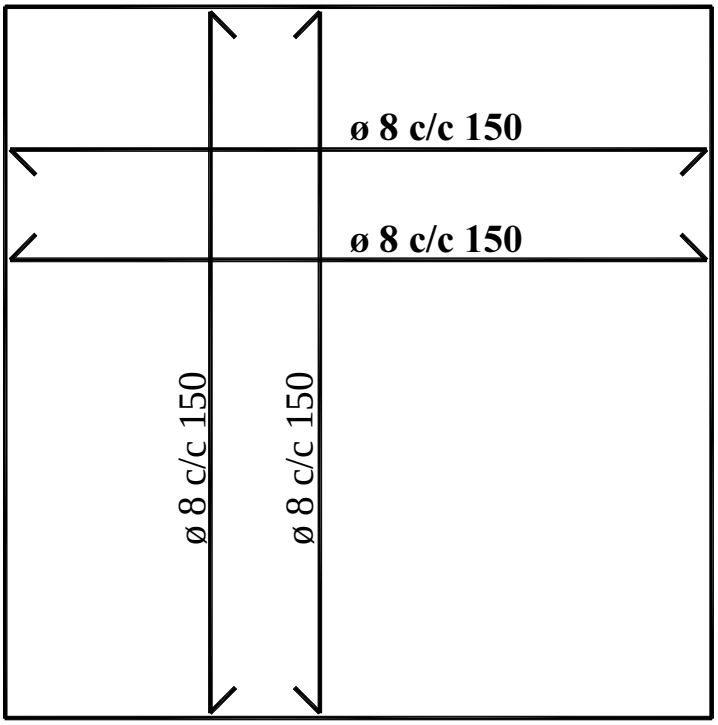

Slab S1, reinforced with net.
Figure 6.1 a

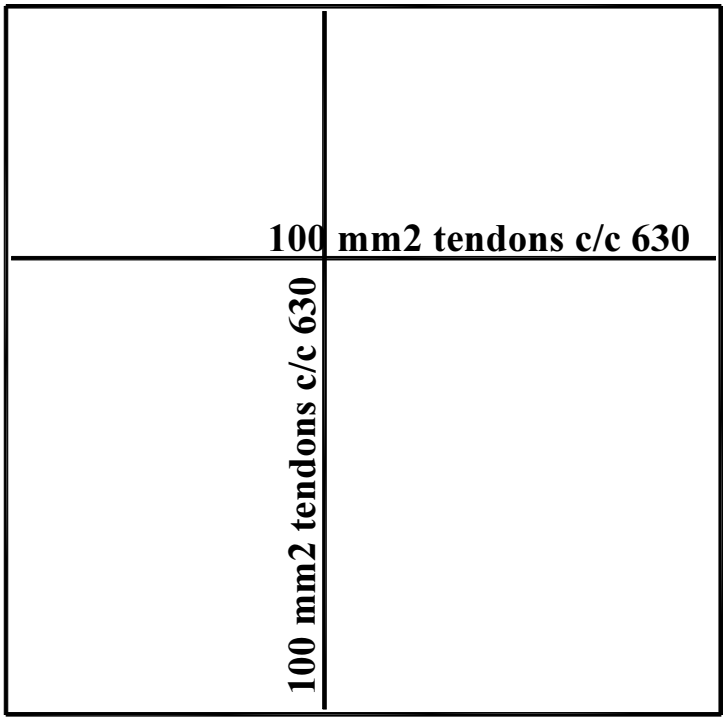

Slab S2, prestressed with 100 mm^2 tendons, c/c 630 mm.
Figure 6.1 b

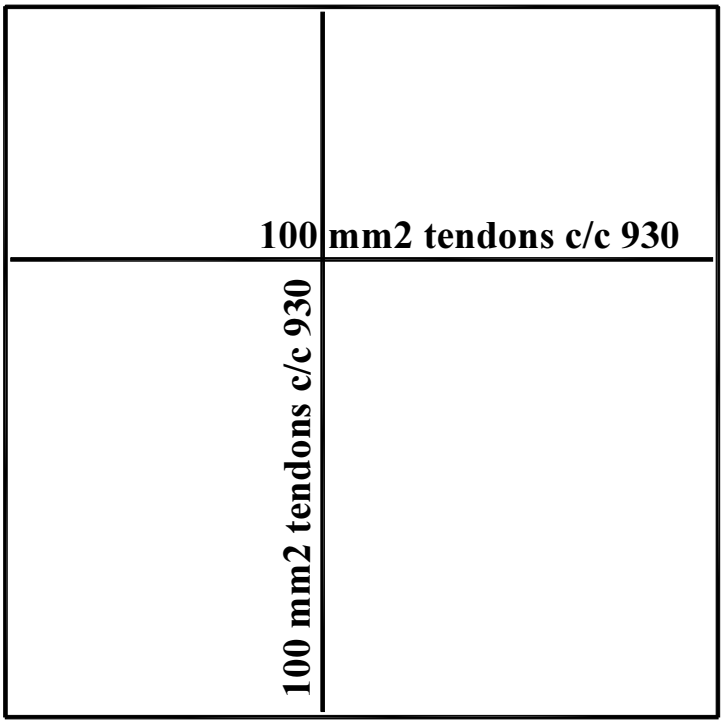

Slab S3, prestressed with 100 mm^2 tendons, c/c 930 mm.
Figure 6.1 c

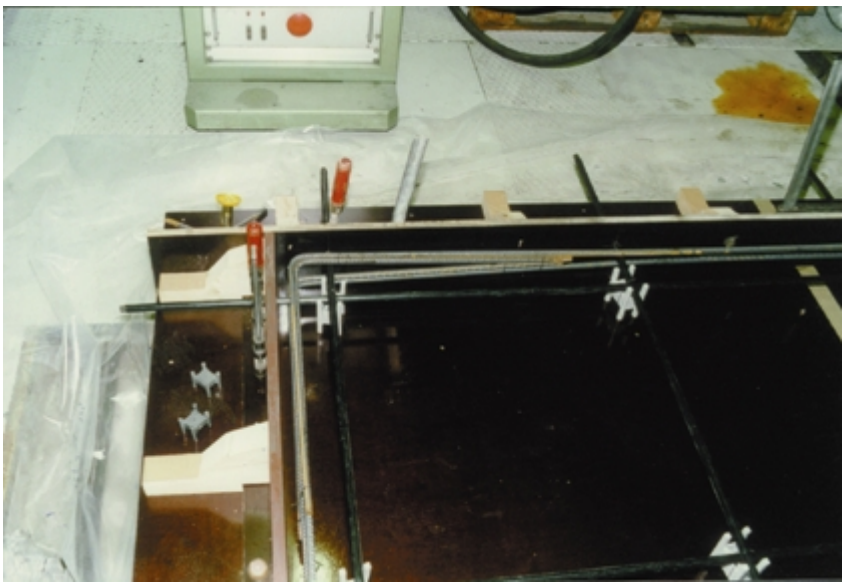

Reinforcement in the anchorage zone.
Figure 6.2

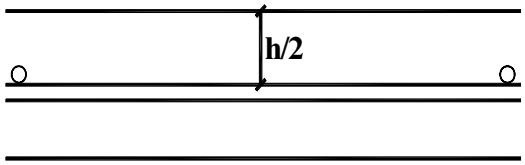

Tendons placed centrically in the slab.
Figure 6.3

S2 and S3 have two 12 mm reinforcement bars around the edge, see fig 6.2. These bars are placed to prevent cracking in the anchorage zone.

The surface was treated with steel trowelling. This makes it easier to see when the cracks start on the surface.

The tendons were located in the middle of the slab, see fig 6.3.

The slabs should represent typical industrial floors, but slab S1 has more reinforcement than normally used in this type of floor. K257 with 257 mm^2/m is a more commonly used reinforcement. The K335 reinforcement is used because of the strain gauges. Recommended reinforcement in slabs on ground is discussed in chapter 5.4. The three slabs before casting are shown in fig 6.4 a, b and c.

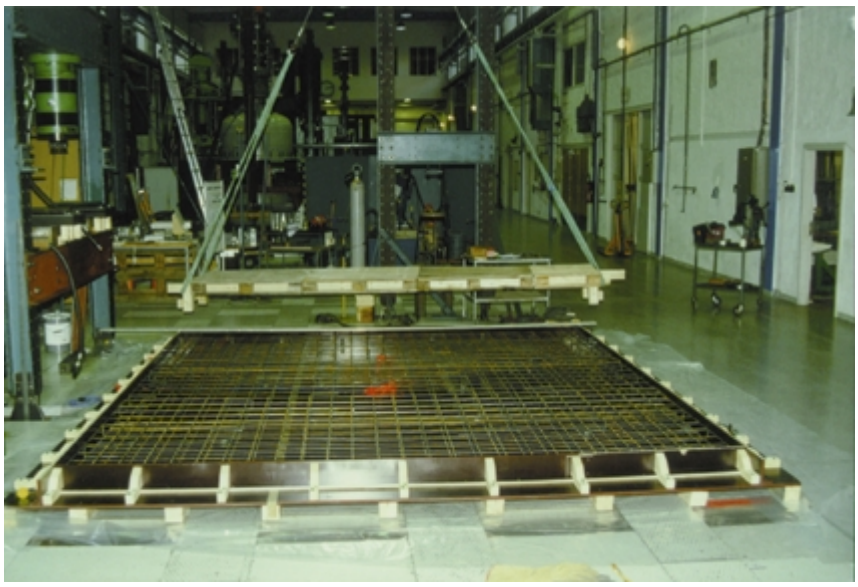

Slab S1 before casting.
Figure 6.4 a

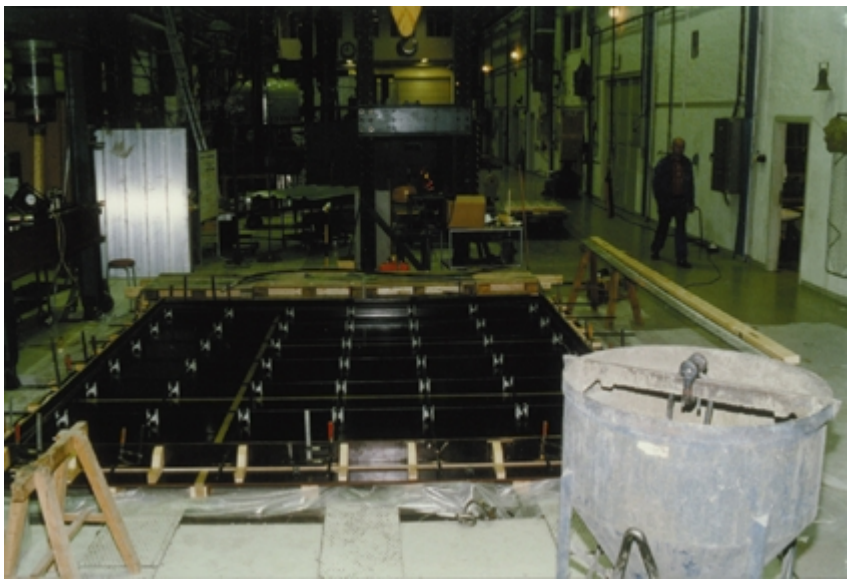

Slab S2 before casting.
Figure 6.4 b

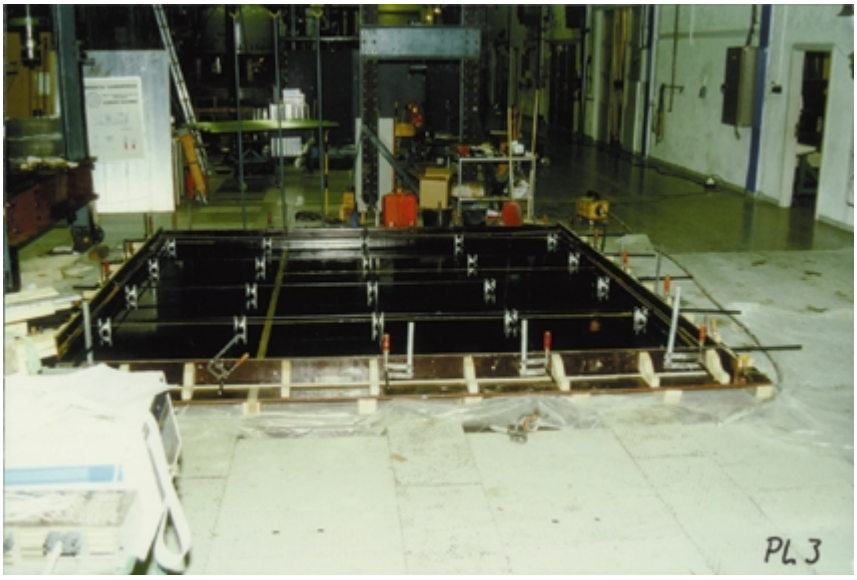

Slab S3 before casting.
Figure 6.4 c

6.3 Materials

6.3.1 Concrete

The concrete quality used in this test was planned to be C35 (28 days characteristic cube strength 35 MPa), but as it can be seen from table 6.1, the compressive strength after twenty-eight days unfortunately varies between 31.3 and 41.0 MPa. The large difference is due to higher air content in the first slab. Six cubes for compressive strength testing were cast for each slab, and for S2 and S3 there were in addition cast cylinders to test the modulus of elasticity and tensile splitting strength. Compressive strength testing of cubes was done after one day, seven days and at the day of loading for S1, after two, three, seven and twenty-eight days for S2, and at one day, two days, seven days and at loading for S3. The modulus of elasticity was determined after the Norwegian standard NS 3676. The modulus of elasticity for S3 is listed in table 6.2 a. Compressive cylinder strength for S3 is presented in table 6.3.

Splitting strength was measured for S3. Tensile strength calculated after EuroCode2, ACI and AS 3600 depends on the concrete compressive strength. Calculated after the Norwegian standard NS 3473, tensile strength depends on splitting strength. In CEB-FIP Model Code 1990 tensile strength can be calculated from the splitting strength if this is known. The equations are shown in chapter 5.3.2, and results plotted in figure 6.5. The splitting tensile strength in test, is calculated to 3.40 N/mm^2 after 28 days, (5.3). This give calculated tensile strength, 28 days after casting, 2.63 N/mm^2 after Model Code (5.7), and 2.27 N/mm^2 after NS 3473 (5.8). The design tensile strength after EuroCode2 is calculated to 2.63 N/mm^2 (5.6), and 1.51 N/mm^2 after NS 3473 (5.9). Modulus of rupture is calculated to 4.35 N/mm^2 (5.4).

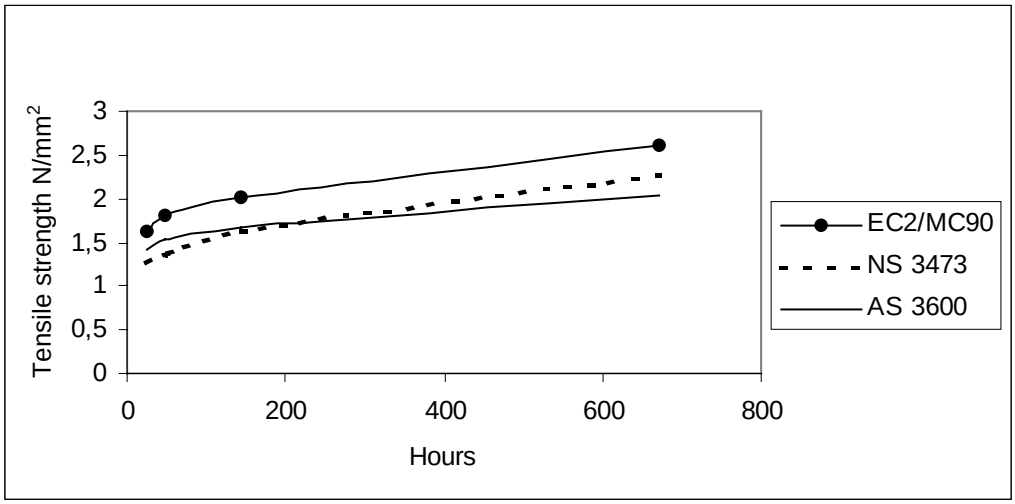

Tensile strength, in slab S3, N/mm^2 after time in hours.
Figure 6.5

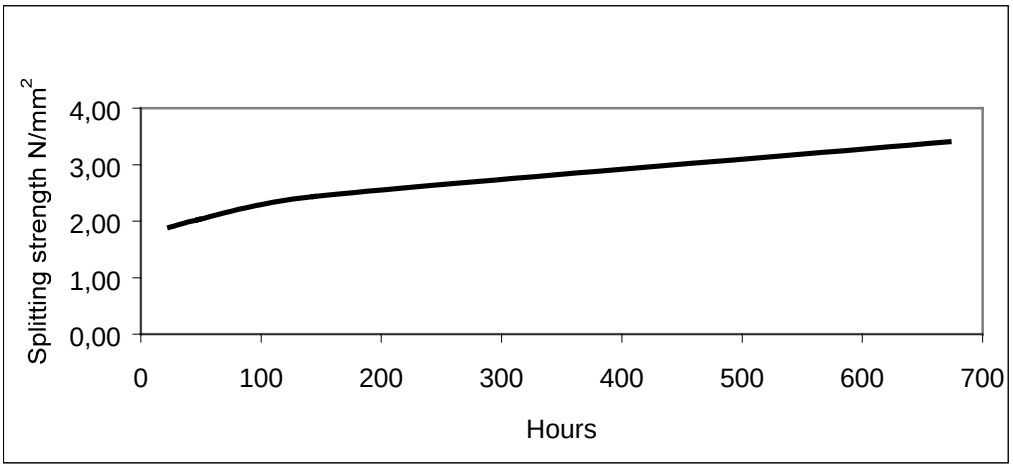

Measured splitting strength for S3, in N/mm^2 after time in hours.
Figure 6.6

The recipe for this concrete is listed in table 6.4. The fresh concrete properties slump and air content are given in table 6.5. The slump is relatively high because superplasticizers are added to give a 'self-levelling' concrete without strength loss.

Age	Slab S1	Slab S2	Slab S3
one day	9.2 N/mm^2		17.3N/mm^2
two days		17.5N/mm^2	21.2N/mm^2
three days		20.8N/mm^2	
seven days	19.8 N/mm^2	25.1N/mm^2	26.1N/mm^2
loading(28- days)	31.3N/mm^2	40.8N/mm^2	41.0N/mm^2

Compressive cube strength.
Table 6.1

Age	E_c
2 days	21400 N/mm^2
	22750 N/mm^2
28 days	29250 N/mm^2
	31900 N/mm^2

Modulus of elasticity, Slab S3.
Table 6.2 a

Age	$f_{ct,sp}$
1 day	1.89 N/mm^2
2 days	2.03 N/mm^2
6 days	2.44 N/mm^2
28 days	3.40 N/mm^2

Splitting strength
Table 6.2 b

Age	f_{cc}
28 days	34,2 N/mm^2
28 days	33,9 N/mm^2

Cylinder compressive strength, Slab S3
Table 6.3

Cement	FA Norcem	276,65	kg/m^3
Plasticity		2	kg/m^3
Water		122,07	kg/m^3
Fine gravel	0-8 mm	621,17	kg/m^3
Gravel	8-16 mm	503,02	kg/m^3
Gravel	16-24 mm	503,01	kg/m^3
Total weight		2493,23	kg/m^3
Total water amount		182,53	kg/m^3
Water/Cement ratio		0,66	
Measured slump		170	mm

Average values in concrete composition recipe.
Table 6.4

Slab	Density	Air	Slump
S1	2421 kg/m^3	6 %	180 mm
S2	2496 kg/m^3	2,7 %	160 mm
S3	2483 kg/m^3	3,6 %	180 mm

Average density, air and slump in slab.
Table 6.5

6.3.2 Prestressing strand and anchorage

The unbonded tendons used in this test were seven wire strands with yield and ultimate stresses 1670/1860 N/mm^2 and total area of 100 mm^2 for each tendon. The diameter of this tendon is 12.7 mm, and inside the plastic sheath and between each strand it is filled with corrosion protective grease. A typical stress-strain curve is shown in fig 6.7, and the modulus of elasticity is 196000 N/mm^2. The tendon was anchored by a steel plate 100 x 60 x 15 mm. The split cone wedges are placed in a conical cylinder in active end, see fig 6.8.

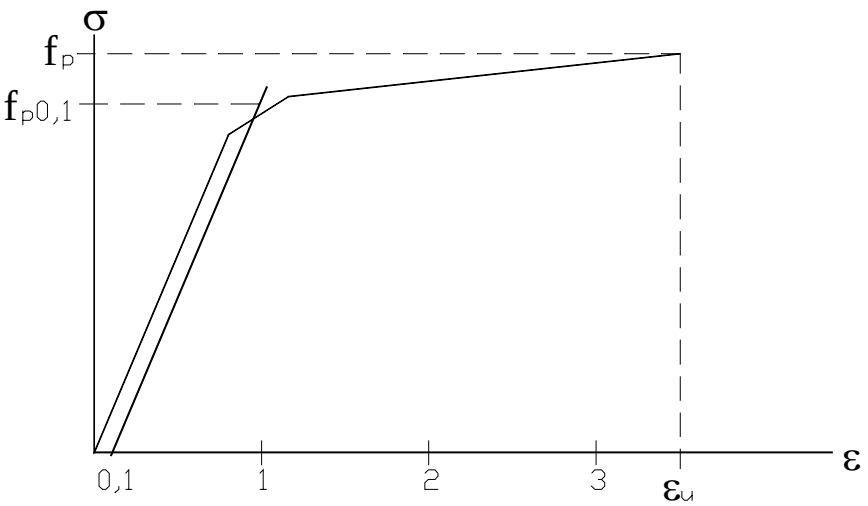

Stress-strain diagram, prestressed tendons.
Figure 6.7

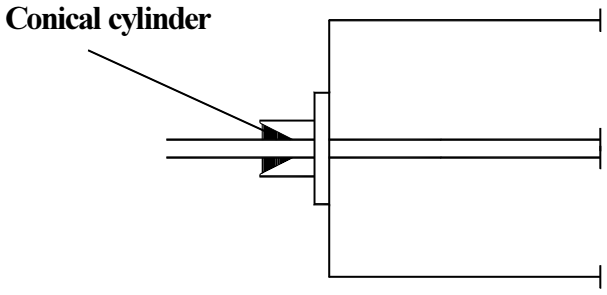

Split cone in cylinder.
Figure 6.8

6.3.3 Sub-base

Since this test was done in the laboratory, it was necessary to find a material with stiffness like compacted ground to get the sub-base and the subgrade, fig 6.9, as close as possible to real ground. To do this, Sundolitt MX300 /54/ with a thickness of 400 mm was chosen. Available data from Sundolitt /54/ reports a modulus of elasticity in the range 12.5 N/mm^2. The modulus of elasticity was tested on two test specimens with b x h x l = 200 x 200 x 400 mm^3 (4 plates), before the slab was tested, and the stress-strain curve for insulation can be seen in figure 6.10. The modulus of subgrade reaction (k-value) is then calculated to 0.03 N/mm^3 as:

$$k = E/h \tag{6.1}$$

E = Sub-base modulus of elasticity
h = Sub-base thickness

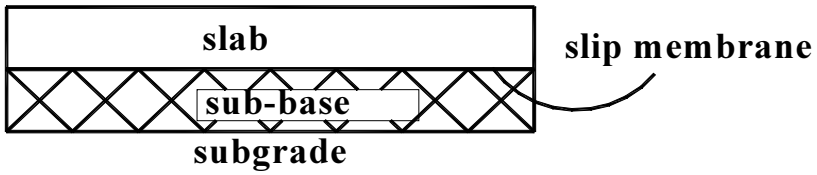

Slabs on ground.
Figure 6.9

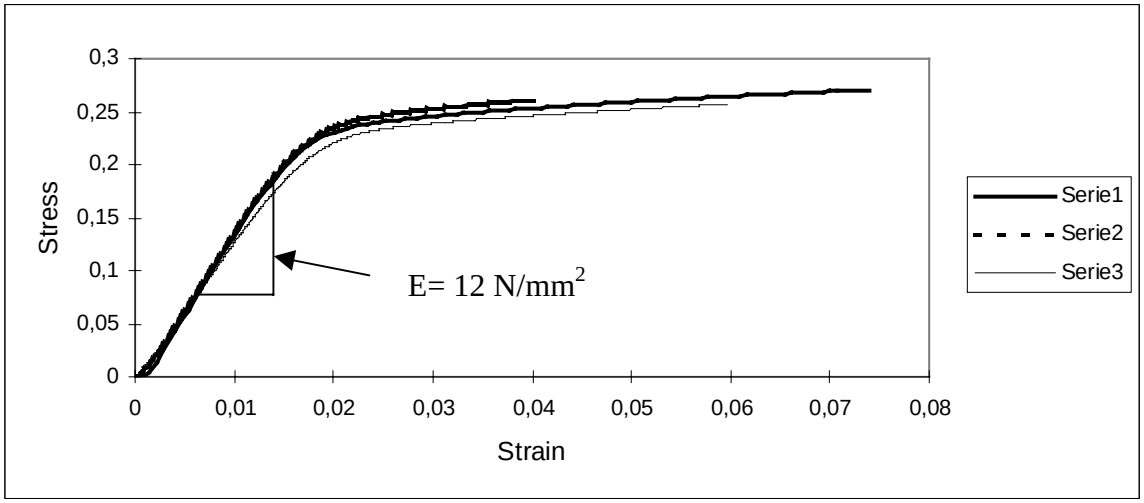

Stress-strain for insulation Sundolitt MX300
Figure 6.10

Sub-base was built with four 100 mm thick insulation plates, and after slab S1 was tested, the top insulation was replaced. The same procedure was followed after slab S2 was tested.

Figure 6.10 shows that the insulation is linear up to a strain on 0.02. For a thickness of 400 mm, this corresponds to 8 mm deflection.

The concrete floor below the test rig is a 1200 mm thick reinforced slab on ground. Compared to the Sundolitt, the stiffness is infinite.

6.4 Load arrangement, Fabrication and Instrumentation of slabs

6.4.1 General

The slabs were cast in a form made of wood. The base and side forms were constructed of 15 mm plywood, and under the base there were 75 x 75 mm timber beams. The test was done in the laboratory and the formwork was supported on concrete floor. The side form was 150 mm high and the edge was used to level the concrete. The same form was used for all three slabs, and the reinforced slab, S1, was cast first.

All data from this test are saved in a computer, Schlumberger Solatron 3531D data logger. The instrumentation was designed to record the data from the strain gauges, load cells, deflection gauges and the load.

6.4.2 Load

The load was applied to the slab by a 300 kN capacity hydraulic jack installed on a steel frame. As the load increases, it is registered in the computer each 10^{th} second. The load increases at a speed of 3 kN / minute. The load surface on the slab was 200 mm x 200 mm and was applied by a steel plate and a 12 mm porous plate, see fig 6.11 and 6.12.

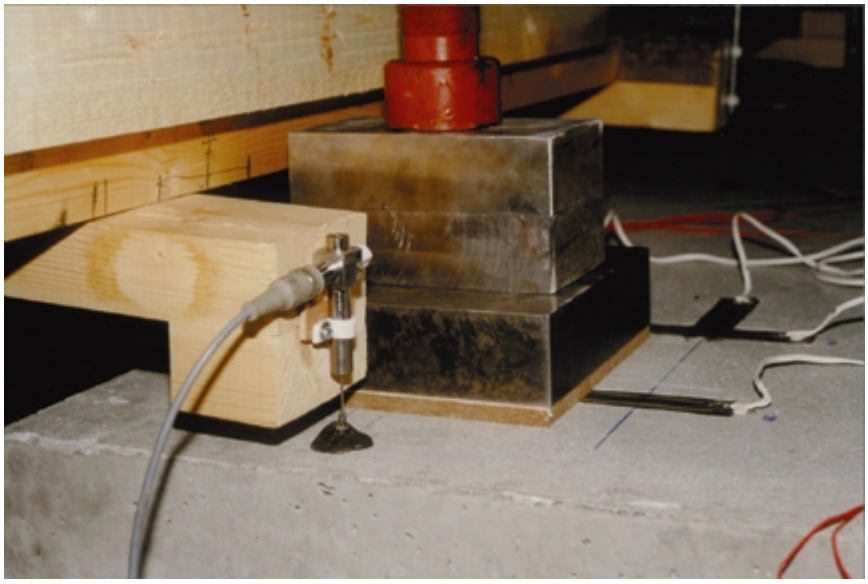

Load surface and deflection gauge.
Figure 6.11

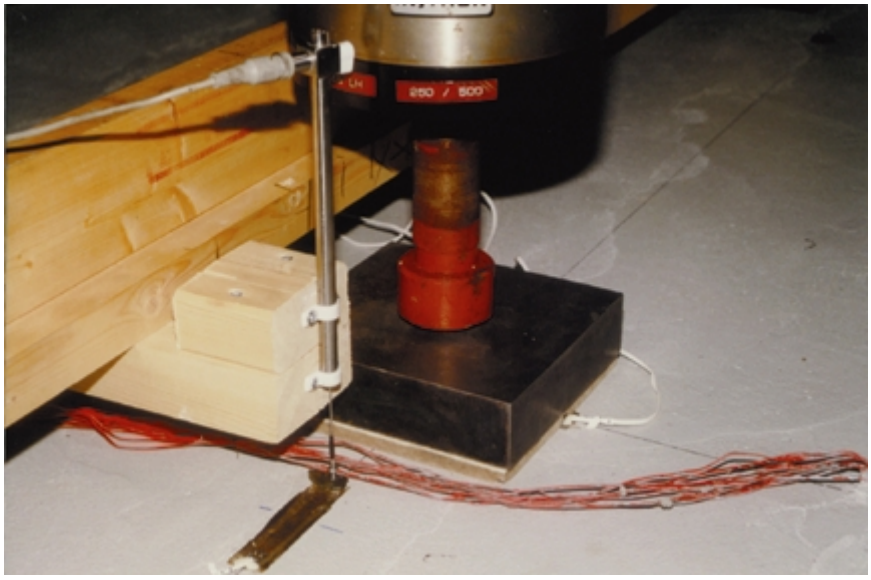

Load surface, concentrated load.
Figure 6.12

Each slab was loaded with three different load cases, and the same procedure was used in each slab. First load case was in the centre of slab, the second at the edge, in a distance of 200 mm from centre of load to edge. In the last load case the load was applied in the corner 200 mm from both edges, fig 6.13.

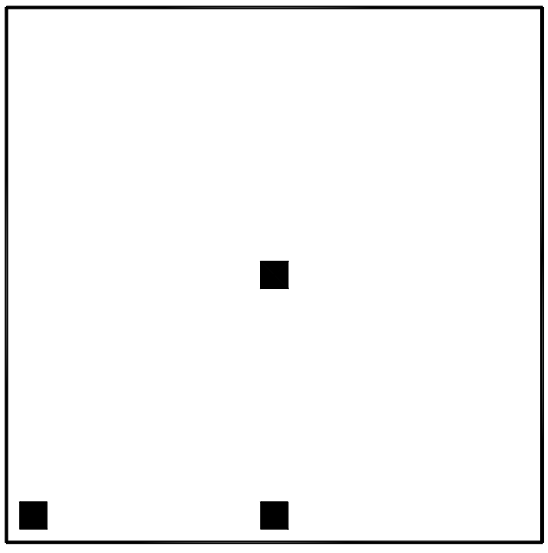

Load in centre, at the edge and in the corner of slab.
Figure 6.13

6.4.3 Load cells on prestressing tendons

In figure 6.14, the position of load cells in S2 and S3 are shown. The change in tendon forces when the load increases is measured each 10th second. Figure 6.15 shows a load cell with strain gauges.

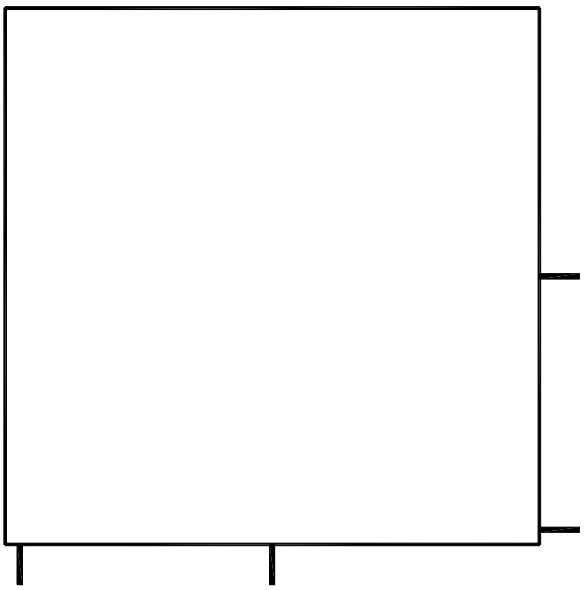

Load cell on the edge of slab S2 and S3.
Figure 6.14

Strain gauges glued to load cells.
Figure 6.15

6.4.4 Deflections

Vertical deflection at a line from one side to the other side was measured. A total of five points were measured when loading in the centre and at the edge, and six points when loading in the corner. The deflection gauges were attached to a wood beam over the slab, and it was glued to the slab with a special glue, see fig 6.11 above. Figure 6.16 shows position of deflection gauges when loading in centre. All deflection gauges were located at the top of the slab.

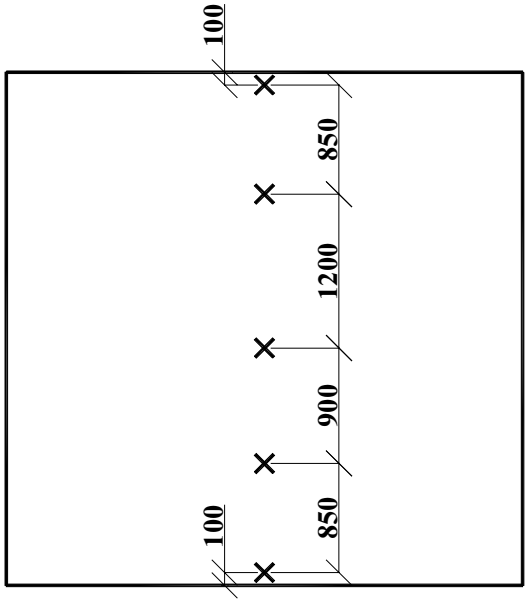

Deflection measure points in slab.
Figure 6.16

6.4.5 Strain gauges

Strain gauges of the type WFLA 3 were glued to the reinforcement at top and bottom of slab S1. In addition strain gauges of the type PL 60 were glued to the top and bottom surfaces. The positions are shown in figure 6.17 and 6.18. Table 6.6 shows position of each strain gauge for slab S1. Strain gauges at the reinforcement were glued at both sides of reinforcement in each point, see fig 6.20. Slab S2 and S3 were instrumented with strain gauges at top and bottom surface. Strain gauges in top of slab were placed after one day, and strain gauges in the bottom were placed before loading. Position of strain gauges can be seen in fig 6.19. Table 6.7 shows position of the strain gauges for S2 and S3.

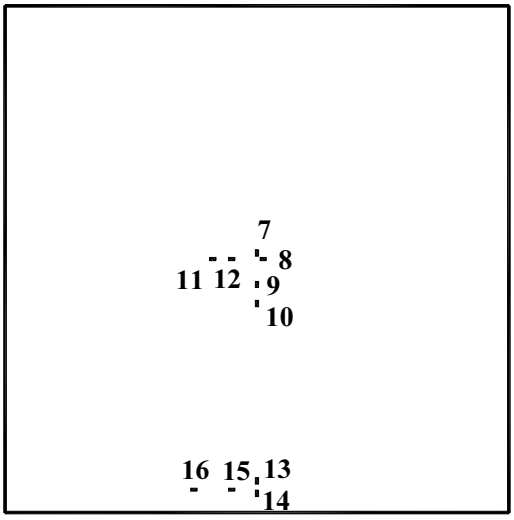

Strain gauges in bottom reinforcement, S1.
Figure 6.17 a

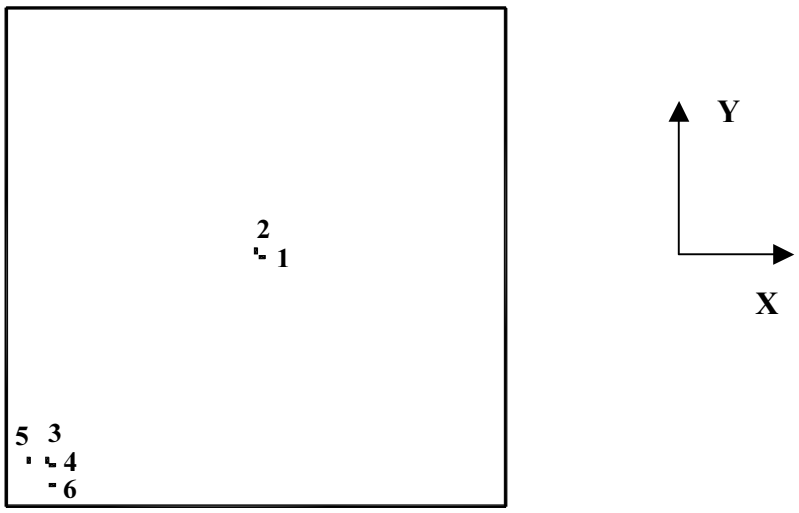

Strain gauges in top reinforcement, S1.
Figure 6.17 b

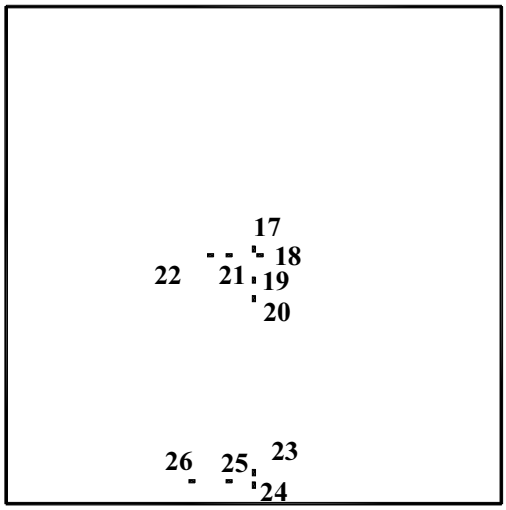

Strain gauges at the bottom surface of slab, S1.
Figure 6.18 a

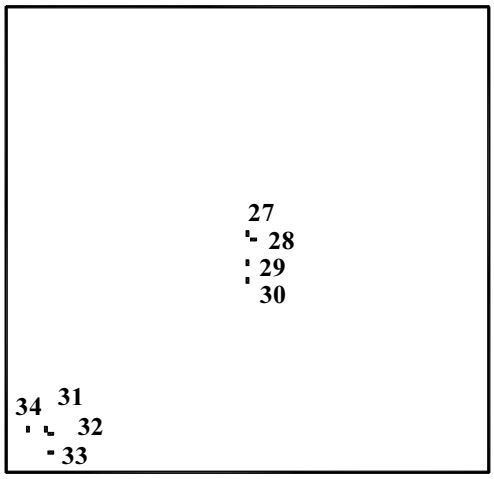

Strain gauges at the top surface of slab, S1.
Figure 6.18 b

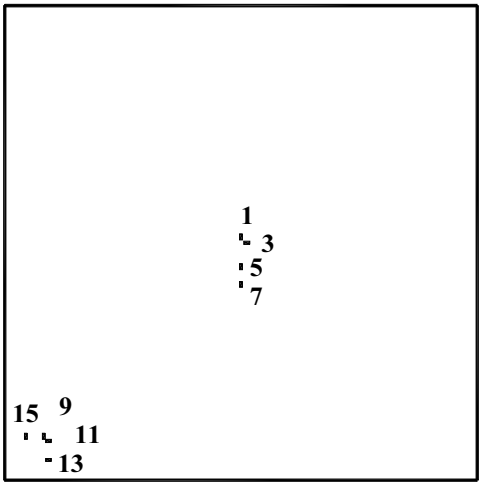

Strain gauges at the top surface of concrete, S2 and S3.
Figure 6.19 a

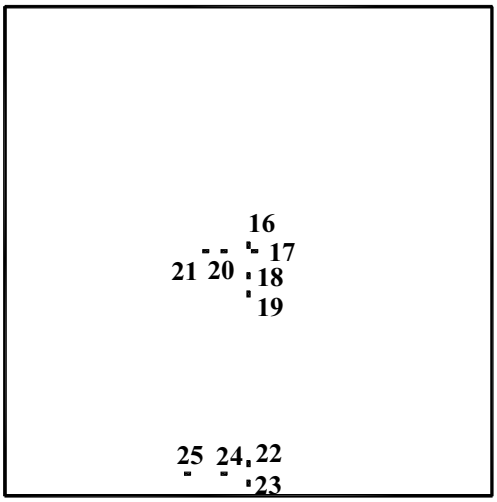

Strain gauges at the bottom surface of concrete, S2 and S3.
Figure 6.19 b

Strain gauge glued at reinforcement.
Figure 6.20

Strain gauge	x-value mm	y-value mm	Gauge at	Direction
1	2050	2000	Reinforcement top	x-dir.
2	2000	2050	Reinforcement top	y-dir.
3	330	370	Reinforcement top	y-dir.
4	370	330	Reinforcement top	x-dir.
5	180	370	Reinforcement top	y-dir.
6	370	170	Reinforcement top	x-dir.
7	2000	2050	Reinforcement bottom	y-dir.
8	2050	2000	Reinforcement bottom	x-dir.
9	2000	1800	Reinforcement bottom	y-dir.
10	2000	1650	Reinforcement bottom	y-dir.
11	1650	2000	Reinforcement bottom	x-dir.
12	1800	2000	Reinforcement bottom	x-dir.
13	2000	200	Reinforcement bottom	y-dir.
14	2000	150	Reinforcement bottom	y-dir.
15	1800	180	Reinforcement bottom	x-dir.
16	1500	180	Reinforcement bottom	x-dir.
17	2000	2050	Concrete bottom	y-dir.
18	2050	2000	Concrete bottom	x-dir.
19	2000	1800	Concrete bottom	y-dir.
20	2000	1650	Concrete bottom	y-dir.
21	1800	2000	Concrete bottom	x-dir.
22	1650	2000	Concrete bottom	x-dir.
23	2000	250	Concrete bottom	y-dir.
24	2000	150	Concrete bottom	y-dir.
25	1800	180	Concrete bottom	x-dir.
26	1500	180	Concrete bottom	x-dir.
27	2000	2050	Concrete top	y-dir.
28	2050	2000	Concrete top	x-dir.
29	2000	1800	Concrete top	y-dir.
30	2000	1650	Concrete top	y-dir.
31	330	370	Concrete top	y-dir.
32	370	330	Concrete top	x-dir.
33	370	170	Concrete top	x-dir.
34	180	370	Concrete top	y-dir.

Position of strain gauges S1

Table 6.6

Strain gauge	x-value mm	y-value mm	Gauge at	Direction
1	2000	2050	Concrete top	y-dir.
2				
3	2050	2000	Concrete top	x-dir.
4				
5	2000	1800	Concrete top	y-dir.
6				
7	2000	1650	Concrete top	y-dir.
8				
9	330	370	Concrete top	y-dir.
10				
11	370	330	Concrete top	x-dir.
12				
13	180	370	Concrete top	y-dir.
14				
15	370	170	Concrete top	x-dir.
16	2000	2050	Concrete bottom	y-dir.
17	2050	2000	Concrete bottom	x-dir.
18	2000	1800	Concrete bottom	y-dir.
19	2000	1650	Concrete bottom	y-dir.
20	1800	2000	Concrete bottom	x-dir.
21	1650	2000	Concrete bottom	x-dir.
22	2000	250	Concrete bottom	y-dir.
23	2000	150	Concrete bottom	y-dir.
24	1800	150	Concrete bottom	x-dir.
25	1500	150	Concrete bottom	x-dir.

Position of strain gauges S2 and S3

Table 6.7

6.4.6 Slab S1, reinforced

Strain gauge at both sides of reinforcement.
Figure 6.21

The strain gauges were installed on the reinforcement before it was placed in the form. Bottom reinforcement was placed exactly by a plastic distance chair. This gives a concrete cover of 25 mm. Before the top reinforcement was placed, there were installed reinforcement stirrups to give the exact distance to the top reinforcement. After all reinforcements were installed, the cables from strain gauges were thoroughly fastened to prevent damage when casting.

When casting the slab, four lift anchors were also installed. The anchors were placed in the 1/4 points of the slab, 1000 mm in from each corner in x- and y- direction, see fig 6.22. This slab was loaded forty-two days after casting.

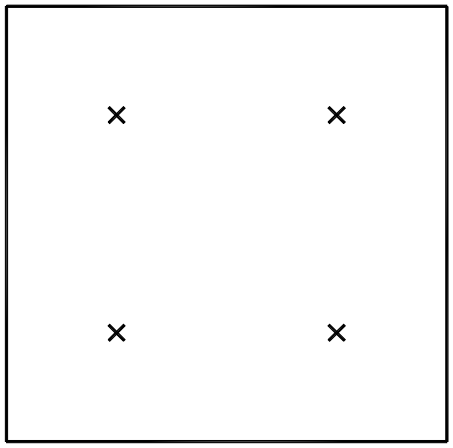

Lift anchors in slab.
Figure 6.22

6.4.7 Slab S2 and S3

In the side form there were drilled a 17 mm hole for each tendon. These holes were exactly in the middle of the slab. Inside the form the tendons were supported by 60 mm plastic distance chairs in one direction while tendons in the other direction were supported by lower tendons. That gives a theoretical concrete cover of 58 mm for the upper tendons. This difference is negligible. Outside the side form the tendons were fixed to prevent tendon deflection when casting.

Slab S2 was loaded thirty-eight days after casting, while S3 was loaded thirty-four days after casting.

6.5 Test procedure

After the strain gauges were glued to the reinforcement of slab S1, the slab was cast, and it was removed from the form after six days. Each slab was covered with a plastic sheet one day after casting, and this sheet was removed after three days.

After the slab was removed from the form, instrumentation on concrete surface in top and bottom started. For S2 and S3 the strain gauges on the concrete surface were installed after one day, before the prestressing operation started. The sub-base made of 400 mm insulation, was placed in an area of 4300 mm x 4300 mm. Slab S1, which was tested first, was centred over the sub-base, and LVDT's were installed in five points on the top surface. Strain gauges and LVDT's were set to zero before loading. After load case with load in centre was finished, the slab and sub-base were moved, and the load applied at the edge of slab. Finally the load was placed in the corner of slab. Slab S2 and S3 were loaded after the same procedure.

6.6 Test results

6.6.1 Prestressing force

S2 and S3 were prestressed to 15% of total force after one day, to 50 % of total force after two days and 100% after three days. This is done to reduce the cracking risk the first days. Typical force in tendon can be seen from fig 6.23, while the strain development is shown in figure 6.24. The computer was restarted when stressing of tendons starts, i.e. time 0 in figure 6.23 and 6.24 is 24 hours after casting.

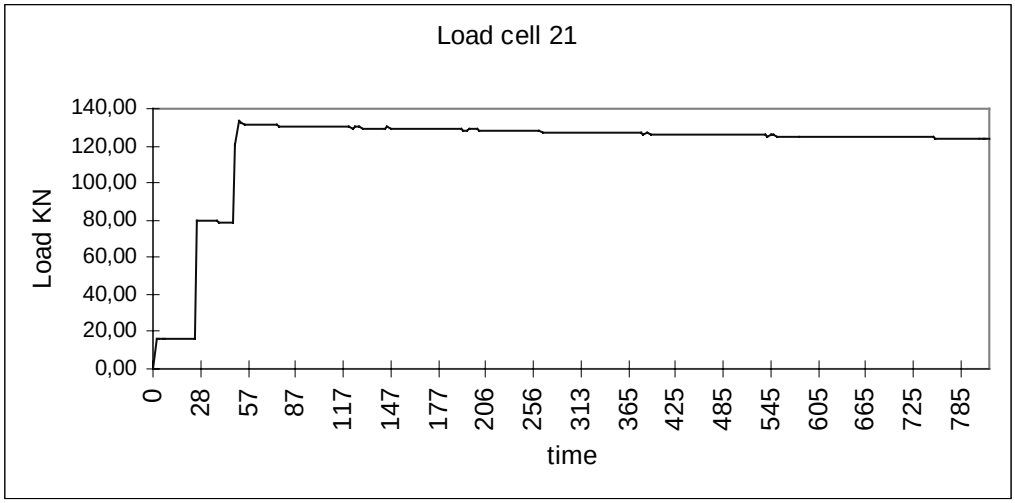

Typical force in tendon after jacking to 15 %, 50% and 100%
Figure 6.23

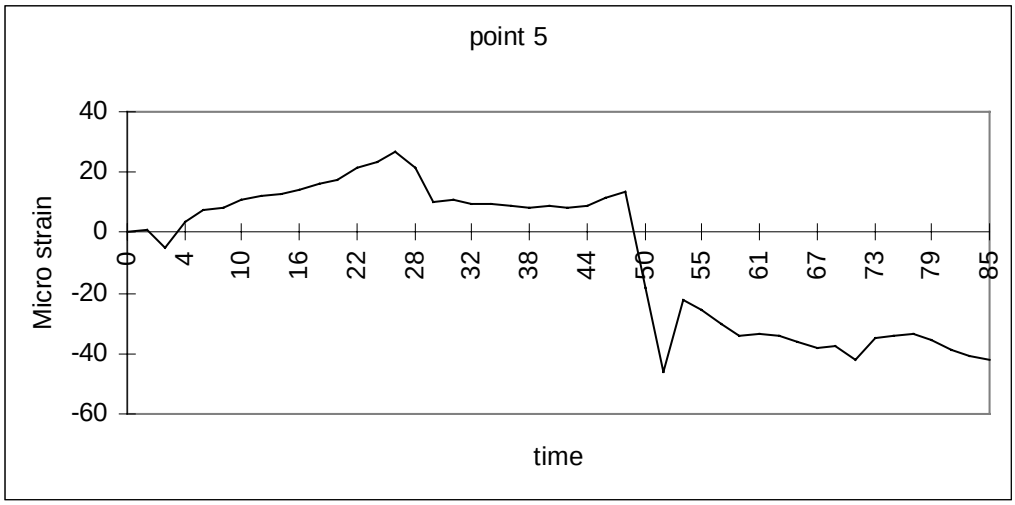

Strain in the middle of slab, at top surface (time in hours).
Start time is 24 hours after casting
Figure 6.24

The planned total force before loss in prestressing was 140 kN, which is near 85% of f_y. To achieve this force accurately was difficult, because the tendons are short. However, it appears that only one tendon has considerably lower stress after jacking.

Figure 6.24 shows that after the first stressing, there is a small compressive strain of 5 micro strain at the top surface in the middle of the slab. Before the next stressing, the strains change sign to expansion which probably is caused by drift in the strain gauges. Some of the reason can also be relaxation in tendons. After the second stressing, the strain gauges still showed expansion. The final stressing gives a compressive strain in the middle of the slab of 45 micro strain. The concrete cube strength when maximal stressing occurred was 25.6 N/mm^2 for slab S2, and 26.6 N/mm^2 for slab S3.

Since the tendons were short, 4000 mm, the elongations after jacking were small, about 20 - 24 mm.

The tendon forces give an average compressive stress in concrete of 1.5 N/mm^2 for S2 and 1.0 N/mm^2 for S3. During the failure test the maximum increase in prestressing force was 2.7 kN (2%).

6.6.2 Temperature in concrete

The temperature sensors in the slabs show the hardening temperatures, fig 6.25. In slab S2 the maximum temperature was 29 ^{o}C, and in slab S3 31 ^{o}C. Maximum temperature occurs after approximately 10.5 hours.

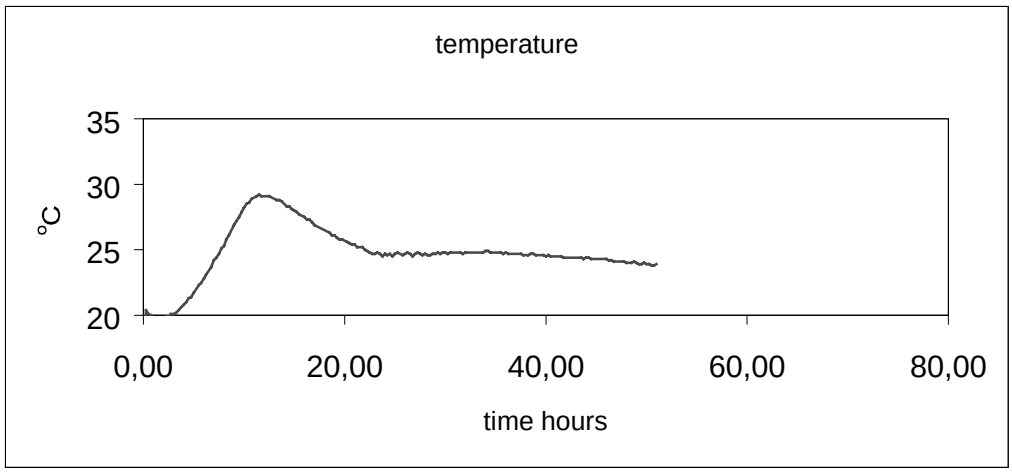

Development of concrete temperature, S2.
Figure 6.25 a

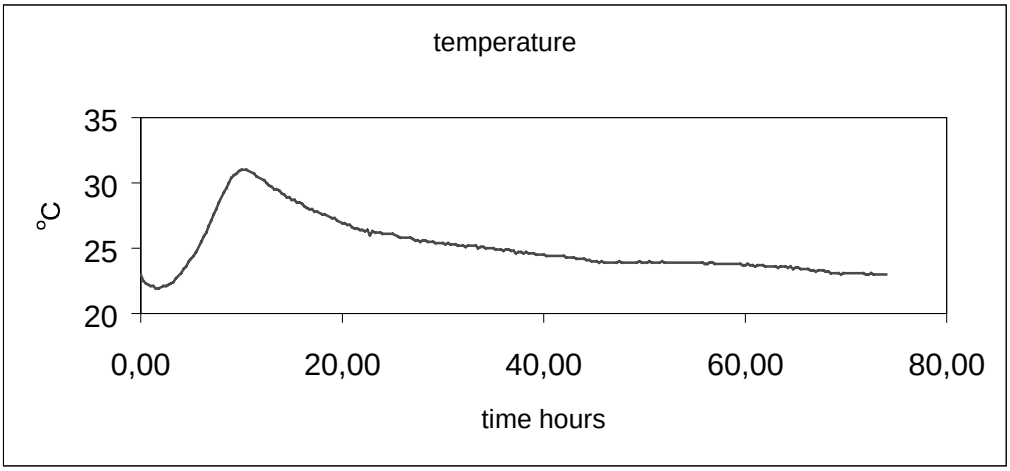

Development of concrete temperature, S3.
Figure 6.25 b

6.6.3 Deflections

All the slabs had the same sub-base, so variations of deflections should ideally depend only on slab stiffness. In figure 6.26 a-i the development in deflections are shown. Location of deflection gauges can be seen in figure 6.16.

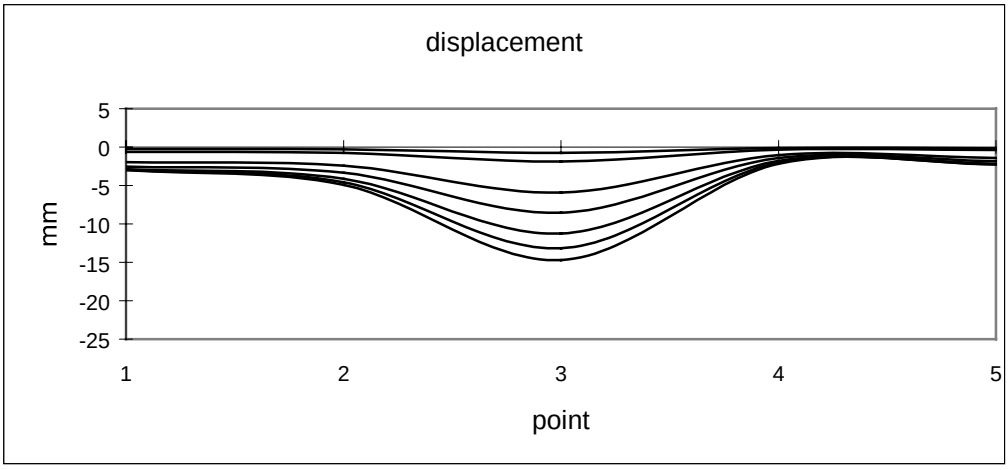

Displacement for S1 loaded in the middle. Load 10, 25, 50, 75, 100, 125, 150 kN.
Figure 6.26 a

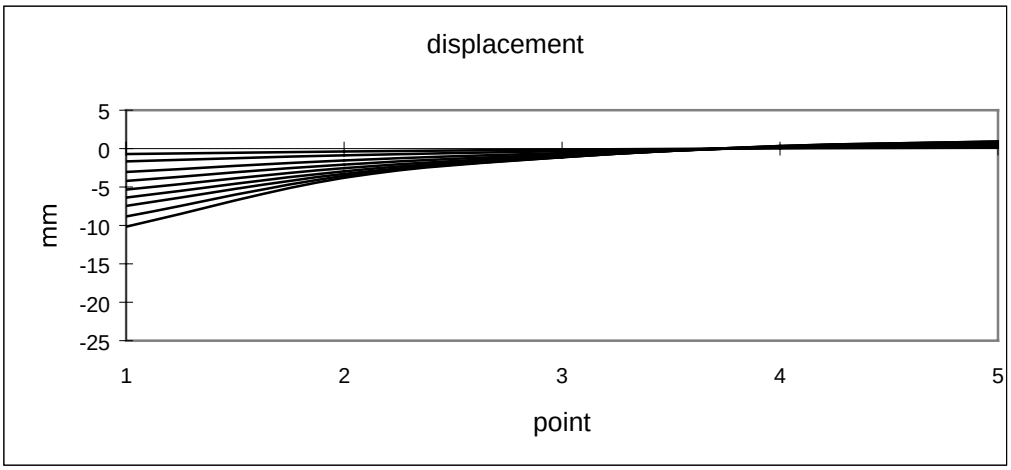

Displacement for S1 loaded at edge. Load 10, 25, 50, 75, 100, 125, 150, 175, 200 kN
Figure 6.26 b

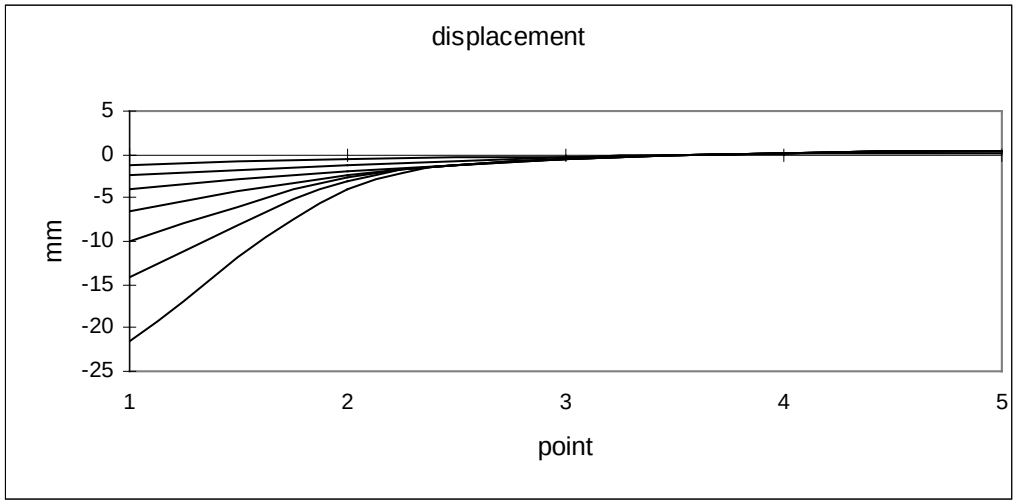

Displacement for S1 loaded in the corner. Load 10, 25, 50, 75, 100, 125, 150 kN
Figure 6.26 c

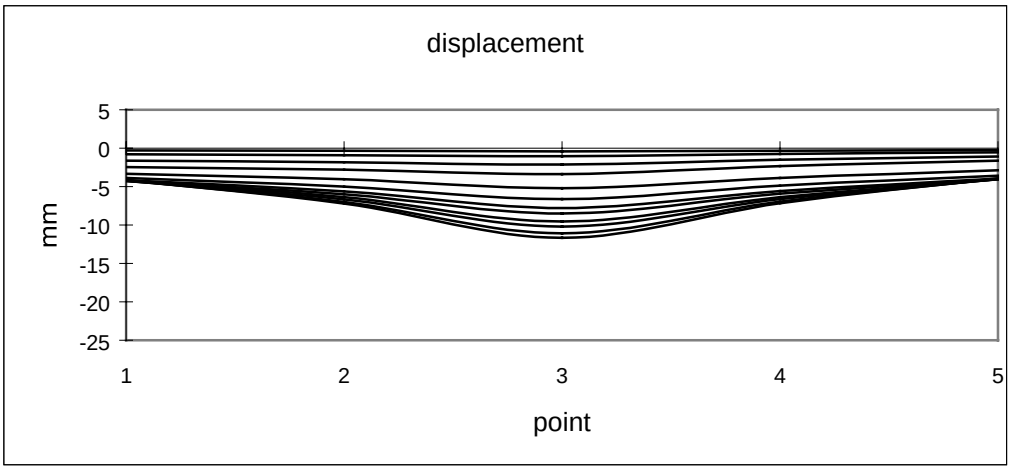

Displacement for S2 loaded in the middle. Load 10, 25, 50, 75, 100, 125, 150, 175, 200, 225, 250, 270 kN.
Figure 6.26 d

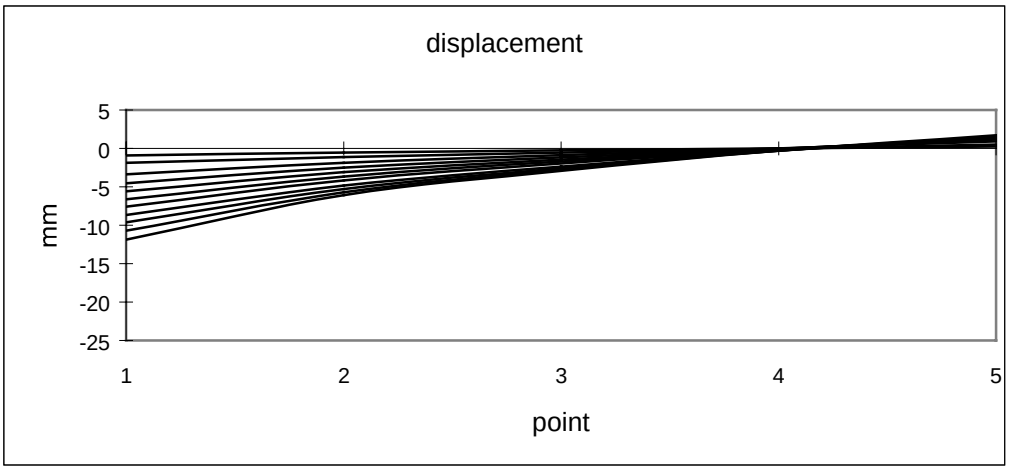

Displacement for S2 loaded at edge. Load 10, 25, 50, 75, 100, 125, 150, 175, 200, 225, 250 kN
Figure 6.26 e

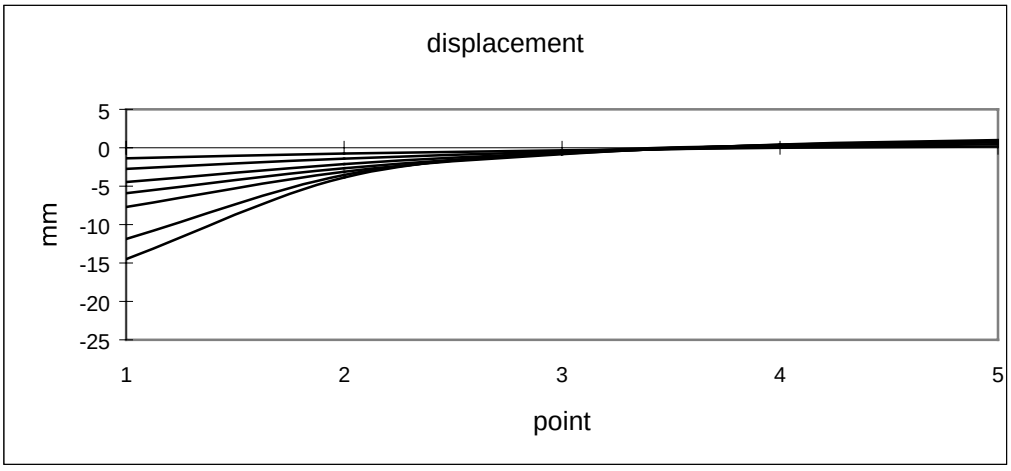

Displacement for S2 loaded in the corner. Load 10, 25, 50, 75, 100, 125, 150 kN
Figure 6.26 f

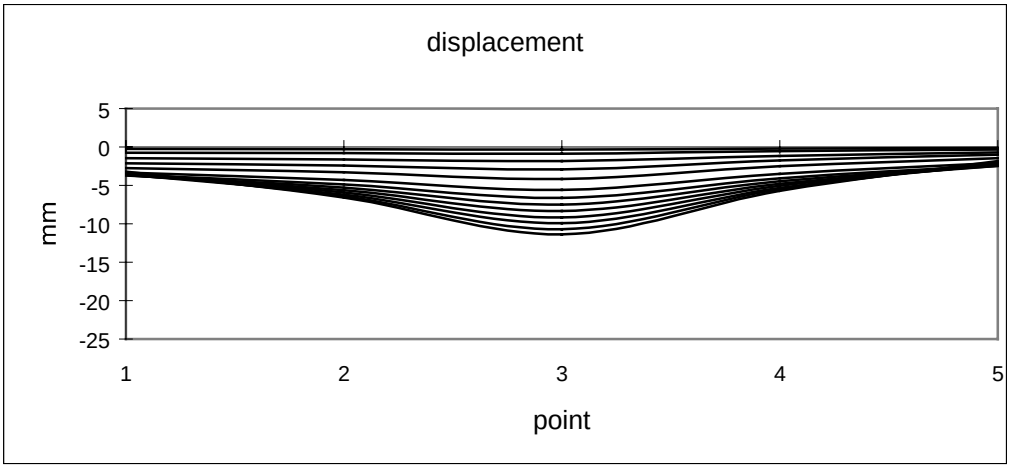

Displacement for S3 loaded in the middle. Load 10, 25, 50, 75, 100, 125, 150, 175, 200, 225, 250, 275, 300 kN.
Figure 6.26 g

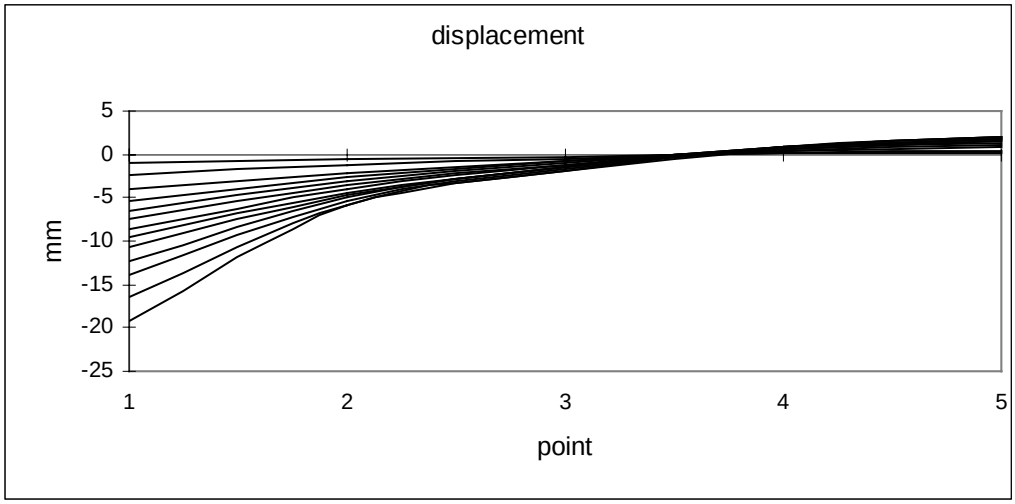

Displacement for S3 loaded at edge. Load 10, 25, 50, 75, 100, 125, 150, 175, 200, 225, 250,275, 290 kN
Figure 6.26 h

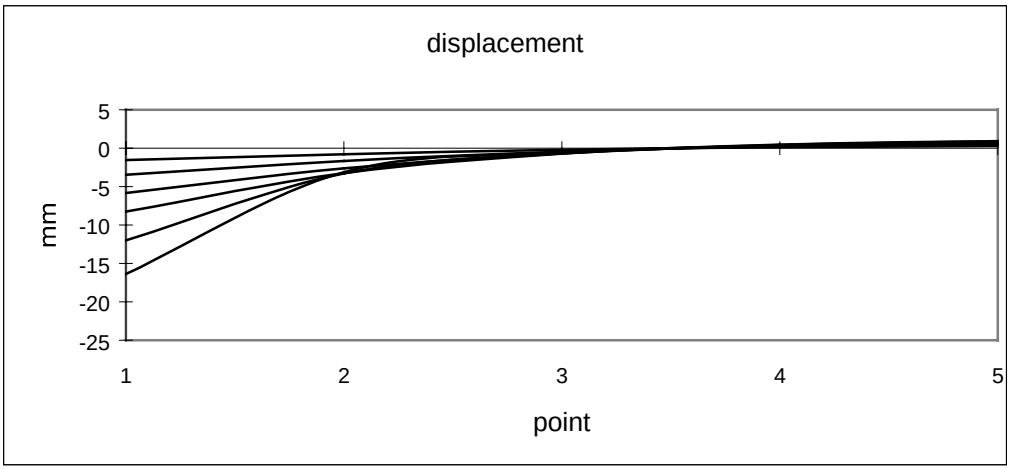

Displacement for S3 loaded in the corner. Load 10, 25, 50, 75, 100, 125 kN
Figure 6.26 i

For load in the corner, the deflections were measured in the opposite corner. This dial gauge gave a positive deflection on 0.5 mm at maximum load. The maximum deflections after unloading were:

S1	Load in the middle	7 mm in point 3
	Load at the edge	2 mm in point 1
	Load in the corner	6 mm in point 1
S2	Load in the middle	3 mm in point 3
	Load at the edge	3 mm in point 1
	Load in the corner	4 mm in point 1
S3	Load in the middle	4 mm in point 3
	Load at the edge	4 mm in point 1
	Load in the corner	4 mm in point 1

To evaluate the results, a simple control of the deflections can be done by comparing the vertical strain in the insulation layer by the following equations:

$$\varepsilon_1 = \frac{\Delta L}{L} \tag{6.2}$$

and

$$\varepsilon_2 = \frac{\sigma}{E} \tag{6.3}$$

For S2 with a load of 150 kN the measured deflection is 7 mm. This gives $\varepsilon_1 = 17.5\,{}^{o}/_{oo}$ when the sub-base is 400 mm thick. With a load area of L/4 x L/4 = $1000 \cdot 1000 = 1 \cdot 10^6\,\text{mm}^2$ and a modulus of elasticity = 12 N/mm^2, $\varepsilon_2 = 12.5\,{}^{o}/_{oo}$. The strains are relatively close, but the result obviously depends on the choice of load area. These strains are inside the linear range in the stress-strain diagram in figure 6.10.

The deflection in S1 with load 150 kN in the middle is much larger than deflection in S2 and S3 at the same load level. The most probable reason is that the sub-base is uneven before the first load case. The subject is further discussed when the results later are compared to finite element analysis.

S3 has a deflection close to deflection in S2 in the middle and at the edge with a load of 150 kN.

6.6.4 Cracking

The cracks at the top surface were marked on the concrete as they appeared. Loads were written on the crack lines and the end of crack from this load was marked perpendicular to the crack. The cracks at bottom of the slab could not be observed, but the strain gauges at the bottom surface and the top surface indicate where and when the cracks occur. The crack width was not measured. There were no cracks on the top surface before loading because there is no restraint and consequently no shrinkage cracking.

6.6.4.1 Slab S1

For all slabs the first load case was in the centre of the slab. Location of strain gauges in S1 are shown in table 6.6 and figure 6.17 and 6.18 above. There were no cracks around the load on the top surface when loading in the middle.

From the measured strains on the bottom surface, figure 6.27, it can be estimated that in point 20, 350 mm from centre of load, the first crack occurs with a load of 28 kN.

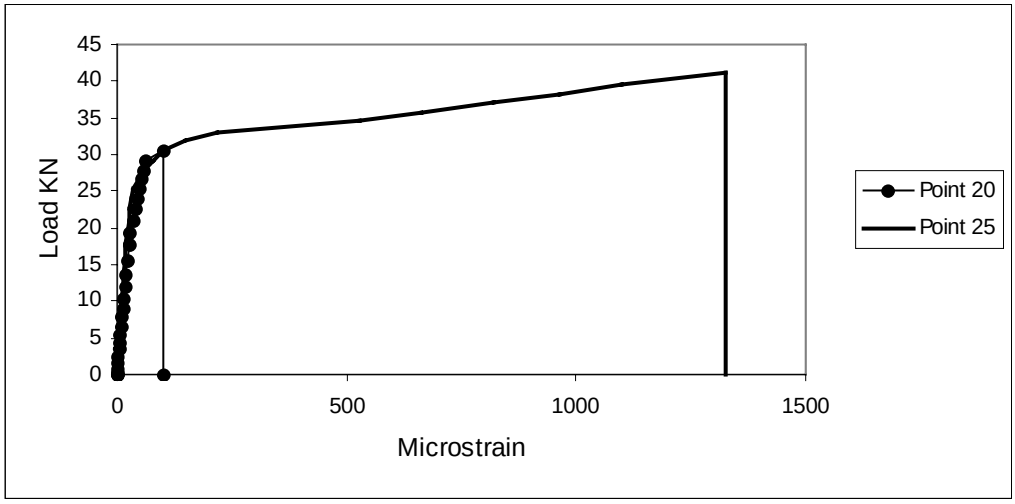

Strain development in point 20 (under the load) and point 25 (at the edge) with load in the middle, S1.
Strain gauges glued to the bottom surface.
Figure 6.27

This was the first crack, and this crack expanded to the edge, where cracks occurred at a load of about 32 kN (100-150 microstrain) in point 25. This crack could at this time also be seen at the vertical side of slab as a crack from bottom to top of the slab. After loading, the slab was lifted up, and it was possible to inspect the bottom surface. There were also some cracks outside the range of the strain gauges, but it is difficult to decide when they occurred. The crack length and form were near equal for all cracks.

For load at the edge, the crack at the edge from the first load step was opening up early, while new cracks occurred at the edge from 30 kN. The distance from centre load was about 300 mm to the first new crack. This load case continued to 200 kN, and during this time there were several cracks at the top surface at a distance of 250 mm to 1000 mm from centre of load. Reinforcement strains are presented in chapter 6.6.5. There were no strain gauges at the top surface or at the top reinforcement at the edge.

In the last load case with load in the corner, the first crack occurs at a load of 30 kN. The crack development can be seen in figure 6.28. The first crack occurred at the edge 600 mm from load centre, and when the load was 73 kN, the crack continued to the other edge. The next crack occurred at a load of 83 - 90 kN at a distance of about 200 mm from the first crack. The distance to the third crack is equal, and it occurred at a load of 90-95 kN. This load case continued to 150 kN. After load 95 kN, there were no more cracks, but the width of the cracks continued to increase.

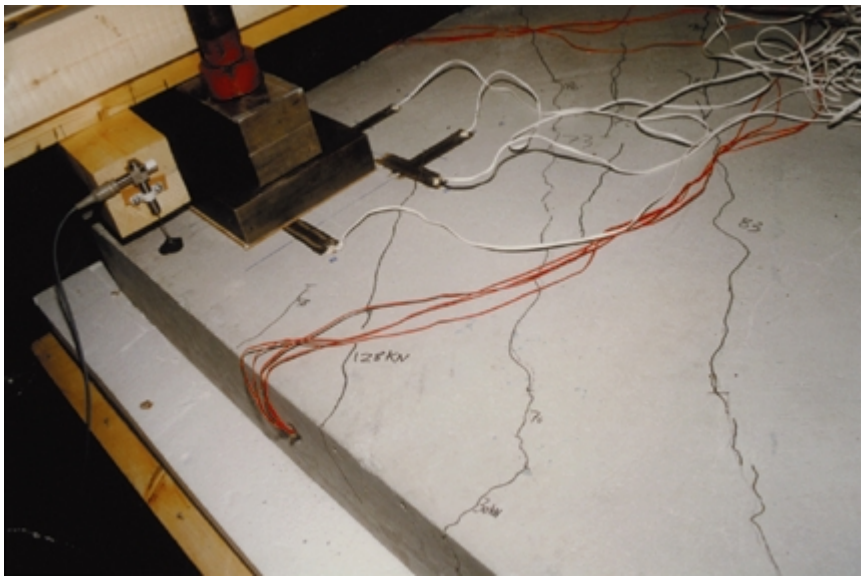

Crack pattern in S1 with load in the corner.
Figure 6.28

6.6.4.2 Slab S2

For this slab with distributed tendons in both directions, (c/c 630 mm), the first crack with load in the centre occurred at approximately 45 kN. The distance from load centre was 50 mm. Cracks occur at the edge in point 24 and 25 with a load of about 95 kN, see figure 6.29.

For load case two with load at the edge, the edge crack from the previous load case reopened at a load of about 45 kN (point 24 in the bottom, 200 mm from load centre). In the first load case the strain in this point decreased from about 110 micro strains before maximum load was reached. The observed cracks, at the top surface, started from the tendons 630 mm and 1260 mm from the load. There were also cracks 200 mm to both sides of the tendon that was nearest the load, at 120 kN. These cracks start in the bottom and cross the vertical edge and continued in the top surface. The situation was similar for both sides of the load. This load increases to 250 kN and during this time only one small crack occur in additional, 500 mm long, at a distance of 1000 mm from centre load. See fig 6.30.

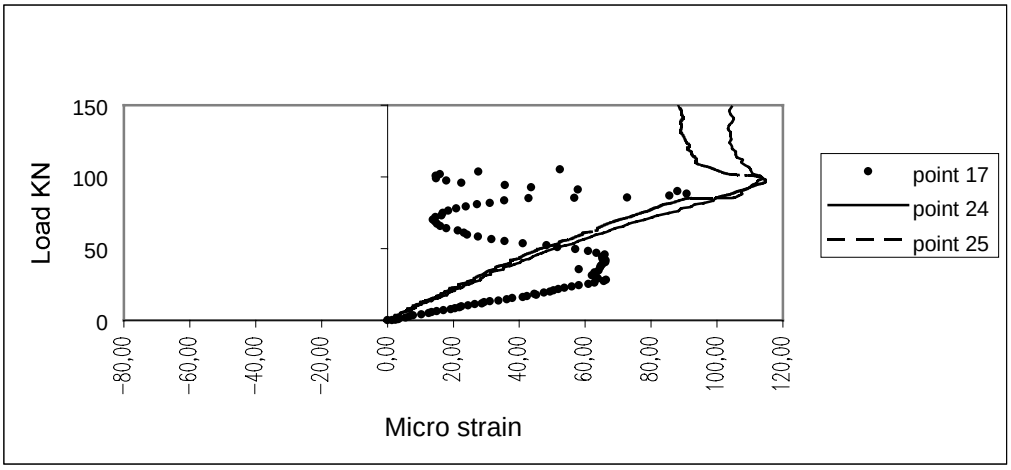

Strains in point 17, 24 and 25 with load in the middle, S2.
Strain gauges glued to the bottom surface.
Figure 6.29

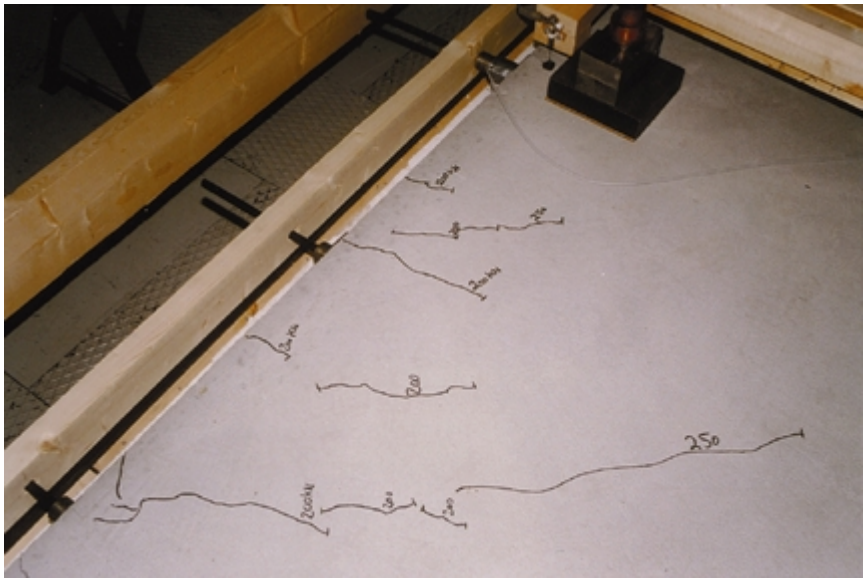

Crack pattern with load at the edge, S2.
Figure 6.30

There were also small cracks at the top of the edge, (vertical side) with a load of 250 kN. These cracks were 100 mm long and ended at the top of anchorage of tendon, 1260 mm from load. The angle of this crack was 45 ^{o} from the vertical.

When loading in the corner, the first observed crack at the top surface, occurred with a load of 107 kN and this crack further developed with a load of 110 kN, see fig 6.31. Because the strain gauges in the corner were placed too close to the load, the strain in the gauges are nearly constant due to the compressive force from tendons.

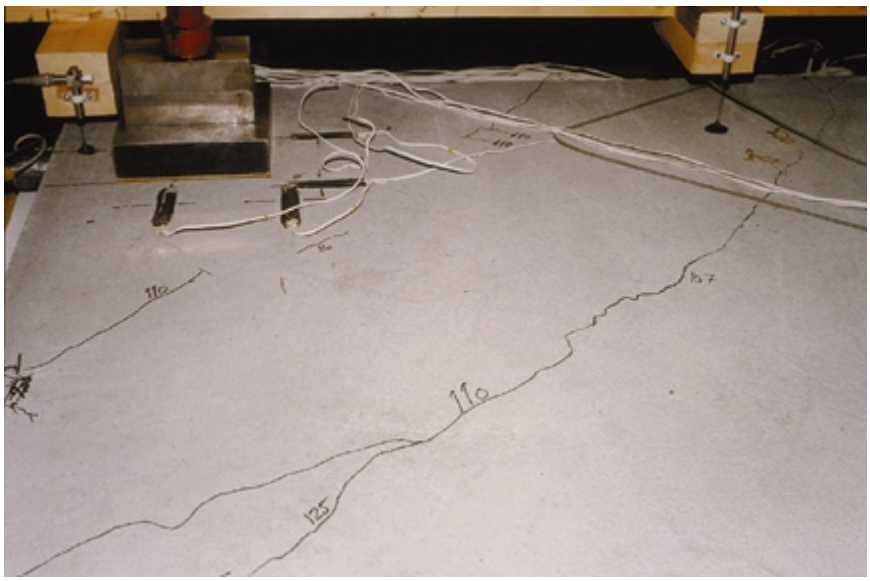

Crack pattern with load in the corner, S2.
Figure 6.31

Two cracks start with the tendons, 630 mm and 1260 mm from the load centre and the crack, 1260 mm from the load, goes to the other edge and ends by the tendons. The load was increased to 150 kN and that does not give any new cracks, but the external cracks are wide at this time.

6.6.4.3 Slab S3

In this slab the tendons are distributed with a distance of 930 mm. The first crack occurred at the bottom surface at a load of about 45 kN in point 20 and the crack reached the edge at a load of about 100 kN in point 25, see figure 6.32. After the test the slab was lifted, and there were other cracks that did not cross the gauges having the same size as the crack that crosses point 18.

The first crack with load at the edge opened at a load of about 60 kN in point 24 (100-150 micro strain) under the load. At the top surface the first crack occurred at a load of 150 kN at a distance of 930 mm from the load, which means at the tendon next to the tendon under the load. When the load increased to 220 kN the crack developed further around the load, see fig 6.33, and when the load increased to 270-280 kN two new similar cracks appeared. As in S2 there was a crack under the load at the vertical side of the edge, at an angle of 45 ^{o} and this occurs at a load of 240 kN.

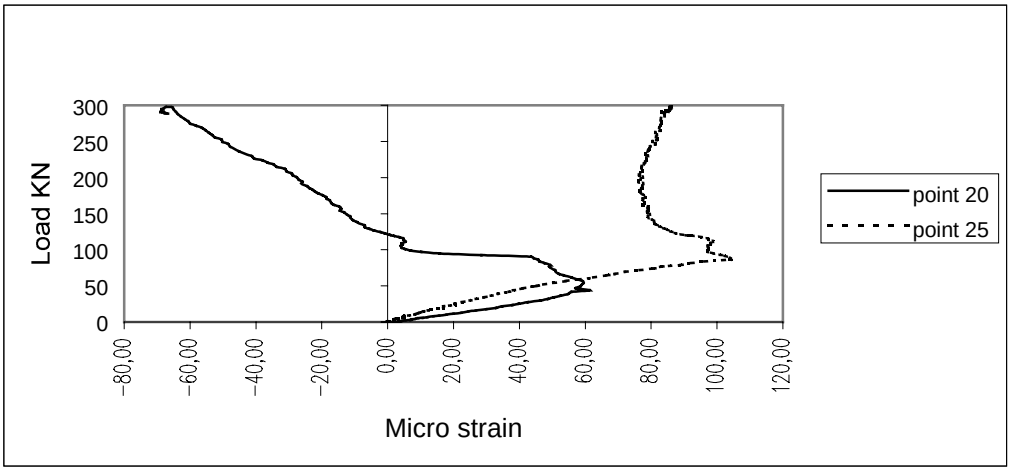

Strain in point 20 and 25 with load in the middle, S3.
Figure 6.32

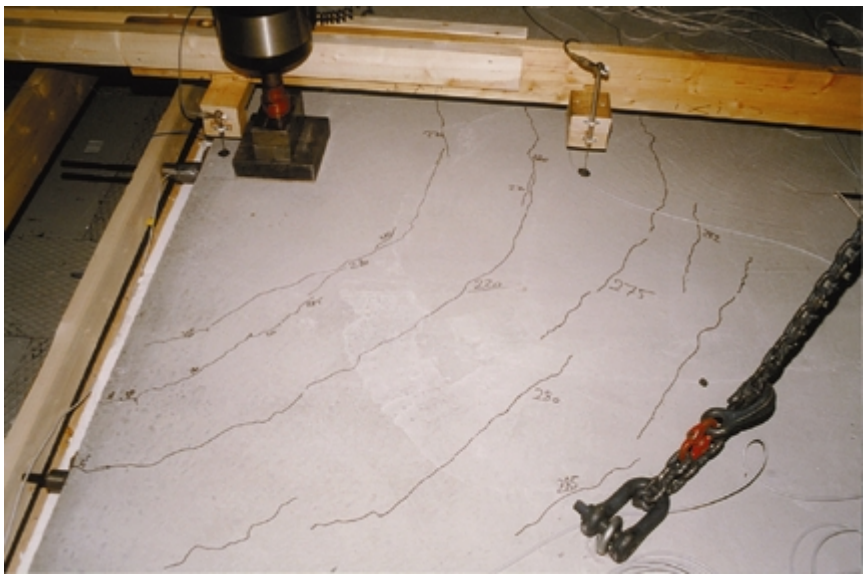

Crack pattern with load at the edge, S3.
Figure 6.33

When loading in the corner the first crack occurred at a load of 75 kN. This crack started by the tendon next to the tendon under the load. With a load of 78 kN this crack crossed the corner and ended by the tendons at the other edge. From this time and until maximal load of 125 kN there were only a few small cracks that occurred at a load of 110 kN. The crack pattern is shown in figure 6.34.

Crack pattern with load in the corner, S3.
Figure 6.34

6.6.5 Steel strain development in slab S1

As previously explained strain gauges were glued to both sides of the reinforcement to determine the average strain. In this test the strain gauges from one side to the other of an 8 mm reinforcement bar, has a maximum difference in point 4 with load in the corner (reinforcement in top in the corner). The average difference in strain from the two sides of reinforcement bar, is about 0.18 $^{o}/_{oo}$ when the load level is 50% of maximum load. The location of the strain gauges can be seen from figure 6.17. Strain development for all gauges is included in appendix B.

6.6.5.1 Load in the centre

Strains in top reinforcement in the centre of the slab have a maximum of 0.34 $^{o}/_{oo}$ in x-direction (point 1) at the maximum load of 150 kN. In y-direction the maximum value, -0.13 $^{o}/_{oo}$, is reached at a load of 82 kN (point 2) before the strains decrease until maximum load. Reinforcement strains in the corner were negligible in this load case. In the bottom reinforcement the maximal strain occurs with maximal load. Strains in point 7 and 8, under the load centre, have a maximum of 1.05 $^{o}/_{oo}$ and 1.6 $^{o}/_{oo}$. At the same time point 9 at a location 200 mm from load centre, has a strain of 0.37 $^{o}/_{oo}$. Point 12 at the same distance from load centre, but in perpendicular direction, has a strain of 0.55 $^{o}/_{oo}$. At a distance of 350 mm from load centre the strain was measured to 0.2 $^{o}/_{oo}$ in y-direction while it was negligible in x-direction. The strain development in these points are presented in figure 6.36.

Strain gauges at the edge give only small strains except for point 16, which is located 500 mm from the centre line of the slab. In this point the strain is 1.1 $^{o}/_{oo}$ at maximum load.

Figure 6.35 indicate that the concrete in point 8 cracked at a load in the range 25 - 30 kN.

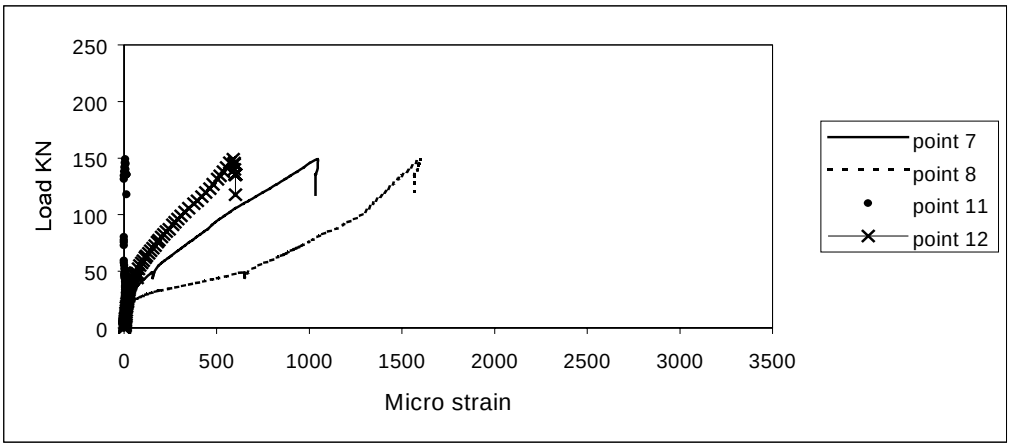

Reinforcement strain in point 7, 8, 11 and 12 with load in the middle.
Figure 6.35

6.6.5.2 Load at the edge

Only strain gauges at the bottom reinforcement were installed at the edge. The strain in the top reinforcement in the middle, was 0.18 $^{o}/_{oo}$ in x-direction with maximum load of 200 kN, while it was negligible in y-direction. The reinforcement strains in the corner were also negligible. The bottom reinforcement strains in point 7, 9 and 10 which lie at the slab's centre line, have a maximum strain of -0.1 $^{o}/_{oo}$ in point 7. Perpendicular to this line in the middle of the slab, the strains in point 8 has a maximum of 0.4 $^{o}/_{oo}$. Reinforcement strains in the bottom of the slab at the edge are shown in figure 6.36. It is important to notice that point 16 has a crack from the first load case with load in the middle.

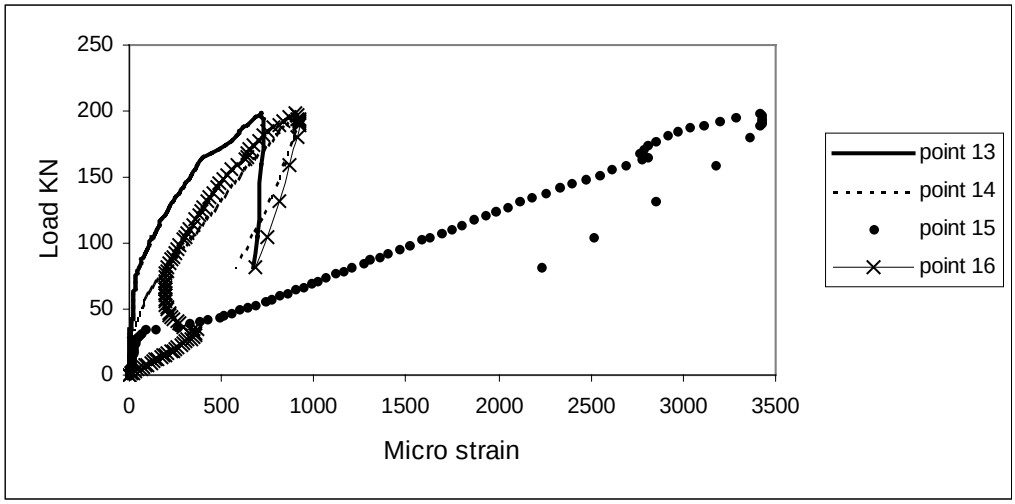

Reinforcement strain in point 13, 14, 15 and 16 with load at the edge.
Figure 6.36

6.6.5.3 Load in the corner

For this load case the top and bottom reinforcement strains in the middle of the slab were negligible. Strain in the bottom reinforcement in the corner is positive. Strains in top reinforcement in the corner vary from 1.1 to 2.5 $^{o}/_{oo}$ in point 3, 4, 5 and 6, see figure 6.37. At the edge point 15 and 16 parallel to the edge and in the middle of the edge length, have strains about -0.25 $^{o}/_{oo}$.

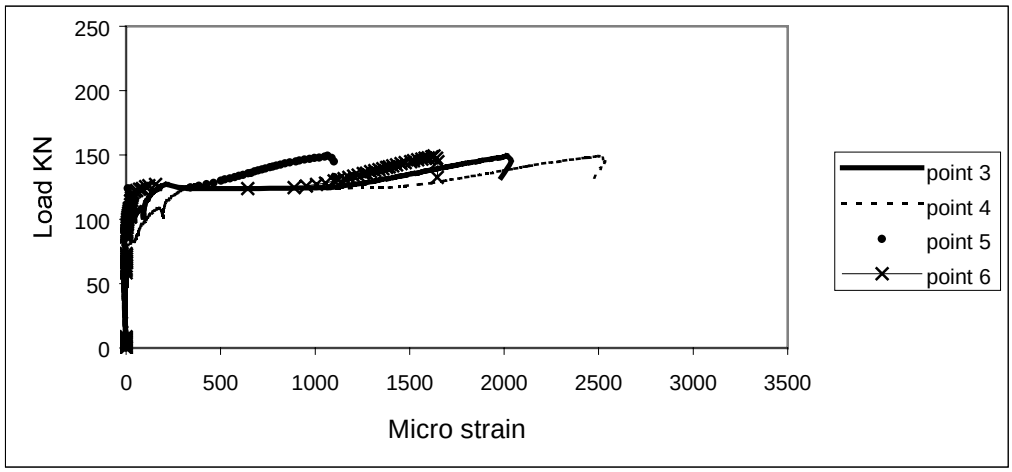

Strain in reinforcement point 3, 4, 5 and 6 with load in the corner.
Figure 6.37

6.6.6 Concrete strain

Location of strain gauges at the bottom and top surface were the same for all slabs, and can be seen from figure 6.18 for S1, and 6.19 for S2 and S3. Strains in concrete are dependent on the position of the gauges related to the cracks.

6.6.6.1 Slab S1

With load in the centre, the strains in point 27 and 28 located at the top surface 50 mm from the centre, increase similarly and end at -1.0 $^{o}/_{oo}$ for the maximum load of 150 kN. The strains decrease rapidly with increasing distance from load centre, as shown in figure 6.38. The strain in the corner is negligible in this load case.

With load at the edge there is a linear increase of strains in points at the top surface that lie on a line from the load point to middle of slab. Maximal strain is in number 27 in the middle of the slab, that point is the farthest from load, and has a strain of 0.12 $^{o}/_{oo}$ with a load of 184 kN. The location for maximum strain is in agreement with figure 6.26 b, deflection with load at the edge. With a more compacted subgrade, a smaller deflection and therefore a smaller strain in the top surface in the middle of the slab is expected.

The strains at top surface in the corner, and bottom surface in the middle, are negligible in this load case. Strain around the load in bottom surface is about 1.0 $^{o}/_{oo}$ with a load of 200 kN.

For load in the corner, the strains in the bottom and top surface in the centre of the slab and by the edge in the bottom are negligible. The strains around the load, recorded in point 31 to 34 at the top surface vary from -0.12 $^{o}/_{oo}$ to -0.31 $^{o}/_{oo}$.

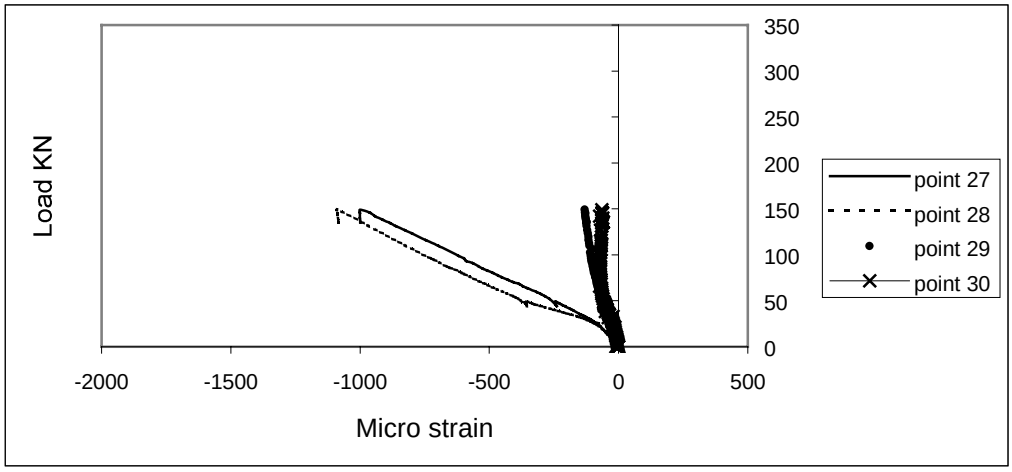

Reinforcement strain in point 27, 28, 29 and 30 for the case with load in the middle, slab S1.
Figure 6.38

6.6.6.2 Slab S2

The expected strain from the distributed tendons only was for this slab about 60 – 70 micro strain. It was also expected some strain from 7 mm eccentricity of tendons, about 15 - 20 micro strain. In figure 6.24 above, it can be seen that after the last stressing the strain in top surface end at 40 micro strain. This includes also strains from drying in concrete.

For the case with load in the centre, the strains under the load at point 1 and 3 at the top surface increase linearly with increasing load to -1.45 $^{o}/_{oo}$ and –1.15 $^{o}/_{oo}$. The strains decrease with increasing distance from load centre and in point 7 they are negligible, see figure 6.39.

With load 300 kN, 200 mm from centre load in the bottom surface, point 18, the strain is 0.1 $^{o}/_{oo}$ and 350 mm away, point 19, the strain is zero. The latter strain decreases to –0.13 $^{o}/_{oo}$ with a load of 270 kN. Strains at the edge have a maximum of 0.12 $^{o}/_{oo}$ in direction parallel to the edge.

In figure 6.38 strain in the middle of the slab, top surface S1, are shown. If these strains are compared with strains in figure 6.39, it can be seen that strains with a load of 150 kN in point 3 (S2) and point 28 (S1) are – 0.65 $^{o}/_{oo}$ and –1.1 $^{o}/_{oo}$. If cracks start at about 150 micro strain, it can be seen that in S1 cracking starts with a load of 30 kN, while it in S2 starts with a load of 45 kN.

With load at the edge the strain for load level 245 kN under the load in point 22 is 0.12 $^{o}/_{oo}$. Point 24 has a maximum of 0.2 $^{o}/_{oo}$ with a load of 145 kN, before the strain decreases while load still increases. This is due to a crack beside of the strain gauge.

When loading in the corner, the strain at the top surface in the middle is negligible. Point 9 to 15 has a jump in strain when the load was 128 kN. This is because a crack occurred at this time, see fig 6.31 chapter 6.6.4.2. There are only small variations in strain at the bottom of the slab when loading in the corner.

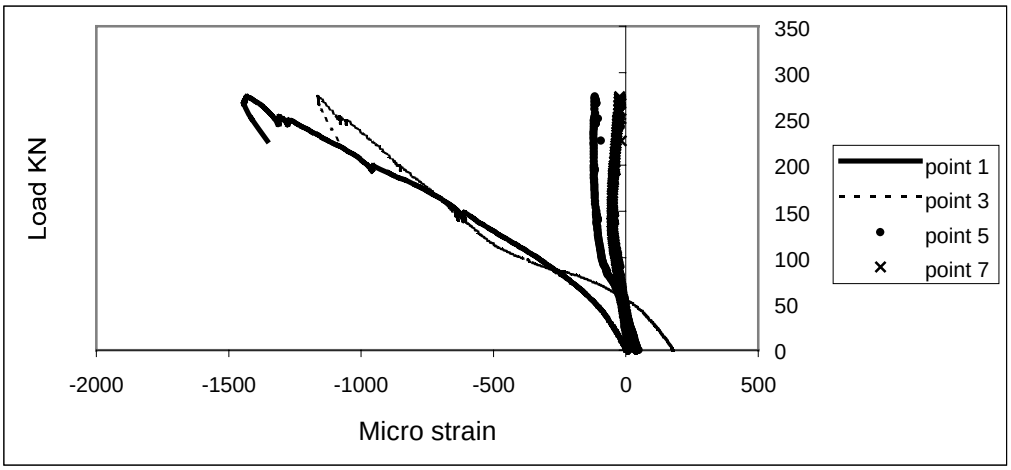

Strain in concrete surface point 1, 3, 5 and 7 with load in the middle, S2.
Figure 6.39

6.6.6.3 Slab S3

Load in the middle of slab S3, gives strains at the top surface of point 1 and 3 of -1.2 $^{o}/_{oo}$ and -1.7 $^{o}/_{oo}$ with a maximum load of 300 kN. At the two other points in the middle of top surface, the maximum strain was reached for a load of 150 kN. This strain was -0.23 $^{o}/_{oo}$ for point 7. At the other point in top surface there was negligible change in strain in this load case, see figure 6.40. At the bottom surface the strains under load increase until about 90 kN, and then decreases until zero strain for point 16, and -0.14 $^{o}/_{oo}$ for point 17. Point 19, 20 and 21 have the same tendency as point 16 and 17. The points at the edge and parallel to this have a maximum strain of 0.2 $^{o}/_{oo}$.

With load at the edge, the strains increase to 0.2 $^{o}/_{oo}$ in point 1, and decrease to -0.2 $^{o}/_{oo}$ in point 3. In point 5 the strain increases to a maximum of 0.45 $^{o}/_{oo}$. In bottom surface in the middle the change in strain is small, with a maximum of -0.15 $^{o}/_{oo}$ in point 19. Under the load the strain in point 22 is 0.14 $^{o}/_{oo}$, point 23 yields at a load of 236 kN. Point 24, parallel to the edge, has a maximum strain of 0.28 $^{o}/_{oo}$ at a load of 130 kN.

The last load case with load in the corner gives negligible strains in the top surface in the centre of the slab. Around the load it gives a maximum strain of -0.25 $^{o}/_{oo}$ in point 11. In the bottom surface this load gives only small strains.

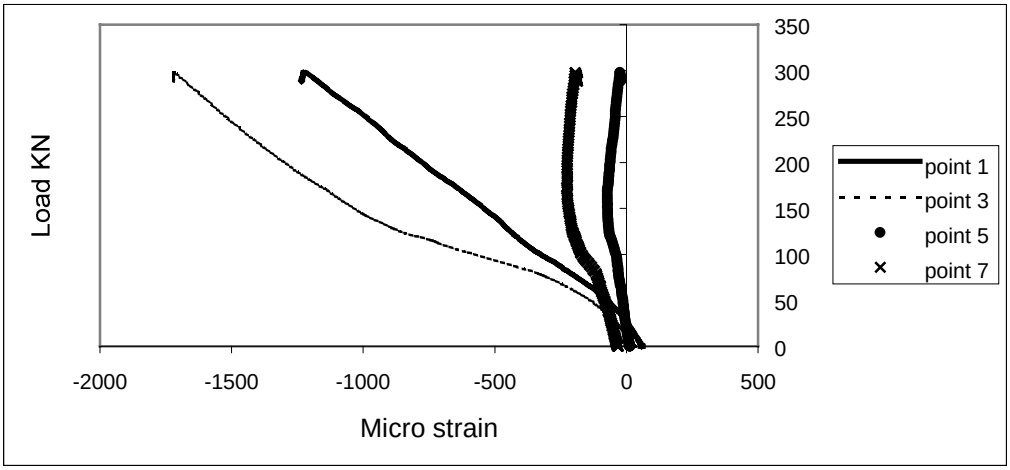

Strain in the concrete surface point 1, 3, 5 and 7 with load in the middle, S3.
Figure 6.40

6.6.7 Summary and discussion of test results

In this test, three slabs on ground were tested, slab S1 was reinforced at top and bottom, while slab S2 and S3 were prestressed with unbonded tendons.

For S1, with load in the middle, the first crack in the bottom occurred at a load of 28 kN. At 32 kN the crack had expanded to the edge. Deflection under the load was 14 mm with a maximum load of 150 kN, and the corresponding deflection at the edge, 2000 mm from load centre, was 3 mm.

With load at the edge, maximum strain in reinforcement at a maximum load of 200 kN, was 3.5 $^{o}/_{oo}$ 180 mm from the edge. The strain increases linearly from a load of 30 kN. Deflection under the maximum load was 10 mm. This is a considerably smaller deflection than with load in the centre, which most probably is due to that the insulation in the first load case was not well enough compressed before loading started. With load in the corner, the first crack occurs with a load of 30 kN at a distance of 600 mm from the load centre, and when the load was 73 kN the crack crossed the corner. Maximum deflection was 22 mm under a load of 150 kN.

Slab S2 was loaded until 45 kN in the centre before the first crack occurred in the bottom of the slab. This slab was loaded until 270 kN, and this crack was the only one registered by the strain gauges at the bottom of the slab. Deflection under maximum load was 11.5 mm. When loading at the edge, crack from the previous load case reopened with a load of 45 kN, and these cracks started by the tendons 630 mm and 1260 mm from load centre. Maximum deflection under the load was 12 mm with a load of 250 kN.

When loading in the corner the first crack occurred at a load of 107 kN, and this crack crossed the corner with a load of 110 kN. This crack started by the tendons 630 mm and 1260 mm from the load centre. Maximum deflection occurred when the load was hold constant at 150 kN, and was measured to 18 mm.

S3 was loaded until 300 kN in the middle of the slab. The first crack occurred with a load of 45 kN. This crack was the only one registered from strain gauges in the bottom of slab. Deflection with maximum load was 11.5 mm in the middle of the slab. When loading at the edge, the first crack in the bottom occurs at 60 kN. At the top surface the first cracks start with a load of 150 kN, and with a load of 220 kN this crack describes a circle around the load. This crack starts from the tendon next to the tendon under load. The maximum deflection occurs with maximum load of 290 kN.

For corner load the first crack occurred at a distance of 930 mm from load. This crack started at 75 kN, and for 78 kN the crack crossed the corner. Maximum deflection under the load was 16 mm with a load of 125 kN.

Figure 6.41 to 6.45 show deflections for different load cases. Figure 6.41 and 6.42 show evident differences from reinforced to prestressed slabs, but a major problem is the influence of the uncertain sub-base stiffness. Furthermore it is also strange that deflection in S3 is smaller than in S2 with load in the middle. With load at the edge and in the corner, deflections are close for all three slabs.

Figure 6.46 presents strain development in the top surface. The strains in S1 start at zero since this slab is reinforced with ordinary reinforcement bars. It is also seen that S3 with 930 mm between tendons has larger stiffness than S2 with tendon spacing 630 mm, which is in agreement with the measured deflections.

Deflection and strain results show that the insulation stiffness influence the results, for instance since the deflections in S2 with most tendons, are higher than in S3. Figure 6.47 to 6.49 show development of deflection with increasing load. Figure 6.47 shows the same as figure 6.41, slab S1 has much larger deflection under load, with load in the middle, than S2 and S3. With load at the edge, the deflections are quite close, see figure 6.48, S1 and S2 have nearly equal results, while S3 has somewhat higher deflection. With load in the corner, fig 6.49, the deflection in S2 is somewhat lower than in the other slabs.

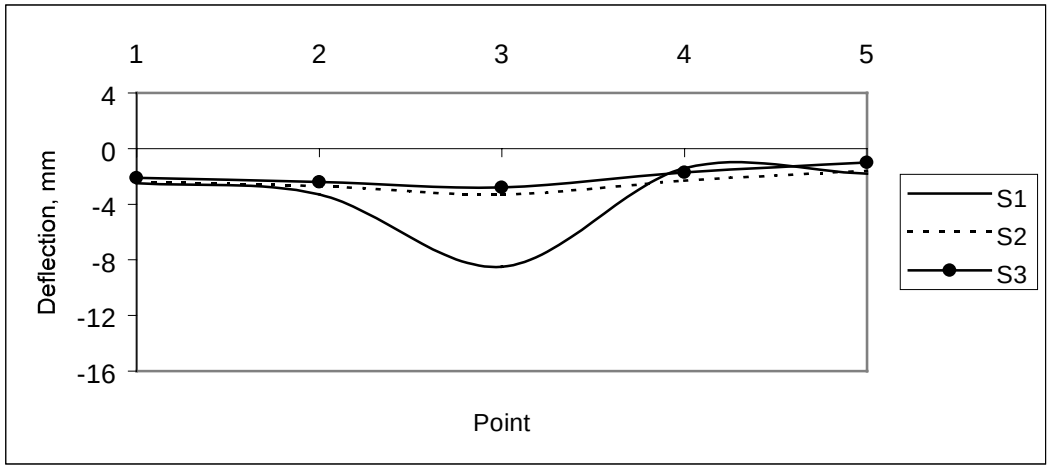

Deflection in the slab with centric load 75 kN.
Figure 6.41

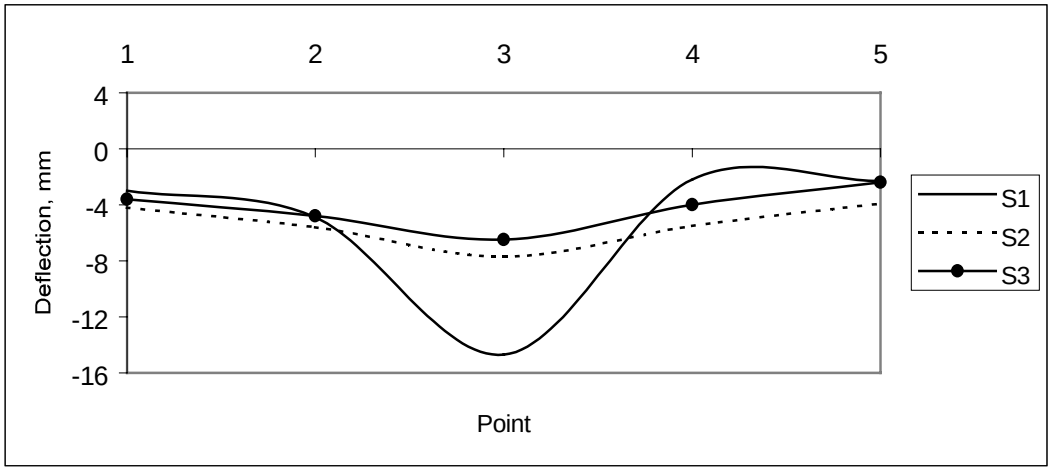

Deflection in the slab with centric load 150 kN.
Figure 6.42

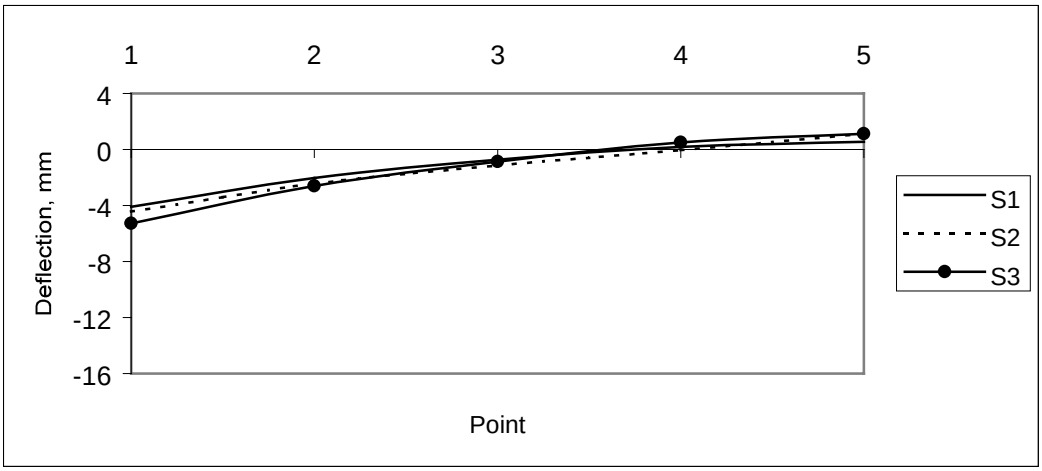

Deflection in the slab with load 75 kN at the edge.
Figure 6.43

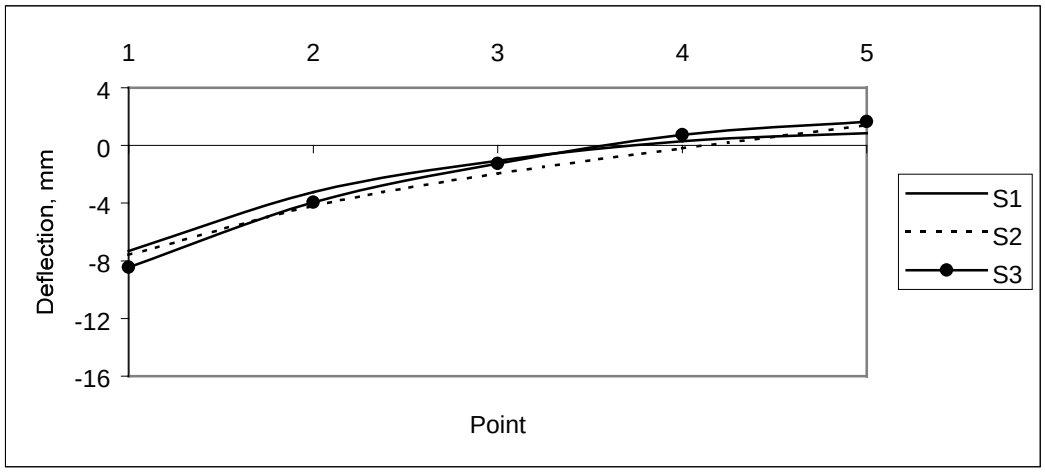

Deflections in the slab with load 150 kN at the edge.
Figure 6.44

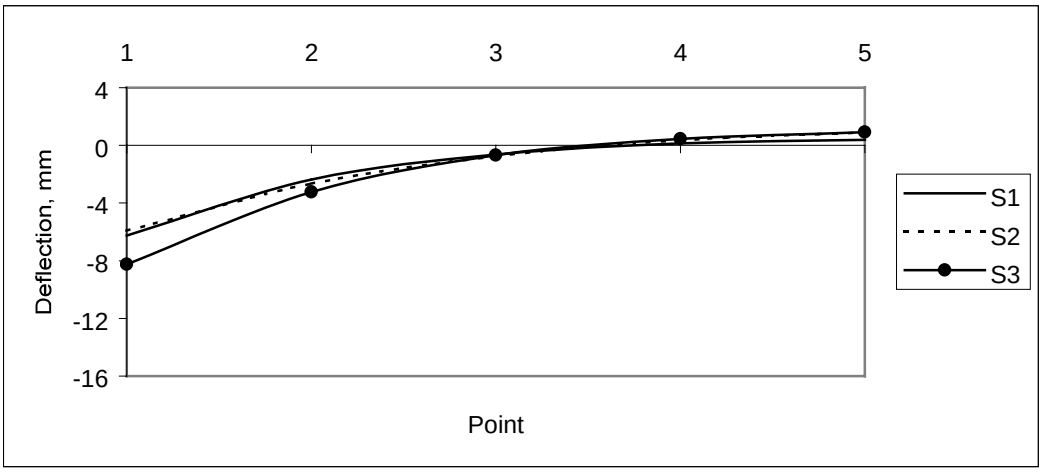

Deflections in the slab with load 75 kN in the corner.
Figure 6.45

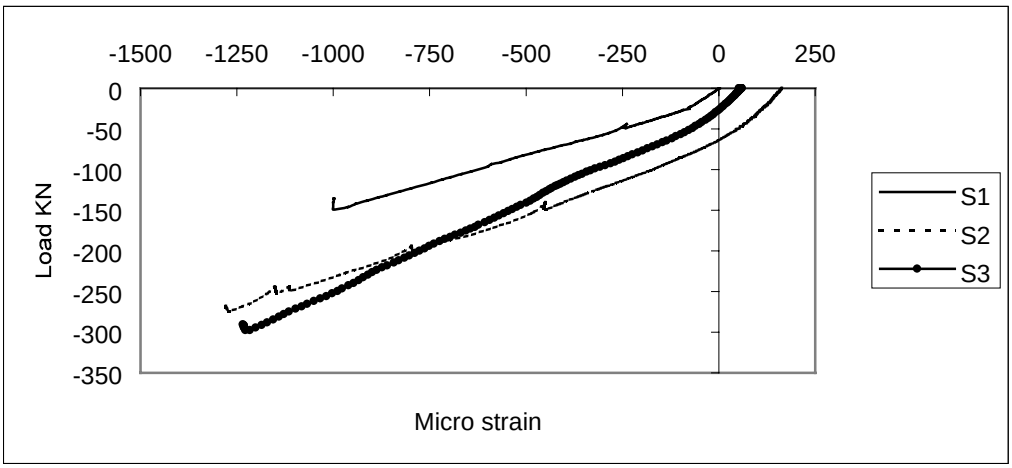

Strain in the top surface by the load when loading in the middle of the slab.
Figure 6.46

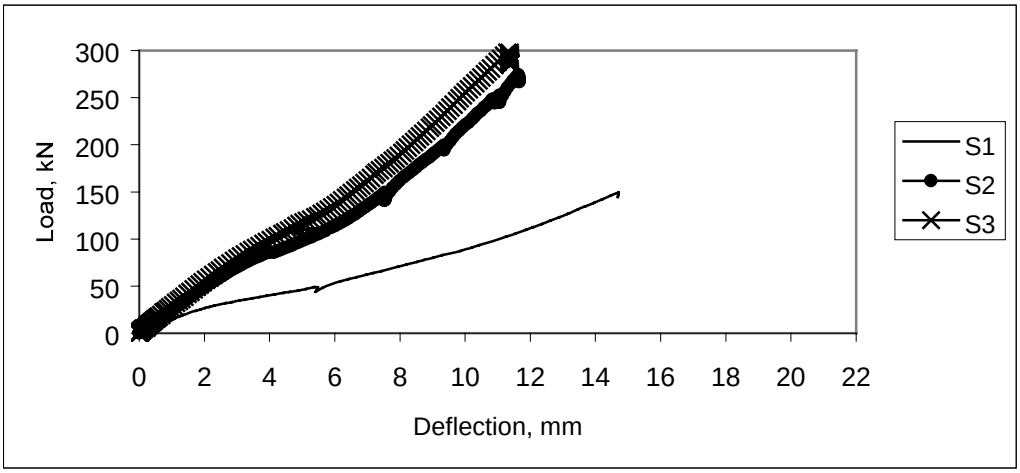

Development of deflection under load, with load in the middle.
Figure 6.47

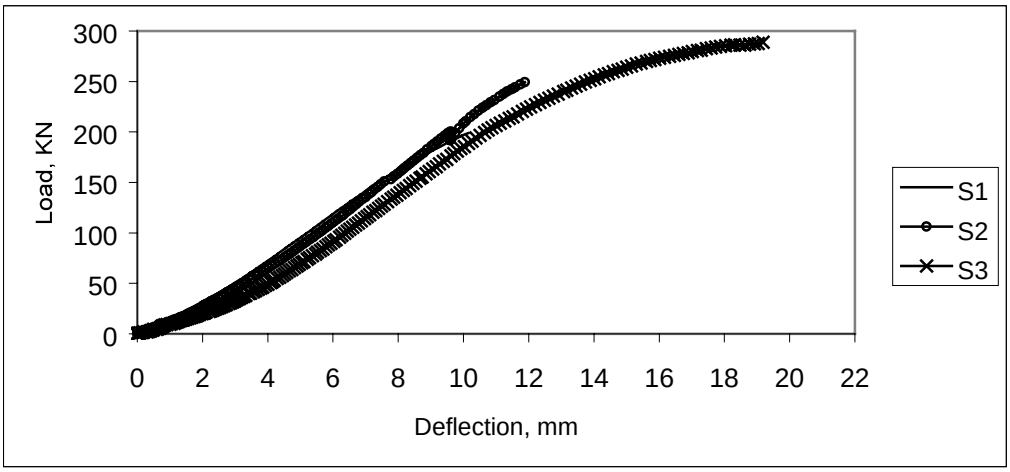

Development of deflection under load, with load at the edge.
Figure 6.48

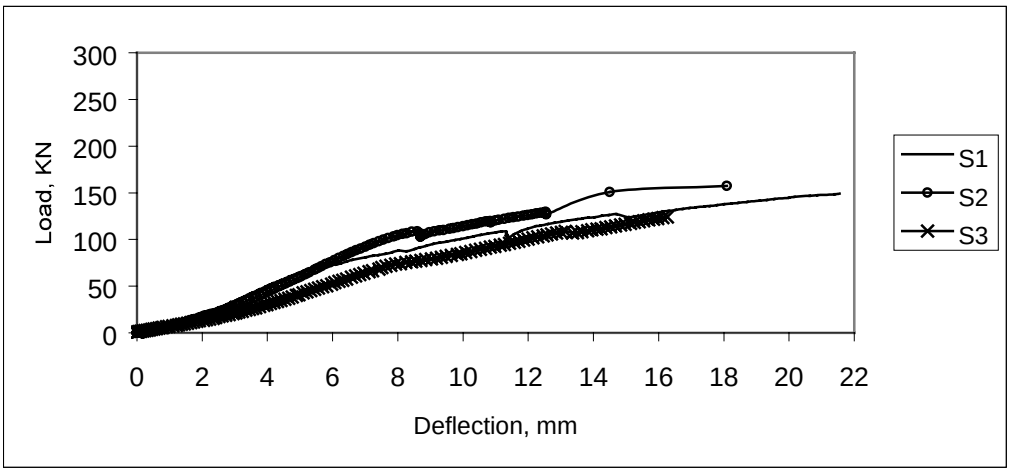

Development of deflection under load, with load in the corner.
Figure 6.49

6.6.8 FE analysis of slabs on ground

The three slabs were analysed with the FE program “Diana”. To simulate concrete a shell-element termed Q20SH was used, and an interface element Q24IF was used to simulate sub-base /52/. Q20SH is a four-node quadrilateral isoparametric curved shell element based on linear Gauss integration over the element area, which is previously described in chapter 4.9.2. Q24IF is an interface element between two planes in a three-dimensional configuration. The element describes a relation between tractions and displacements across the interface. The default integration scheme for the Q24IF element is 2 x 2 Gauss.

The prestressed slabs, S2 and S3, are analysed with a distributed load from prestressed tendons at the edge. This load is given in a grid and starts from an anchorage, which must be positioned at an end point of the reinforcement. Both end points have to be anchored. The initial stress in x- and y-direction must be given, and in this test the stress is reduced with theoretical prestress loss. It is also possible to calculate this loss

in the finite element analysis. This is discussed in the chapter considering flat slabs. Since all three load cases not are symmetrical, the whole slab was modelled. The slab was divided into 256 elements in a mesh, see figure 6.51. With centric load the four elements in the middle were loaded. Two elements were loaded for edge load, while only one element was loaded for corner load. This gives a load area of 200x200 mm^2 in each load case, see figure 6.52. Element size varies from 100x100 mm^2, to 400x400 mm^2. Sequence of loading was first self-weight, then load from prestressed tendons, and finally point load in steps of 1 kN.

The modulus of subgrade reaction, k-value, was previously in chapter 6.3.3 calculated to 0.03 N/mm^3. In table 6.8 the most important input data used in the finite element analysis are given. In appendix B, a more complete description of the input data is given.

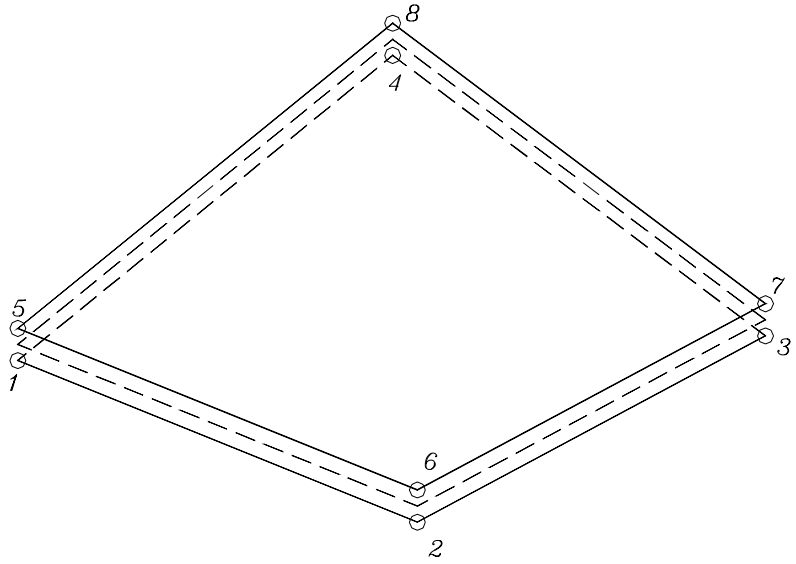

Topology of a Q24IF element.
Figure 6.50

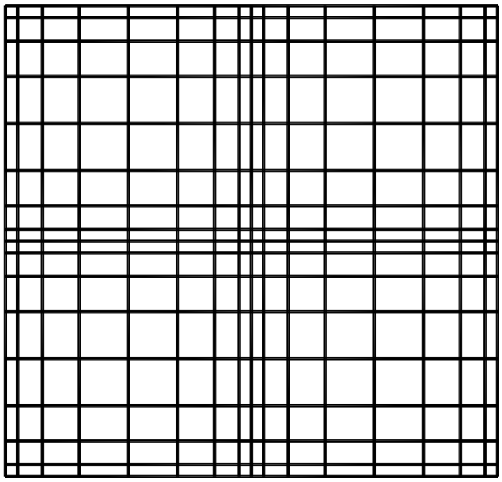

Slab divided in mesh, FE analysis.
Figure 6.51

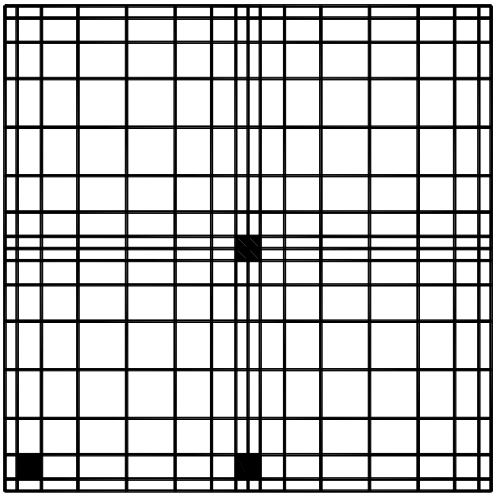

Loaded element in FE analysis.
Figure 6.52

To describe the post-cracking behaviour, the tension softening model shown in figure 6.53 is used. The tensile strength is 3.0 N/mm^2. This is close to the tensile strength calculated from MC /33/, 3.06 N/mm^2, with measured splitting strength from S3 after 28 days. The tensile strength calculated after NS 3473 /9/, is 2.27 N/mm^2.

Concrete		
	Modulus of elasticity	25000 N/mm^2
	Poisson's ratio	0.2
	Concrete yield stress	30.0 N/mm^2
	Thickness	150 mm
	Post cracking stress / strain diagram σ_{nn} / ε_{nn} (fig 6.55)	3.0 / 0.0 0.5 / 0.00025 0.01 / 0.0025 0.0 / 1000.0
Sub-base		
	k-value	0.03 N/mm^3
Tendons		
	Modulus of elasticity	196000 N/mm^2
	Yield value	1860 N/mm^2

Data used in finite element analysis.
Table 6.8

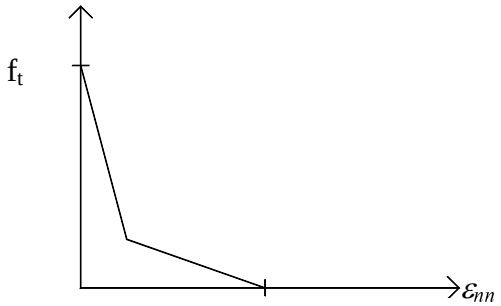

Tension softening model according to the smeared crack method.
Figure 6.53

6.6.8.1 FE analysis of slab S1

For S1 loaded with centric concentrated load, it was not possible to observe cracks visually in the bottom of slab. From the measured strains the crack load was determined to 28 kN. In the FE analysis the first crack starts at 19 kN in the 4 elements below the load. In figure 6.54 the measured and calculated development of strain in the top of slab, is presented. This point is located 50 mm from the centre of the slab. In figure 6.55 the development of deflection under load is plotted. The finite element analysis, did not converge after 212 kN.

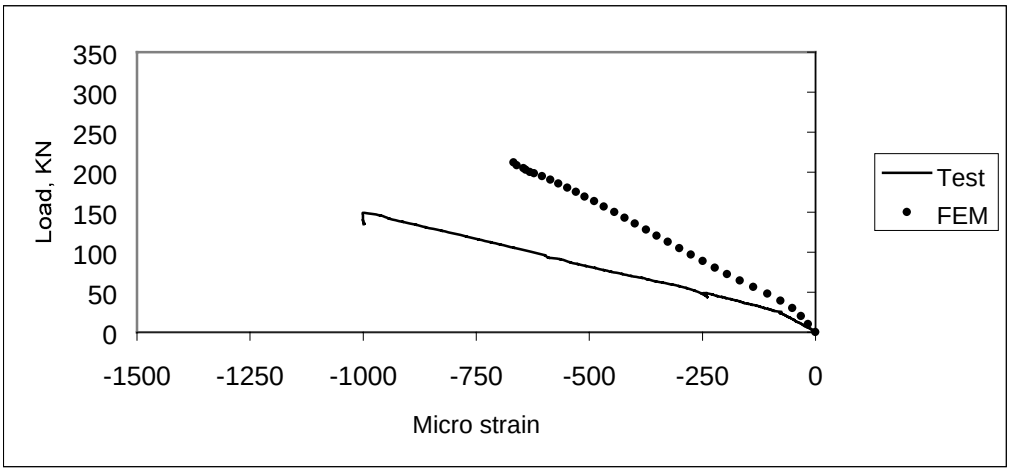

Development of strain under load in the middle, test and FE-analysis, S1.
Figure 6.54

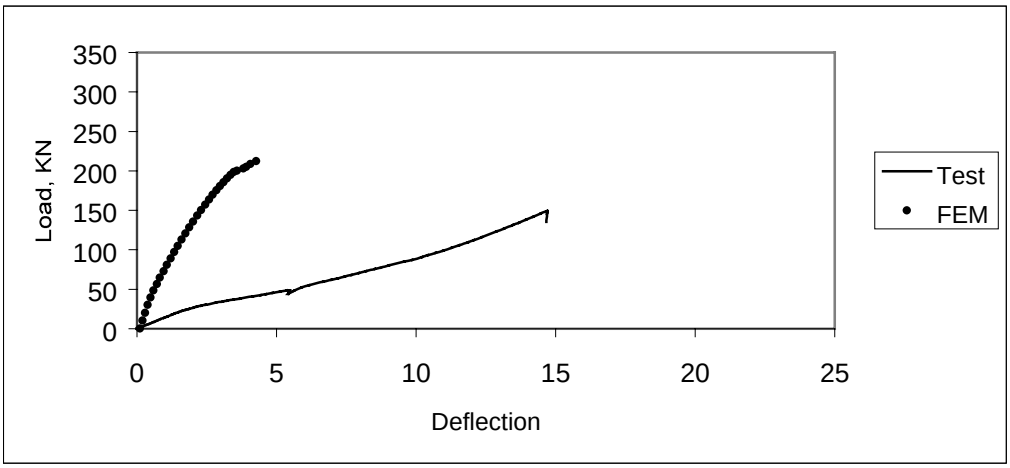

Development of deflection under load in the middle, test and FE-analysis, S1.
Figure 6.55

In the test the first new crack with load at the edge occurs with a load of 30 kN at a distance of 300 mm from load. It is important to note that cracks at the edge from the first load case, load in the middle, opened earlier. Cracks in the FE analysis start at 13 kN in the elements below the load. This crack was closed, and then opened again with a load of 29.5 kN. Since there was no strain gauge on top surface at the edge, only strain in the reinforcement 200 mm from centre load is shown in figure 6.56, and deflection below the load is presented in figure 6.57. The finite element analysis ends at 218 kN, while the test was stopped at 198.8 kN.

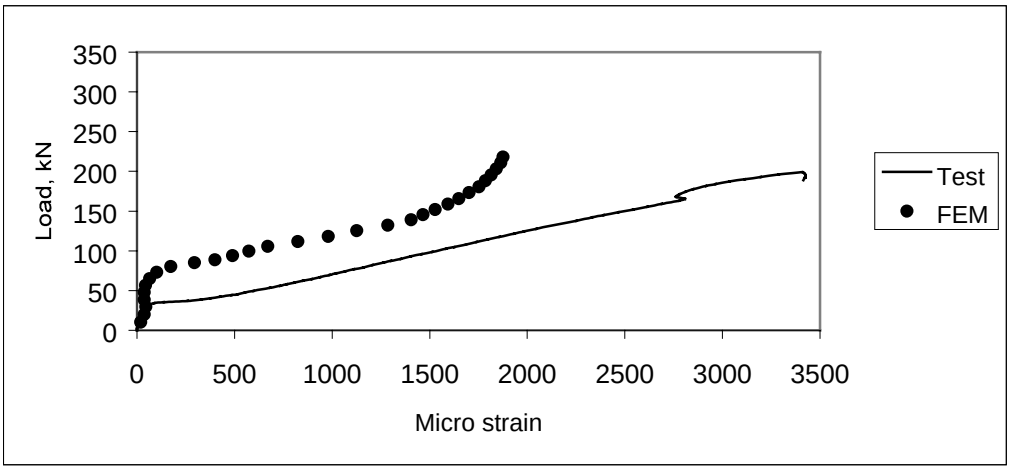

Development of strain in reinforcement under load at the edge, test and FE-analysis, S1.
Figure 6.56

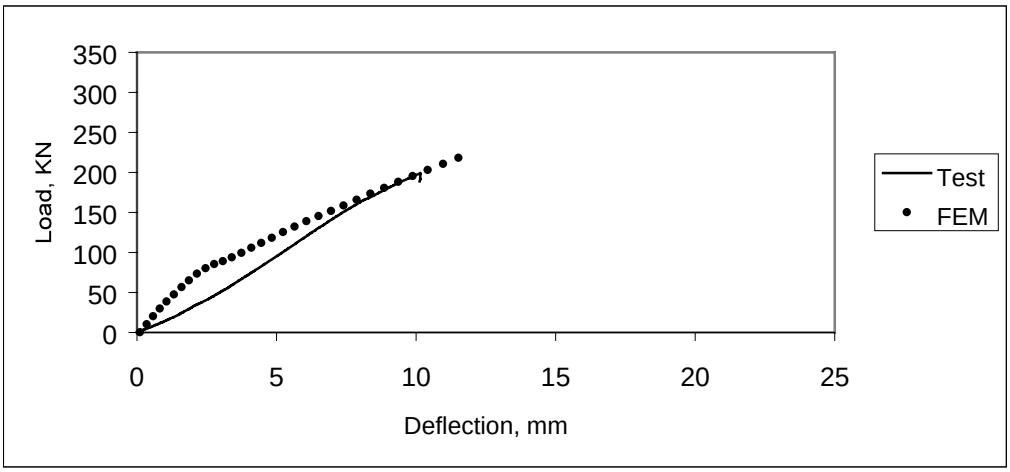

Development of deflection under load at the edge, test and FE-analysis, S1.
Figure 6.57

For the last load case for S1, load in the corner, cracking starts at 30 kN 600 mm from the load. In the analysis the first crack starts at 17 kN, and the distance from load is about the same as in the test. Development of strain and deflections are shown in figure 6.58 and 6.59. In the test, there were no new cracks observed after a load of 95 kN.

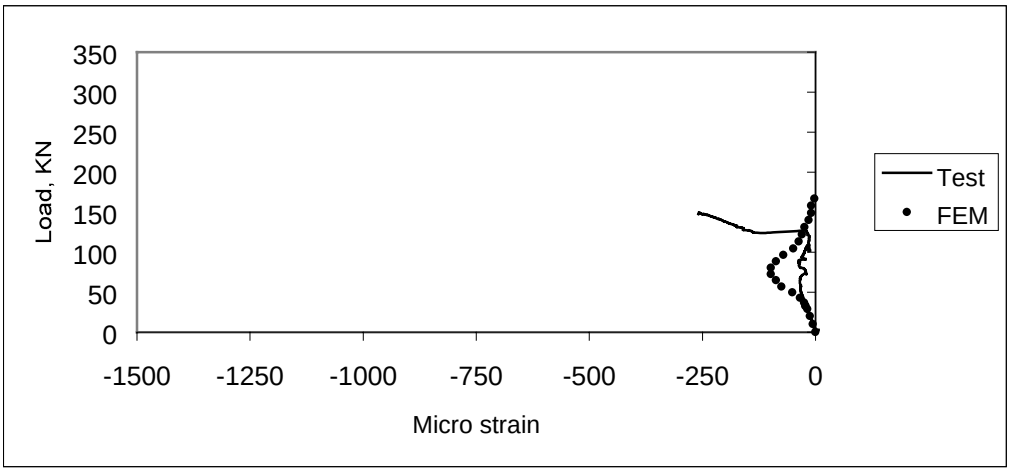

Development of strain under load in the corner, test and FE-analysis, S1.
Figure 6.58

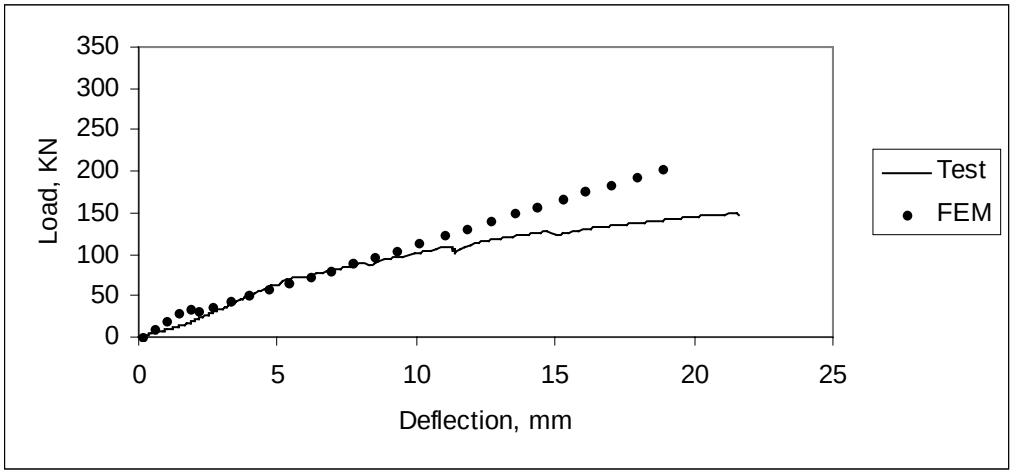

Development of deflection under load in the corner, test and FE-analysis, S1.
Figure 6.59

6.6.8.2 FE analysis of slab S2

In the analysis the first crack, with load in the middle, starts at 41 kN, while strain measurements indicate that this happened at 45 kN. Figure 6.60 and 6.61 compare the measured and calculated strains and deflections.

With load at the edge the crack in the bottom was reopened at a load of 45 kN in the test, and the crack load was 28 kN in the analysis. The observed cracks in the top surface started at the tendons 630 mm and 1260 mm from the load, and increase slowly until load level of 250 kN. The analysis stopped at the maximum load of 232.9 kN.

The first crack in the analysis with load in the corner, starts with a load of 38 kN, while the corresponding crack load was 107 kN in the test. The analysis stopped with a load of 174.1 kN. Figure 6.63 and 6.64 show the development of strain and deflection under load in test and analysis.

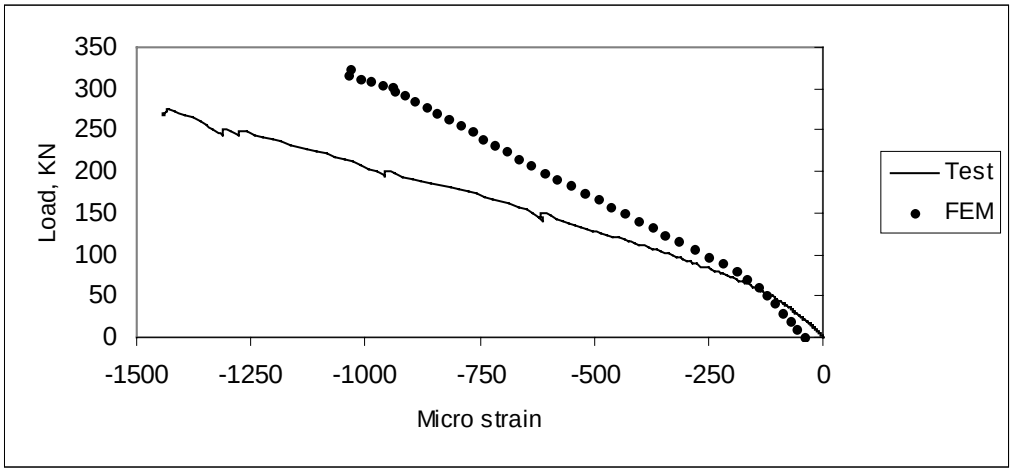

Development of strain under load in the centre, test and FE-analysis, S2.
Figure 6.60

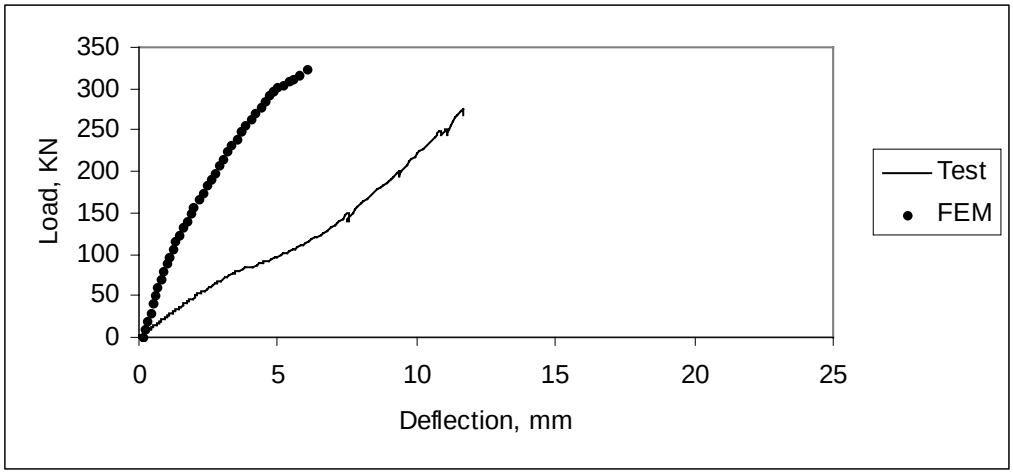

Development of deflection under load in the centre, test and FE-analysis, S2.
Figure 6.61

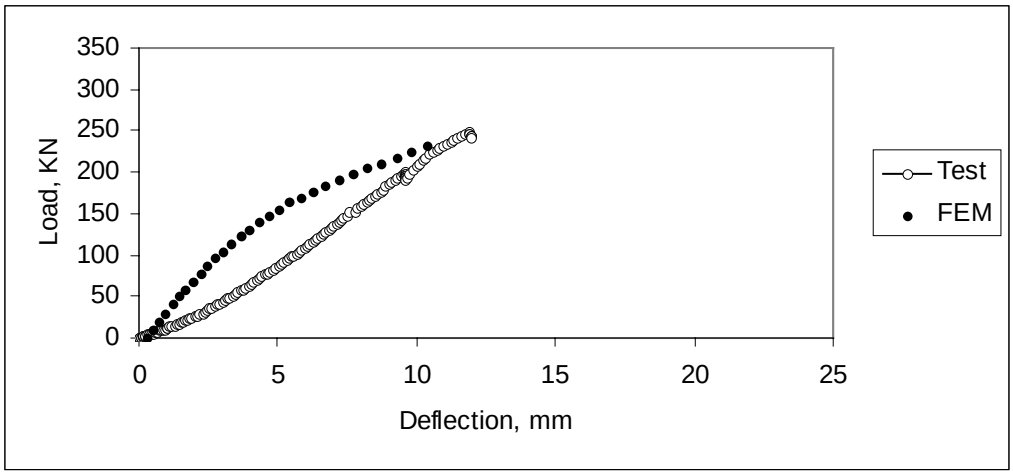

Development of deflection under load at the edge, test and FE-analysis, S2.
Figure 6.62

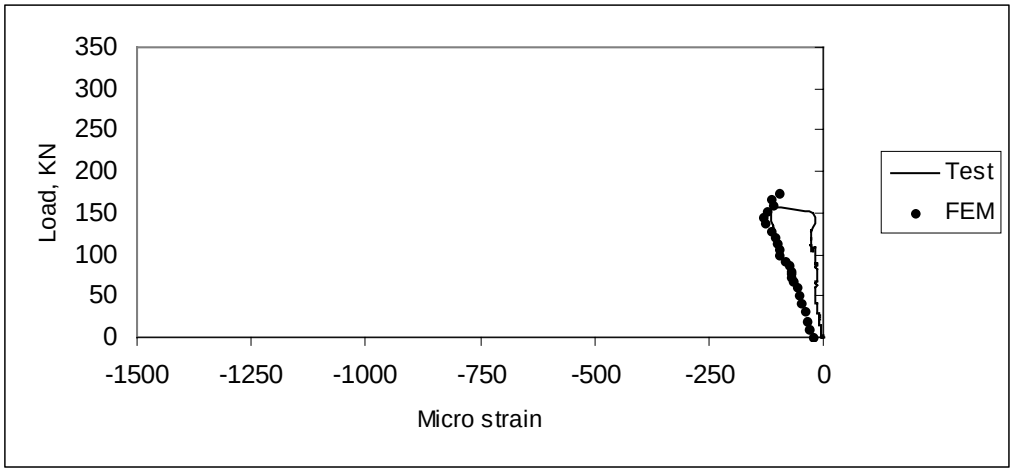

Development of strain under load in the corner, test and FE-analysis, S2.
Figure 6.63

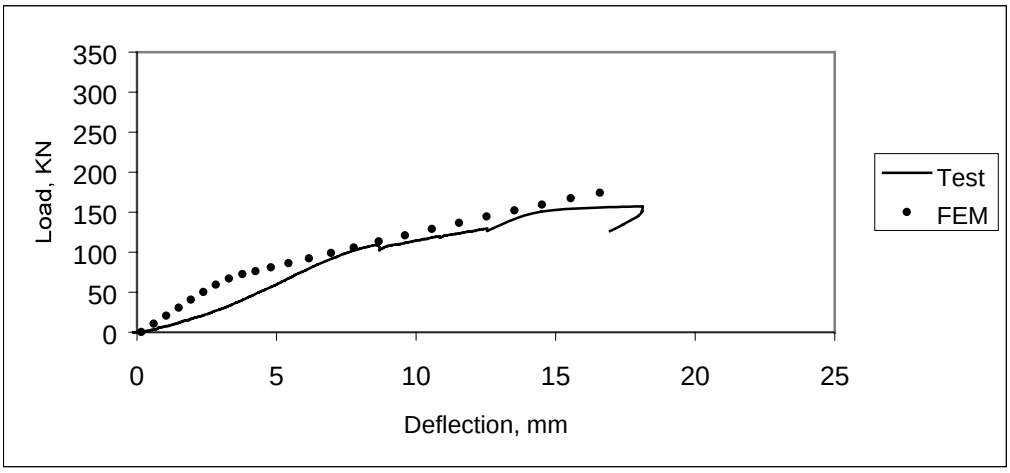

Development of deflection under load in the corner, test and FE-analysis, S2.
Figure 6.64

6.6.8.3 FE analysis of slab S3

With load in the centre the first crack in the bottom surface occurs at approximately 45 kN while in the FE analysis the first crack occurs at 34 kN. Figure 6.65 and 6.66 show development of strain and deflection under load.

With load at the edge the experimental and calculated crack loads were respectively 60 kN and 23 kN. Development of deflection under load at the edge is plotted in figure 6.67.

The first observed crack load with load in the corner, was 75 kN, while in the analysis the first crack starts with a load of 31 kN. Development of strain and deflection for this load case is presented in figure 6.68 and 6.69.

In the subsequent chapter, 6.6.10, the comparison between theoretical and experimental results is more thoroughly discussed.

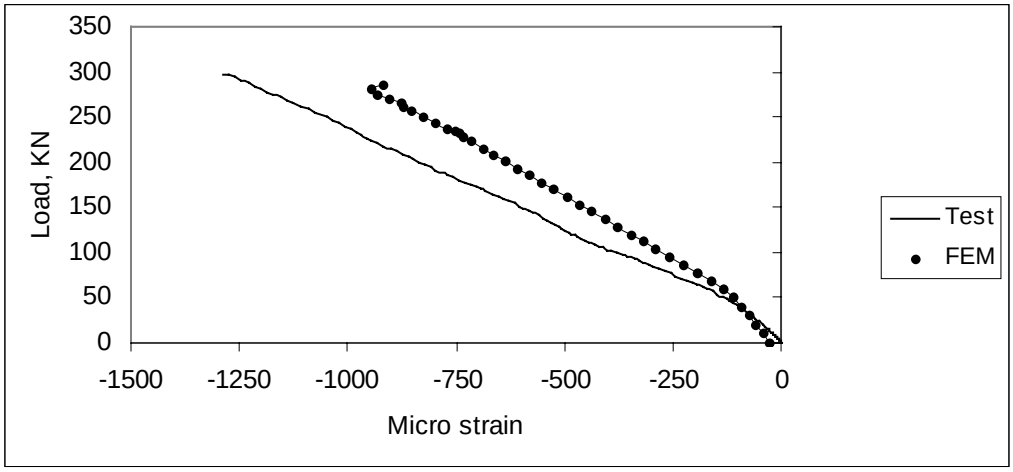

Development of strain under load in the centre, test and FE-analysis, S3.
Figure 6.65

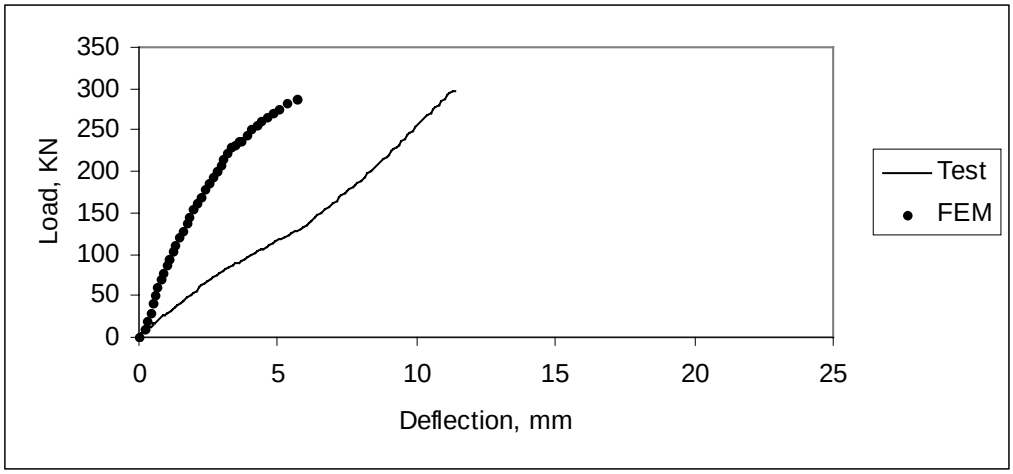

Development of deflection under load in the centre, test and FE-analysis, S3.
Figure 6.66

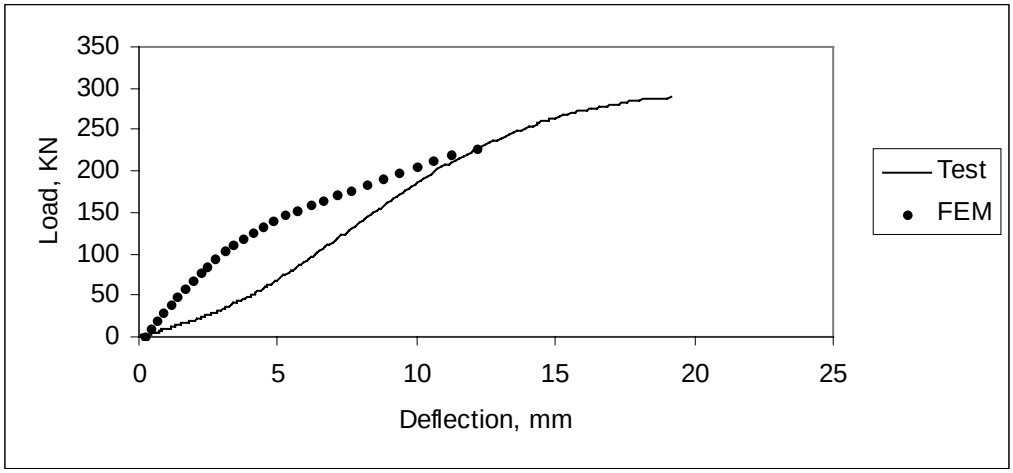

Development of deflection under load at the edge, test and FE-analysis, S3.
Figure 6.67

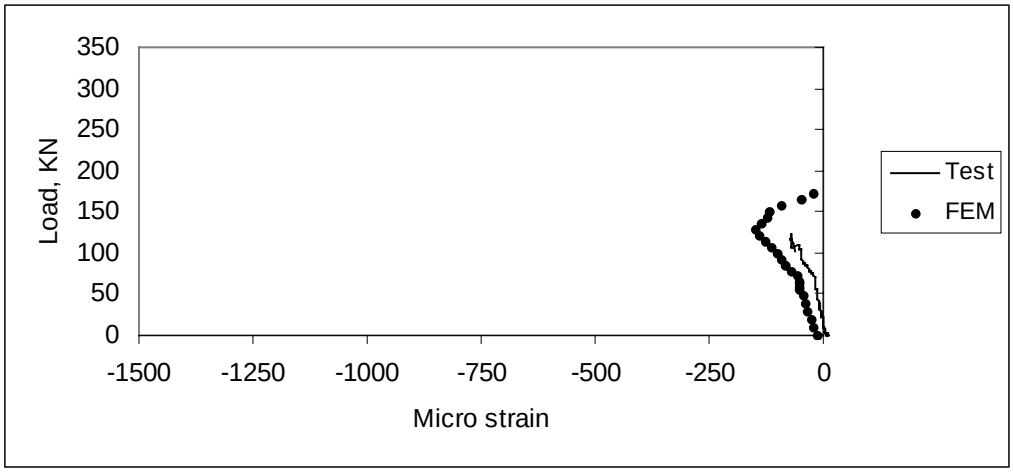

Development of strain under load in the corner, test and FE-analysis, S3.
Figure 6.68

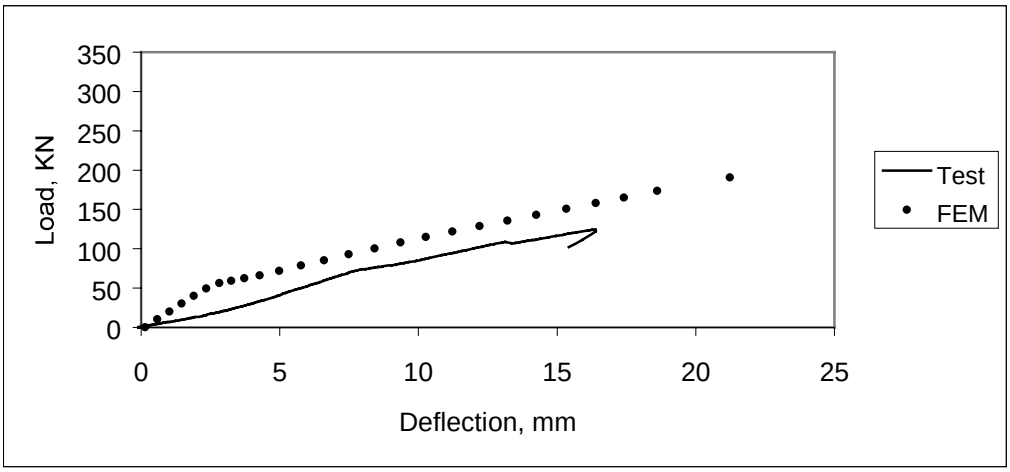

Development of deflection under load in the corner, test and FE-analysis, S3.
Figure 6.69

6.6.9 Shrinkage in slabs on ground

Because shrinkage probably is the most common reason for cracking in concrete slabs on ground, the concrete used in slab S3 was tested in a shrinkage (free movement) rig and a stress rig, fig 6.70. In this stress rig, the concrete is 100 % restrained, and the stress development caused by thermal dilation and autogenous shrinkage is measured. This test is done by Bjøntegaard, and the method is described in the dr. ing. thesis /55/.

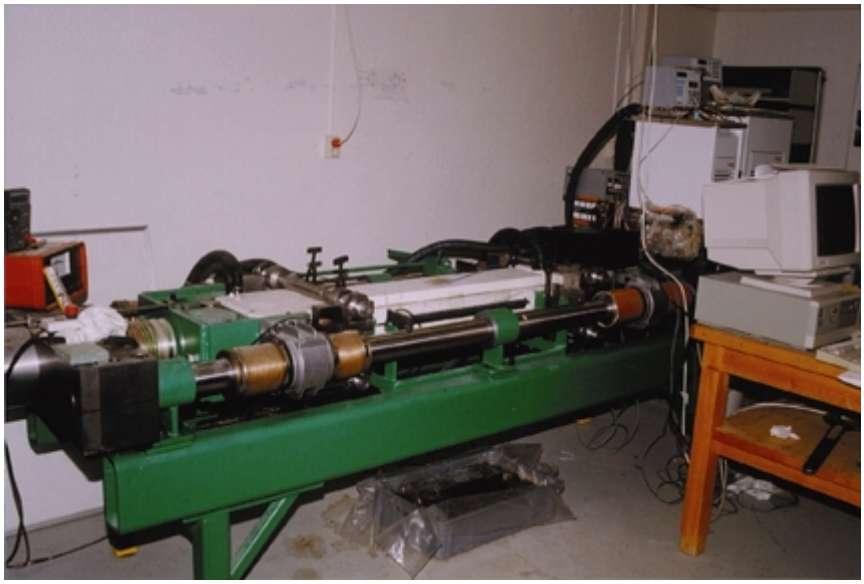

The stress rig.
Figure 6.70

A temperature control system kept the concrete specimen at a constant temperature of 20-degree Celsius for the first 24 hours, and then the temperature in specimen was the same as the temperature in laboratory, between 19- and 21-degree Celsius for the next 35 days. The concrete specimen was insulated to prevent drying. Total time duration of this test was 36 days. After 36 days the specimen was "loaded" to fracture. Fracture occurred at the stress 2.8 N/mm^2 and the self-induced stress at this time was 1.7 N/mm^2.

Autogenous shrinkage in concrete is caused by the hydration process. Due to the hydration of the cement paste, the free water content will decrease, which leads to shrinkage of the paste and thus to shrinkage of the concrete. Development of autogenous shrinkage and stress are shown in figure 6.71. Description or models for the autogenous shrinkage is presently not included in the concrete standards and design rules. The explanation is partly due to older experimental results, which have shown that the autogenous shrinkage is negligible for normal strength concretes. The results in fig 6.71 clearly demonstrate that this is not so.

In figure 6.72 the development of the thermal dilatation coefficient versus time, measured in the shrinkage rig, is shown /55/.

Drying shrinkage is calculated after Norwegian Standard NS 3473, EuroCode2, AS3600, ACI 209 and CEB-FIP Model Code 1990, and the results are presented in figure 6.73. Shrinkage is calculated under the following assumption:

RH = 60 %
Slab thickness 150 mm
Compressive strength 34.25 N/mm^2

In addition for ACI:
Fine aggregate 40 %
Air 5 %

Except for ACI 209, the agreement is satisfactory. One reason for this might be some high percentage fine aggregate or to much air. If the fine aggregate is reduced to 20 %, the drying shrinkage calculated after ACI is close to the other codes.

When drying shrinkage is measured, the registrations usually start at the time when the specimen is exposed to drying. Consequently autogenous shrinkage from the curing period is not included in the measurements an in the codes.

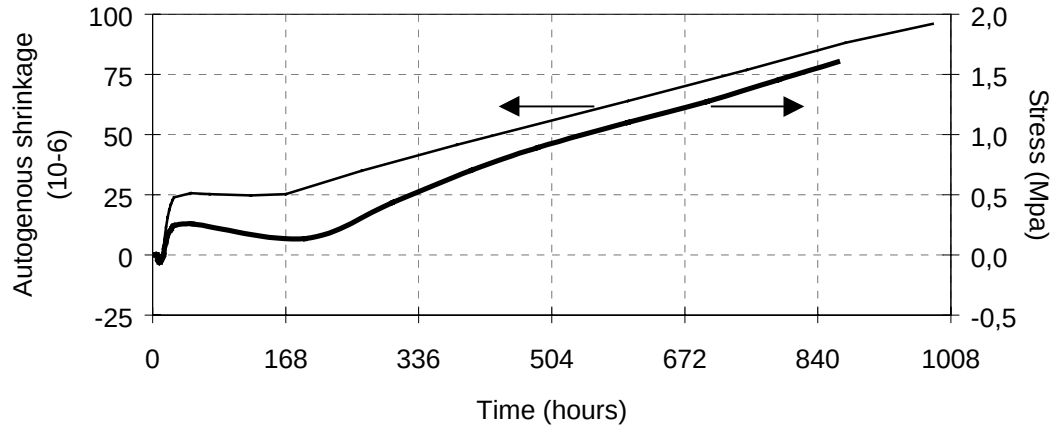

Autogenous shrinkage measured in the shrinkage rig and stress measured in the stress rig, after time (168 hours = 1 week).
Figure 6.71

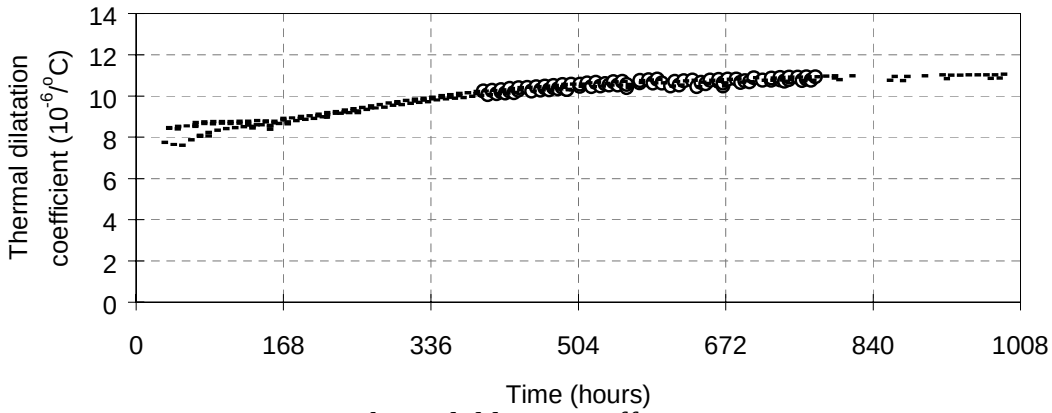

Thermal dilation coefficient.
Figure 6.72

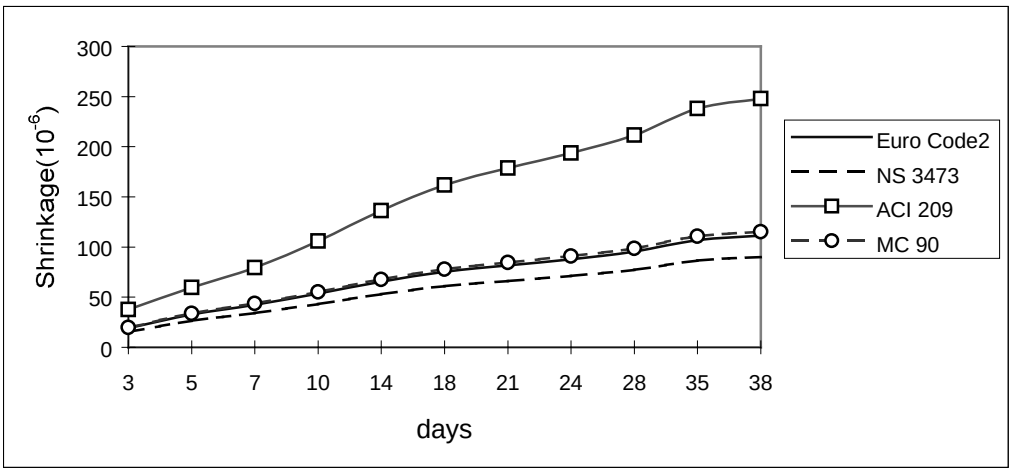

Development of drying shrinkage after different codes.
Figure 6.73

6.6.10 Discussion related to theoretical and experimental results

Because the sub-base stiffness is very important for the structural behaviour of slabs on ground, it was measured prior to the test. Unfortunately, the test results still show that there are considerable sub-base stiffness variations between the different load cases. The major problem is the low stiffness of the first test, S1 with load in the middle. The explanation might be insufficient plane ness of the insulation layers before the test started.

The test results are compared with results from Westergaards equations, and finite element analysis, and some of them are listed and discussed here:

- For S1 with load in the middle the deviations between results from the FE analysis and the test is large. As mentioned above the reason is low sub-base stiffness. For S1 with load at the edge and in the corner the deflections agree well, while it seems to be more difficult to predict the strain.
- In S2 and S3, prestressed slabs, the agreement between observed and calculated strains and deflections is reasonably good, except for the development of deflection in the middle where observed deflection is somewhat higher than deflection from the FE analysis. Again, the reason for this might be that the insulation is not compressed well enough when the test starts. The stiffness of four insulation layers, as used in this test, can also be different from one thicker layer.
- Deflections depend strongly on the sub-base stiffness, and deflections under loads and the crack loads are also calculated by the Westergaards theory presented in chapter 7.2.2 /53/, and compared to the FE analysis. Table 6.9 presents deflections for S1.

Load case	Load	Deflection, Westergaard	Deflection, FE analysis	Deflection, observed
Centre load	25 kN	0.20 mm	0.23 mm	1.87 mm
Edge load	25 kN	0.39 mm	0.59 mm	1.60 mm

Deflection from Westergaards formulas, and FE analysis, S1.
Table 6.9

- There are small deviations between deflection calculated after Westergaards theory and FE analysis, but there are large deviations from these two calculations to observed deflection. Deviations between results from Westergaards equation and FE analysis mainly arise from the effect of the slab size which in Westergaards equations is assumed to be infinite. With load at the edge, the modulus of sub-grade reaction had to be changed from 0.03 N/mm^3 to 0.003 N/mm^3, to get deflection calculated after Westergaards equation equal the observed deflection.

- The crack observation method is uncertain because cracking can start in other places than where the strain gauges are placed. Still the observed crack loads give a good indication of the effect of prestressing because in the prestressed slabs the crack load is close to two times the crack load in the reinforced slab. Crack loads for prestressed slabs S2 and S3 are close when loading in the middle and at the edge, while S2 have a higher crack load when loading in the corner. In the FE analyses cracks generally start earlier than in the test, (again, location of strain gauges) but it gives a good indication of where cracks start.
- For S1 the crack loads calculated by Westergaards equations, are 54 kN with centric load, and 31 kN with load at the edge. The corresponding observed crack loads are 28 kN and 30 kN. It is important to note that S1 is reinforced, while Westergaards equations assume no reinforcement.

The crack loads are calculated under the following assumptions:

k = 0.03 N/mm^3
E = 25.000 N/mm^2
v = 0.2
Tensile strength = 3 N/mm^2

Since shrinkage is an important factor in slabs on ground, autogenous shrinkage was measured in one of the three concrete mixture, while drying shrinkage was calculated after EuroCode2, NS 3473, ACI 209 and Model Code 1990.

Autogenous shrinkage in the curing period is usually not recorded in drying shrinkage tests. Consequently this is also neglected in the codes, which then might underestimate shrinkage in real concrete structures.

6.6.11 Conclusion

Three concrete slabs on ground were tested in the laboratory, each with three different load cases; concentrated load in the centre, at the edge and in the corner. Tests in the shrinkage and stress rigs were done to give a better understanding of the shrinkage problem in a concrete floor. The slabs were analysed by the finite element program Diana, and the results compared to measured values. The slab thickness was 150 mm for all slabs. Slab S1 was reinforced with 8 mm bars with 150 mm spacing in both directions in top and bottom. Slab S2 and S3 were prestressed in both directions with 100 mm^2 tendons in the middle of slab thickness, with spacing 630 and 930 mm, respectively. Load surface was 200 x 200 mm^2 in each load point, and strain gauges were placed at concrete surface and on reinforcement bars. In S2 and S3 four load cells were connected to tendons.

On basis of the test results from the three slabs on ground, the following conclusions can be made:

1. With load in the middle the strain gauges at the bottom surface gives an indication of when cracking starts. In S1 the first crack appears with a load of approximately 28 kN, and in both prestressed slabs the first crack at 45 kN. Load at the edge gives crack in S1 at 30 kN, 45 kN in S2 and 60 kN in S3. Cracking in S3 probably starts earlier, but this is the first observed crack. Finally load in the corner gives the first observed crack at 30 kN for S1, 107 kN for S2 and 75 kN for S3.
2. Crack load calculated with FE analysis with load in the middle, at the edge and in the corner are respectively 19 kN, 13 kN and 17 kN for S1. 41 kN, 28 kN and 38 kN for S2. 34 kN, 23 kN and 31 kN for S3. This test shows that prestressed concrete slabs on ground have a great advantage to reinforced concrete slabs, with crack load 115 % higher in S2 than in S1, 80% higher in S3 than in S1. This shows also that cracks probably start earlier than the observed cracks.
3. There are few problems related to cracks in the bottom of the slab from concentrated loads. The experimental and theoretic load / deflection plots of all three slabs show that these cracks most likely do not have any significant influence on deflections, since the deflections increase approximately linearly with increasing load.
4. Deflections calculated in the FE analysis are in reasonable agreement with the observed deflections when loading at the edge and in the corner. With load in the middle, the observed deflections are considerably larger than the calculated deflections. As discussed in the previous chapter, this is a result of uneven sub-base.
5. Finite element analysis is a useful tool for calculation of slabs on ground, but it is important to have a reliable value for the sub-grade stiffness, *k*-value, to achieve reliable results. This test shows that results from FE analysis possibly give the best indication of crack load and deflection.
6. As a result of this test and other slabs on ground, the author recommends a structure with prestressed tendons for industrial slabs on ground and other slabs where a crack free surface is important.

Chapter 7

Considerations for design and construction of prestressed concrete slabs on ground

7.1 Introduction

In this chapter some of the necessary data and procedures used to design slabs on ground are discussed, and the author's recommendations presented. Results of the non-linear finite element analysis from section 6.6.8, are compared with calculated results.

7.2 Design of slabs on ground

7.2.1 General

As an alternative to reinforcement in concrete slabs on ground, prestressed tendons have been used in some countries. It is vital that the prestressed tendons are properly designed and installed. By pre-compressing the concrete from stressed tendons, the amount of cracks can be controlled before the hydration is effectively completed. This can be done in two or three stages, with for instance 10 % stressing after one day, 50 % stressing after two days and 100 % stressing after three days, of course under the precondition that compressive strength of concrete is high enough.

By use of prestressed concrete the compressive stress from the prestressing can be added to the modulus of rupture in the design formulas. Normally slabs on ground are stressed with 1.0 - 1.5 N/mm^2 after loss in prestressing force. The author recommends this as a minimum. By use of prestressed tendons it is important to have low friction between subgrade and concrete slab, which can be obtained by placing a membrane between them. It is also important that the subgrade is as plane as possible. Columns, walls or other installations must not prevent the slab movement. Prestressed concrete slabs on ground are normally about 20-25 % thinner than plain or reinforced concrete slabs

The stress ratio, SR, between maximum allowable tensile stress, f, and modulus of rupture, MR, in a slab is given by:

$$SR = \frac{f}{MR}$$

Depending on safety factors, allowable tensile stress can be chosen between characteristic tensile strength and design tensile strength. If characteristic tensile strength is used, some cracking can occur, but since MR depends on design compressive strength, design tensile stress is normally used to calculate SR. This gives a SR in range 0.45-0.60 after the Norwegian standard.

In chapter 6.3.1, tensile strength is calculated after the Norwegian standard and EoroCode2. The deviation between these two values are relative large, with the highest value, which is the mean axial tensile strength from EuroCode2, 2.63 N/mm^2. Results from the test in the stress rig, described in chapter 6.6.9, give a failure at 2.8 N/mm^2. This shows that the characteristic design strength from the Norwegian standard, 1.51 N/mm^2, is too low for the slab tested in the laboratory. It is important to note that the result from the stress rig is from only one specimen.

As other concrete structures, slabs on ground should be designed with a safety factor. This factor has to be selected before the thickness and other dimensions can be determined. Safety factors (SF) depend on designers choice, since this factor is not dictated in building codes. The allowable tensile stress is then:

$$MR/SF$$

The most common values for safety factors are between 1.4 and 2.0, Ringo and Anderson /41/ recommend 1.7 as an acceptable value, when loading is frequent and design parameters are reasonably well known. The Norwegian standard, NS 3473 /9/, and EuroCode2 /16/ recommends safety factors 1.4.

The shear strength of the concrete is rarely decisive to slab design. Punching shear can, however be decisive in cases with large concentrated loads, especially when the load area is small.

Soil bearing capacity, soil compressibility, and the modulus of subgrade reaction are parameters that need to be considered in a design procedure. It is also important that the slabs on ground should have a possibility to move independently of other structures like walls, columns and sub-base. To design a slab on ground, the subgrade and sub-base normally will be changed to give a good bearing capacity. This is a geotechnical problem and will not be discussed here, but a modulus of subgrade reaction about 0.03 N/mm^3 or higher should be pursued. The modulus of subgrade reaction, k-value, for some subgrades are shown in table 5.1 from /34/.

7.2.2 Westergaard's equations /36, 53/

Westergaard's equations, based on the theory of elasticity, are the most commonly used theoretical equations to calculate stress in concrete slabs on ground. Westergaard developed these equations to find the maximum stress caused by load in the middle of slab, at the edge and in the corner of a slab with infinite length in both directions.

The major assumptions for these equations are that the slab is homogeneous, isotrop and in accordance with Hooke's elasticity law, and finally the deformation of the sub-base is inversely proportional to the stiffness of the sub-base. One consequence is that they are strictly valid only for uncracked concrete.

The original equations from 1926 are quoted here by /36/:

Load in the middle $$\sigma_i = \frac{0.316}{h^2} \cdot P \cdot \left(4 \cdot \log_{10}\left(\frac{l}{b}\right) + 1.069 \right) \qquad (7.1)$$

Load at edge $$\sigma_k = \frac{0.572}{h^2} \cdot P \cdot \left(4 \cdot \log_{10}\left(\frac{l}{b}\right) + 0.359 \right) \qquad (7.2)$$

Load in the corner $$\sigma_h = \frac{3 \cdot P}{h^2} \cdot \left(1.0 - \left(\frac{a_1}{l}\right)^{0.6} \right) \qquad (7.3)$$

The new modified Westergaards formulas from 1948 /53/ are given as:

Maximum tensile stress under load, with load in the centre of the slab:

$$\sigma = \frac{P}{h^2}\left[0.275(1+\nu)\log_{10}\left\{ \frac{E \cdot h^3}{k\left(\frac{a+b}{2}\right)^4} \right\} + 0.239(1-\nu)\frac{a-b}{a+b} \right] \qquad (7.4)$$

Deflection under load, with load in the centre of the slab:

$$\delta = \frac{P}{8 \cdot k \cdot l^2}\left[1 - \frac{a^2+b^2+4\cdot x^2+4\cdot y^2}{16 \cdot \pi \cdot l^2}\log_{10}\left\{ \frac{E \cdot h^3}{k\left(\frac{a+b}{2}\right)^4} \right\} - \frac{a^2+4\cdot a\cdot b+b^2}{16\cdot\pi\cdot l^2} + \frac{(a-b)(x^2-y^2)}{2\cdot\pi\cdot l^2(a+b)} \right] \qquad (7.5)$$

Tensile stress under load, with load at the edge:

$$\sigma = \frac{2.2(1+\nu)\cdot P}{(3+\nu)\cdot h^2}\log_{10}\left\{\frac{E\cdot h^3}{100\cdot k\left(\frac{a+b}{2}\right)^4}\right\}+$$
$$\frac{3(1+\nu)\cdot P}{\pi(3+\nu)\cdot h^2}\left[1.84-\frac{4}{3}\cdot\nu+(1+\nu)\frac{a-b}{a+b}+2(1-\nu)\frac{a\cdot b}{(a+b)^2}+1.18(1+2\cdot\nu)\frac{b}{l}\right] \qquad (7.6)$$

Deflection under load, with load at the edge:

$$\delta = \frac{P\sqrt{2+1.2\cdot\nu}}{\sqrt{E\cdot h^3\cdot k}}\left[1-(0.76+0.4\cdot\nu)\cdot\frac{b}{l}\right]\cdot\left[1-(0.76+0.4\cdot\nu)\cdot\frac{y}{l}\right] \qquad (7.7)$$

where

P = load with circular load surface (elliptic load surface in new formulas).
h = thickness of the slab.
ν = Poisson's ratio.
E = modulus of elasticity.
k = modulus of sub-grade reaction.
a = radius of load surface
a, b = semiaxes of an ellipse in new formulas.
x, y = horizontal rectangular coordinates.
l = radius of relative stiffness.
a_l = distance from load centre to corner of slab (mm)

$$b = \sqrt{1.6\cdot a^2+h^2}-0.675\cdot h \quad \text{if} \quad a < 1.724\cdot h \qquad (7.8)$$

$$b = a \quad \text{if} \quad a > 1.724\cdot h \qquad (7.9)$$

$$l = \sqrt[4]{\frac{D}{k}} = \sqrt[4]{\frac{Ec\cdot h^3}{12\cdot(1-\nu^2)\cdot k}} \qquad (7.10)$$

Frans Van Cauwelaert /42/ concludes by " The original formula from 1926 for the deflection at the edge is fairly correct, the original formula from 1926 for the stress at the edge (7.2) is not correct and the new formula from 1948 for the stress at the edge is correct (7.6)".

7.2.3 Other stress calculation methods

Stresses in rigid slabs can be set up as a result of uniform temperature change that causes the slab to contract or expand. The size of stress depends on friction between concrete and subgrade, and the length of concrete slab is also important here.

There are also many different influence charts for calculation of moments, deflections and stresses in concrete slabs on ground. These diagrams are most often used for estimation of thickness and forces, and are mainly used in pavement design. Some of the most frequently used methods are /41/:

- Portland Cement Association (PCA) method
- Wire Reinforcement Institute (WRI) method
- United States Army Corps of Engineers (COE) method
- Post-Tensioning Institute (PTI) method
- ACI Committee 223 (ACI 223) method

In addition to concentrated load, uniform loads distributed over partial areas of slabs might produce the critical design condition. Slabs where clear aisles between heavy distributed loads occur, can obtain large negative moments, and in the centre line of aisle this moment can be expressed by (7.11) /40/. This equation will not be more discussed here.

$$M_c = \frac{w}{2 \cdot \lambda^2} \cdot e^{-\lambda a} \sin \lambda a \qquad (7.11)$$

where

M_c = slab moment (Nmm/mm)

$$\lambda = \sqrt[4]{k / 4EI} \qquad (7.12)$$

a = half-aisle width (mm)
w = uniform load (N/mm^2)
k = modulus of subgrade reaction (N/mm^3)
e = base of natural logarithms

7.2.4 FE analysis of slabs on ground

At low load levels the slab elements are uncracked and the actions and deformations could be calculated, using the uncracked flexural stiffness of the slab elements. After cracking, linear finite element analysis will give results that do not take care of the stress and strain redistribution. A typical average stress-strain relation for cracked concrete in tension can be seen in figure 7.1 a. Correlation of test data for cracked concrete in tension is shown in figure 7.1 b /3/.

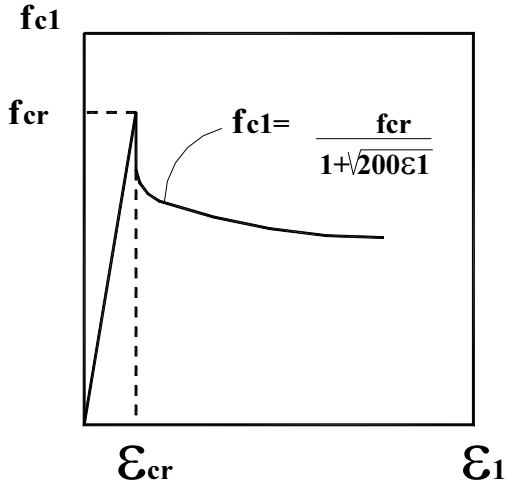

Stress-strain relation for cracked concrete in tension.
Figure 7.1 a

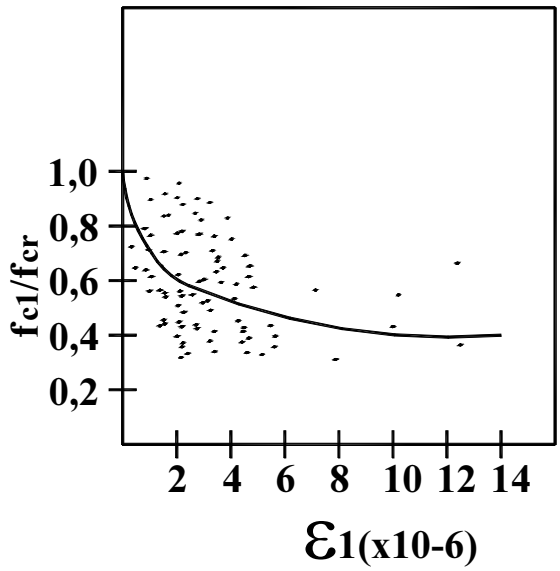

Correlation of test data for cracked concrete in tension.
Figure 7.1 b

Prestressed concrete slabs are subjected to both bending and membrane forces, so to analyse the slab it is necessary to use elements that handle this case. To simulate subgrade and sub-base springs or interface element can be used.

7.3 Recommendation for calculating slabs on ground

7.3.1 Introduction

As discussed previously design of slabs on ground is not discussed as much as design of other structures in buildings like slabs, beams and columns. The use of table and diagram to design structures is not “up to date”, and computer programs should have been developed. The author will in this chapter give some formulas for calculations of slabs on ground, and some of them should be applied in computer programs. This is done for prestressed slabs on ground, and in chapter 7.4 results are compared with data from tests of slabs loaded in the middle, at the edge and in the corner.

7.3.2 Moment and stress in slabs on ground

G.H. Tsohos /44/ has designed concrete pavement on ground derived from following assumptions:

- It consists of homogeneous, isotropic, and elastic materials.
- It is of uniform thickness.
- The range of relative thickness is such that the theory of thin plates may be applied.
- The load upon the top surface and the subgrade reactions at the bottom surface are applied vertically to these surfaces.

These equations can also be used for slabs on ground and are described below.

The design of a concrete slab on ground is usually based on a slab on elastic foundation. In general the stresses in x- and y-direction, can be expressed as a function of the deflection, *w(x,y)* by the following well-known equations /43/:

$$\sigma_x = -\frac{Ez}{1-\nu^2}\left(\frac{\partial^2 w}{\partial x^2} + \nu\frac{\partial^2 w}{\partial y^2}\right) \tag{7.13}$$

$$\sigma_y = -\frac{Ez}{1-\nu^2}\left(\frac{\partial^2 w}{\partial y^2} + \nu\frac{\partial^2 w}{\partial x^2}\right) \tag{7.14}$$

$$\tau_{xy} = -\frac{Ez}{(1+\nu)}\frac{\partial^2 w}{\partial_x \partial_y} \tag{7.15}$$

These stresses vary linearly through the thickness of the slab and are equivalent to moment per unit length acting on an element of the plate. Moments are given by:

$$M_x = \int_{-h/2}^{h/2} z\sigma_x dz \qquad = \qquad -D\left(\frac{\partial^2 w}{\partial x^2} + \nu\frac{\partial^2 w}{\partial y^2}\right) \tag{7.16}$$

$$M_y = \int_{-h/2}^{h/2} z\sigma_y dz \qquad = \qquad -D\left(\frac{\partial^2 w}{\partial y^2} + \nu\frac{\partial^2 w}{\partial x^2}\right) \tag{7.17}$$

$$M_{xy} = \int_{-h/2}^{h/2} z\tau_{xy} dz \qquad = \qquad -D(1-\nu)\frac{\partial^2 w}{\partial_x \partial_y} \tag{7.18}$$

where the flexural rigidity D of the slab is :

$$D = \frac{E \cdot h^3}{12\left(1-\nu^2\right)} \tag{7.19}$$

In a slab on elastic foundation there will be a load from subgrade reaction, $q = k \cdot w$ where k = stiffness modulus of the subgrade. The general differential equation of this problem can be expressed as /42/:

$$\left(\frac{\partial^2}{\partial x^2} + \frac{\partial^2}{\partial y^2}\right)\left(\frac{\partial^2 w}{\partial x^2} + \frac{\partial^2 w}{\partial y^2}\right) + k \cdot \frac{w}{D} = \frac{p}{D} \tag{7.20}$$

Deflection under the load for a beam on elastic foundations is /45/ :

$$w_o = \frac{p \cdot \lambda}{2 \cdot k} \tag{7.21}$$

and zero point of the line is where $\cos\lambda x + \sin\lambda x = 0$, that is, at the consecutive values of $\lambda x = \frac{3}{4}\pi, \frac{7}{4}\pi, \frac{11}{4}\pi, etc.$

where

$$\lambda = \sqrt[4]{\frac{k}{4EI}} \tag{7.22}$$

Deflections in centre of load for a slab on elastic foundation can be expressed by /42/:

$$w = \frac{p}{8 \cdot k \cdot l^2} \tag{7.23}$$

where

$$l^4 = D/k \tag{7.24}$$

This is in accordance with the first part of Westergaards equation (7.5).

7.3.3 Prestressed tendons, loss in prestressing force, shrinkage

By use of prestressed tendons in slabs on ground, there are some criteria that have to be met to get the best solution. With plane subgrade a plastic membrane between concrete and subgrade will reduce the friction, and this has a positive effect on crack development in concrete. When using prestressed slabs, the number of joints can be reduced since the concrete has a compressive force all over the slab thickness. A combination of prestressed tendons and high strength concrete can reduce the slab thickness in slabs on ground. Thickness under 150 mm is however not recommended since, for the tendon geometry, a small deviation from centre line gives moment in slab, and with small thickness, this can be critical and give cracks. To get the force from tendons distributed over a length of the slab, more and smaller tendons are preferred. The first tendons should be placed at a certain distance from the edge, so there is a compressive force along the edge. This is because the concentrated tendons force will be distributed at an angle of about 45^o, and this gives a zone with no compression force in that direction, se figure 7.2. Tendons perpendicular to this tendon give a compressive force in this area. If the first tendon in this direction can not be placed at the edge, the slab has to be reinforced with minimum reinforcement in this area.

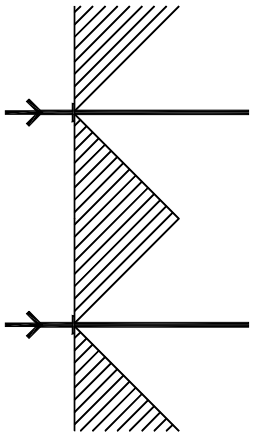

Zone with no compression force.
Figure 7.2

When stressing tendons, there will be some loss in prestressing force, see appendix A5. Friction loss depends on total drape between inflection points, and then total angle change at a distance from stressing point. Slabs on ground should have straight tendons, which results in a simpler friction loss equation:

$$P_x = P_o \cdot e^{-\mu \Delta \alpha \cdot x} \tag{7.25}$$

where

P_x = tendon force in a distance x from stressing point
P_o = tendon force at active end of tendon
μ = Friction coefficient
$\Delta\alpha$ = Wobble friction coefficient
x = distance from stressing point to inspected point

This loss is 2 - 5 %, and depends on the tendon length.

Number of tendons depends on slab thickness and length of slab, but with a 200 mm thick slab and total 15 % loss in prestressing force, a distance of 400 mm between tendons (Ap =100 mm^2) will give a compressive stress of about 1.5 N/mm^2.

To calculate creep and shrinkage the design rules in EuroCode2 can be applied. In figure 6.71 the measured autogenous shrinkage in slabs on ground test is given, while figure 6.73 shows drying shrinkage calculated after different codes.

7.3.4 Calculation

In this chapter one possible procedure to design prestressed concrete slabs on ground is presented. The most critical load cases for slabs on ground are normally concentrated loads, effects of temperature variation and shrinkage. The procedure will only take care of these load cases.

A useful design procedure is developed by J. A. Sindel /48/ and this method is reproduced here in detail. This procedure takes care of concentrated load distributed over a circular contact area with load placed away from corner and edge. Concentrated load stress is based on Westergaard's modified equation /7.4/ for a homogeneous, isotropic solid. The method can easily be extended to also cover load at the corner and at the edge. A commonly used relation is:

$$f_t - f_p - f_F \geq f_{\Delta T} + f_L \tag{7.26}$$

where tensile stresses are positive

and

f_t = Maximum allowable concrete tensile stress
f_p = Effective prestress
f_F = Subgrade friction stress loss
$f_{\Delta T}$ = Stress due to temperature and shrinkage effects
f_L = Stress due to concentrated load
$(f_{\Delta T} + f_L)$ = Tensile stress in the bottom of slab due to temperature and concentrated load.

To determine the minimum compression required in the concrete slab, equation 7.26 can be rewritten:

$$-f_p \geq f_{\Delta T} + f_L + f_F - f_t \tag{7.27}$$

The maximum allowable concrete tensile stress, f_t, can be chosen between characteristic tensile strength, design tensile strength and modulus of rupture. As described previously, the result from the stress rig give a failure in concrete specimen at 2.8 N/mm^2, which is a representative value for the tensile strength of the slabs tested in the laboratory. The maximum stress in concrete is normally in the bottom of the slab, under the load. There is normally no problem if some cracks occur in the bottom of the slab, but crack development can be reduced with choice of a higher safety factor.

Subgrade friction stress loss is normally a small value and it is not a big mistake to ignore this, but equation for this loss is given here:

$$f_F = \mu \cdot \rho \cdot \chi \tag{7.28}$$

where μ is the coefficient of subgrade friction, ρ is the concrete density and χ is the distance from the edge with a maximum value of $L/2$, where L is the total length of the slab.

If a linear temperature gradient is assumed, $f_{\Delta T}$ is given by (assumed no rotation):

$$f_{\Delta T} = \frac{E_c \cdot \alpha_c \cdot \Delta T}{2 \cdot (1 - \upsilon)} \tag{7.29}$$

Where E_c is the concrete modulus of elasticity, α_c is a coefficient of thermal expansion, ΔT is the assumed temperature differential and υ is Poisson's ratio.

Stress due to concentrated load is given by:

$$f_L = \frac{0.275 \cdot P}{h^2} \cdot (1+\upsilon) \cdot \left(\log_{10}\left(\frac{E_c \cdot h^3}{k \cdot b^4} \right) - 0.44 \right) \qquad (7.30)$$

which has been modified in accordance with the suggestion of Teller and Sutherland /59/.

Where k is the modulus of the subgrade reaction, h is the slab thickness, a and b are given by (7.8) and (7.9).

P is the concentrated load.

These equations give the necessary prestressing forces and the number of tendons needed in the slab. In appendix B some calculations are done for slabs with different load case and different distance between tendons.

These equations are also tested and compared with observations from an industrial slab in Brisbane where high concentrations of lift trucks are expected /56/. Results from this test are in good accordance with theoretically calculated values.

7.4 Comparison of theoretical and experimental results

The deflection calculated after the equations in 7.3.2, is 1.2 mm with modulus of elasticity = 30000 N/mm^2, k = 0.03 N/mm^3, ν = 0.2, slab thickness = 150 mm and load = 150 kN. The test described in chapter 6, shows that a load of 150 kN gives a deflection of 6 mm for prestressed slabs and 14 mm for reinforced slab. The main reason for the large deviation between theoretically calculated and observed result in prestressed test slab, is small test slab and low stiffness in sub base. In the test slab, there was a large deflection at the edge (2000 mm from the load centre). The moment distribution in a large floor will reduce the deflection in this point, and as an estimate this reduction can be around 50 %. That means 3 mm for prestressed specimen and this is close to the calculated deflection. The reinforced specimen cracked at an early stage.

The crack loads calculated by the equations in chapter 7.3.4, tensile strength 2.8 N/mm^2, and other data as described above in calculation of deflection, is about 37.5 kN for the reinforced slab, 65 kN with tendon spacing 630 mm, and 56 kN with tendon spacing 930 mm (load in the middle).

In table 7.1, crack load from FE-analysis, Westergaards new equations (chapter 7.2.2) and observed values are given.

Load case	Crack load FE- analysis. kN	Crack load Westergaards. kN	Crack load Observed. kN
Load in the middle.			
S1	19	32	28
S2	41	56	45
S3	34	49	45
Load at the edge.			
S1	13	19	30
S2	28	32	45
S3	23	28	60

Comparison of crack load.
Table 7.1

In S3, with load at the edge, the observed crack load is probably too high. In S1, load at the edge, the first crack from FE analysis opened with a load of 13 kN, then it closed, and opened again with a load of 29.5 kN. It is important to notice that all equations used to calculate concrete slabs on ground have some uncertainty in choice of parameters. In appendix B different choices and the results from calculations with the equation given in chapter 7.3.4 are listed.

When the results from equation 7.1, 7.4 and 7.30 are compared, the stress due to concentrated load is lowest in equation 7.30. Equation 7.1 gives a result 16 % higher, and finally 20 % higher in equation 7.4 than in 7.1.

As shown in table 7.1 the results from Westergaards new equation (7.4) are somewhat higher than observed values and results from FE analysis with load in the middle of the slab. In this test, equation 7.30 gives the best results compared with observed values.

The difference between FE analysis and Westergaards equation can be explained by that the Westergaards equation assumes a slab with infinite length, compared to the finite length in FE analysis. This gives a deviation in moment distribution in the slab, and different stress in the two cases.

7.5 Conclusion

In this project, the author's intention was to find possible solutions of some main problems related to design and construction of slabs on ground, and contribute to a general improvement of the design rules. In this test the low and variable sub-base stiffness was a main problem, which might explain some unexpected results.

S2 and S3 with tendons distributed at a distance of 630 mm and 930 mm, and load in the middle, give a calculated crack load of 65 kN, and 56 kN with equations in 7.3.4. S1, slab without prestressing, gives a calculated crack load of 37.5 kN. Some of the deviation from observed crack load, 45 kN in S2 and S3, can be explained by small specimens.

Since the test slabs were relatively small, it is difficult to give absolute descriptions of moment distribution, deflection, loss in prestressing force and other size dependent effects.

The author concludes that the equations in chapter 7.3.4 give good indications of stress in slabs on ground, and recommends these equations as a first estimate of development of cracks in slabs on ground. Deflection calculated after equations in 7.3.2 is recommended since the result seems to be in relatively good accordance with observed values. As shown in table 7.1 above, the FE-analysis gives somewhat lower values than results from Westergaards equations. The reason is that the Westergaards equations calculate the slab with infinite length, and in FE-analysis the real length is used. This gives a distribution of moment different from what the Westergaards equation assumes, which gives earlier cracks in FE analysis. A larger test slab would give a better understanding of moment distribution, a better control of the Westergaards equation and the accuracy of FE analysis.

In the test, the prestressed slabs have an observed crack-load 60 % higher than in the reinforced slab. FE analysis gives twice crack-load in prestressed slab compared with reinforced slab.

In this test, FE-analysis gives in some load cases a good indication of development of deflections and cracks in slabs, but it is shown that small deviations in material parameters can give large deviations in results.

By use of prestressed tendons in this type of structure the builder will get a better product than with ordinary reinforced slabs.

It is surprising that lack of design rules for slabs on ground is a general problem for the different standards, since cracks in this type of structure is a well known problem. This test shows also that it is important to have a good sub base before the slab is casts, since development of cracks in concrete depends of the stiffness in sub base. The observed crack loads in prestressed slabs are equal with load in the middle. At the edge the most stressed slab, S1, cracks with a higher load than S2. This shows that stress level can be reduced if load occurs only away from the edge.

If this test should be done again, some points that might give better results can be listed as:

- Larger test specimen to obtain a more representative moment distribution.
- A more reliable material in the sub-base.
- More comprehensive FE-analysis before the test to locate the strain gauges.

Chapter 8

Final conclusions

On the basis of the reported test results and analyses, the following conclusions can be made about prestressed flat slabs and slabs on ground:

Flat slabs

Prestressed flat slabs are economically favourable structures that give possibility to combine long span width and thinner slab thickness. This gives the user greater possibility for a reduced number of columns, while no beams under the slab simplify technical installations. Prestressed flat slabs also give small deflections.

The critical area for prestressed flat slabs is around the column. Shear reinforcement, drop panels or increased length of the critical section are possible ways to increase the shear capacity.

This full-scale test of flat slab with two spans of 9000 mm in x-direction and two spans of 7500 mm in y-direction represents the most used span widths in office buildings and parking houses. The slab was designed with a distributed load of 2.5 kN/m^2.

The slab was loaded until failure with a uniformly distributed load of 6.5 kN/m^2. The shear capacity calculated after the Norwegian standard, NS 3473 /9/, was passed with 58 percent when the failure occurred. Relation between shear force when failure occurs, and capacity was also calculated after ACI, EuroCode2 and AS3600. Like the Norwegian standard, the capacity was passed when calculating after ACI and EuroCode2, but the Australian standard AS3600 gives capacity close to observed shear force when failure occur.

Difference in calculated and observed prestressing force was after short time losses and long time losses (until 18 days) 12 percent, with 115 kN observed force and 129 kN theoretically.

With a load of 2.5 kN/m^2 there was only 5 mm deflection of the slab. This is in good accordance with calculated deflection.

FE-analysis is a powerful tool to calculate concrete structures, and this slab was analysed with the FEM program “DIANA”. First a long-time analysis was carried out to find an indication of development of strain in the slab, but it was difficult to obtain close agreement between the analysis and the measured results. In general, strains from analysis and the failure test are in a reasonably good accordance until a load of 4 kN/m^2, except in the observed point over the middle column. The major reason for the deviation between observed strain and strain from FE-analysis in this point is due to

the development of cracks around the column. These cracks start earlier in the test than in the analysis.

This test shows that this type of structure is complex to calculate, including long-time effects, two-ways effects and change in moment when cracks occur. FE-analysis is still likely to be the best tool to predict moment, forces and deflections in concrete structures of this type.

Slabs on ground

As a part of this thesis, three concrete slabs on ground were tested in the laboratory. Each specimen was 4000 mm x 4000 mm and 150 mm thick. The slabs were loaded with concentrated load in the middle, at the edge and in the corner. The first slab was reinforced and the two last specimens were prestressed.

Insulation was used as a sub-base in this test. The stiffness of the sub-base is one of the most important parameters when calculating slabs on ground, and this was measured before loading started.

The deviations between experimental and theoretical results are mainly caused by the low and uncertain sub-grade stiffness. One reason for this can be that the insulation is not compressed well enough when the test starts, and that the stiffness is changed between the load cases.

In S1, reinforced with 8 mm bars in top and bottom, cracking was observed with a load about 30 kN for all three load cases. Specimen S2 and S3 were prestressed with distributed tendons in both directions at a distance of 630 mm in S2 and 930 mm in S3. In both, cracking was observed with a load of 45 kN with load in the middle. With load at the edge cracking starts at 45 kN in S2 and at 60 kN in S3. In the final load case, load in the corner, cracking starts at 107 kN in S2 and at 75 kN in S3.

With load in the middle of the slab, the first crack starts in the bottom of slab. With load at the edge, crack starts in the bottom, and at higher load levels cracks also occur at the top surface. When loading in the corner, crack starts in the top surface.

Each specimen was analysed with the FEM program “DIANA”, and based on this analysis cracks start earlier than observed cracks do. One reason for this might be that cracks in the test might have started other places than where the strain gauges are placed.

It is observed that cracks do not have any significant influence on deflection in prestressed slabs, since deflection increases linearly with increasing load. The structural behaviour of the reinforced slab is quite different from the prestressed slabs.

There are relatively small deviations between deflections calculated after Westergaards equation and FE-analysis, while there are large deviations between these two calculations and observed deflections.

This test shows that prestressed concrete slabs on ground have a great advantage compared to reinforced concrete slabs, with less cracking. Since crack in top surface is the critical crack for the user, it is more interesting to find the load level when cracks start, than deflection, for the slab.

J. A. Sindel /48/ developed a design procedure that takes care of concentrated load placed away from corner and edge. These equations, which partly are base on the Westergaards theory, are compared with results from test in full-scale done in Brisbane /56/, and are in good accordance with this. The same equations are also used to find the crack load in the two prestressed specimens in this test, and they give a good indication of crack load, and can be a simple alternative to a more demanding and exact FE-analysis.

Chapter 9

Suggestions for further work.

Flat slabs

Still many open questions about prestressed concrete structures exist and some suggestions for further work can be summarised as:

In the full-scale test of the flat slab, the shear capacity calculated after the Norwegian standard was passed with 58 percent when failure occurred. This is an adequate safety factor, but additional research needs to be done to find an optimum solution by use of drop panel, shear reinforcement, or increased critical section around the column.

The area around tendon anchorage is important, and the reaction in concrete when stressing the tendons is also a part where more information is needed. Observations here can be taken from tests in small scale 1:3 – 1:4, but the most correct results will come from a full-scale test, since there is some uncertainty with scaling up results from tests. Observations from anchorage in groups are most interesting, but also reactions from single anchorage on active and passive side might be interesting.

Additional experimental data and theoretical work need to be obtained to explain moment and shear reaction and distribution in prestressed slabs, especially flat slabs with small supports are interesting.

Since the prestressing force in this test gives a deviation of 12 percent between theoretical and observed values, a test with longer tendons might give a better understanding of prestress loss due to long time and short time effects.

Deflections measured in the flat slab test are in good accordance with theoretical deflections, but it might be of interest to control deflections in the “inner” span, that means in a slab with three or more spans.

There are some FEM programs that take care of prestressed tendons in slabs, but further development of the FEM programs, which take care of three dimensional cracking, combined with prestressed tendons, will provide a powerful tool for calculation of punching shear failures.

A parameter study and FE-analysis is important before a test like this is done. This will increase the possibility to chose the best materials and tendon geometry and also simplify the location of strain gauges in the test slab for an optimum result.

Slabs on ground

Prestressed slabs on ground are structures that are relatively new and not well known in Norway. Additional research is therefore interesting to give an adequate understanding of reactions in slabs on ground were prestressed tendons can be applied. Tests with large slabs on ground loaded with point load, groups of point load and distributed loads are all interesting cases here.

Few prestressed slabs on ground are controlled with strain gauges and load cells, and then compared with theoretically calculated values when loading. This is interesting for control and verification of existing design equations and FE-analysis.

More research is needed to understand development of moment and shear forces in slabs on ground, and also the effect of the distance between tendons in this type of structures.

As for flat slabs, FEM programs, which take care of shear in slabs on ground, will be powerful tools to help designers of slabs on ground.

FE-analysis is a powerful tool to calculate concrete structures, and the author's opinion is that most of concrete structures will be calculated with this tool in the future. The FEM program used in this test seems to be a bit difficult to apply, since designers in general are most comfortable with Window's programs.

Chapter 10

References

1 British Design Code BS8110 (1985) part 1-2

2 Ritz, P., Matt, P., Tellenbach, Ch., Schlub, P., and Aeberhard, H.U. (1981). Post-Tensioned Slabs, Losinger Ltd.- VSL International, Bern, Switzerland.

3 Collins, M.P., Mitchell, D. (1991). Prestressed Concrete Structures, Prentice-Hall, Inc New Jersey, USA.

4 Post-Tensioning Institute. (1977). Design of Post-Tensioned-Slabs, Post-Tensioning Institute, Glenview, USA.

5 Stemland Hans. (1983). Forspenning av flatdekker med uinjiserte kabler, Institutt for betongkonstruksjoner, NTH, Trondheim.

6 Magura, D., Sozen, M.A., and Siess, C.P., A Study of Stress Relaxation in Prestressing Reinforcement. PCI Journal, Vol 9, No. 2, Mar.-Apr. 1964

7 Magura, D., Sozen, M.A., and Siess, C.P. (1964). A Study of Stress Relaxation in Prestressing Reinforcement, PCI Journal, Vol 9, No 2.

8 OHBDC, Ontario Highway Bridge Design Code. (1983). Ontario Minisstry Of Transportation and Communications, Toronto, Canada.

9 NS 3473. (1989). Prosjektering av betongkonstruksjoner, beregnings- og konstruksjonsregler. Norges Standardiseringsforbund.

10 Recommendations for Concrete Members Prestressed with Unbonded Tendons ACI-ASCE Committee 423 (1983)

11 Building Code Requirements for Reinforced Concrete (ACI 318-89)(Revised 1992) and Commentary-ACI 318R-89 (Revised 1992). Reported by ACI Committee 318, (1992)

12 ACI Manual of Concrete Practice Part 3-1987, American concrete institute.

13 Warner, R.F., Faulkes, K.A. (1988). Prestressed Concrete 2nd edition. Longman Cheshire Pty Ltd, Australia.

14 Australian Standard. AS 3600 Concrete structures. Standards Association of Australia (1994).

15 AS 3600 Supplement 1-1990 Concrete structures-Commentary. (Supplement to AS 3600-1988). Standards Association of Australia (1990).

16 Eurocode 2, Design of concrete structures, ENV 1992-1-1 December 1991

17 Eurocode 2, part 1-5 ENV 1992 Unbonded end external prestressing tendons

18 Concrete structures Euro design handbook 1994/96,Josef Eibl, Germany.

19 Technical report no 43. (1994). Post tensioned concrete floors design handbook. The concrete society, United Kingdom.

20 Rusch Hubert, Jungwirth Dieter, Hilsdorf Hubert K.. Creep and Shrinkage. Their Effect on the Behavior of Concrete Structures. Technische Universitat, Munich, Dyckerhoff & Widmann AG, Munich, Universitat Karlsruhe, Karlsruhe, Germany.

21 Daye Marwan A. (1992). Creep and Shrinkage of Concrete: Effect of materials and environment. American Concrete Institute, Detroit, Michigan, USA.

22 McHenry, D.A. (1943). A new aspect of creep in concrete and its application to design ATMS Proc., 43.

23 The design of post-tensioned concrete flat slabs in buildings. Recommendations of The Concrete Society Working Party on post-tensioned flat slab construction. The Concrete Society (1974), United Kingdom.

24 Eugene J. O'Brien & Andrew S. Dixon. (1995) Reinforced and prestressed concrete design. The complete process. Department of Civil Structural and Environmental Engineering, Trinity College, Dublin, KML Consulting Engineers, Dublin, Ireland.

25 Reinforced concrete floors slabs-research and design. American Society of Civil Enginers. The Reinforced Concrete Research Council. Bulletin No. 20

26 K.W. Johansen. (1972). Yield-line formulae for slabs. Cement and Concrete Association. Technical University of Denmark.

27 The university of Sydney. School of civil engineering. Post graduate course, prestressed concrete. May 1979. Lecture 17, Diffusion of concentrated loads, R. J. Wheen.

28 Harianto Sundidja. Urbana, Illionis. (1982). Response of prestressed concrete plate-edge column connections. Doctoral thesis.

29 Westergaard, H. M. (1927). Theory of Concrete Pavements Design, Proceedings. Highway Research Board. USA

30 R. Colin Deacon. (1976). Concrete ground floors: Their design construction and finish. Cement and Concrete Association. England.

31 ACI 224.1R. Causes, Evaluation, and Repair of Cracks in Concrete Structures. Reported by ACI Committee 224. 1984

32 ACI 224.2R. Cracking of Concrete Members in Direct Tension. Reported by ACI Committee 224. 1986

33 CEB-FIP Model Code 1990, First predraft. Comite Euro-International du Beton. (1978).

34 Concrete industrial ground floors. The Concrete Society in association with the British Industrial Truck Association and the Storage Equipment Manufacturers Association. Concrete Society Technical Report No 34. (1988)

35 Robert G. Packard. (1976).Slab Thickness Design for Industrial Concrete Floors on Grade. Portland Cement Association. Illinois, USA.

36 Bjørn Hakvaag. (1977). Dimensjonering av betongvegdekker.. Institutt for veg- og jernbanebygging. Universitetet i Trondheim, Norges Tekniske Høgskole. Trondheim. (In Norwegian)

37 ACI 302-69 Recommended Practice for Concrete Floor and Slab Construction. American concrete institute. (1969).

38 E. J. Yoder, M. W. Witczak. (1975). Principles of pavement design. Second edition. A Wiley-Interscience Publication.

39 Slab on ground, a symposium. The cement & concrete association of Australia August, 1970.

40 George Winter, L. C. Urquhart, C. E.O'Rourke, Arthur H. Nilson. (1964). Design of concrete structures. Seventh Edition. International Student Edition. McGraw-Hill Book Company.

41 Boyd C. Ringo and Robert B. Anderson. (1992). Design Floor Slabs On Grade. Step-by-Step Procedures, Samples Solutions, and Commentary. Cement and Concrete Association of Australia. Queensland Regional Office.

42 Fifth International Conference on Concrete Pavement design and Rehabilitation
April 20-22, 1993 Purdue University West Lafayette, Indiana USA. Volume 1

43 E.H. Mansfield. (1964). The Bending and Stretching of Plates. Senior Principal Scientific Officer, Structures Department, Royal Aircraft Establishment, Farnborough. England.

44 Airfields, heavy duty areas and railways. Noise reducing surface. Skid resistance and ridability. 7th International Symposium on Concrete Roads, Vienna October 1994

45 M. Hetenyi. (1983). Beams on elastic foundation. Theory with applications in the fields of civil and mechanical engineering.

46 Kanstad, T. (1990). Nonlinear analysis considering timedependent deformations and capacity of reinforced and prestressed concrete. Doctoral thesis. Division of Concrete Structures. The Norwegian Institute of Technology. The University of Trondheim, Norway.

47 Standard Practice for the Use of Shrinkage - Compensating Concrete (ACI 223-83) Reported by ACI Committee 223 1983

48 J.A. Sindel. (1983). A Design Procedure for Post-Tensioned Concrete Pavements. VSL Prestressing, Queensland, Australia.

49 VSL Construction system. VSL prestressing (AUST.) PTY.LTD. 1995

50 Trygstad, S. (1996). Fullskalaforsøk flatdekke med etteroppspente uinjiserte kabler. Aalesund. Norway. (In Norwegian)

51 ACI 209R-92. Prediction of Creep, Shrinkage, and Temperature Effects in Concrete Structures.

52 DIANA, Finite Element Analysis, User's Manual Nonlinear Analysis, Release 6.1 May 1996. TNO. The Netherlands.

53 Westergaard H. M, Bone Evan P. (1947). New formulas for stresses in concrete pavements of airfields. USA.

54 Mx-spesifikasjoner. Sundolitt 10-1997. Aalesund. Norway. (In Norwegian)

55 Bjøntegaard, Ø. Thermal Dilation and Autogenous Deformation as Driving Forces to Self-Induced Stresses in High Performance Concrete. Doctoral thesis, Department of Structural Engineering, Norwegian University of Science and Technology, Trondheim, Norway. (1999).

56 Sindel J. A. and Friberg Bengt F. Discussion of article by J. A. Sindel. Concrete International (1983). Queensland.

57 Roongroj Hemakom. (1975). Strength and behaviour of post-tensioned flat plates with unbonded tendons. Doctoral Thesis. The University of Texas, USA

58 Recommendations for the design of post-tensioned slabs and foundation rafts. FIP Commission on Practical Design. (1998).

59 Teller, L.W., and Sutherland, E. C., The Structural Design of Concrete Pavements. Part 5, An Experimental Study of the Westergaards Analysis of Stress Conditions in Concrete Pavements Slabs of Uniform Thickness, “Public Roads”, V. 23, No 8, (1943). USA.

60 Pettersson Dan. (2000) Control of Cracking due to Imposed Strains in Concrete Structures. Doctoral Thesis. Lund University. Sweden. Division of Structural Engineering.

Appendix A, flat slab

A.1.1 Introduction

As a introduction to appendix, some general rules and material parameters that are used to calculate the flat slab in the failure test are given. This start with chose of tendon geometry, balanced load concept, stress calculation and moment distribution, time dependent material properties, and finally some about shear reinforcement.

A.1.2 Tendon geometry

After the slab thickness and concrete cover are determined, tendon geometry can be calculated. Normally horizontal length between top point over column and the inflection point is 10 % of span width. This depends on minimum radius of tendons. When calculating the balanced load, the prestressing forces are usually reduced with about 10-20 %, loss in prestressing force is about 15 %.

The idealised tendon profile for slabs with two or more spans are shown in fig 1.1 a.

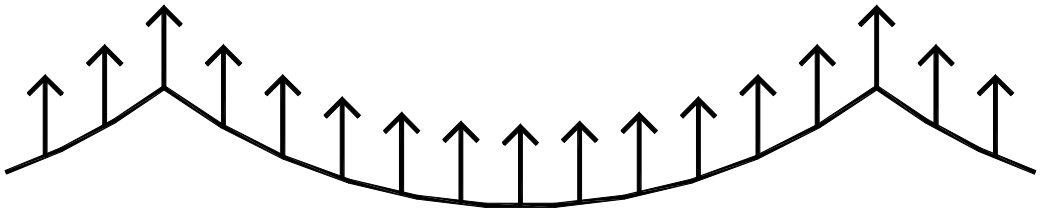

Idealised tendon profile
Figure 1.1 a

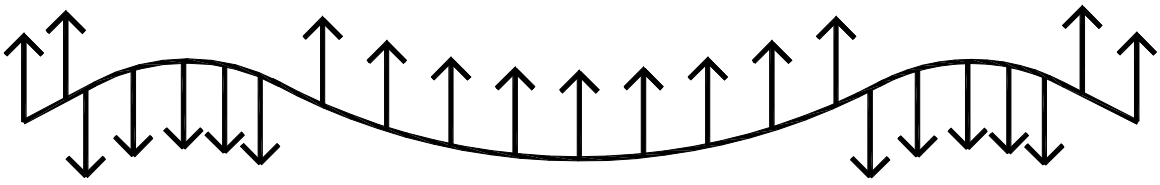

Tendon profile in practice.
Figure 1.1 b

In practice this is not possible, so we have to make an adaptation, see fig 1.1 b, if this should be possible to achieve. There are some recommendations /2/ for a minimum radius of curvature.
Most of the tendons used in slabs, are 13 mm or 16 mm strands, and this recommends a minimum radius on 2500 mm. The parabola over the column has to be as short as possible, but not shorter than the minimum radius recommended. Usually the length of the convex segment is about 10 % of the span at each side from centre column for the interior span, and 5 - 10 % of the span at end columns. Since the upward and downward load must be equal, there can be large shear forces around the columns, especially around the inner columns. In flat slabs the tendons usually are placed in both directions.

Examples of tendon distributions are shown in fig 1.2.

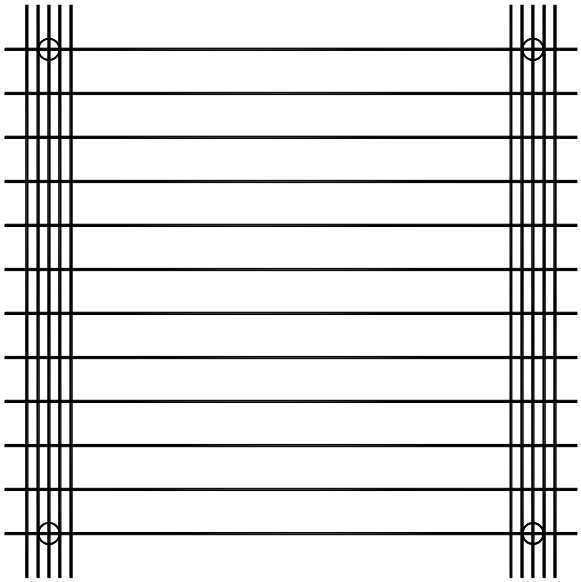

Combination of concentrated
and distributed tendons
Figure 1.2 a

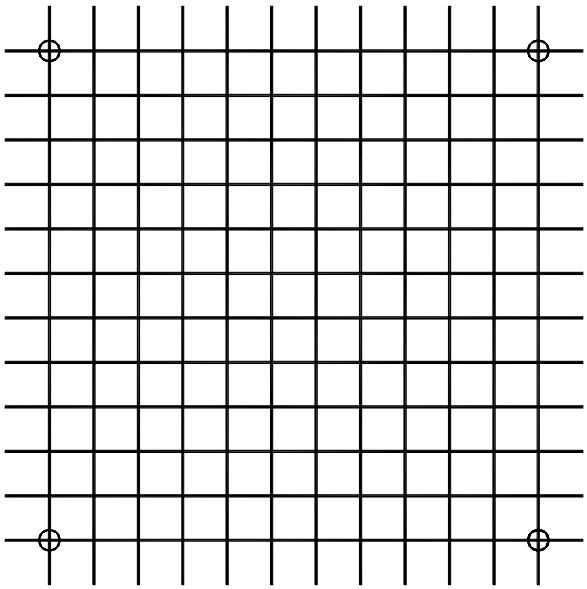

Distributed tendons in
both directions
Figure 1.2 b

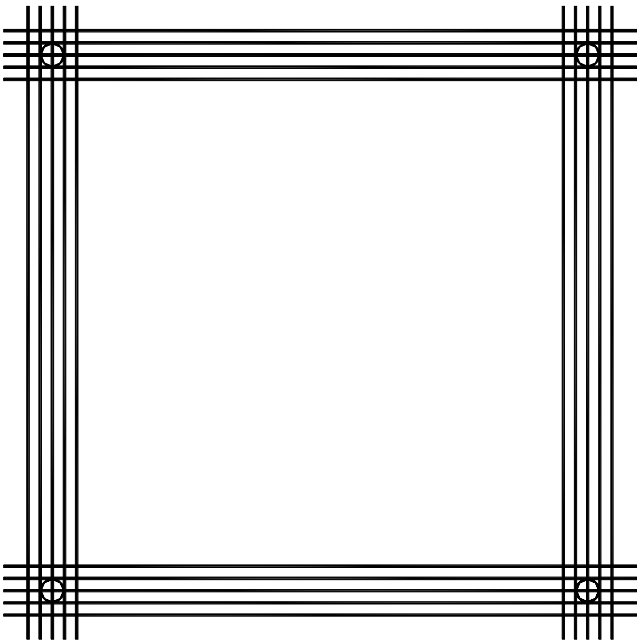

Concentrated tendons in
both directions.
Figure 1.2 c

Figure 1.2 a shows a combination of tendon distributions in figure 1.2 b and c, which is the most used method as it is easier to install, especially compared to the system shown in fig 1.2 b.

When starting the calculation of tendon geometry, it is necessary to divide the tendon in each span into three parts. This is the same for interior and for exterior spans. The first part of the tendon in outer span starts at the edge and in the middle of the slab thickness fig 1.3. For an interior span it starts at the end and at the top of the slab fig 1.4.

First part of tendon from edge.
Figure 1.3

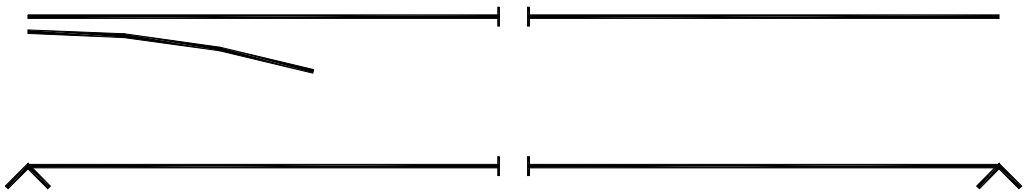

First part of tendon in an interior span.
Figure 1.4

Part number two starts where part number one ends, this point, inflection point, is the point where the tendons have a contraflexure. This part is the longest one and ends at the inflection point near next column fig 1.5. Part three is like part one.

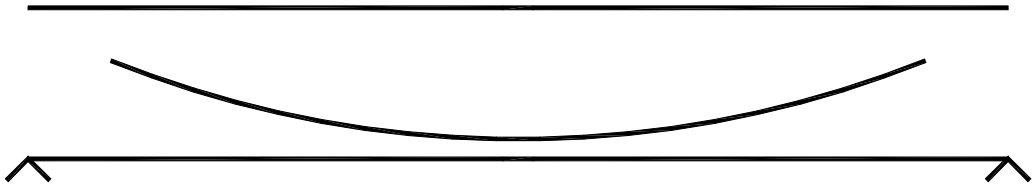

Tendon in bottom of the slab.
Figure 1.5

Before the calculation of the tendon geometry starts, there are some values to be given. The tendon usually starts and ends in the middle of the slab thickness. Then we need the concrete cover at the top and at the bottom of the slab, and the distance from the centrelines of the column to the inflection point. To calculate the tendon profile there are three equations:

1. Parabola from A to B:

$$y_1 = k_1 \cdot x_1^{\,2} \qquad (1.1)$$

When $x_1 = l_{AB}$ then $y_1 = -a_B$

2. Parabola from B to D:

$$y_2 = k_2 \cdot x_2^{\,2} \qquad (1.2)$$

When $x_2 = -l_{BC}$ then $y_2 = a_A - a_C - a_B$

When $x_2 = l_{CD}$ then $y_2 = a_E - a_C - a_D$

Where

a_A = distance from bottom of the slab to point A.
a_B = vertical distance from point A to point B.
a_C = distance from bottom of the slab to point C.
a_D = vertical distance from point E to point D.
a_E = distance from bottom of the slab to point E.

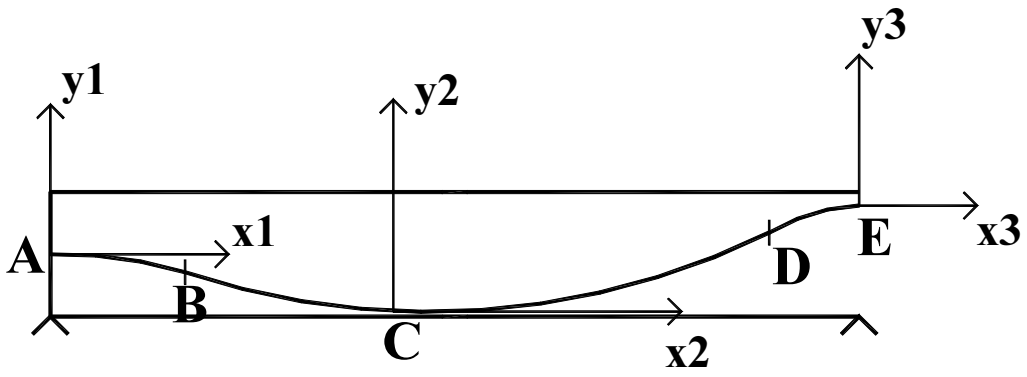

Tendon geometry.
Figure 1.6

3. Parabola from D to E:

$$y_3 = k_3 \cdot x_3^{\,2} \qquad (1.3)$$

When $x_3 = -l_{DE}$ then $y_3 = -a_D$

The parabola tangents for parabola one and parabola two have to be equal in point B, and for parabola two and parabola three in point D.

Point B: $\frac{dy_1}{dx_1} = \frac{dy_2}{dx_2} \Rightarrow 2k_1 \cdot l_{AB} = 2k_2 \cdot \left(-l_{BC}\right) \Rightarrow k_1 = \frac{-k_2 \cdot l_{BC}}{l_{AB}}$ (1.4)

Point D: $\frac{dy_2}{dx_2} = \frac{dy_3}{dx_3} \Rightarrow 2k_2 \cdot l_{CD} = 2k_3 \cdot \left(-l_{DE}\right) \Rightarrow k_3 = \frac{-k_2 \cdot l_{CD}}{l_{DE}}$ (1.5)

This gives:

$$a_B = k_2 \cdot l_{BC} \cdot l_{AB} \qquad (1.6)$$
$$a_D = k_2 \cdot l_{CD} \cdot l_{DE} \qquad (1.7)$$

The vertical distance from the tendon in point A to bottom of the slab in point C:

$$a_A = a_C + a_B + k_2 \cdot l_{BC}^{\,2} \qquad (1.8)$$

and the vertical distance from the tendon in point E to bottom of the slab in point C:

$$a_E = a_C + a_D + k_2 \cdot l_{CD}^{\,2} \qquad (1.9)$$

Solving for k_2 in each case gives the solution:

$$Ax^2 + Bx + C = 0 \tag{1.10}$$

where:

$$A = a_A - a_E$$
$$B = (a_A - a_C) \cdot (l_{DE} - 2L) + l_{AB}(a_E - a_C)$$
$$C = L \cdot (L - l_{DE}) \cdot (a_A - a_C)$$

and *x* is the horizontal distance from point A to point C, l_{AC}

This gives:

$$k_2 = \frac{a_A - a_C}{(l_{AC} - l_{AB})^2 + (l_{AC} - l_{AB}) \cdot l_{AB}} \tag{1.11}$$

$$k_1 = \frac{-k_2 \cdot (l_{AC} - l_{AB})}{l_{AB}} \tag{1.12}$$

$$k_3 = \frac{-k_2 \cdot (L - l_{AC} - l_{DE})}{l_{DE}} \tag{1.13}$$

The distance from bottom and up to the tendon can then be found in each point in the slab.

$$0 \le x \le x_B \qquad y = a_A + k_1 \cdot x^2 \tag{1.14}$$
$$x_B \le x \le x_C \qquad y = a_A + k_1 \cdot l_{AB}{}^2 - k_2 \cdot x^2 \tag{1.15}$$
$$x_C \le x \le x_D \qquad y = a_C + k_2 \cdot x^2 \tag{1.16}$$
$$x_D \le x \le x_E \qquad y = a_C + k_2 \cdot l_{CD}{}^2 - k_3 \cdot x^2 \tag{1.17}$$

This gives a good curvature for tendons in slabs loaded with distributed load. With a concentrated load on the slab, the normal tendon curvature will have the lowest drape of tendons under that load, if possible.
The curvature should be controlled at the top of each column. In the middle of the span there is usually no problem with the curvature. After calculating the distance from top of tendon to the inflection points, it is possible to find the radius fig 1.7 /3/.

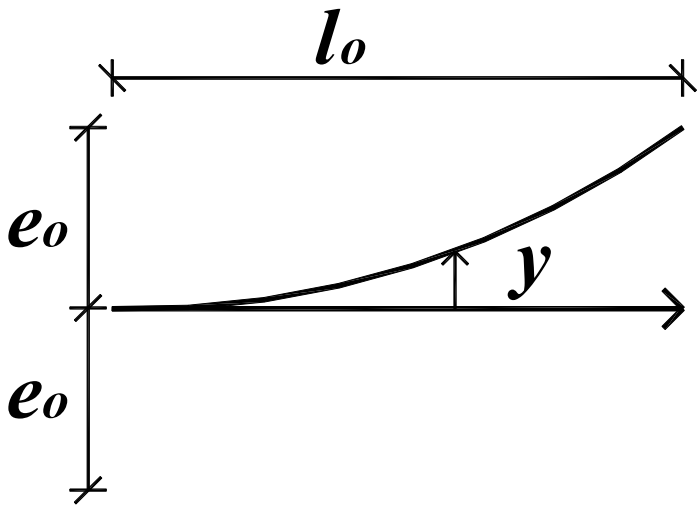

Radius of tendon.
Figure 1.7

$$y = e_0 \cdot \left(\frac{x}{l_0}\right)^2 \quad (1.18) \qquad R = \frac{{l_0}^2}{2e_0} \quad (1.19)$$

Since the tendon has a curved geometry, the total length of the tendon is longer than the horizontal distance between start and end point, active and passive anchorage.
Total length of a curved tendon can be calculated as:

$$L = \sum x\left(1 + \tfrac{2}{3} \cdot \left(\tfrac{y}{x}\right)^2 - \tfrac{2}{5} \cdot \left(\tfrac{y}{x}\right)^4\right) \quad /50/ \quad (1.20)$$

A.1.3 Balanced load concept

The load from tendons between inflection points will be a distributed load, *w*. This load gives the same moment in the middle of span as a simple supported single span slab gives:

$$M = \frac{1}{8} \cdot q \cdot l^2 \qquad (1.21)$$

where

q is the distributed load, dead load *g* and live load *p*.

The eccentricity of the tendon gives also a moment in the slab.

$$M = P_p \cdot f \qquad (1.22)$$

where

P_p is the average prestressing force and *f* is the total drape between inflection point.

If the tendon should take all dead load, *q* had to be changed with *g*, and the moment from distributed load and the moment from tendons are equal.

$$\frac{1}{8} \cdot g \cdot l^2 = P_p \cdot f \cdot n$$

This gives the number of tendons: $n = \frac{g \cdot l^2}{8 \cdot P_p \cdot f}$ (1.23)

or load from one tendon: $w = \frac{8 \cdot P_p \cdot f}{l^2}$ (1.24)

Number of tendons if tendon should take all dead load:

$$n = \frac{g}{w} \qquad (1.25)$$

where

g = balanced load (dead load or dead load plus 10 – 20 % live load)

Balanced load for cantilevers.
The moment at a cantilever from dead weight is:

$$M = \frac{g \cdot l^2}{2} \tag{1.26}$$

and with a total drape from inflection point until end of the tendon, *f*, which gives a moment from tendons:

$$M = P \cdot f \tag{1.27}$$

That gives load from one tendon:

$$w = \frac{2 \cdot P \cdot f}{l^2} \tag{1.28}$$

The concrete stress after all tendons are stressed, is about 2.0 N/mm^2. Another way to find the number of tendons and tendon eccentricity is to calculate maximal permissible stress, try a slab thickness from span to depth ratio and than plot the relation between number of tendons and eccentricity. This is done in spans where the maximal moment occurs. Around the column the shear capacity is most critical.

A.1.4 Stress calculation

A.1.4.1 General

In America and Europe most of the prestressed slabs and beams are built with unbonded tendons. ACI have "recommendations for concrete members prestressed with unbonded tendons" /10/ in addition to ACI's "building code requirements for reinforced concrete (ACI 318-83)" /11/. ACI gives relatively detailed rules in chapter 18 "Prestressed concrete". It does not accept the same stress in tendons as the Norwegian standards do. ACI : $0.82f_{py}$ after stressing. ACI also describes each loss of prestress and some rules for the anchorage zone.

The stress in bottom of a slab after jacking is calculated as:

$$\sigma_b = \sigma_N + \sigma_M \tag{1.29}$$

where

$$\sigma_N = -\frac{P}{A}$$

and

$$\sigma_M = \left(M_o + M_f + \Delta M_f\right)/W \tag{1.30}$$

P = Force in concrete from jacking, positive as tension.
A = Cross-sectional area of the slab.
M_o = Moment from dead load.
M_s = Moment from dead load and live load.
M_f = Moment from tendons with an eccentricity f. $M_f = P \cdot f \cdot n$
ΔM_f = Secondary moment from prestressing.
W = Section modulus.

For a slab with positive moment in the middle of the span, tension in bottom fibres, this gives a stress in bottom as:

$$\sigma_b = -\frac{P}{A} + \left(M_o - P \cdot f \cdot n + \Delta M_f\right)/W \le \sigma_{Max} \qquad (1.31)$$

after stressing. After time t the force is reduced due to loss in prestressing. Since this loss is about 15 %, a normal estimate is to use a force after long time as: $0.85 \cdot P$ This gives a stress in bottom fibres after long time as:

$$\sigma_{t,l} = -\frac{0.85 \cdot P}{A} + \left(M_s - 0.85 \cdot P \cdot f \cdot n + \Delta M_f\right)/W \qquad (1.32)$$

These two equations represent a relation between number of tendons, n, and eccentricity, f.

A.1.4.2 Example

This is shown for a slab with one span of 9000 mm, live load of 2.5 kN/m^2 and concrete C35, figure 1.8. Since one span gives small eccentricity of tendons (no top over column) the span to depth ratio is chosen to 36. This gives a slab thickness 9000/36 = 250 mm. The relation between number of tendons and eccentricity is shown in fig 4.2 a and b.

Dead load: $g = 25KN/m^3 \cdot 0.25m = 6.25KN/m^2$

Live load: $p = 2.5KN/m^2$

Moment:
$$M_o = \frac{1}{8} \cdot 6.25 \cdot 9^2 = 63.3KNm$$
$$M_s = \frac{1}{8} \cdot (6.25 + 2.5) \cdot 9^2 = 88.6KNm$$

Cross-sectional area of the slab: $A = 250 \cdot 1000 = 2.5 \cdot 10^5 mm^2$

Section modulus $W = \frac{1}{6} \cdot 1000 \cdot 250^2 = 1.04 \cdot 10^7 mm^3$

Tendons with area 100 mm^2 and stressing to 85 % of f_y that gives a jacking force:

$$P = 0.85 \cdot 1670N/mm^2 \cdot 100 = 141950N \approx 141KN$$

Maximal tension stress from NS 3473 before cracking occurs is:

$$\sigma_{Max} \leq k_w \cdot f_{tn} / k_t$$

k_w = 1.5-h/h_1 h_1= 1.0m h= slab thickness, 0.25 m => k_w = 1.25
f_{tn} = tensile strength f_{tn} =1.70 N/mm^2
k_t = environment conditions, NA, after NS 3473 k_t = 1.0

This gives $\sigma_{Max} = 2.13 N / mm^2$

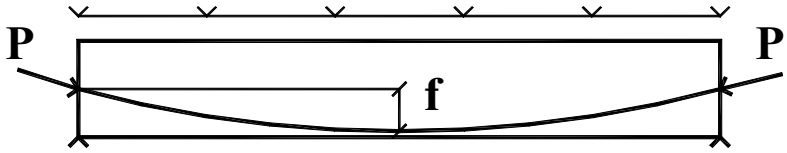

Tendon in slab with jacking force P and maximal drop f.
Figure 1.8

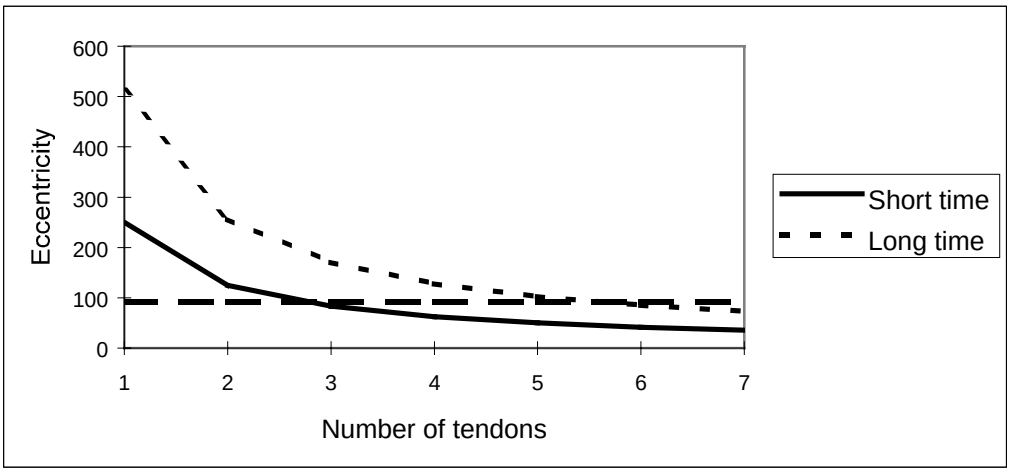

Relation between number of tendons and eccentricity, tension in bottom fibre.
Figure 1.9 a

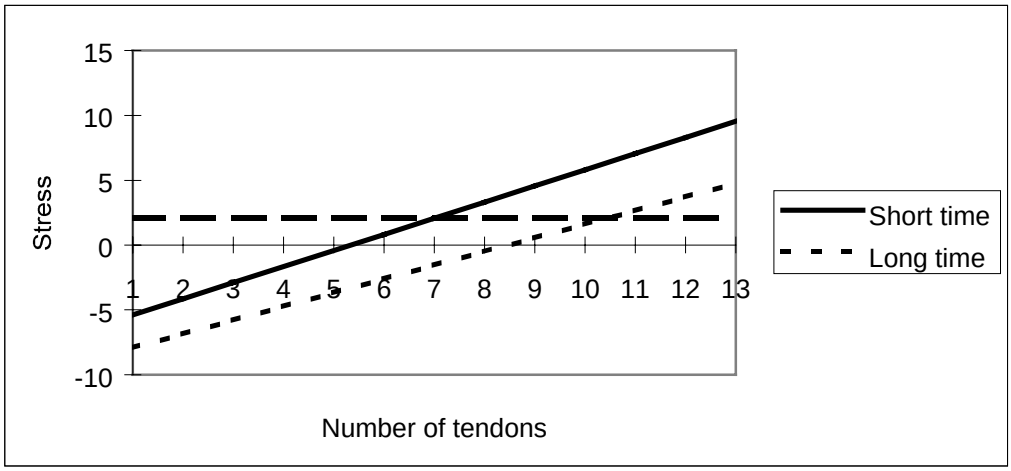

Relation between number of tendons and stress, tension in top fibre.
Figure 1.9 b

Since the slab thickness was chosen as 250 mm, the maximal drop in 16 mm tendon with cover of 25 mm is:

$$f = \frac{250}{2} - 25 - \frac{16}{2} = 92mm$$

Five to six tendons pr m, figure 1.9 a, will give tensile strength in bottom of concrete lower than the maximum tension after long time. Figure 1.9 b shows that more than seven tendons give higher tension in top fibre after short time than maximum tension.

A.1.5 Moment distribution

Calculation of moment in flat slab can be done either by using equivalent frame method or yield-line calculation. BS8110 /1/ recommends that the column strip is assigned as 75 per cent of total hog moment and 55 per cent of the sag moment. The middle strip is designed to resist the remaining 25 per cent of hog moment and 45 per cent of the sag moment.

As ACI also describes how to calculate moment in column strip and middle strip, this will not be repeated here.

In EuroCode /16/ the following methods of analysis are acceptable: linear analysis with or without redistribution, plastic analysis based either on the kinematics method (upper bound) or on the static method (lower bound), and numerical methods taking account of the non-linear material properties. Current methods of plastic analysis are the yield-line theory and the strip method. EuroCode uses the width of $0.3 \cdot l_x$ and $0.3 \cdot l_y$ for column strip with inner columns and $0.15 \cdot l_x$ and $0.15 \cdot l_y$ for column strip with exterior column. K.W.Johansen /26/ has described the yield-line theory and only some possible yield-lines for flat slabs are shown here, fig 1.10 a and b.

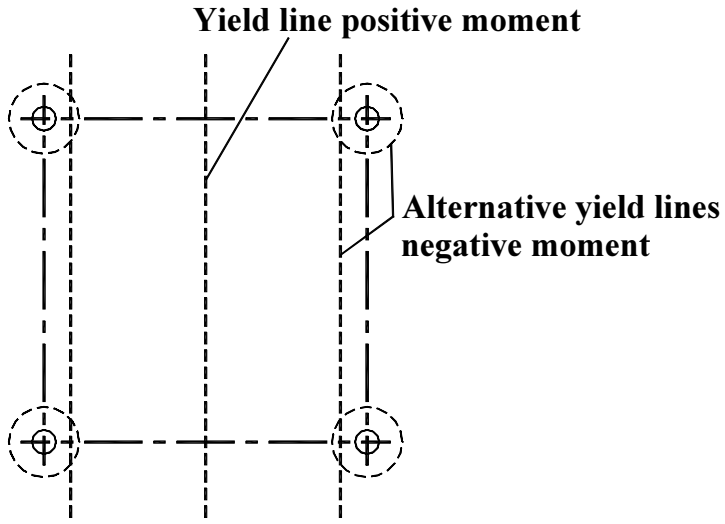

Possible yield-lines for flat slab. K.W. Johansen /26/.
Figure 1.10 a

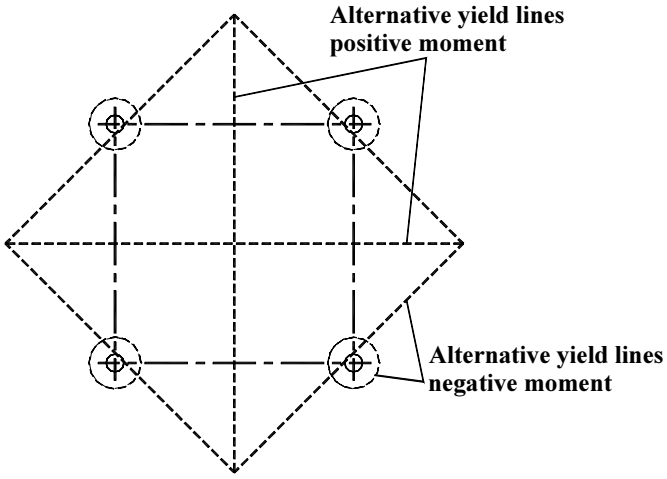

Possible yield-lines for flat slab. K.W. Johansen /26/.
Figure 1.10 b

This method assumes a ductile cross section, and this can be done either by using some reinforcement or bonded prestressing.

Rules in Euro Code and ACI are for reinforced slabs.

In a test described in chapter four, the frame method is used to calculate moment in span and over the column. The static system used in this test, gives deflections close to the observed values, but there might always be a discussion about parameters as column strip width, stiffness of column strip and size of load area that should be included in this width. In the Norwegian standard from 1973, a table with moment distribution in column strip and span strip increased the moment in column strip with 33 % and reduce the moment in slab strip with 33 %. Column strip width in this case was ½ of span width. The author finds it more practical to use smaller column strip width, and calculate moment and stiffness with this width, but load the "frame" with load from ½ of span width.

There can also be a discussion of load area in a exterior span if there is a wall as a support in one end of this span, and a column strip in the other end. The column strip is prestressed with tendons, and they are distributed at about one metre. This is like a beam, and the load in the rest of the span should be distributed 50 % to the wall and 50 % to "beam". With small span or if there are several tendons in the column strip, the beam will be a larger part of span, and load in column strip will be more than 50 % of total load.

In the test described in chapter four, the column strip width was set to 1/3 of span width. This is close to rules used in Euro Code. There are no rules given in the Norwegian standard for choice of column strip width or load distribution in flat slabs. In the frame method, loads from tendons are given as load upwards in the span between inflection point, and load downwards over column between inflection point.

A.1.6 Moment capacity

Moment capacity in prestressed concrete is calculated as in reinforced concrete, but the increase of stress in tendons has to be calculated.

ACI recommends an equation for predicting the stress in tendons when the ultimate moment of the slab is reached:

$$f_{ps} = f_{se} + 10000 + \frac{f'_c}{300 \cdot \rho_p} \text{ (psi).} \qquad (1.33)$$

For a member with unbonded tendons and with span to depth ratio greater than 35, Sunidja, Harianto /28/ means that the increased stress in tendons is expressed explicitly as a function of the span to depth ratio as:

$$f_{ps} = f_{se} + \Delta f_{ps} \qquad (1.34)$$

where

f_{se} = effective prestress at service load, after loss.

$$\Delta f_{ps} = \phi \cdot \varepsilon_c \cdot \left(1 - \frac{a}{d_{ps}}\right) \cdot \frac{d_{ps}}{L_{ps}} \cdot E_p \qquad (1.35)$$

where

ϕ is a coefficient around 9.0 for span to depth ratio typical for slabs.
a = depth of equivalent rectangular compression zone.
d_{ps} = distance from extreme compression fibre to centre of prestressed reinforcement.
L_{ps} = initial length of tendon.
E_p = modulus of elasticity of tendon.

A.1.7 Time dependent material properties (modulus of elasticity)

Since the modulus of elasticity of concrete depends on the modulus of elasticity of the aggregate, Hubert /20/ has taken this into account in the following formula:

$$E_o = 4.3 \cdot \beta_a \cdot w_c \cdot \sqrt[3]{f'_c} \qquad (1.36)$$

where β_a is a coefficient that is dependent on the type of aggregate.

$\beta_a \approx 0.7$ for sandstone
$\beta_a \approx 0.9$ for limestone and granite
$\beta_a \approx 1.0$ for quartzite
$\beta_a \approx 1.1$ for basalt or dense limestone.

w_c is the weight density of the concrete and f_c' is the compressive strength in N/mm^2 at the moment of change in the stress. These coefficients are also used in MC90.

With β_a =1.0 and w_c = 2400 kg/m^3 this gives a modulus of elasticity close to the modulus used in the EuroCode.

Hubert has also a relation between modulus of elasticity after time = t and time = 28 days as:

$$\frac{E_t}{E_{28}} = \frac{w_t}{w_{28}} \sqrt[3]{\frac{f'_{ct}}{f'_{28}}} = \frac{w_t}{w_{28}} \sqrt[3]{\beta_t} \ . \qquad (1.37)$$

Since drying has little influence on weight density, $\frac{w_t}{w_{28}} \approx 1.01$ after seven days and $\frac{w_t}{w_{28}} \approx 0.99$ after t = 1 year, the function seems to be equal:

$$E_t = \beta_e \cdot E_{28} \qquad (1.38)$$

where

$$\beta_e = \sqrt[3]{\beta_t} \qquad (1.39)$$

or

β_e is taken from fig 1.11.

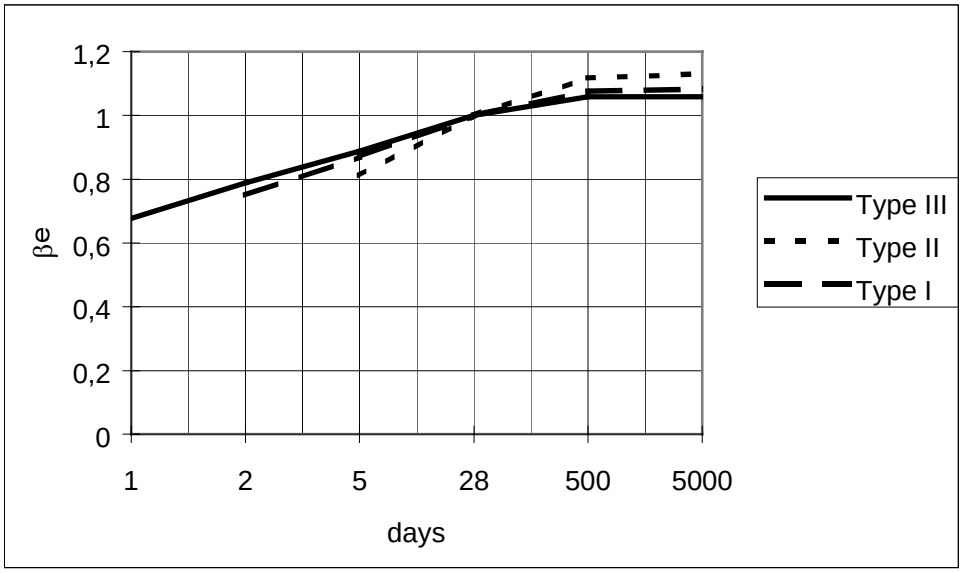

Coefficient β_e after time in days /20/.
Figure 1.11

In an ACI publication /21/ Muller proposes a tangent modulus of elasticity as:

$$E_c = E_{co} \cdot \left(\frac{f_{cm}}{f_{cmo}} \right)^{1/3} \qquad (1.40)$$

where

f_{cm} is the mean compressive strength of concrete cylinder tested at an age of 28 days.
E_{co} =21500 N/mm^2 and f_{cmo} = 10 N/mm^2.

The modulus of elasticity at an age of $t \neq 28$ days, Ec(t), may be estimated as:

$$E_c(t) = E_c \cdot \exp\left[\frac{s}{2} \cdot \left(1 - \left(28 / \left(t / t_1 \right) \right)^{0.5} \right) \right] \qquad (1.41)$$

where s = coefficient which depends on the type of cement, s = 0.2, 0.25 , 0.38 for concrete made with rapid hardening high strength cement (RS), normal or rapid hardening cement (N, R) and slowly hardening cement (SL).
t = age of concrete in days t_1 = 1 day.
This equation is also used in 1990 CEB-FIP Model Code.
Fig 1.12 shows Hubert and Muller's modulus of elasticity.

The modulus of elasticity designed in AS 3600 is given by:

$$E_{cj} = (\rho)^{1.5} \cdot \left(0.043 \cdot \sqrt{f_{cm}}\right) \tag{1.42}$$

and with a density $\rho = 2400 kg/m^3$ it gives $E_{cj} = 5055 \cdot \sqrt{f_{cm}}$ (1.43)

f_{cm} = the mean value of the compressive strength of concrete at the relevant age.

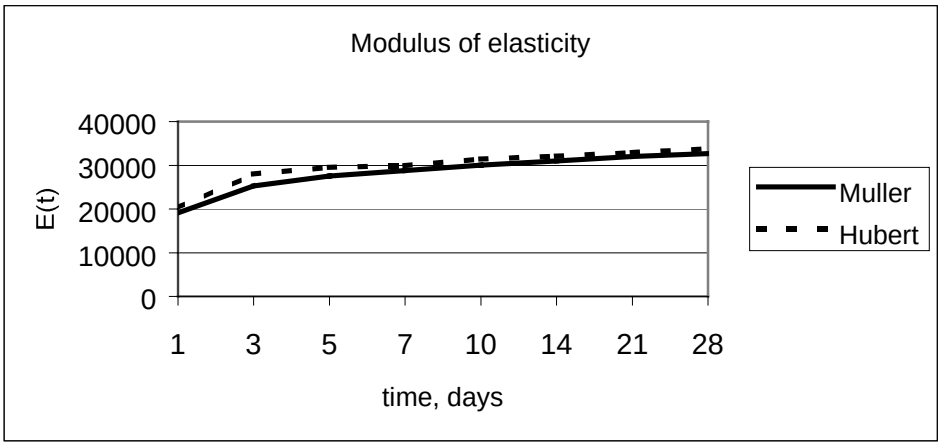

Modulus of elasticity after Hubert and Muller.
Figure 1.12

In figure 1.13 the modulus of elasticity calculated after different codes can be seen in relation to the compressive strength. NS 3473 is based on characteristic compressive strength to calculate modulus of elasticity. Euro Code, ACI and AS3600 apply mean value of the compressive strength.

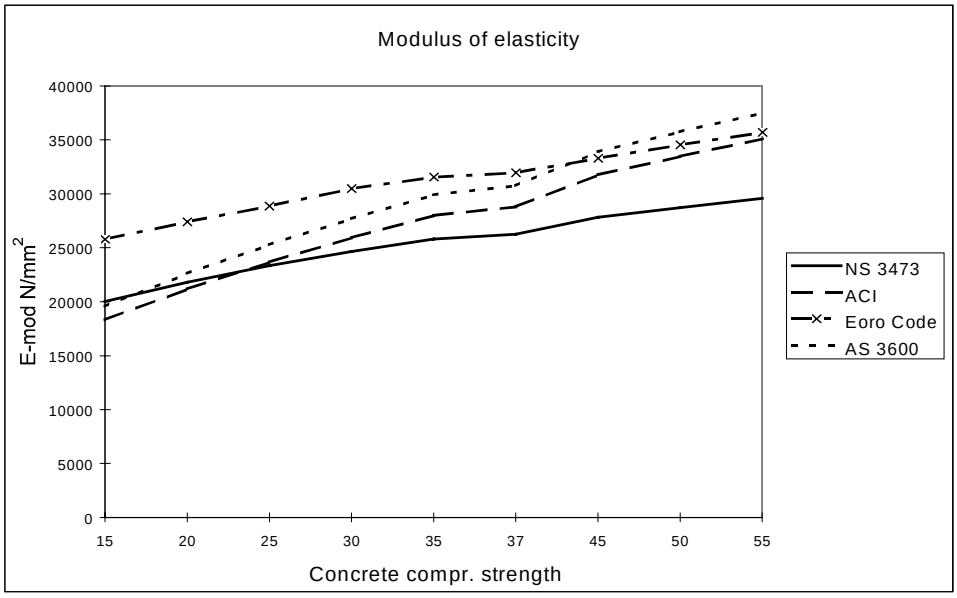

Modulus of elasticity calculated after different codes.
Figure 1.13

A.1.8 Shear reinforcement

In flat slabs the shear force around the column is often more critical than the moment in spans and over the column. The shear capacity is controlled at a distance from column to critical section, and if there is a drop panel, it is controlled at the same distance from this. In flat slabs shear stirrups are often necessary in the sections close to the column. As the only one of the studied standards, ACI gives guidance in the design of shear heads, fig 1.14 /23/.

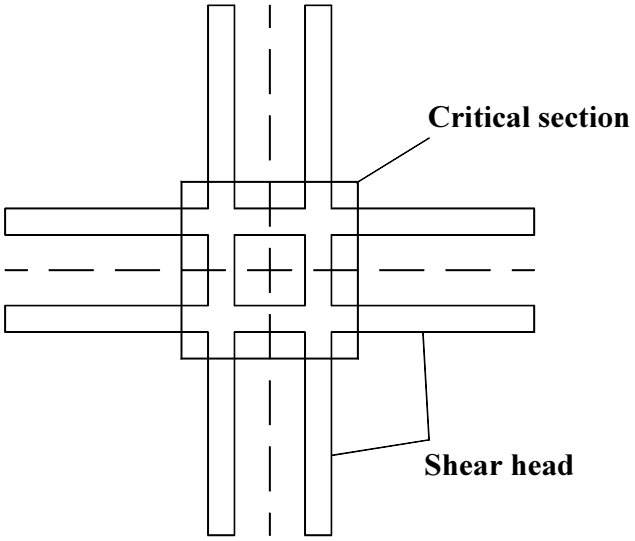

Shear heads after ACI.
Figure 1.14

With use of shear heads, reinforced shear stirrups and/or steel beams can be used, fig 1.15 a, b.

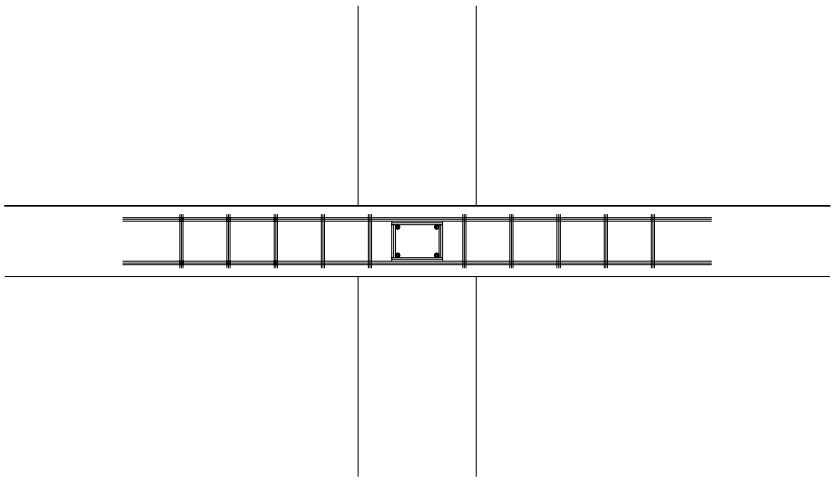

Shear reinforcement.
Figure 1.15 a

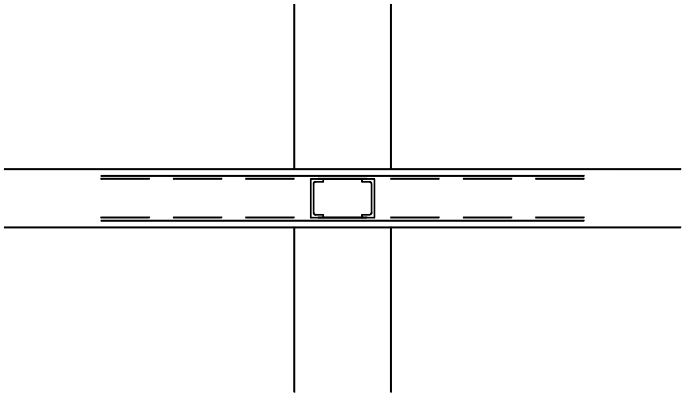

Welded shear head
Figure 1.15 b

Calculation of shear heads is not shown here, but it is described in ACI.

With shear stirrups there are different types of reinforcement and shear studs to use, see fig 1.16.

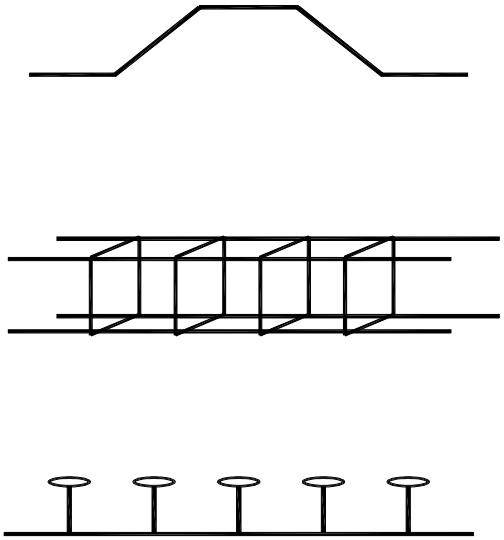

Shear reinforcement and shear studs
Figure 1.16

The most commonly used shear stirrup is reinforcement at an angle of 45 or 90 degree to the length axis.

A.2 Shrinkage and creep

A.2.1 Shrinkage

Shrinkage is defined as the reduction in volume of unloaded concrete at constant temperature. The shrinkage depends on age of concrete, type of cement, relative humidity and thickness of concrete. There are different ways to calculate creep and shrinkage in different standards.

ACI does not calculate creep coefficient or shrinkage in building code, ACI 318-89, but in ACI 209R-92 /51/. Formulas in this code is independent of concrete compressive strength, but depend on cement content for shrinkage, loading age for creep and relative humidity, average thickness, concrete slump, ratio of fine aggregate to total aggregate and air content in concrete for both creep and shrinkage.

The Norwegian standards do not consider the compressive strength of the concrete when calculating shrinkage. There is only a time dependent function and a function of relative humidity.

The Euro Code takes care of the compressive strength in concrete when calculating shrinkage. In the Australian standard AS 3600 shrinkage can be taken from the table, with thickness as the only variable.

The shrinkage calculated after NS 3473 /9/, in concrete is defined as:

$$\varepsilon_{cs}(t,t_s) = \varepsilon_s \cdot \beta_s(t - t_s) \tag{2.1}$$

where

t_s is the age of concrete when drying occur

$$\varepsilon_s = -550 \cdot 10^{-6} \cdot \left(1 - \left(\frac{RH}{100}\right)^3\right) \quad \text{for } RH \geq 40\% \tag{2.2}$$

RH = relative humidity

and the time function is

$$\beta_s(t - t_s) = \left(\frac{t - t_s}{0.035 \cdot h_o^{\,2} + t - t_s}\right)^{0.5} \tag{2.3}$$

h_o = notional size in mm

Rules in EuroCode 2 for calculation of shrinkage are given as:

$$\varepsilon_{cs}(t - t_s) = \varepsilon_{cso} \cdot \beta(t - t_s) \tag{2.4}$$

this is the same as in Norwegian standard but the notional shrinkage coefficient may be obtained from:

$$\varepsilon_{cso} = \varepsilon_s(f_{cm}) \cdot \beta_{RH} \quad \text{with} \tag{2.5}$$

$$\varepsilon_s(f_{cm}) = \left[160 + \beta_{sc} \cdot (90 - f_{cm})\right] \cdot 10^{-6} \tag{2.6}$$

$$\beta_{RH} = -1.55 \cdot \beta_{sRH} \quad \text{for} \quad 40\% \le RH \le 99\% \tag{2.7}$$

$$\beta_{sRH} = 1 - \left[RH/100\right]^3 \tag{2.8}$$

f_{cm} = mean compressive strength of concrete in N/mm^2 at the age of 28 days.
β_{sc} = Coefficient that depends on type of cement:
= 4 for slow hardening cements, S
= 5 for normal or rapidly hardening cements, N, R
= 8 for rapid hardening high strength cements, RS

These equations regard concrete strength and cement type as both depends on shrinkage strain. Shrinkage calculated after Australian Standard /15/ depend only on one coefficient, shrinkage strains coefficient k_1, from fig 2.1, for various environments.
Shrinkage is given by:

$$\varepsilon_{cs} = k_1 \cdot \varepsilon_{cs,b} \tag{2.9}$$

where

$$\varepsilon_{cs,b} = 700 \cdot 10^{-6} \tag{2.10}$$

k_1 depends on thickness of slab, and geographic position in Australia.
AS 3600: “Consideration shall be given to the fact that ε_{cs} has a range of $\pm 30\%$.” With this range, this standard does not need to be commented any more.

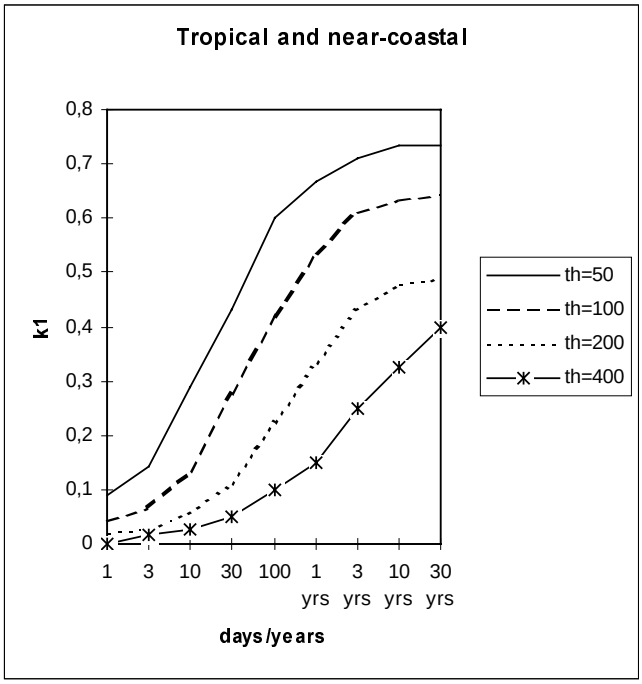

Coefficient to calculate shrinkage after AS3600.
Figure 2.1

Calculation of shrinkage after CEB-FIP Model Code 1990 /33 and 46/ are nearly the same as in EuroCode, and given by:

$$\varepsilon_{cs}(t,t_o) = \varepsilon_s(f_{cm}) \cdot \beta_{RH} \cdot \beta_s(t - t_o) \tag{2.11}$$

$$\beta_s(t - t_o) = \beta_s(t - t_s) \quad \text{above} \tag{2.12}$$

$$\beta_{RH} = 1.55 \cdot \left(1 - \left(RH/100\right)^3\right) \tag{2.13}$$

$$\varepsilon_s(f_{cm}) = \left(250 + \beta_{sc} \cdot \left(75 - f_{cm}\right)\right) \cdot 10^{-6} \geq 250 \cdot 10^{-6} \tag{2.14}$$

β_{sc} is a coefficient dependent on the cement type:
= 3 for normal and slowly hardening cements, N, S
= 5 for rapid hardening cements, R
= 9 for rapid hardening high strength cements, RS

ACI 318-89 /11/ references to ACI 209R-92 /49/ with calculation of shrinkage, and this is given by: $(\varepsilon_{sh})_t = \frac{t}{35+t}(\varepsilon_{sh})_u$ (2.15)

where

t = time in days after initial wet curing

$(\varepsilon_{sh})_u = 780 \cdot \gamma_{sh} \cdot 10^{-6}$ (2.16)

γ_{sh} = product of correction factors depending on:

Relative humidity	$\gamma_\lambda = 1.40 - 0.010 \cdot \lambda$	λ = relative humidity, in %
Slab thickness	$\gamma_h = 1.17 - 0.00114 \cdot h$	h = thickness, in mm
Slump	$\gamma_s = 0.89 + 0.00161 \cdot s$	s = slump, in mm

Percentage of fine aggregate

$\gamma_\psi = 0.30 + 0.014 \cdot \psi$ for $\psi \le 50\%$

$\gamma_\psi = 0.90 + 0.002 \cdot \psi$ for $\psi > 50\%$

ψ = Ratio of the fine aggregate to total aggregate by weight, in %

Cement content	$\gamma_c = 0.75 + 0.00061 \cdot c$	c = cement content, in Kg/m^3
Air content	$\gamma_\alpha = 0.95 + 0.008 \cdot \alpha$	α = air content, in %

With the same values as for creep calculation in chapter 3, and with an age of concrete in days at the beginning of shrinkage, t_s = 10 days, this gives shrinkage as in fig 2.2.

Shrinkage calculated after different codes.

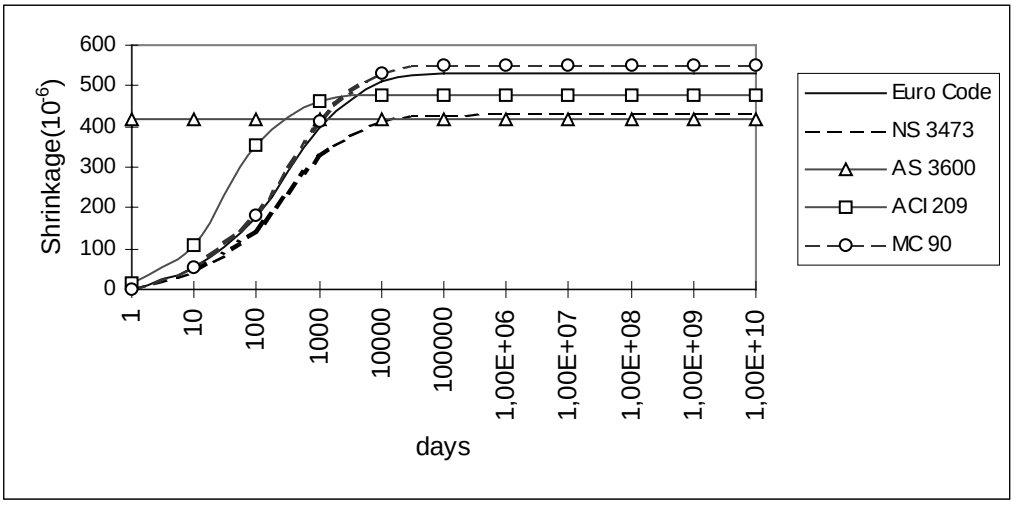

Figure 2.2

It is not correct to compare shrinkage calculation after AS 3600 with other standards, since this standard is developed for tropic areas.

A.2.2 Creep

Loss in prestressing force from creep and shrinkage is about 5 - 7 % of total jacking force. This depends on temperature, time when stressing the tendons, relative humidity and the compressive strength of concrete. Hubert /20/ divided creep into delayed elastic deformation and flow, fig 2.3 a, or basic creep and drying creep, $\varepsilon_c = \varepsilon_d + \varepsilon_f$, fig 2.3 b.

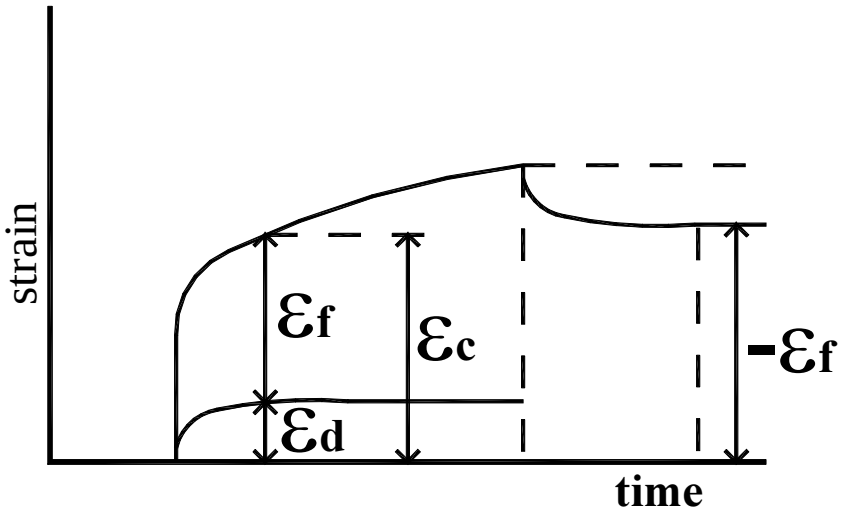

Delayed elastic deformation and flow.
Figure 2.3 a

Delayed elastic strain can be observed only after the load has been removed. In a test done by McHenry /22/ with sealed specimens a relation between observed creep strain and strain from superpositioning two different load cases is shown. Fig 2.4 a-d show that the creep recovery of specimen C is overestimated when applying superposition.

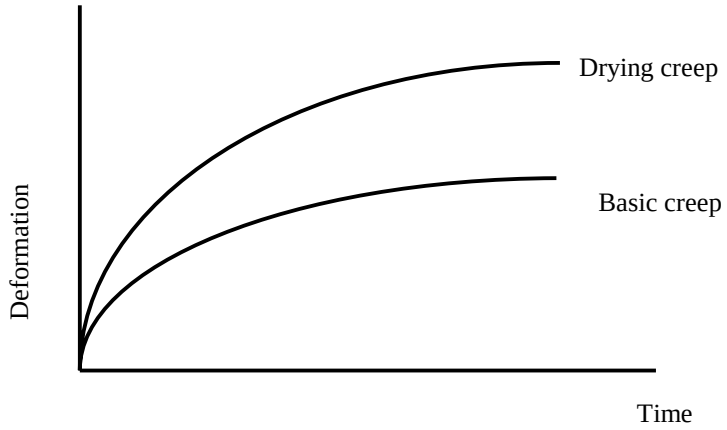

Basic and drying creep.
Figure 2.3 b

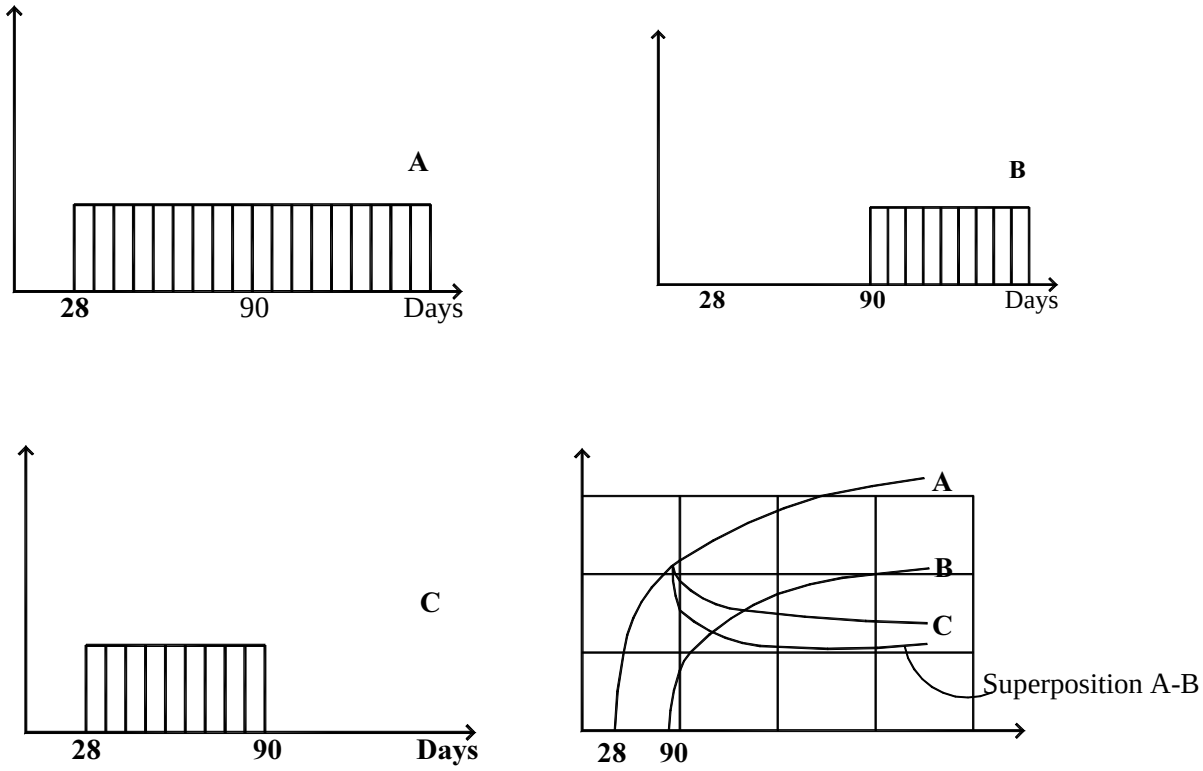

Creep from superpositioning two load cases. Test results from Mc Henry /22/.
Figure 2.4

For prestressed concrete the load from stressed tendons will not be removed, but after time this load will decrease because of long-time loss in prestress force.

The stress dependent creep strain at time t, calculated after NS 3473 /9/ is given as:

$$\varepsilon(t) = \frac{\sigma_c}{E_{cj}} + \frac{\sigma_c}{E_{ck}} \cdot \varphi(t, t_o) \qquad (2.17)$$

where

E_{cj} : modulus of elasticity at time of loading, t_o
E_{ck} : modulus of elasticity after 28 days
$E_{ck} = 9500 \cdot (f_{cck})^{0.3}$

The creep coefficient is calculated as:

$$\varphi(t,t_o) = \varphi_o \cdot \beta_1 \cdot \beta_2 \cdot \beta_c(t-t_o) \tag{2.18}$$

where

φ_o is defined as the influence of the relative humidity, and is calculated as:

$$\varphi_o = 1 + \frac{1 - RH/100}{0.08 \cdot (h_o)^{1/3}} \tag{2.19}$$

$$\beta_1 = \frac{8.3}{3 + \sqrt{f_{cck}}} \tag{2.20}$$

$$\beta_2 = \frac{2.4}{0.1 + t_o^{\,0.18}} \tag{2.21}$$

and the time function is defined as:

$$\beta_c(t-t_o) = \left(\frac{t-t_o}{\beta_h + (t-t_o)} \right)^{0.3} \tag{2.22}$$

This function depends on relative humidity and the section size $h_o = 2 \cdot A_c \cdot U$ in β_h

$$\beta_h = 1.5 \cdot \left[1 + 0.00012 \cdot \left(\frac{RH}{50} \right)^{18} \right] \cdot h_o + 250 \le 1500$$

The Australian standard AS 3600 does not calculate creep as the other standards do. Design creep factor in AS 3600 is $\varphi_{cc} = k_2 \cdot k_3 \cdot \varphi_{cc,b}$ where k_2, k_3 and $\varphi_{cc,b}$ are obtained from fig 2.5 a, b and c.
For tropical and near coastal area the factor k_2=0.1 for t-t_o=20 days and h_o=200 mm. k_3=1.1 for f_{cm}/f_c'=1.0 .

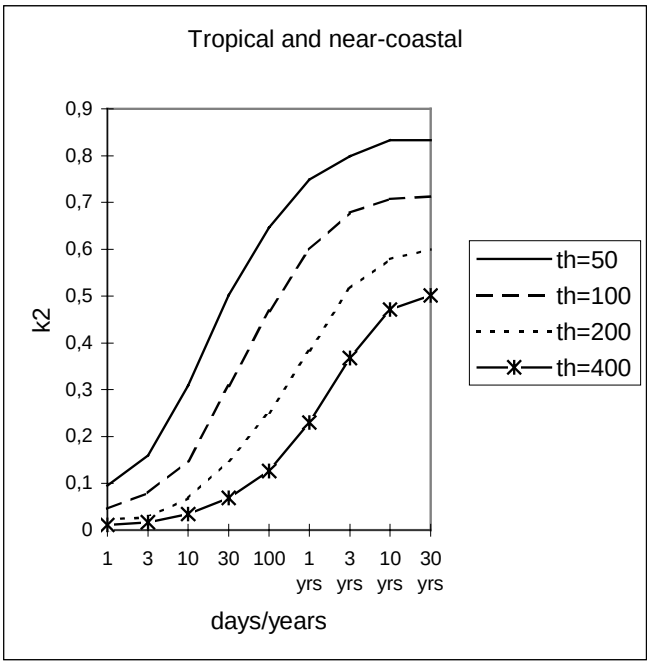

Coefficient k_2 in AS 3600
Figure 2.5 a

Characteristic strength, f'_c, MPa	20	25	32	40	50
Creep factor $\phi_{cc,b}$	5.2	4.2	3.4	2.5	2.0

Creep factor in AS 3600
Figure 2.5 b

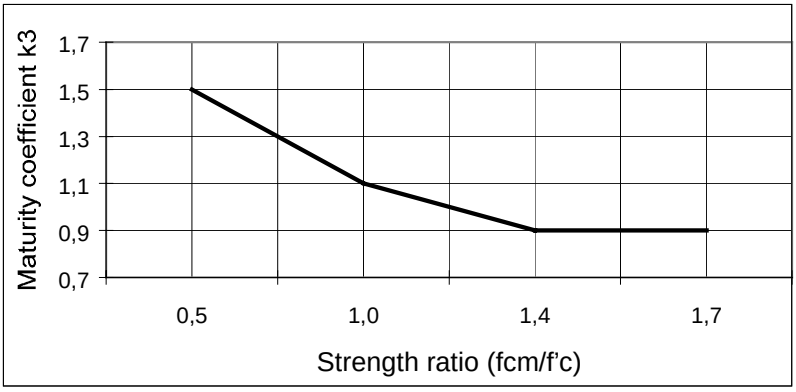

Maturity coefficient in AS 3600
Figure 2.5 c

A.3 Allowable stress and cracking

NS 3473 /9/ does not give any exact calculation rules for prestressed concrete in detail. Stress in tendons can be up to $0.85\,f_y$ or $0.85\,f_{02}$ after stressing, if documented that it does not give any damage on tendons. This is a higher stress level than some other standards give. The stress level in the tendons should never, for any combination of load, be higher than $0.80\,f_y$ or $0.8\ f_{02}$ after short time losses. This means that the jack force can be unto $0.85 \cdot 1670 N / mm^2 \cdot 100 mm^2 = 141950 N$ for a $100 mm^2$ tendon.

There is no crack if:

$$\left(\sigma_N + \sigma_M\right) < k_w \cdot f_{tn} / k_t \qquad (3.1)$$

where

σ_N = stress from normal force
σ_M = stress at the edge from moment
k_w = 1,5-h h: slab thickness in meters
k_t = coefficient depending on the reinforcement and environment.

This relationship is normally satisfied. Minimum reinforcement at the column is necessary anyway.

A.4 Details in flat slab test

A.4.1 Location of strain gauge

Locations of strain gauge in both directions in top and bottom of slab are listed in table 4.1 measured from middle column.

Channel Number	x-direction mm	y-direction mm	Gauge location
1	9000	-7500	Top y-dir.
3	9000	-7500	Top x-dir.
5	9000	-7500	Bottom y-dir.
7	9000	-7500	Bottom x-dir.
9	4500	-7500	Top y-dir.
11	4500	-7500	Top x-dir.
13	4500	-7500	Bottom y-dir.
15	4500	-7500	Bottom x-dir.
17	0	-7500	Top y-dir.
19	0	-7500	Top x-dir.
21	0	-7500	Bottom y-dir.
23	0	-7500	Bottom x-dir.
25	4500	-3750	Top y-dir.
27	4500	-3750	Top x-dir.
29	4500	-3750	Bottom y-dir.
31	4500	-3750	Bottom x-dir.
33	0	-3750	Top y-dir.
35	0	-3750	Top x-dir.
37	0	-3750	Bottom y-dir.
39	0	-3750	Bottom x-dir.
41	9000	0	Top y-dir.
43	9000	0	Top x-dir.
45	9000	0	Bottom y-dir.
47	9000	0	Bottom x-dir.
49	4500	0	Top y-dir.
51	4500	0	Top x-dir.
53	4500	0	Bottom y-dir.
55	4500	0	Bottom x-dir.
57	0	0	Top y-dir.
59	0	0	Top x-dir.
61	0	0	Bottom y-dir.
63	0	0	Bottom x-dir.
65			Reference
67			Reference
69	0	-3750	Temp. top
70	0	-3750	Temp. middle
71	0	-3750	Temp. bottom
72			Temp. air.

Location of strain gauge
Table 4.1

A 4.2 Reaction in strain gauge when loading.

In this chapter strain in reinforcement in each measured point is listed under loading of the slab in figure 4.1 – 4.17. Temperatures after casting are listed in figure 4.18 and 4.19. Forces in load cell are listed in figure 4.20 – 4.24.

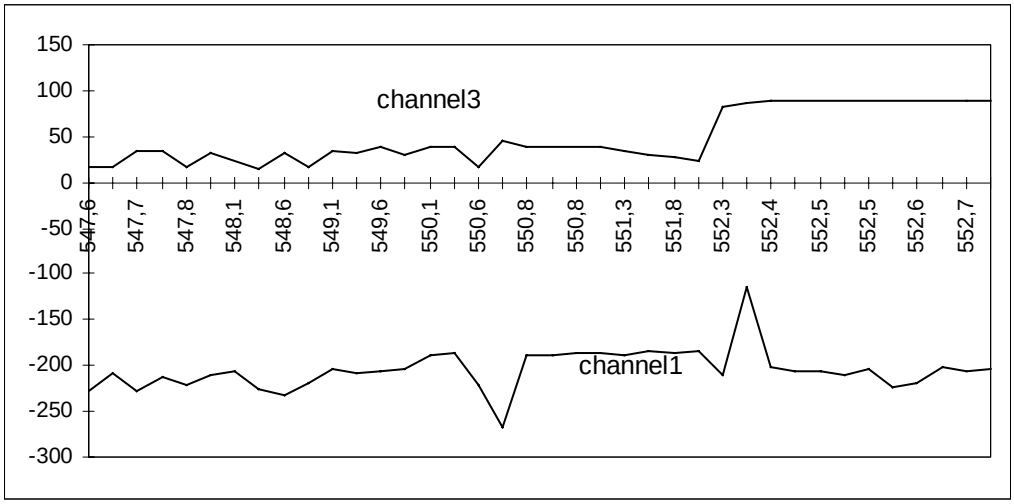

Micro strain after time in hours.
Figure 4.1

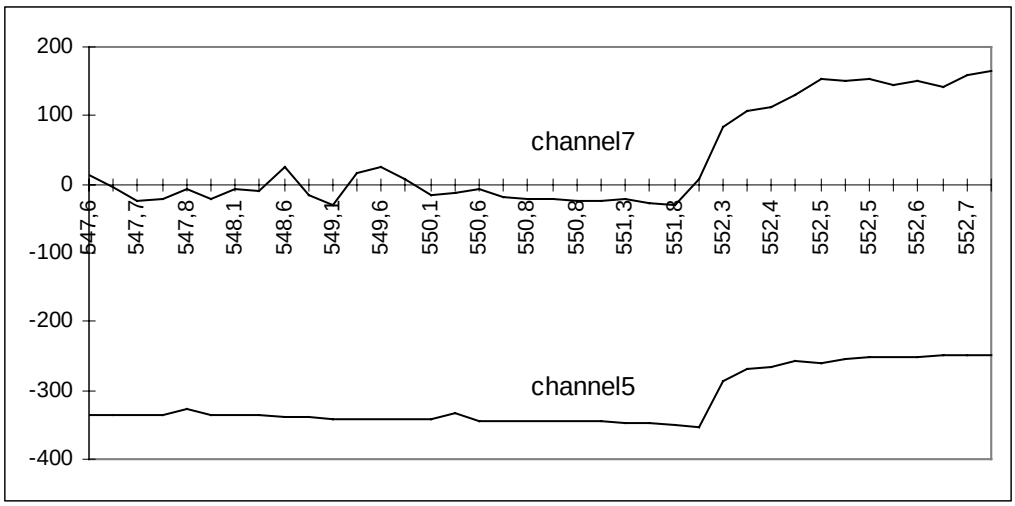

Micro strain after time in hours.
Figure 4.2

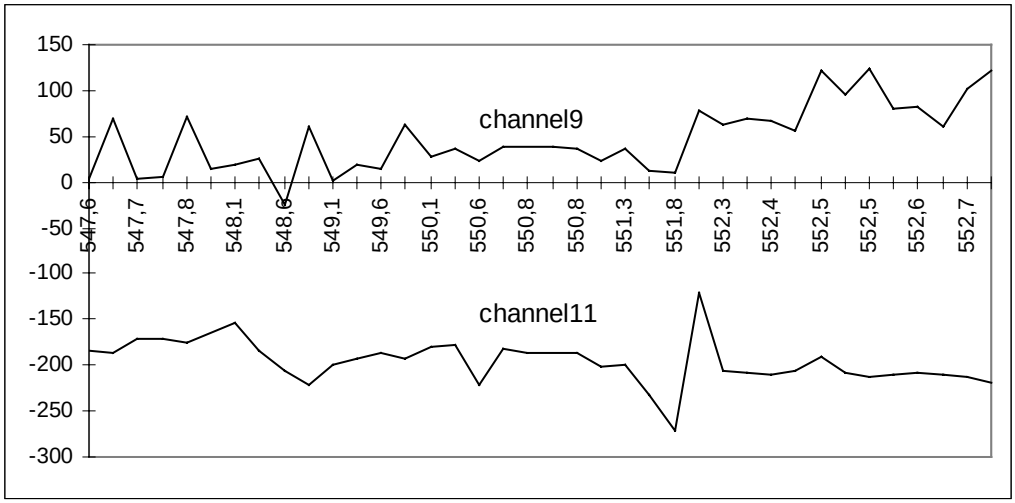

Micro strain after time in hours.
Figure 4.3

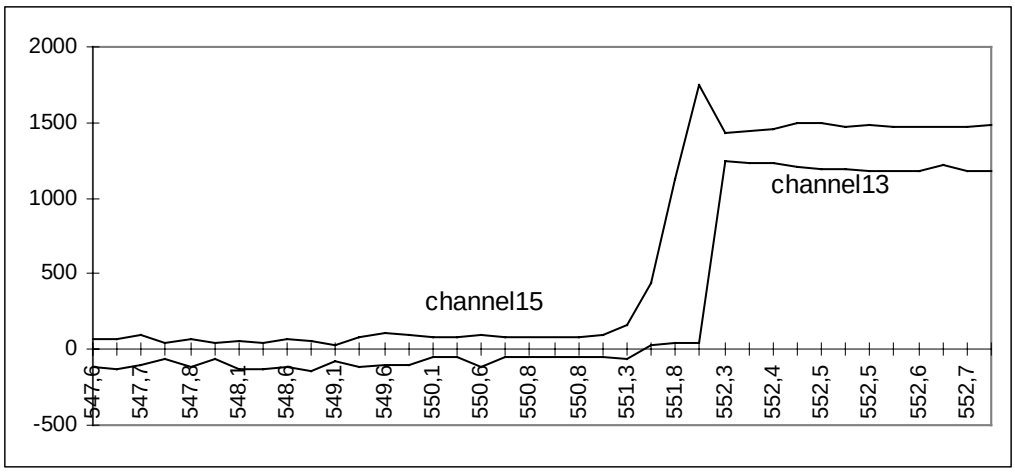

Micro strain after time in hours.
Figure 4.4

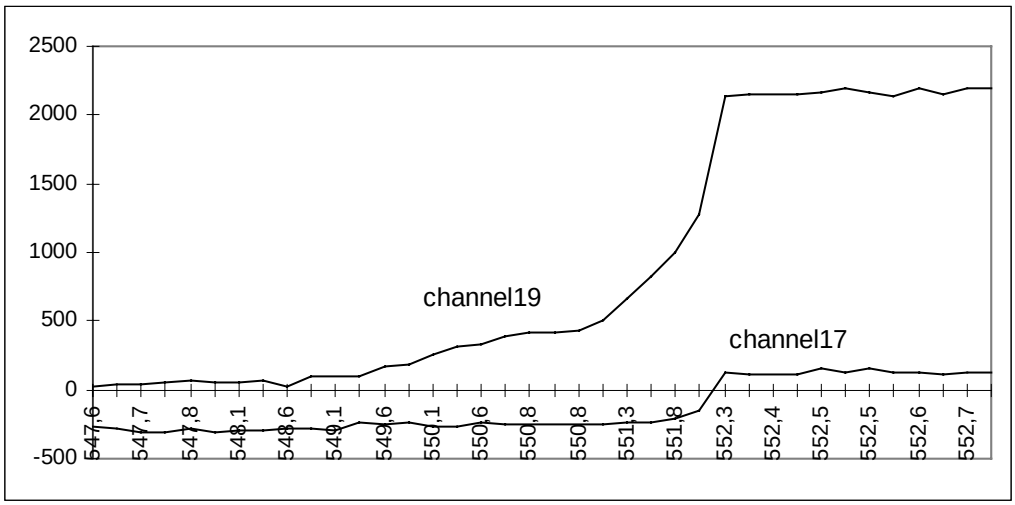

Micro strain after time in hours.
Figure 4.5

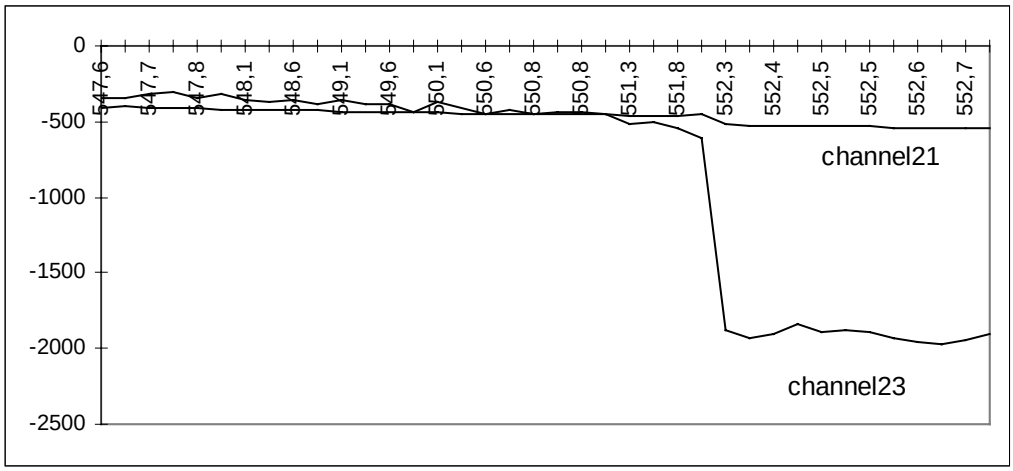

Micro strain after time in hours.
Figure 4.6

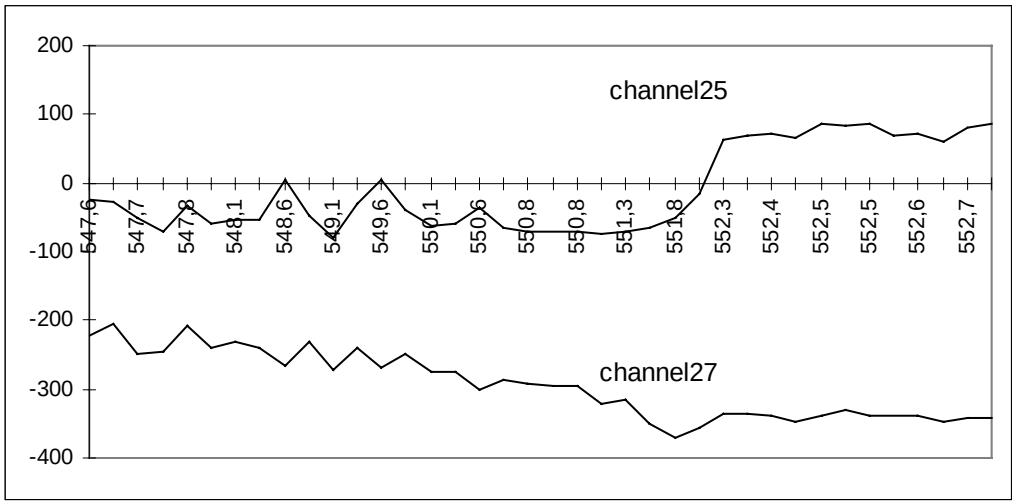

Micro strain after time in hours.
Figure 4.7

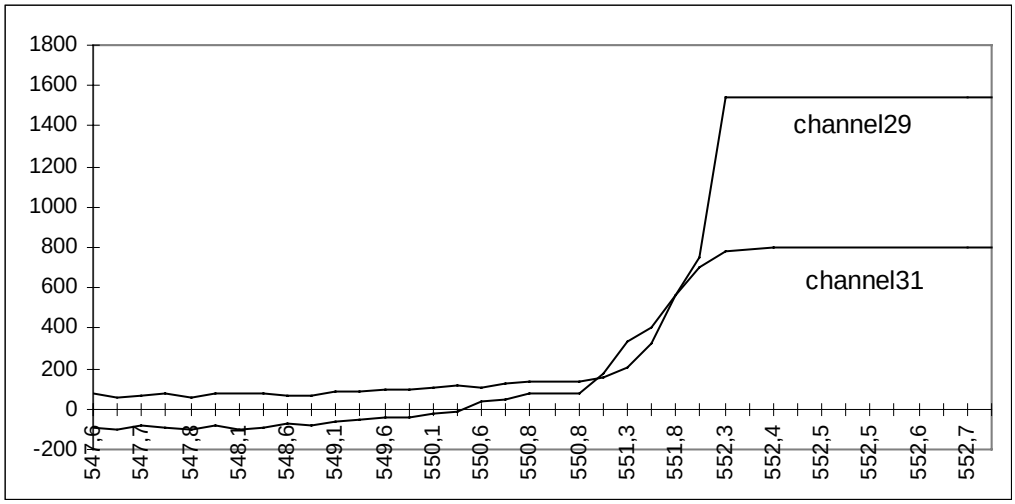

Micro strain after time in hours.
Figure 4.8

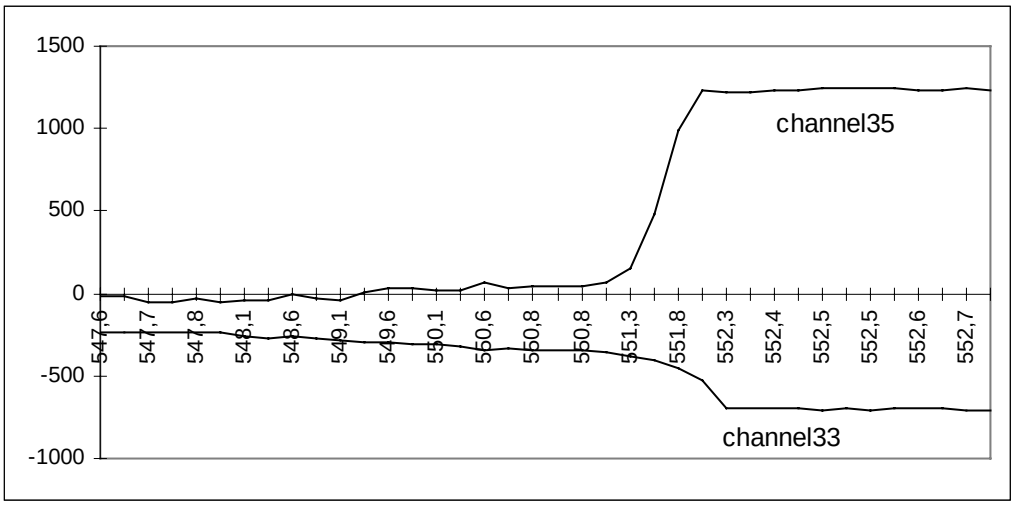

Micro strain after time in hours.
Figure 4.9

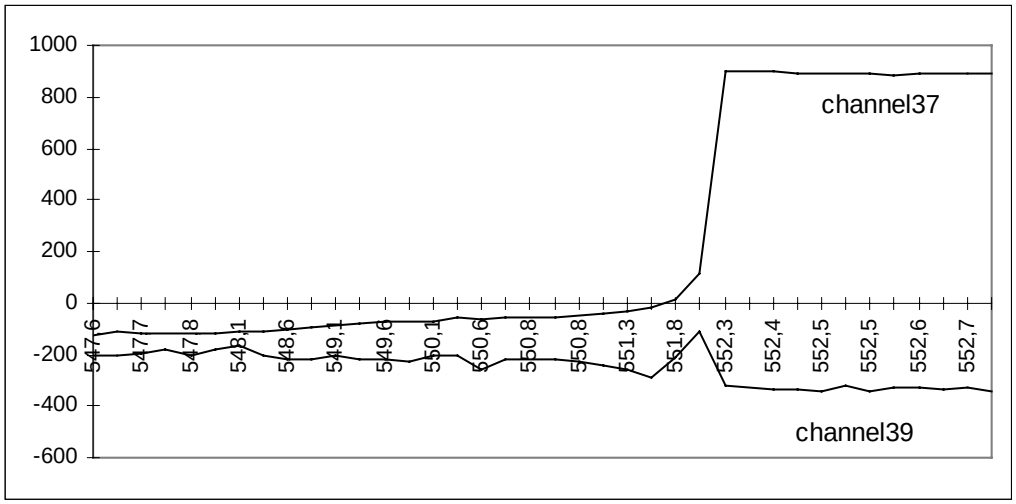

Micro strain after time in hours.
Figure 4.10

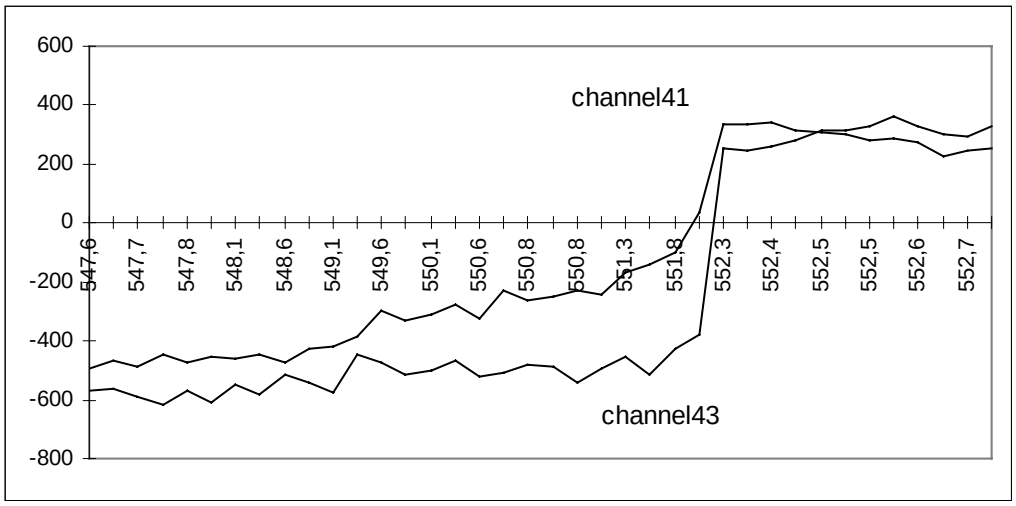

Micro strain after time in hours.
Figure 4.11

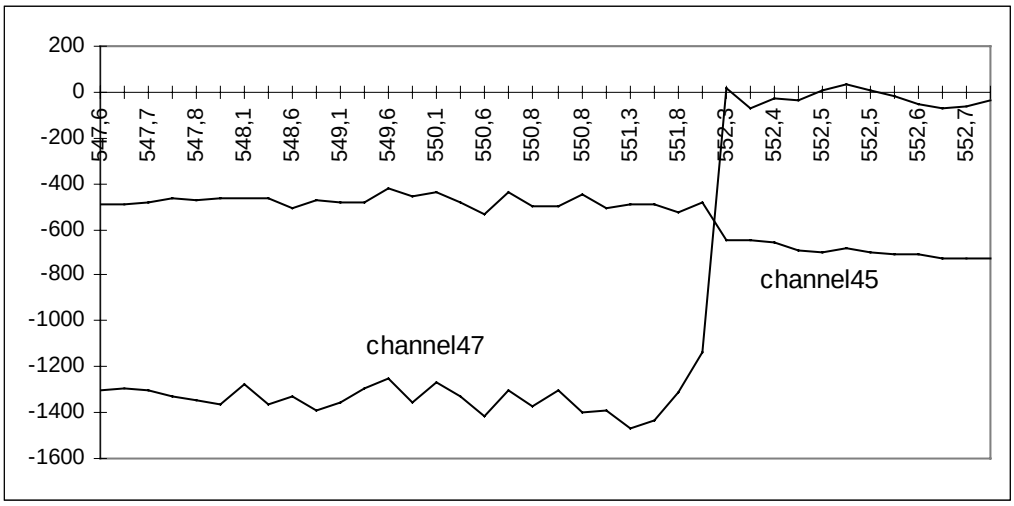

Micro strain after time in hours.
Figure 4.12

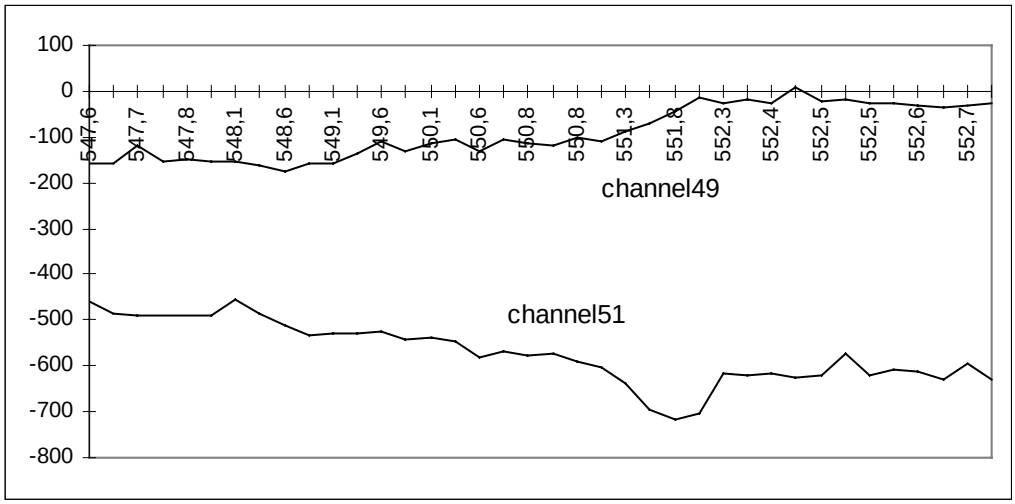

Micro strain after time in hours.
Figure 4.13

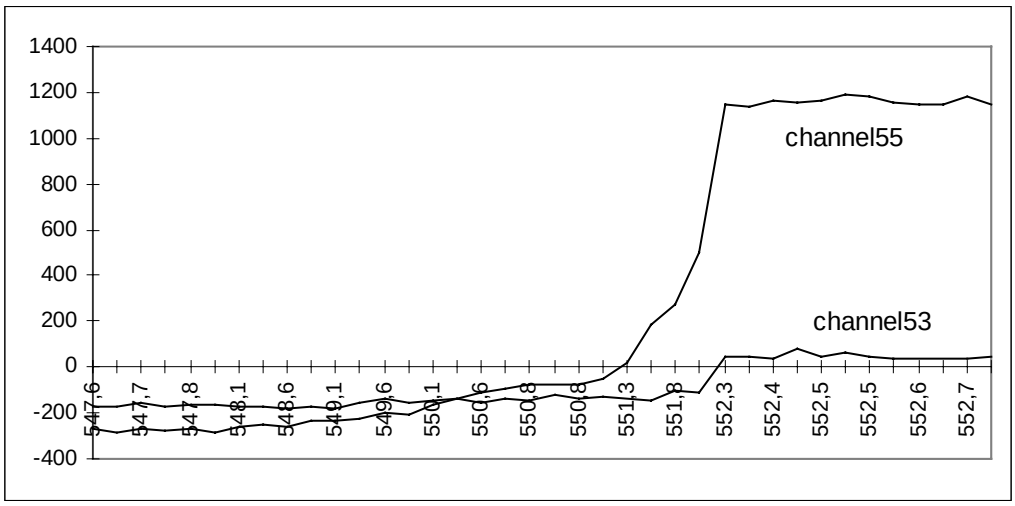

Micro strain after time in hours.
Figure 4.14

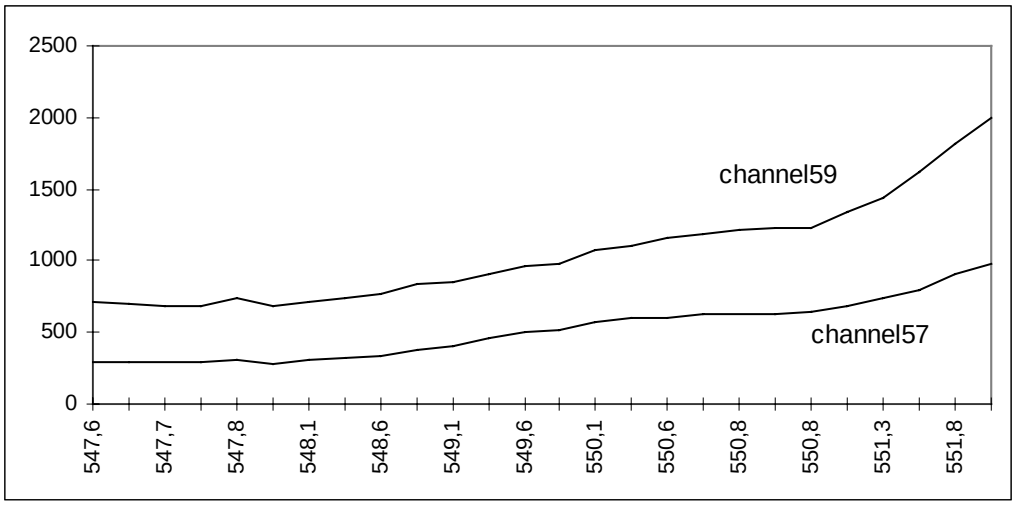

Micro strain after time in hours.
Figure 4.15

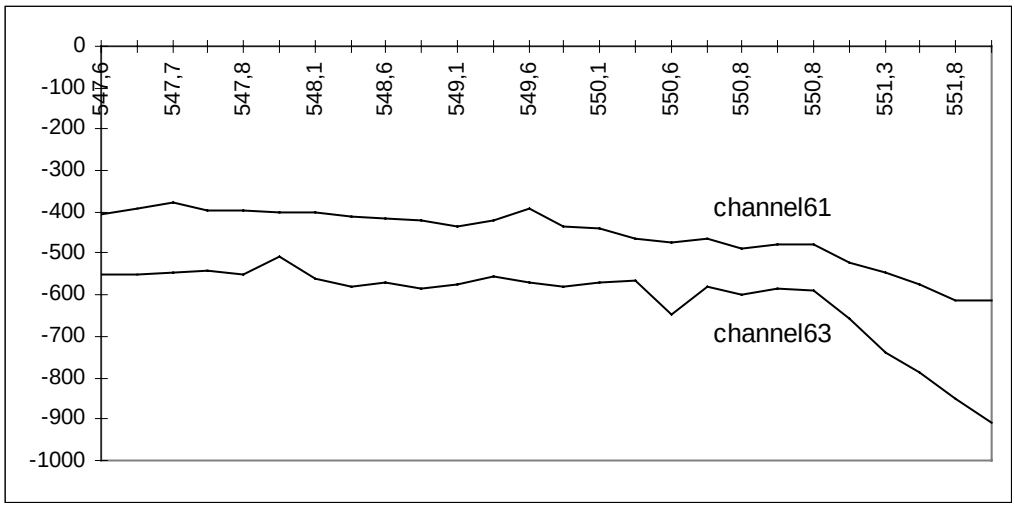

Micro strain after time in hours.
Figure 4.16

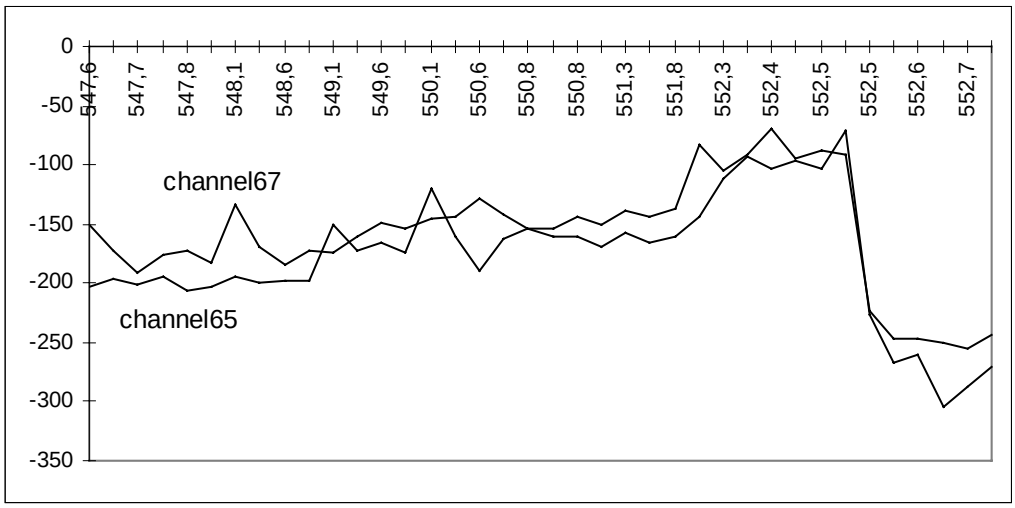

Micro strain after time in hours.
Figure 4.17

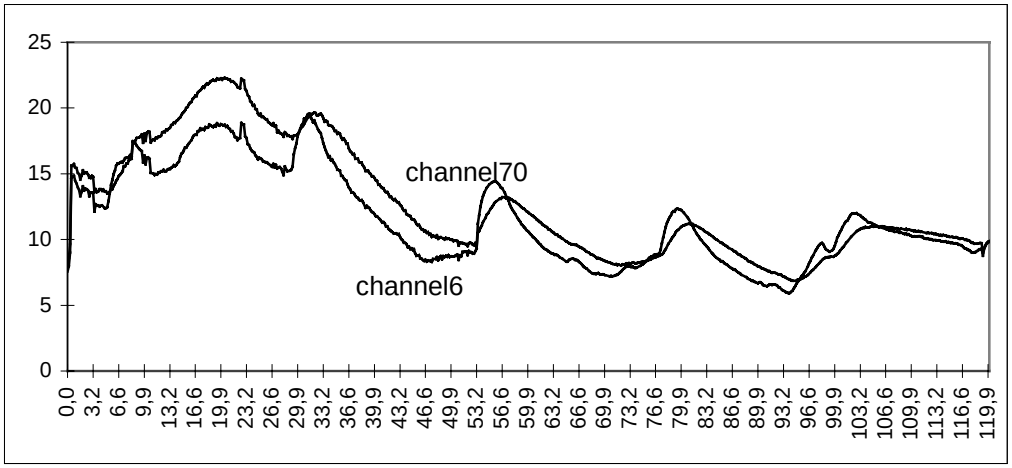

Temperature ^{o}C after time in hours.
Figure 4.18

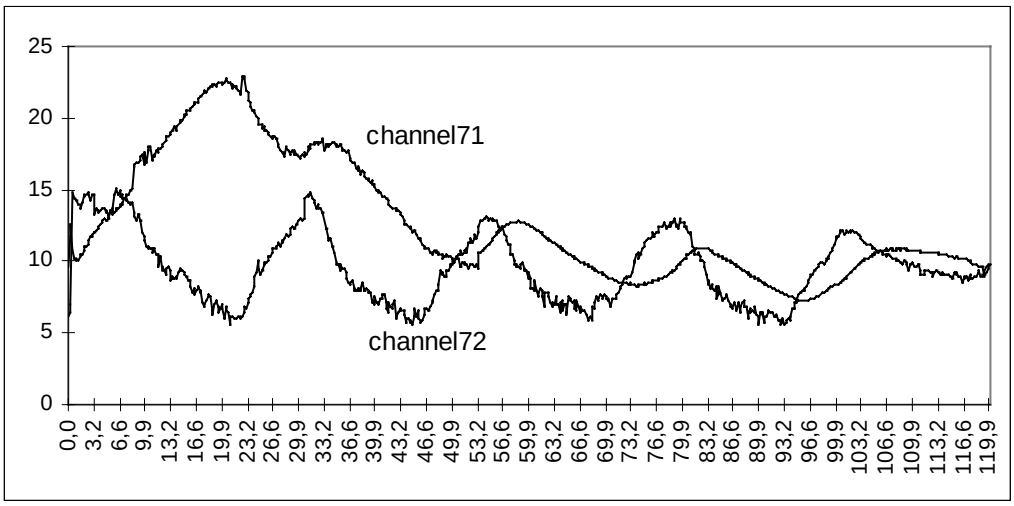

Temperature ^{o}C after time in hours.
Figure 4.19

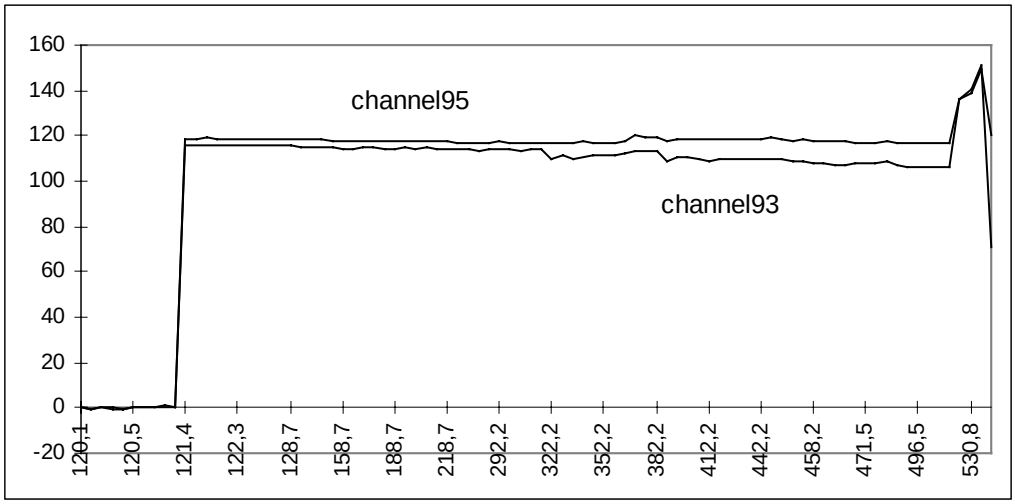

Force in tendons after time in hours.
Figure 4.20

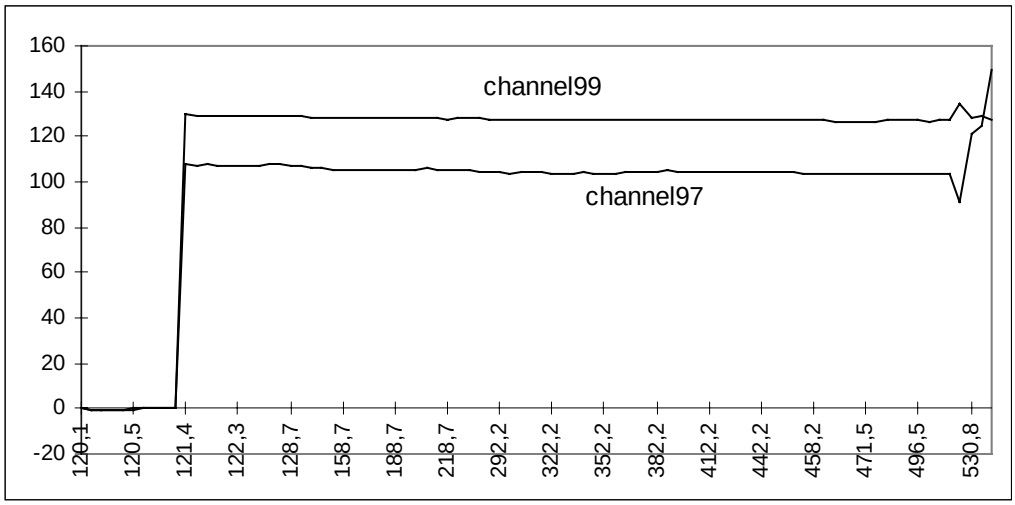

Force in tendons after time in hours.
Figure 4.21

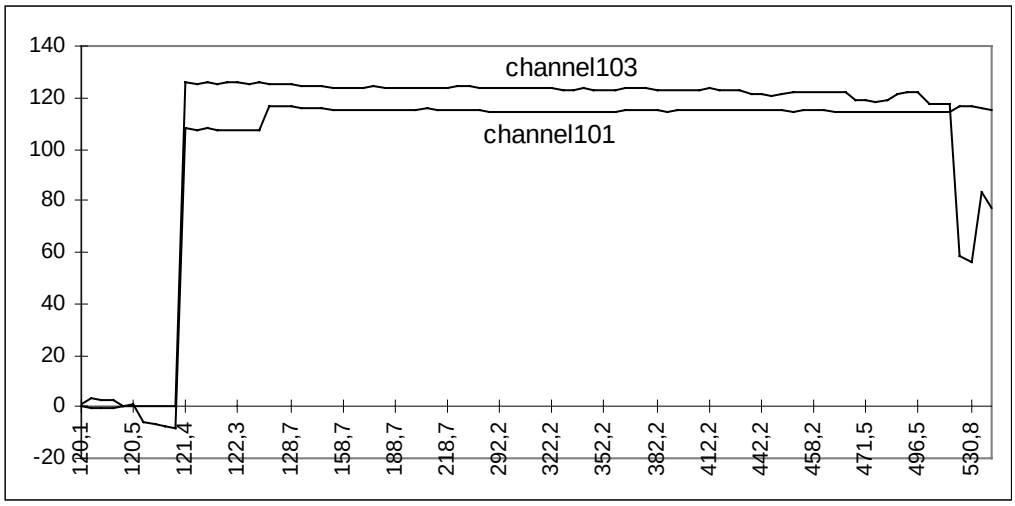

Force in tendons after time in hours.
Figure 4.22

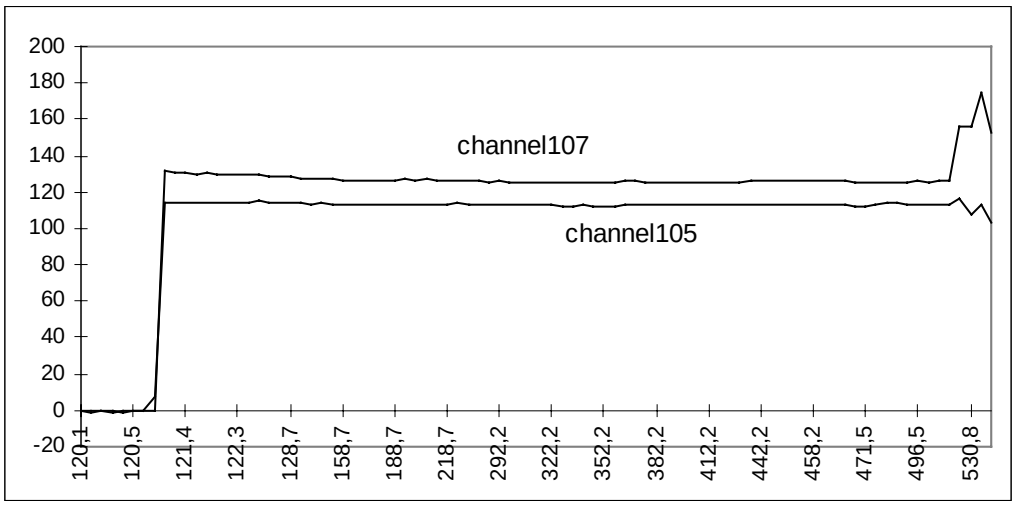

Force in tendons after time in hours.
Figure 4.23

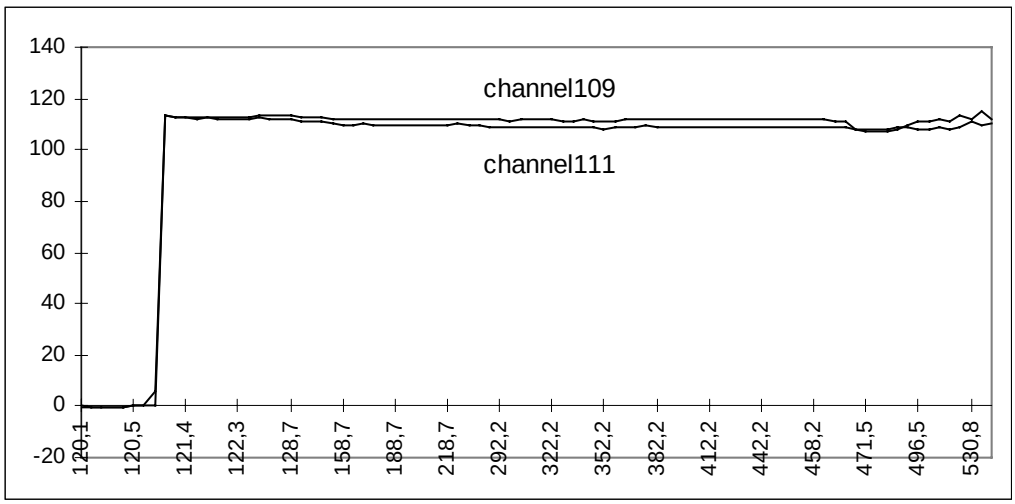

Force in tendons after time in hours.
Figure 4.24

A.4.3 Data for materials used in full scale of prestressed flat slab.

In this chapter materials data used in test slab and data used in FEM analysis are listed. Concrete with cube strength 35 N/mm^2 after twenty-eight days, reinforcement with 500 N/mm^2 yield strength and with diameter 10 mm in bottom and 12 mm over column, prestressed tendons A_p = 100 mm^2 with minimum tensile strength 1860 N/mm^2 and yield strength 1670 N/mm^2 were used. Tendons were stressed when concrete has a minimum of 22 N/mm^2 cube strength.

Data file in FEM analysis program "DIANA" was as follows:

```
FULL-SCALE
'UNITS'
 TIME     DAY
 LENGTH   MM
 MASS     7.46496E+12   0.
: FORCE   7.46496E+12  *KG*MM/DAY**2
'COORDINATES'
   1    .000000E+00    .000000E+00    .000000E+00
   2   2.500000E+02    .000000E+00    .000000E+00
   3   5.000000E+02    .000000E+00    .000000E+00
.
.
303   9.250000E+03   8.000000E+03    .000000E+00
 304   9.500000E+03   8.000000E+03    .000000E+00
'DIRECTIONS'
   1   1.00000E+00    .00000E+00    .00000E+00
   2    .00000E+00   1.00000E+00    .00000E+00
   3    .00000E+00    .00000E+00   1.00000E+00
```

```
'ELEMENTS'
CONNECT
   1 Q20SH  1 2 21 20
   2 Q20SH  2 3 22 21
   3 Q20SH  3 4 23 22
.
.
269 Q20SH  283 284 303 302
 270 Q20SH  284 285 304 303
MATERI
 / 1-270 / 1
GEOMET
  / 1-270 / 1
DATA
  / 1-270 / 1
'MATERIALS'
 1   YOUNG  23635.
     POISON 0.2
     DENSIT 3.348979E-19
     CRACK  1
     CRKVAL 2.
     TAUCRI 1
     BETA   0.2
     TENSIO 1
     TENVAL 0.0015
 2   YOUNG  200000
     POISON 0.2
     DENSIT 0
     YIELD  VMISES
     YLDVAL  500
 3   YOUNG  196000
     POISON 0.2
     DENSIT 0
     YIELD  VMISES
     YLDVAL  1860
     NOBOND
'REINFO'
LOCATI
: reinforcement in x-direction bottom
 1   GRID
     LOCALZ
     / 1-270 /  -85.
.
.
: tendons
 6   GRID
     PLANE   8499. -1. 0.  9501. -1. 0.  9501. 501. 0.
             8499. 501. 0.
     PLANE   8499. 499. 0.  9000. 499. 0.  9501. 499. 0.
             9501. 3875. -82. 9501.
             7251. 38. 9000. 7251. 38.  8499. 7251. 38.
```

URN:NBN:no-2318

```
              8499. 3875. -82.
      PLANE   8499. 7249. 38. 9000. 7249. 38.  9501. 7249.
              38. 9501. 7500. 52. 9501.
              8001. 66. 9000. 8001. 66.  8499. 8001. 66.
              8499. 7500. 52.
.
.
'DATA'
 1   NGAUS  2  2  7
'GEOMETRY'
 1   THICK 230
 2   THICK 0.157  0.
     XAXIS 1. 0. 0.
 3   THICK 0.    0.262
     XAXIS 1. 0. 0.
 4   THICK 2.062 0.
     XAXIS 1. 0. 0.
 5   THICK 0.294  0.
     XAXIS 1. 0. 0.
 6   THICK 0.    0.8
     XAXIS 1. 0. 0.
 7   THICK 0.    1.
     XAXIS 1. 0. 0.
 8   THICK 0.  2.987
     XAXIS 1. 0. 0.
 9   THICK 0.157  0.
     XAXIS 1. 0. 0.
'SUPPORTS'
 / 41 57 288 304 / TR 3
 / 286-304 / TR 2 RO 1
 / 19-304(19) / TR 1 RO 2
'LOADS'
CASE 1
WEIGHT
:   GRAVITY  = 9.81 M/SEC^2
  3  -73231258.E6
CASE 2
REINFO
  / 4 /
      PRESTR  1200. 0.
CASE 3
REINFO
  / 5 /
      PRESTR  0. 1200.
CASE 4
REINFO
  / 6 /
      PRESTR  0. 1200.
CASE 5
ELEMEN
  / 1-270 /
```

```
      FACE
      FORCE  -2.5D-3
      DIRECT  3
:COMBIN  2  1.0  3 1.0  4 1.0

'END'
```

A.5 Prestress loss

A.5.1 General

After jacking, there will be some losses in the tendon force. These losses are friction loss, loss from anchor set, creep and shrinkage, elastic shortening and relaxation of prestressing. Losses are varying along the tendon because the friction in the tendon gives a smaller force at the passive ends than at the active end of tendons. The active end of a tendon is the jacking end, but it is also possible to stress the tendons from both ends. The loss from the anchor set decreases from stressing point at same grade as friction losses do, see fig 5.1.
The other losses, creep and shrinkage, elastic shortening and relaxation, are calculated as constant losses in the length of the tendon, as far as the structure can have free displacement, and is not restrained.

Long-time loss in prestressing force is loss from creep, shrinkage and relaxation. This loss is about 9-10 % of jacking force. Creep and shrinkage from NS 3473, ACI, Euro Code and AS 3600 are described in chapter 3.

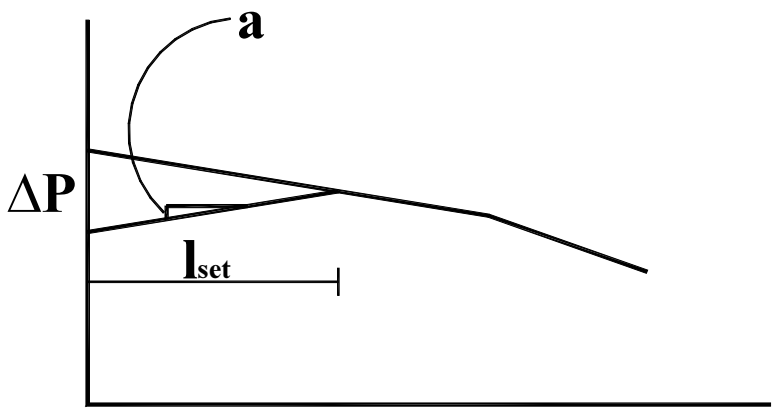

Force variation with anchorage set.
Figure 5.1

A.5.2 Friction loss

The chosen equation calculates the friction loss /5/.

$$P_x = P_o \cdot e^{-\mu(\alpha + \Delta\alpha \cdot x)} \tag{5.1}$$

where

P_x = tendon force in a distance x from stressing point
P_o = tendon force at active end of tendon
μ = friction coefficient
α = total angle change in a distance x from stressing point
$\Delta\alpha$ = wobble friction coefficient
x = distance from stressing point to inspected point.

The friction loss is resulting from the change of angle in tendon curvature, see fig 5.2 /3/, and the wobble friction coefficient takes care of the effect of deviations from perfect geometry in tendons. In a length of dx, the tendon changes its angle $d\alpha$, which gives $N = 2 \cdot P \cdot \sin(d\alpha / 2)$ from fig 5.2. With a friction coefficient μ, the friction loss in dx will be μN. Since the angle is very narrow, the friction loss can be simplified to $P\mu$. Equilibrium can then be used to establish a differential equation to give a solution of this.

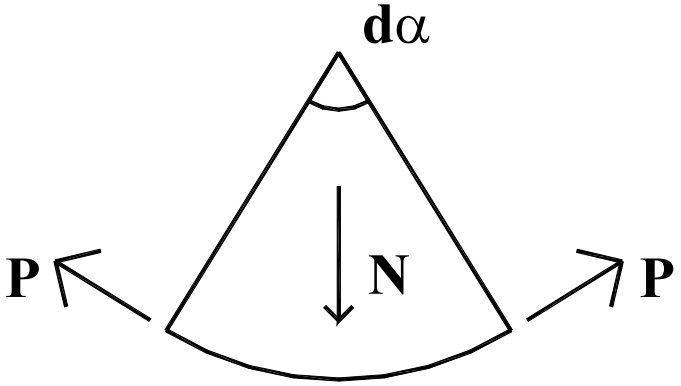

Change of angle in tendon curvature.
Figure 5.2

When stressing from both ends, the tendon forces from both ends have to be controlled, see fig 5.3 a, b. Use the highest value from both ends in further calculation.

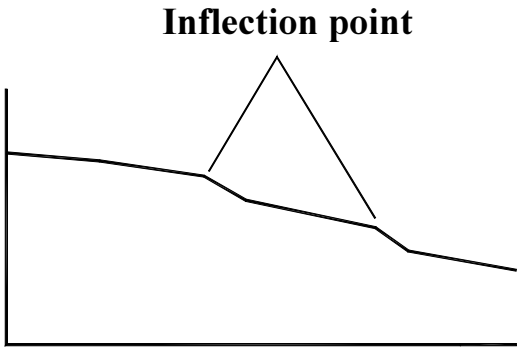

Force in tendon when stressing from one end.
Figure 5.3 a

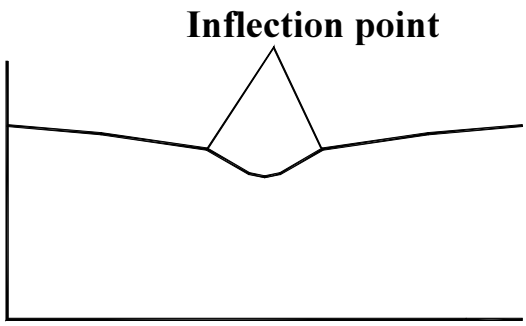

Force in tendon when stressing from both ends.
Figure 5.3 b

A.5.3 Loss from anchorage set

Transferring the force from jack to anchor causes the loss in tendon force from anchorage set. When jack drops the force, the wedge slides a few mm before it stops, and this gives a loss in the tension force. With short tendons, effective length of loss can be longer than the tendons. That gives an anchor loss in both ends. All this is well-known equations, and shown only shortly here. The effective length of loss because of anchor set, is shown in fig 5.1.

$$l_{set} = \sqrt{\frac{s \cdot E_p \cdot A_p}{a}} \qquad (5.2)$$

s = anchor set
Ep = Young's modulus of tendon
Ap = cross-sectional area of tendon
a = gradient, from fig 5.1

If l_{set} is longer than the length of the tendon, there is anchor loss in the passive end too. The loss caused by anchor slip in active ends is then:

$$\Delta P = \frac{s \cdot E_p \cdot A_p}{l} + a \cdot l \tag{5.3}$$

and in passive ends:

$$\Delta P = \frac{s \cdot E_p \cdot A_p}{l} - a \cdot l \tag{5.4}$$

With l_{set} smaller than the length of the tendon, there is no anchor slip in passive ends, and the anchor slip in active ends is then:

$$\Delta P = 2 \cdot a \cdot l_{set} \tag{5.5}$$

A.5.4 Loss from elastic shortening

Loss in tension force caused by elastic shortening as:

$$\Delta P = \varepsilon_{cs} \cdot E_p \cdot A_p \tag{5.6}$$

where

$$\varepsilon_{cs} = \frac{\sigma_c}{E_c} \tag{5.7}$$

if stressing all the tendons at the same time, but since the most normal procedure is to stress one by one, the strain is

$$\varepsilon_{cs} = \frac{\sigma_c}{2 \cdot E_c} \tag{5.8}$$

this because the last tendon to be stressed will not been influenced by elastic shortening. So ε_{cs} gives the average elastic shortening
These are all short time losses, and the long time losses are relaxation of steel, creep and shrinkage.

A.5.5 Relaxation.

When the steel is creeping (relaxation), there will be a decrease in prestress force after long time. This variation of relaxation is shown in fig 5.4 /6/

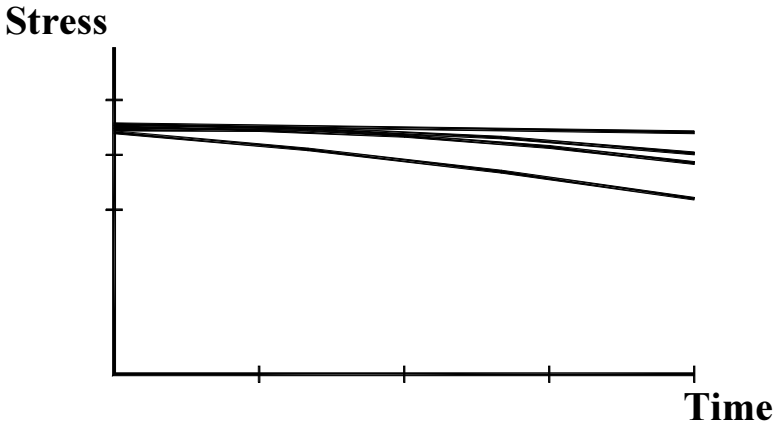

Relaxation in prestressed steel.
Figure 5.4

Magura, Sozen and Siess /7/ recommended the following equation to calculate relaxation in prestressing steel:

$$\frac{f_p}{f_{pi}} = 1 - \frac{\log t}{10}\left(\frac{f_{pi}}{f_{py}} - 0.55\right) \qquad (5.9)$$

For low-relaxation steel $\frac{\log t}{10}$ can be changed by $\frac{\log t}{45}$ /8/

A.5.6 Creep and shrinkage

Loss from creep ε_{cc} , and shrinkage ε_{sh} in prestressed steel can be estimated to:
Creep:

$$\Delta P = \varepsilon_{cc} \cdot E_p \cdot A_p \qquad (5.10)$$

Shrinkage:

$$\Delta P = \varepsilon_{sh} \cdot E_p \cdot A_p \qquad (5.11)$$

For further information about creep and shrinkage, see chapter 3.

EuroCode 2, ENV 1992-1-1 /16/ is a new standard which now can be used all over Europe. Part 1 of EuroCode 2 is supplemented by further parts, and especially interesting for this investigation is "1-5 Unbonded and external prestressing tendons" /17/. According to this standard the maximum force applied to a tendon P_o, immediately after stressing, shall not exceed:

$$A_p \cdot \sigma_{0,\max}$$

where $\sigma_{0,\max} \le |0.80| \cdot f_{pk}\, or \le |0.90| \cdot f_{p01k}$

this gives almost the same tendon force as the Norwegian standards. ENV 1992-1-1 gives a detailed description of calculation of prestress loss in tendons. Time dependent loss should be calculated from:

$$\Delta\sigma_{p,c+s+r} = \frac{\varepsilon_s(t,t_o)E_s + \Delta\sigma_{pr} + \alpha\phi(t,t_o)\left(\sigma_{cg} + \sigma_{cp0}\right)}{1 + \alpha \cdot \frac{A_p}{A_c}\left[\left(1 + \frac{A_c}{I_c} \cdot z_{cp}{}^2\right)\left(1 + 0.8\phi(t,t_o)\right)\right]} \qquad (5.12)$$

where:

$\Delta\sigma_{p,c+s+r}$	= the variation of stress in tendons due to creep, shrinkage and relaxation at location *x*, at time *t*.
$\varepsilon_s(t,t_o)$	= the estimated shrinkage strain, derived from the values in table 3.4 /16/ for final shrinkage.
$\alpha = E_s/E_{cm}$	
E_s	= the modulus of elasticity for the prestressing steel.
E_{cm}	= the modulus of elasticity for the concrete.
$\Delta\sigma_{pr}$	= the variation of stress in the tendons at section *x* due to relaxation.
$\phi(t,t_o)$	= a creep coefficient.
σ_{cg}	= the stress in the concrete adjacent to the tendons, due to self-weight and any other permanent actions.
σ_{cpo}	= the initial stress in the concrete adjacent to the tendons, due to prestress.
A_p	= the area of all the prestressing tendons at the level being considered.
A_c	= the area of the concrete section.
I_c	= the second moment of area of the concrete section.
z_{cp}	= the distance between the centre of gravity of the concrete section and the tendons.

A.6 Prestressing steel relaxation

Relaxation in tendons depends on which type of tendon is used. /16/ Certificates accompanying the consignments shall indicate the class and relevant relaxation data of the prestressing steel. As an indication of relationship between relaxation losses and time up to 1000 hours: 15 % after 1 hour, 25 / 5, 35 / 20, 55 / 100, 65 / 200, 85 / 500, 100 / 1000 can be used. The long-term values of the relaxation losses may be assumed to be three times the relaxation losses after 1000 hours.

NS 3473 /9/ shows a diagram for calculation of relaxation in tendon, this diagram is reproduced in figure 6.1.

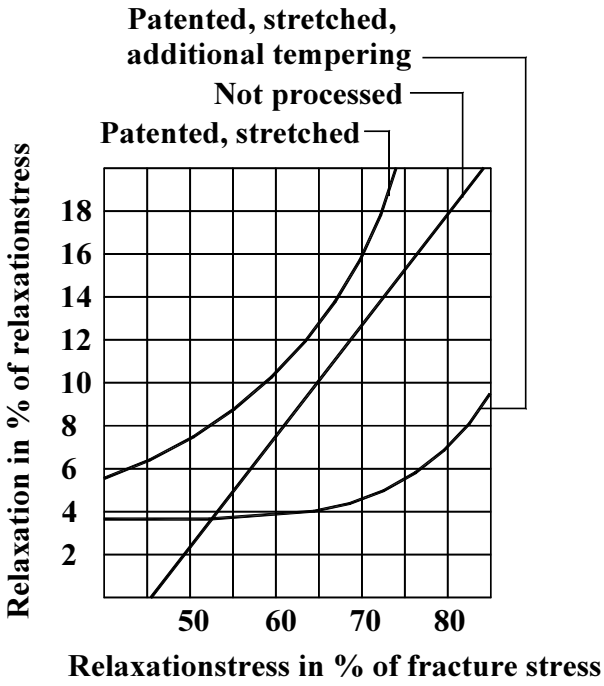

Relaxation in tendons after long time, NS 3473 /9/.
Figure 6.1

Australian standard AS 3600 /14/ gives an equation for calculation of relaxation as:

$$R = k_4 \cdot k_5 \cdot k_6 \cdot R_b \qquad (6.1)$$

where

k_4 = coefficient dependent of the duration of the prestressing force
= $\log\left[5.4(j)^{1/6}\right]$ j = time after prestressing in days

k_5 = coefficient dependent on the stress in the tendon, fig 6.2

k_6 = T/20 but not less than 1.0

T = average temperature

R_b = 1 % for low-relaxation wire
= 2 % for low-relaxation strand
= 3 % for alloy-steel bars

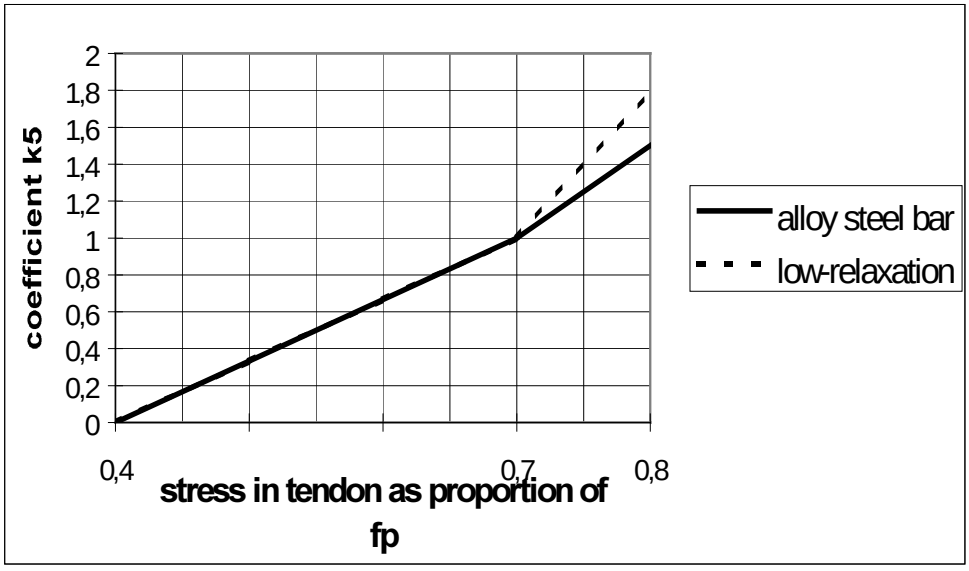

Coefficient dependent on the stress in the tendon.
Figure 6.2

Appendix B, slabs on ground.

B.1 Tendon force after jacking.

In this chapter force in tendons specimen S2 are listed in figure 1.1 – 1.2 and for specimen S3 in figure 1.3 – 1.4.

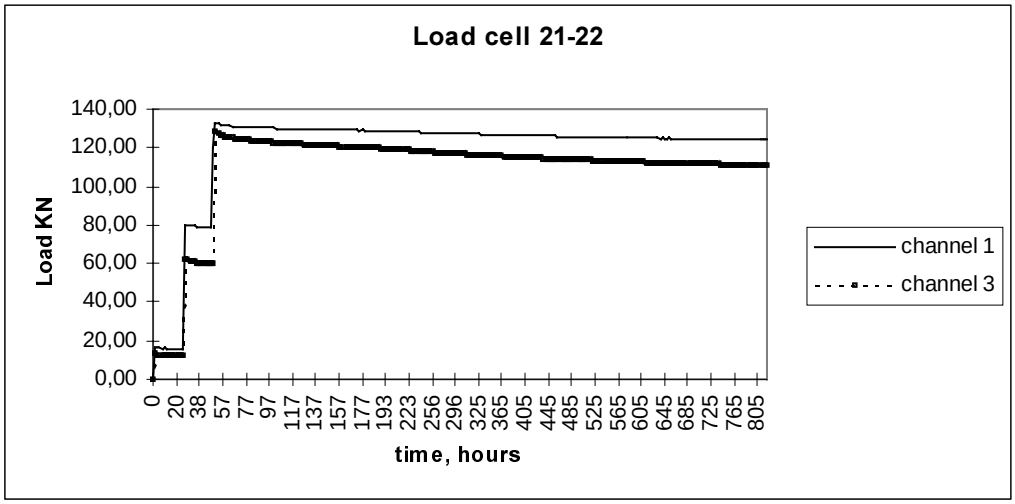

Force in tendons.
Figure 1.1

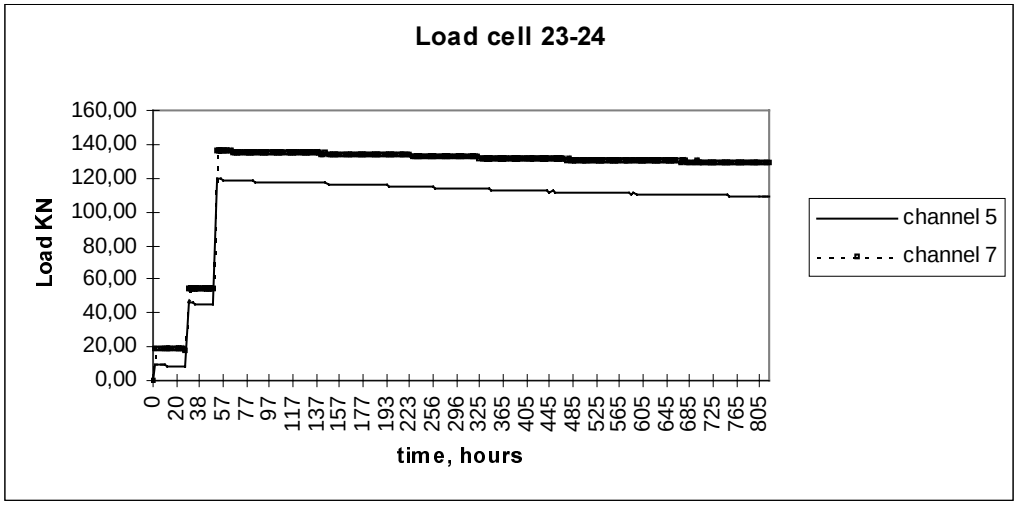

Force in tendons.
Figure 1.2

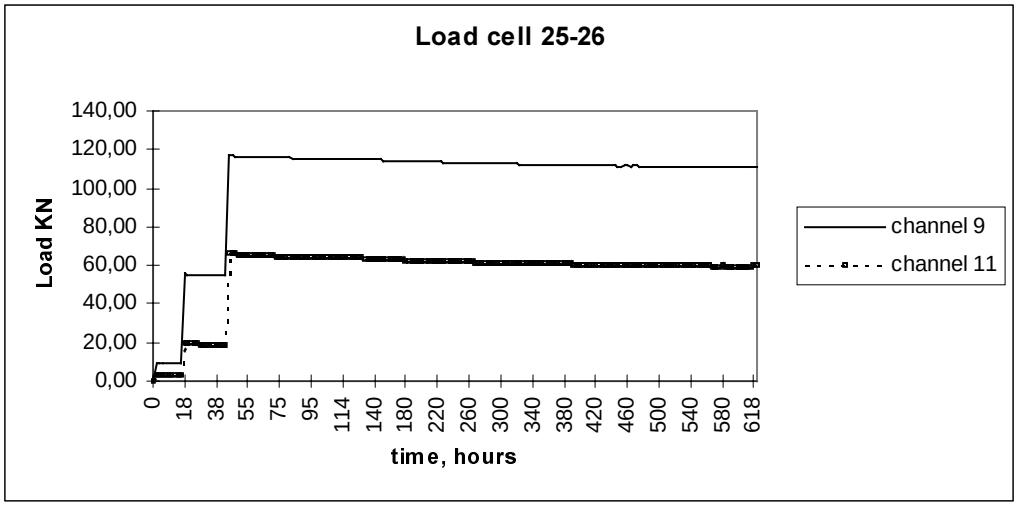

Force in tendons.
Figure 1.3

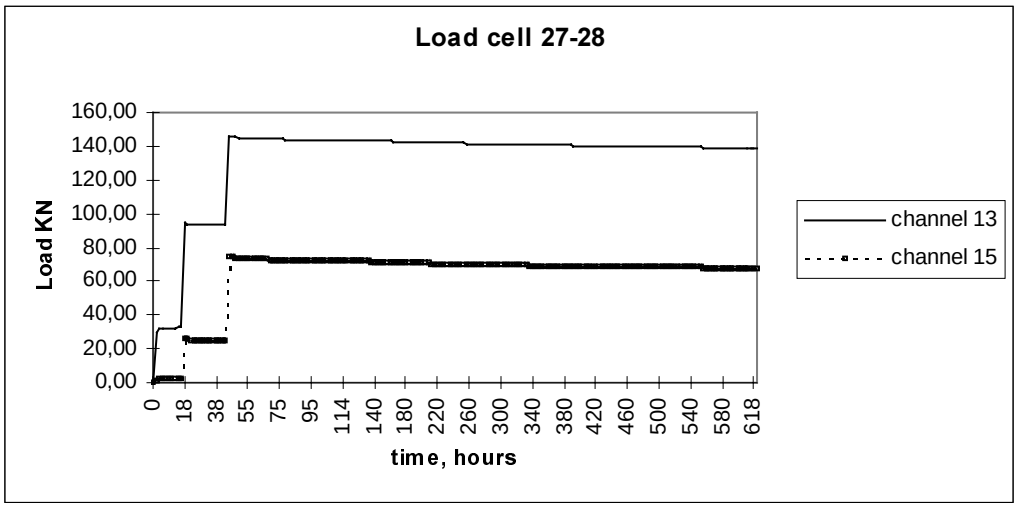

Force in tendons.
Figure 1.4

B.2 Development of strain.

In figure 2.1 – 2.17 the development of strain in reinforcement and at the top and bottom surface of concrete for specimen S1 with load in the middle is listed. Strain in specimen S1 with load at the edge is listed in figure 2.18 – 2.33 and S1 with load in the corner is listed in figure 2.34 – 2.49.

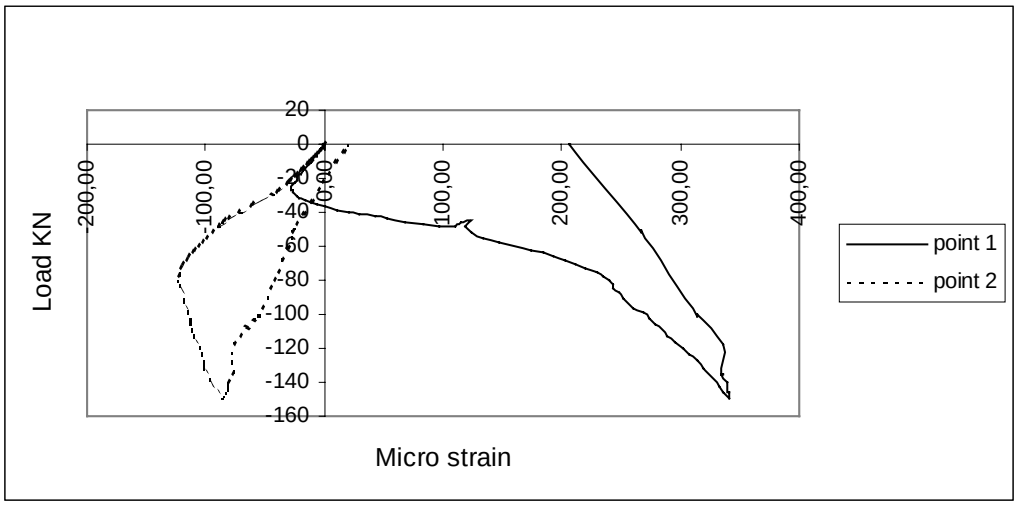

Strain in reinforcement.
Figure 2.1

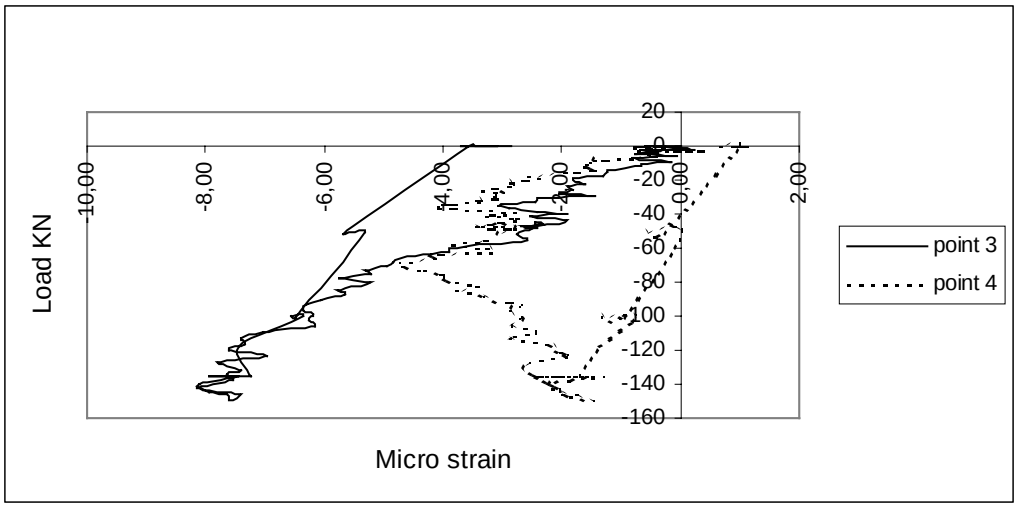

Strain in reinforcement.
Figure 2.2

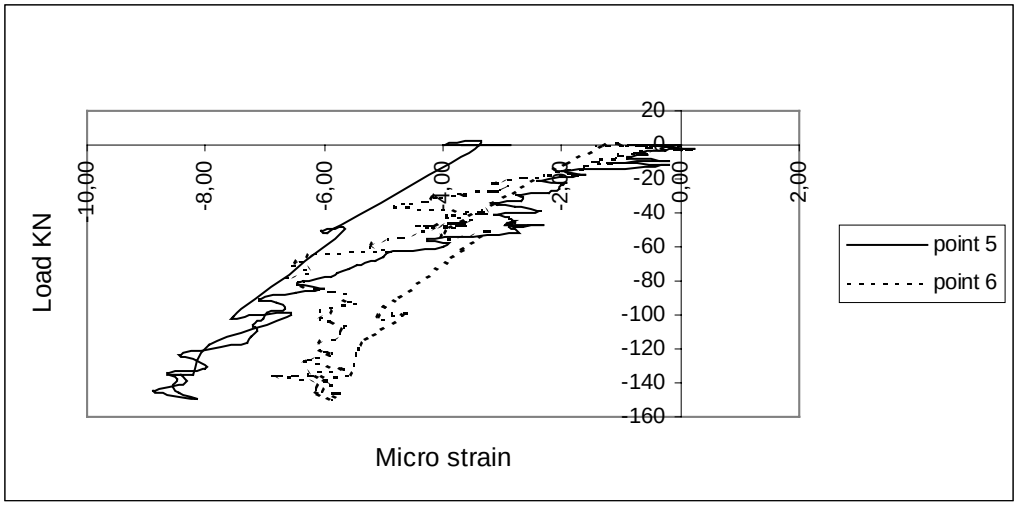

Strain in reinforcement.
Figure 2.3

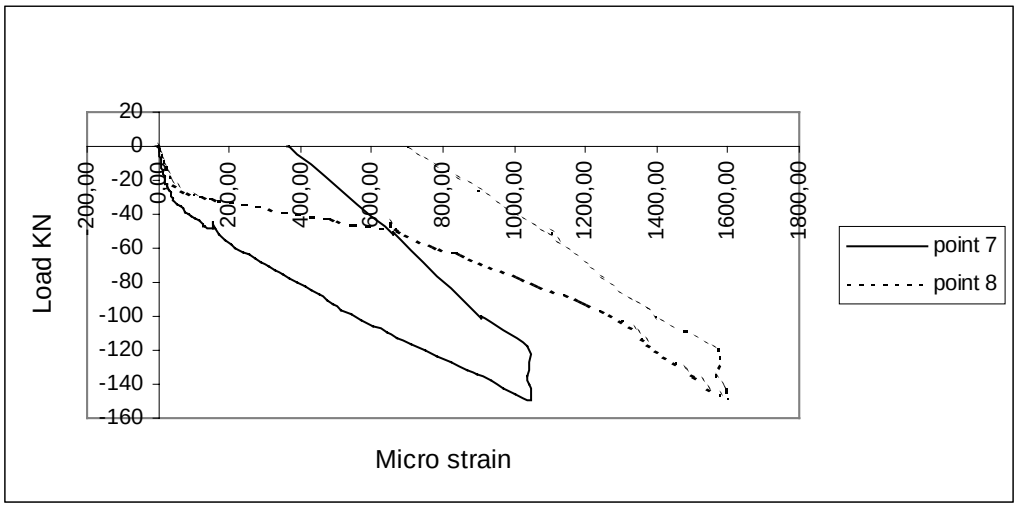

Strain in reinforcement.
Figure 2.4

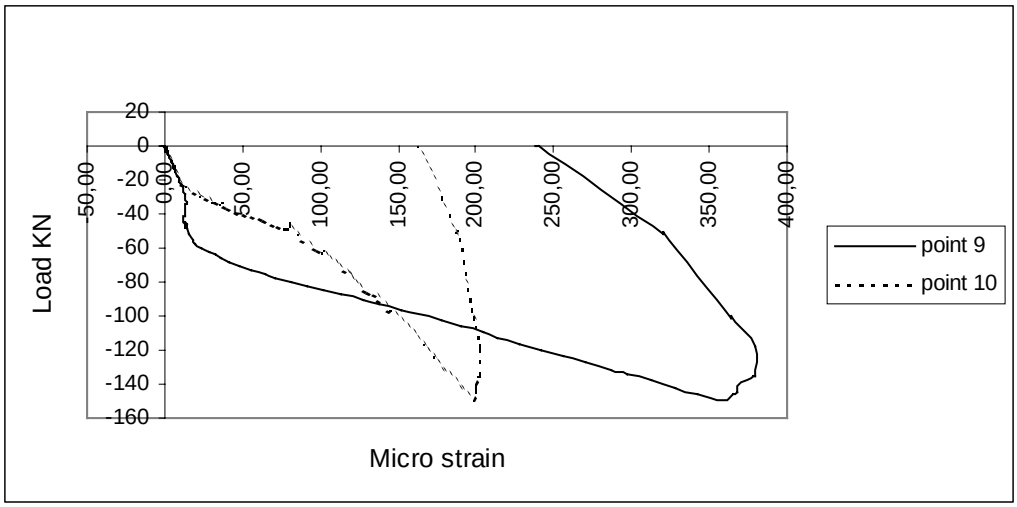

Strain in reinforcement.
Figure 2.5

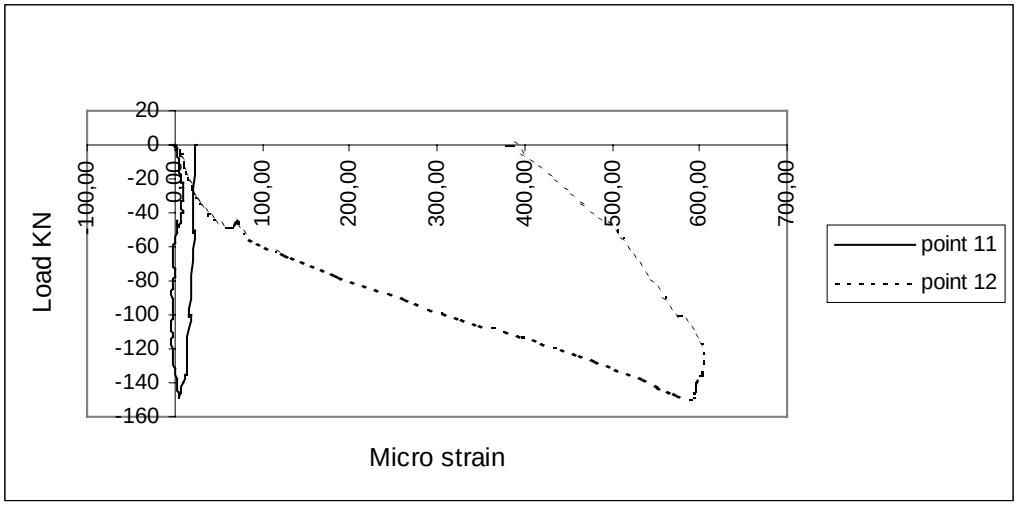

Strain in reinforcement.
Figure 2.6

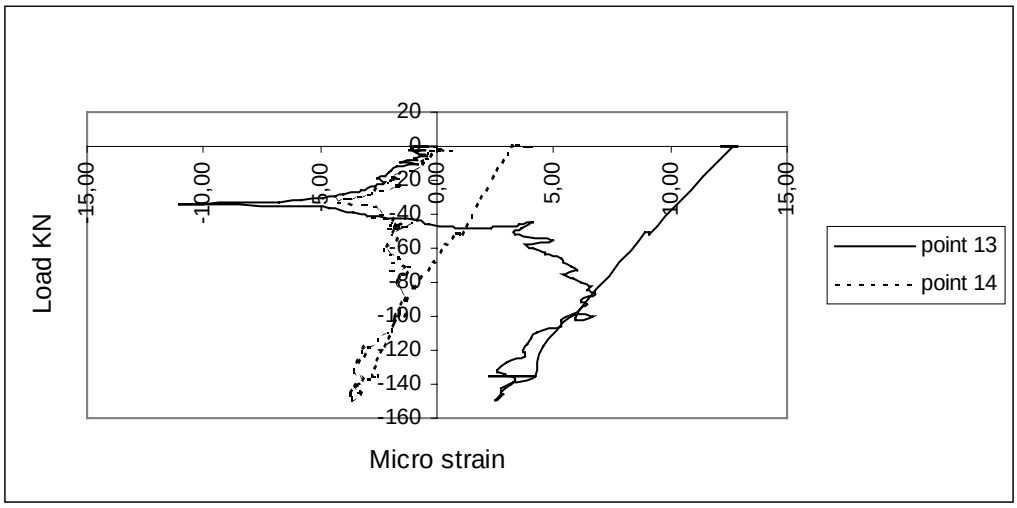

Strain in reinforcement.
Figure 2.7

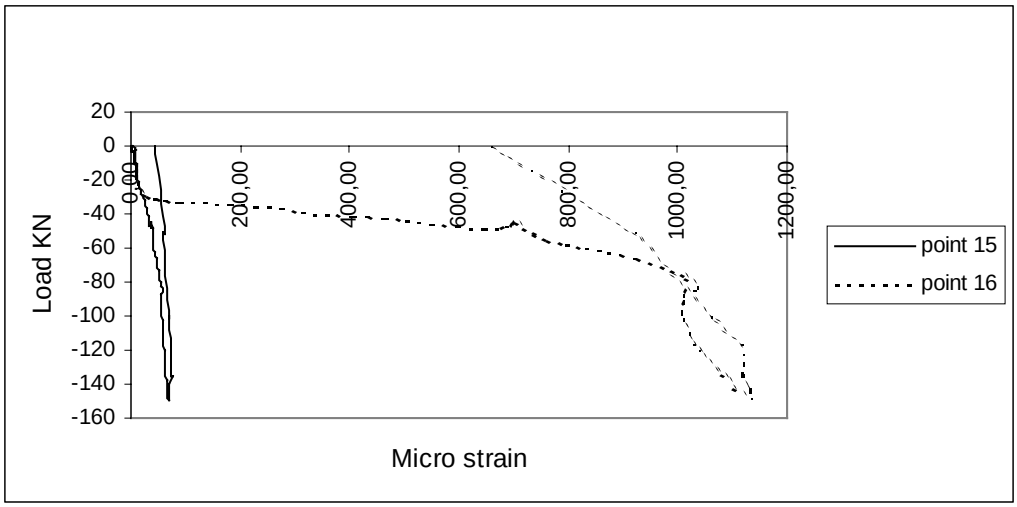

Strain in reinforcement.
Figure 2.8

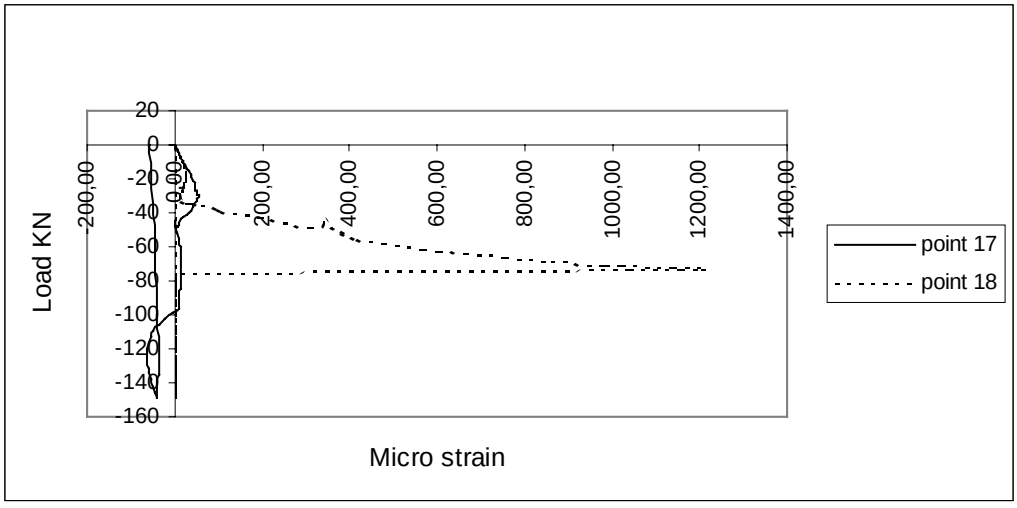

Strain in concrete.
Figure 2.9

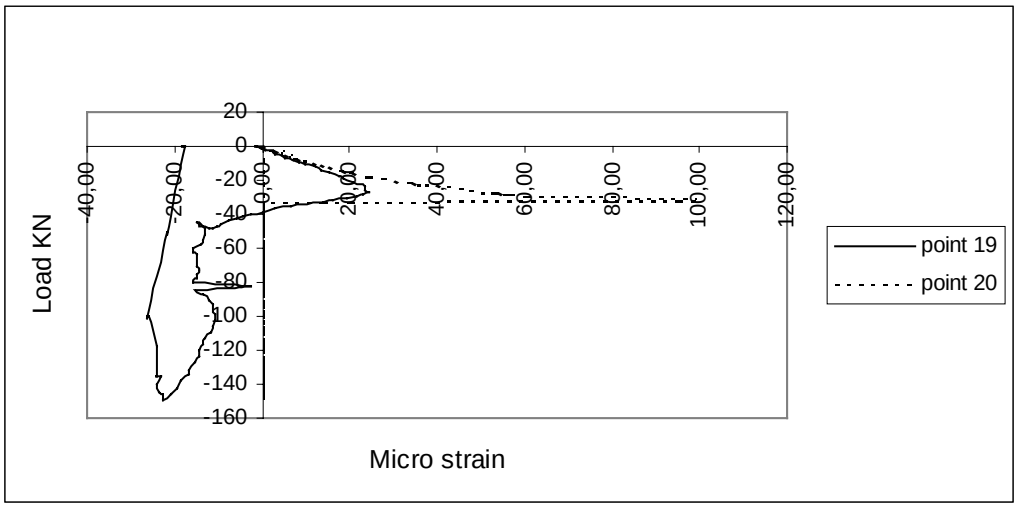

Strain in concrete.
Figure 2.10

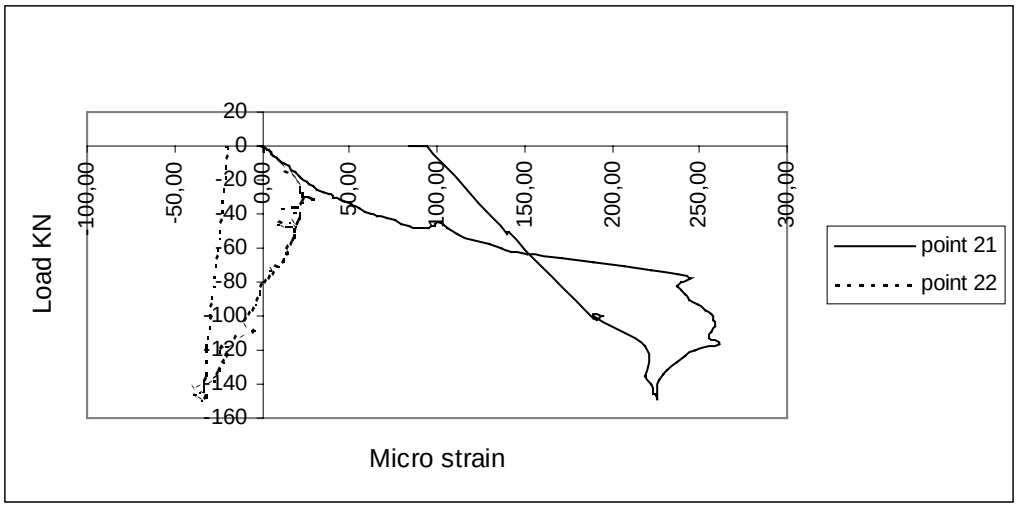

Strain in concrete.
Figure 2.11

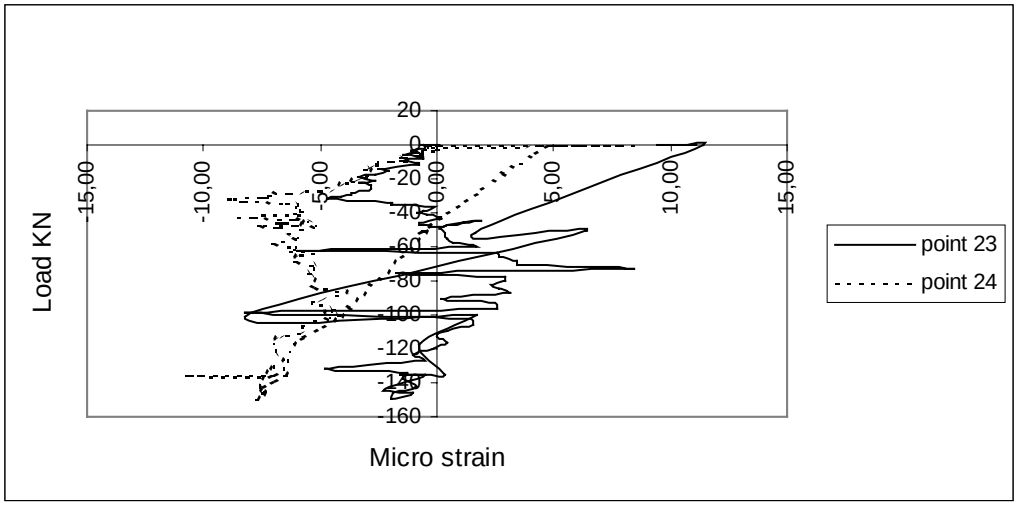

Strain in concrete.
Figure 2.12

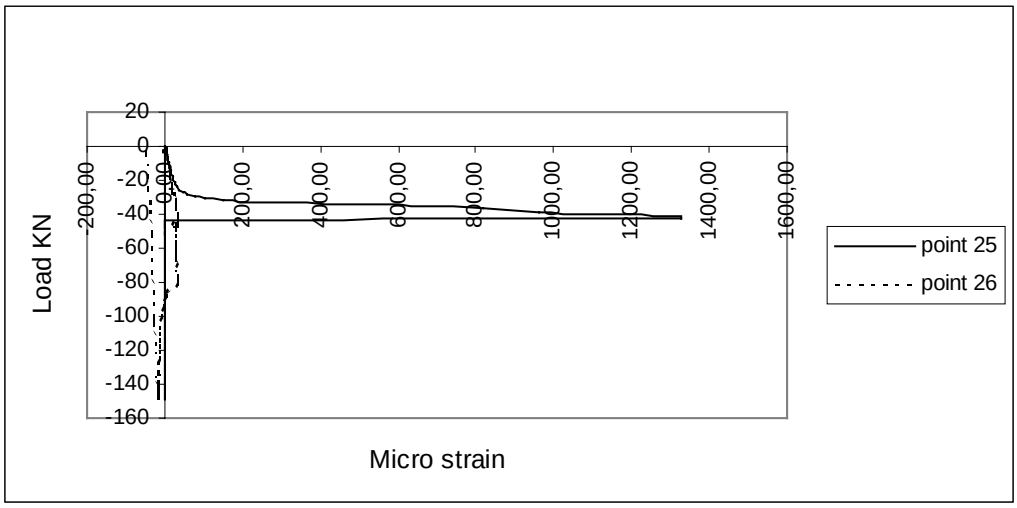

Strain in concrete.
Figure 2.13

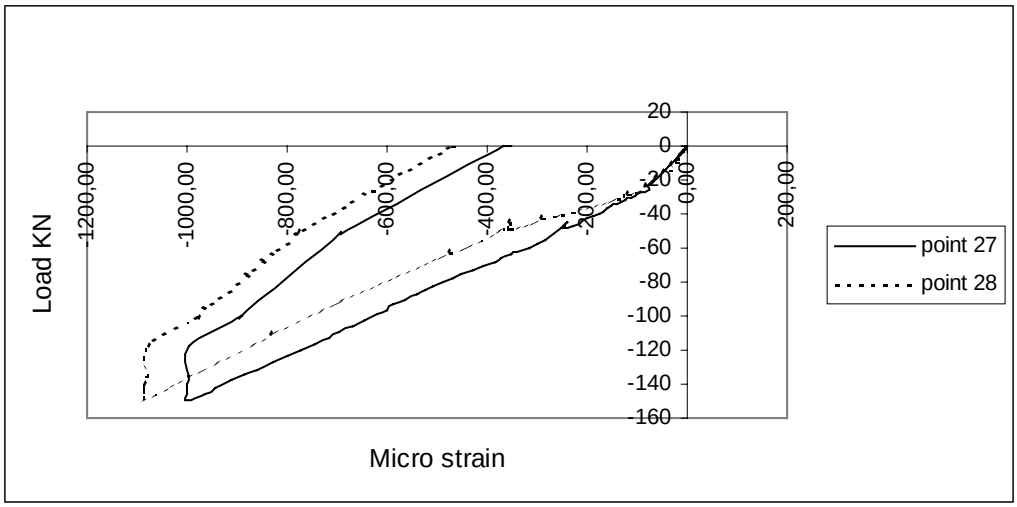

Strain in concrete.
Figure 2.14

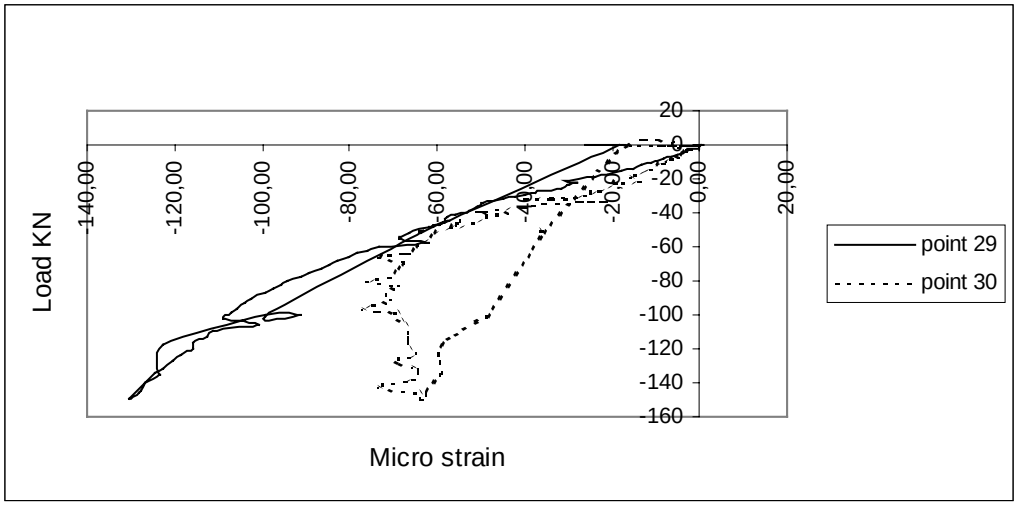

Strain in concrete.
Figure 2.15

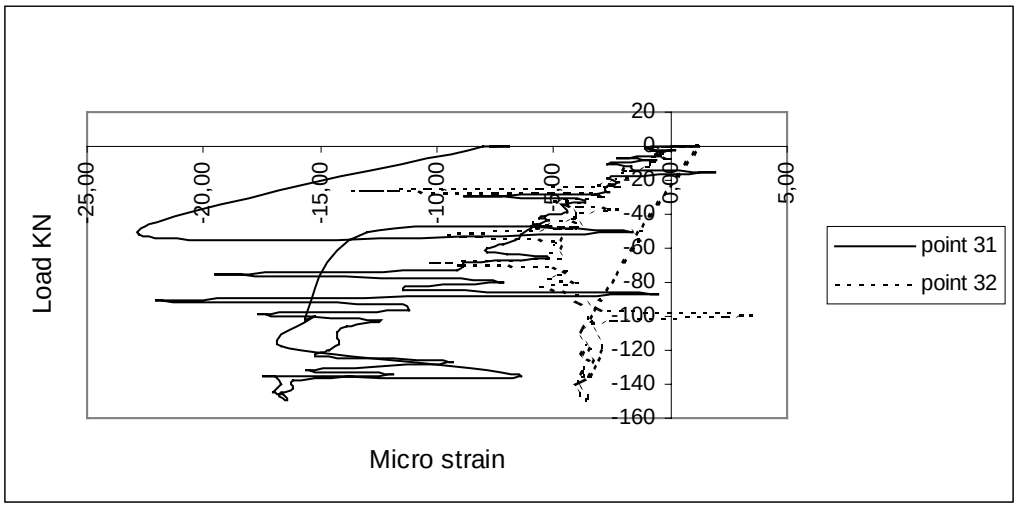

Strain in concrete.
Figure 2.16

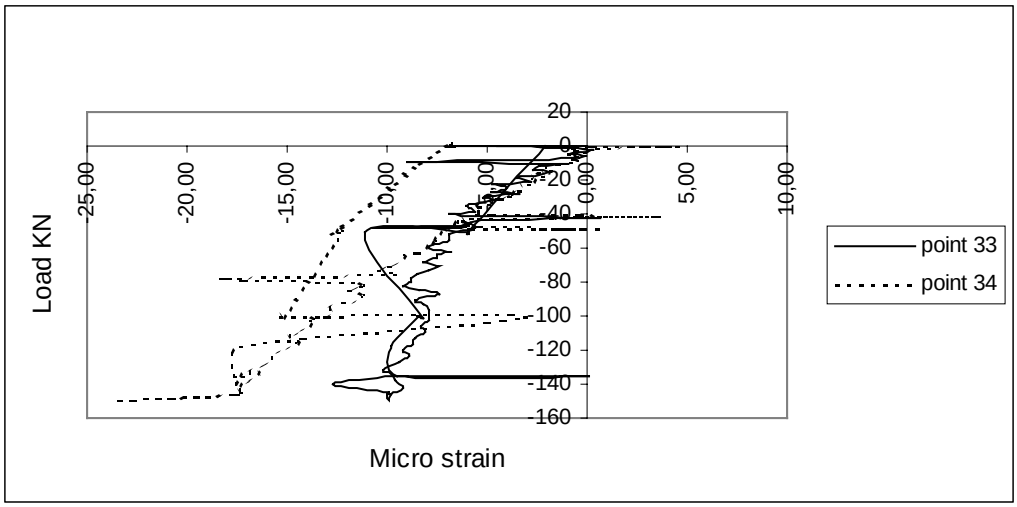

Strain in concrete.
Figure 2.17

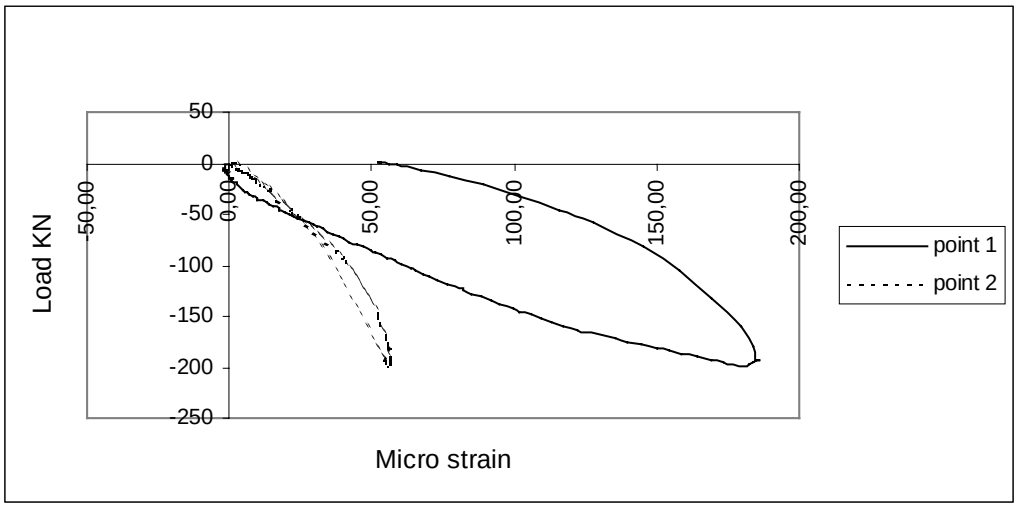

Strain in reinforcement.
Figure 2.18

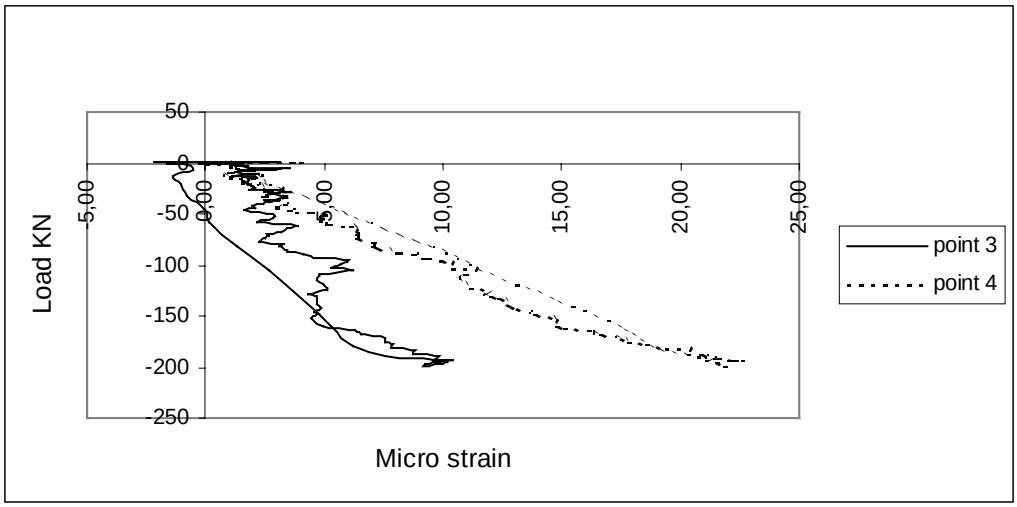

Strain in reinforcement.
Figure 2.19

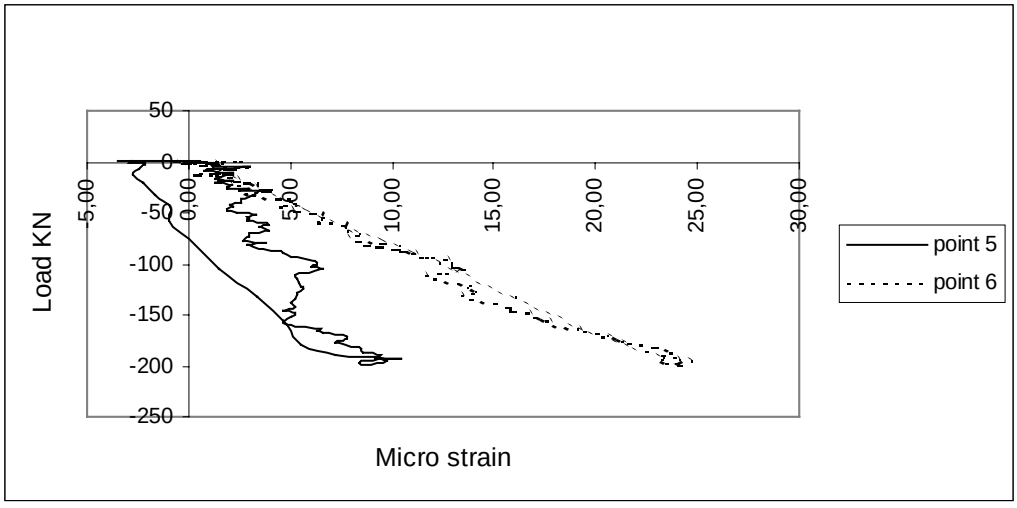

Strain in reinforcement.
Figure 2.20

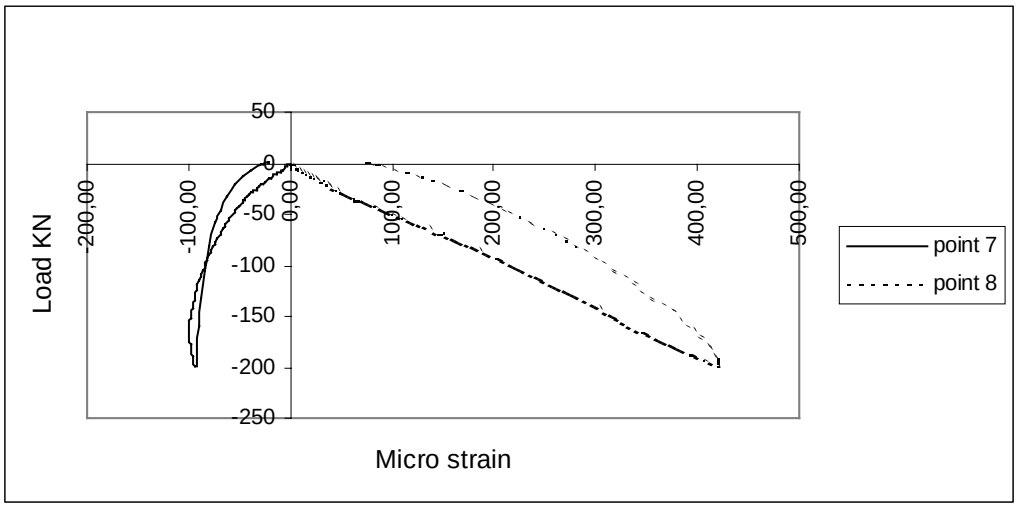

Strain in reinforcement.
Figure 2.21

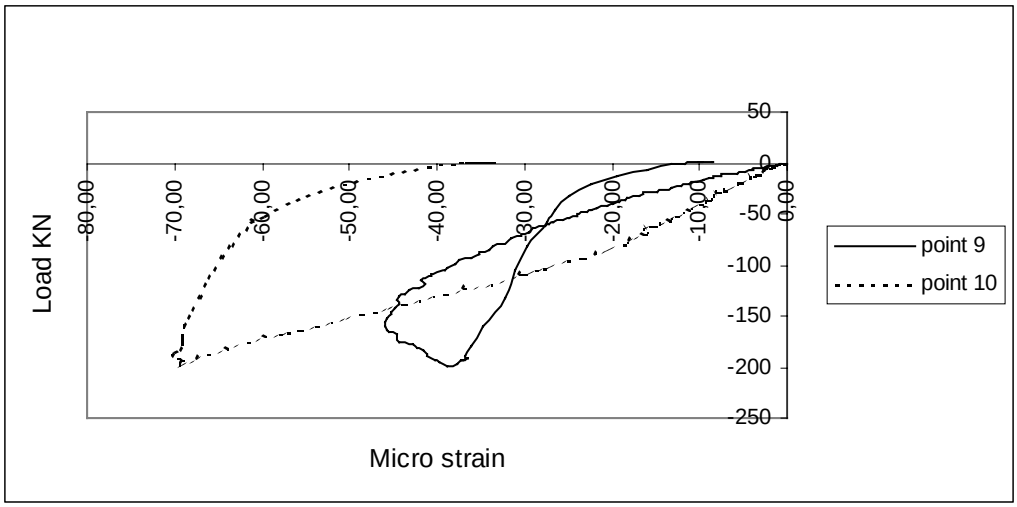

Strain in reinforcement.
Figure 2.22

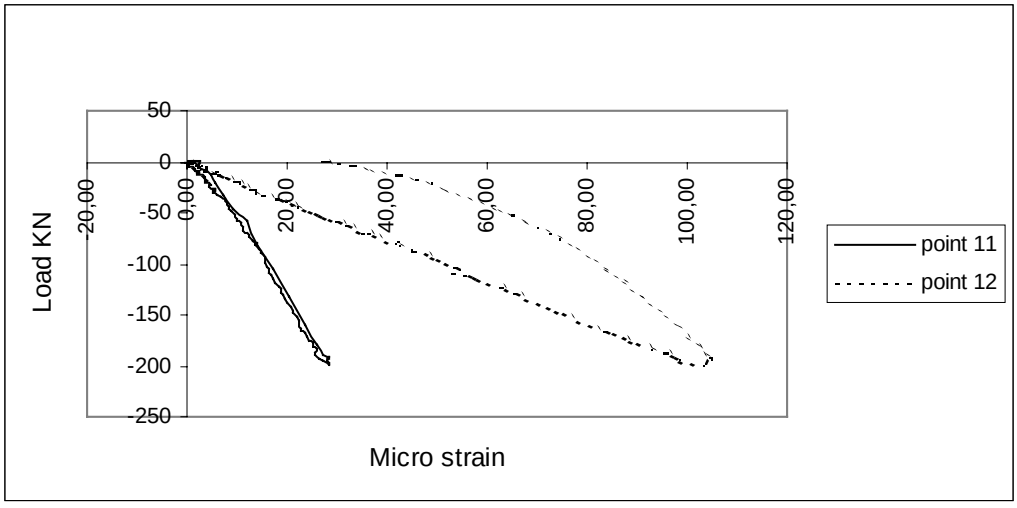

Strain in reinforcement.
Figure 2.23

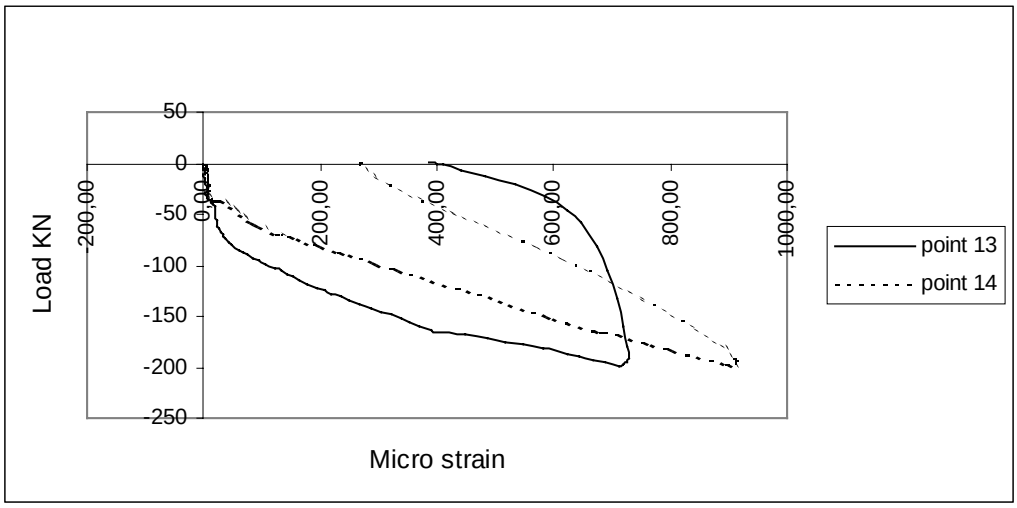

Strain in reinforcement.
Figure 2.24

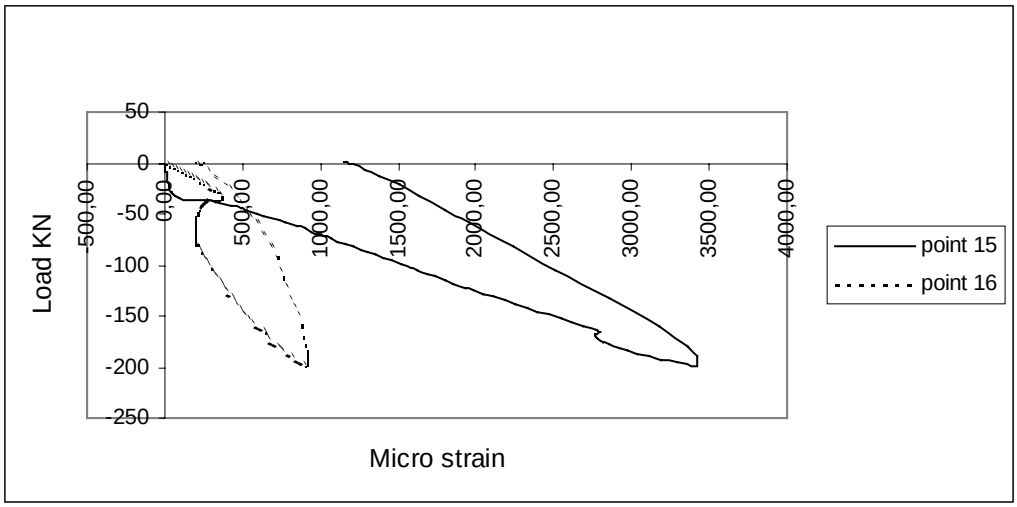

Strain in reinforcement.
Figure 2.25

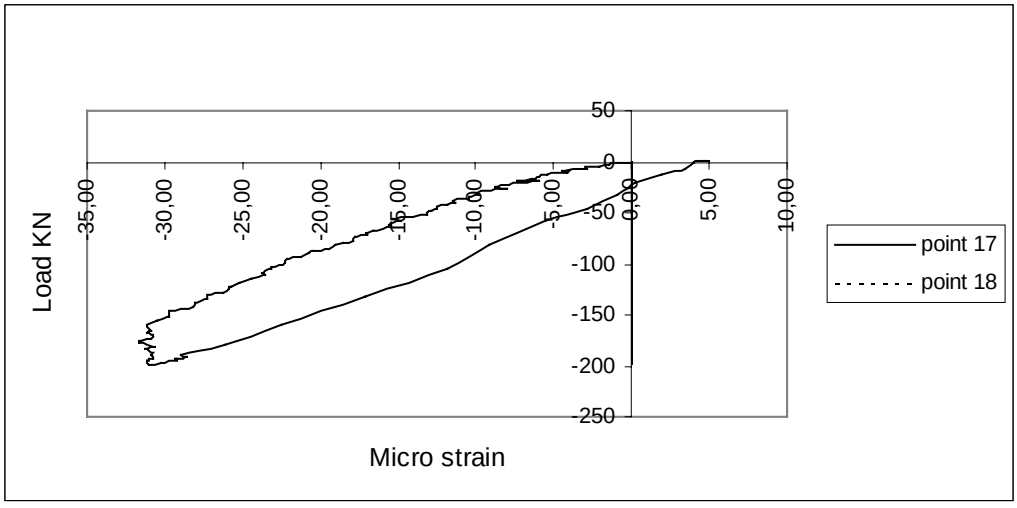

Strain in concrete.
Figure 2.26

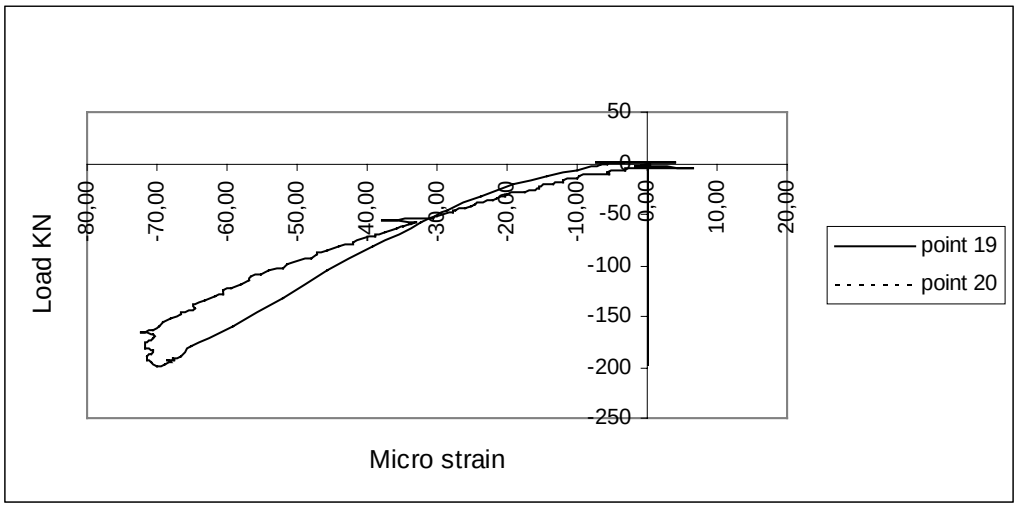

Strain in concrete.
Figure 2.27

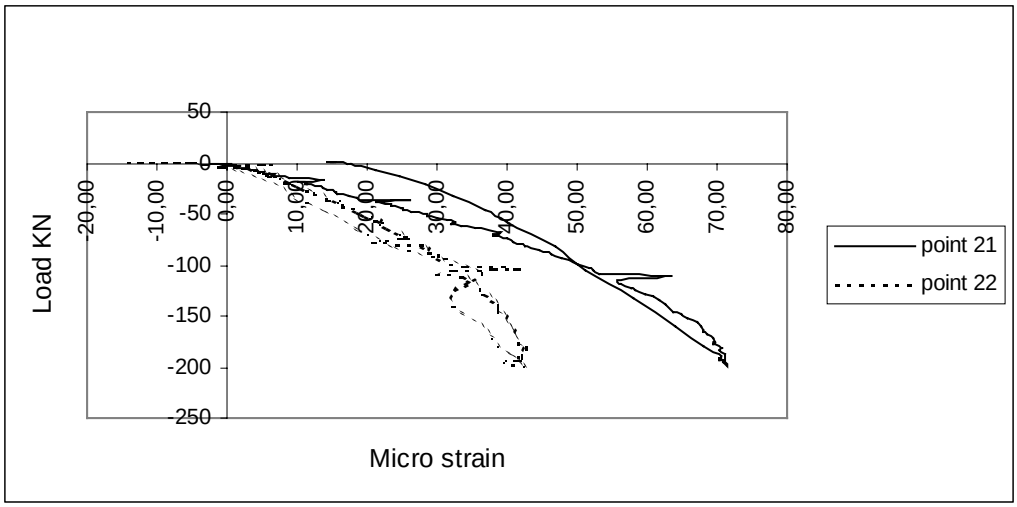

Strain in concrete.
Figure 2.28

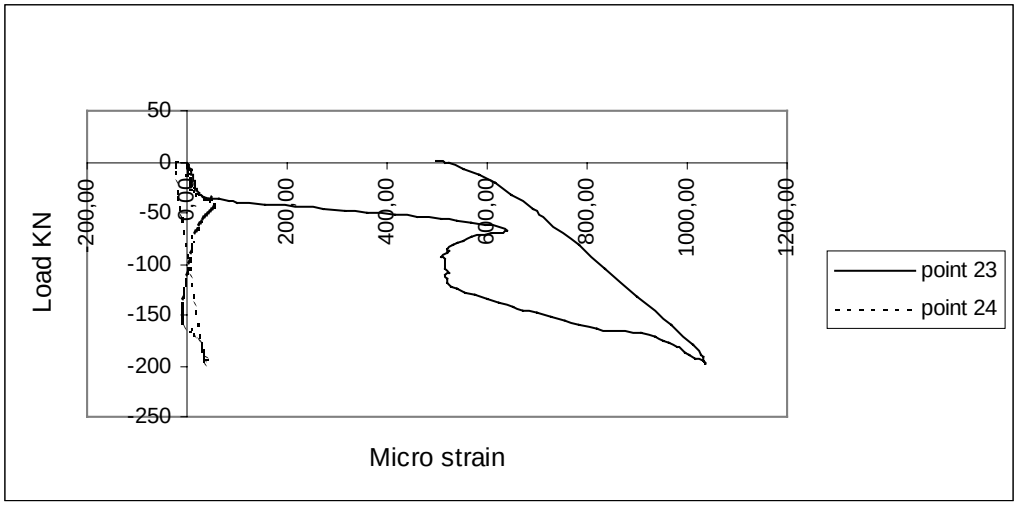

Strain in concrete.
Figure 2.29

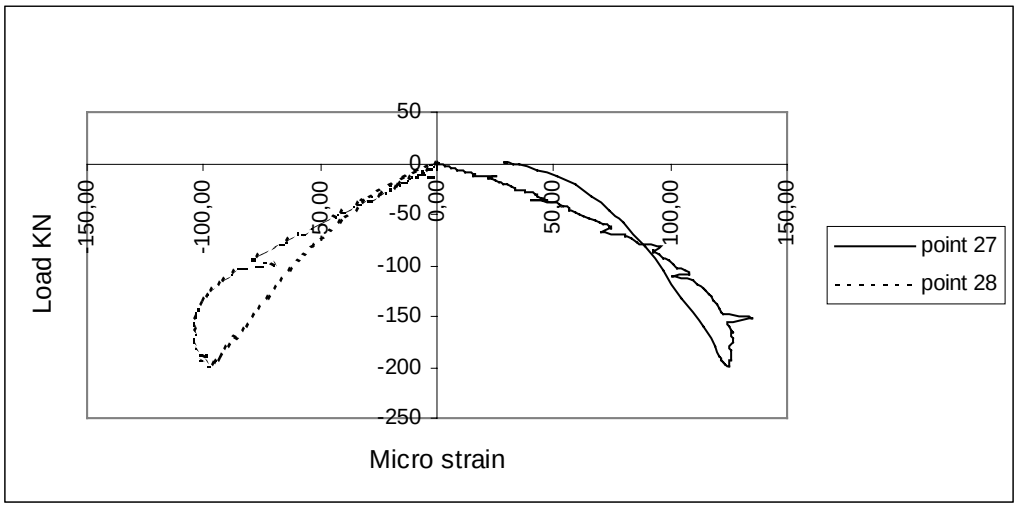

Strain in concrete.
Figure 2.30

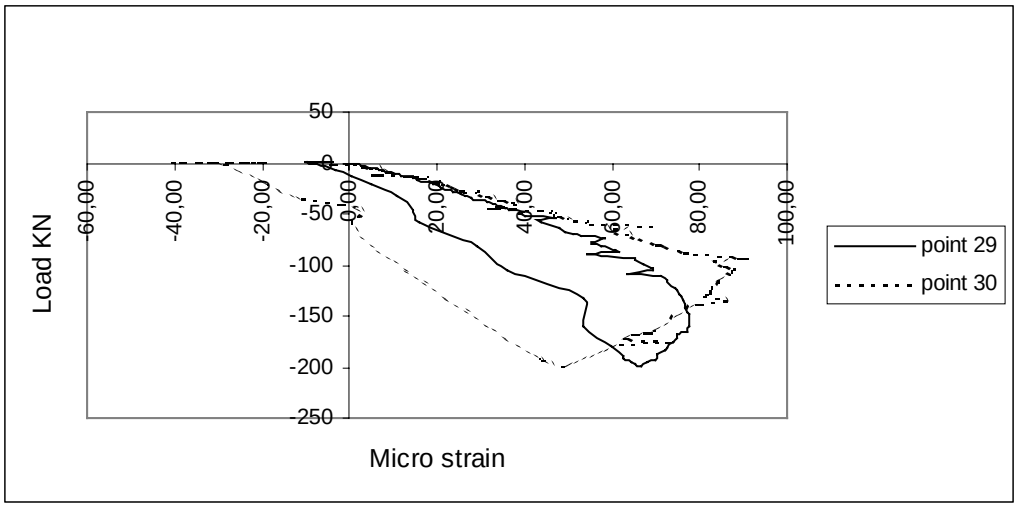

Strain in concrete.
Figure 2.31

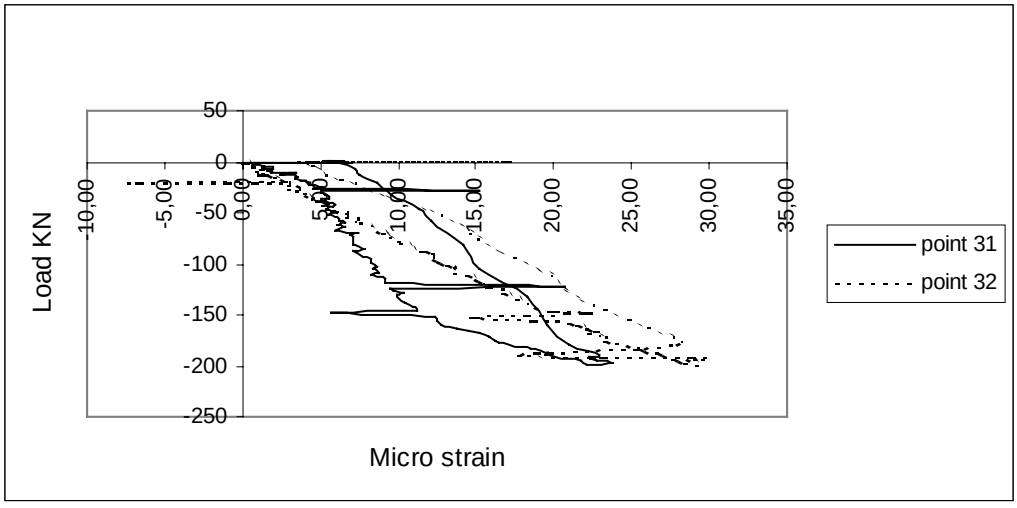

Strain in concrete.
Figure 2.32

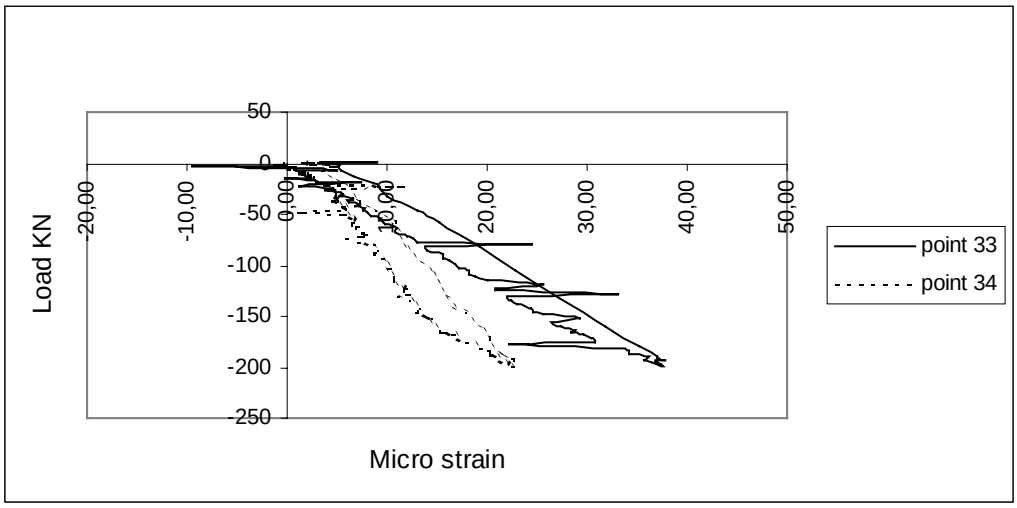

Strain in concrete.
Figure 2.33

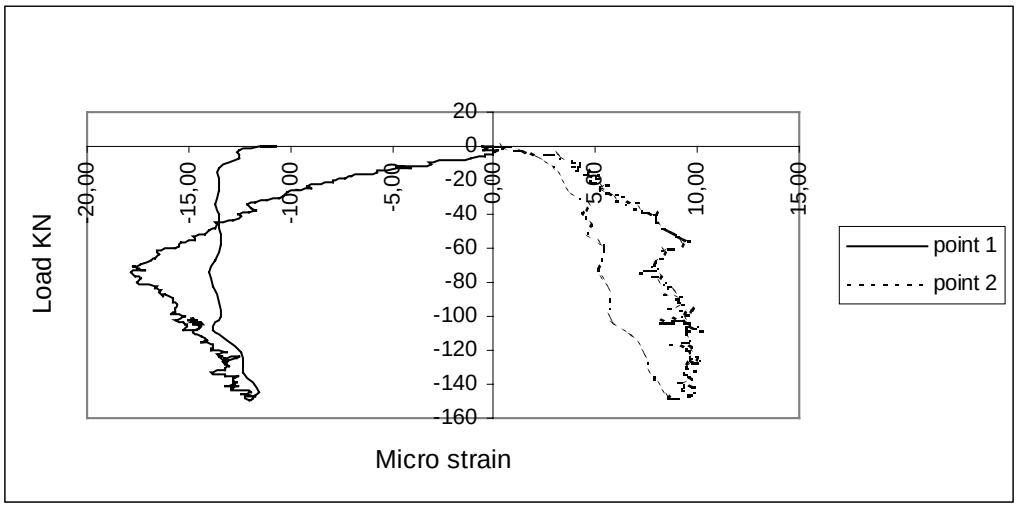

Strain in reinforcement.
Figure 2.34

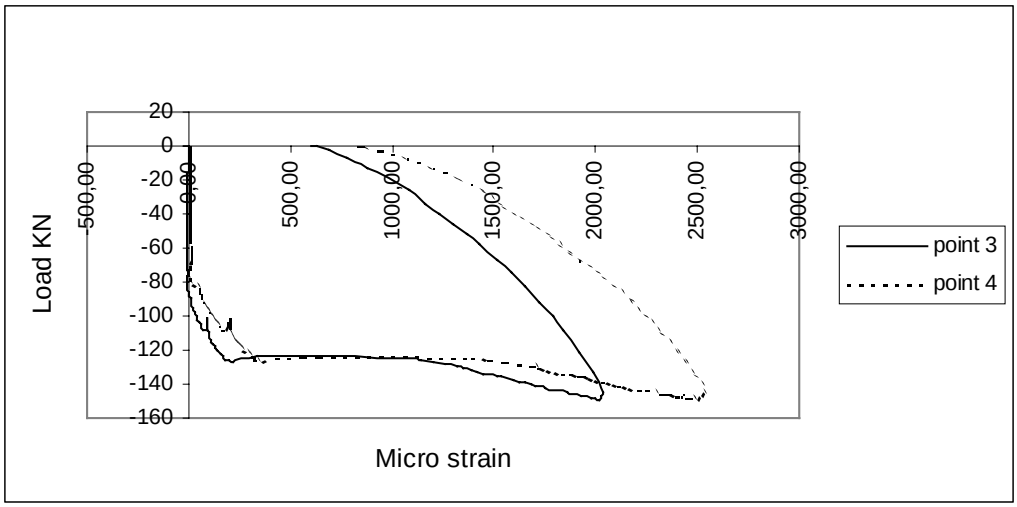

Strain in reinforcement.
Figure 2.35

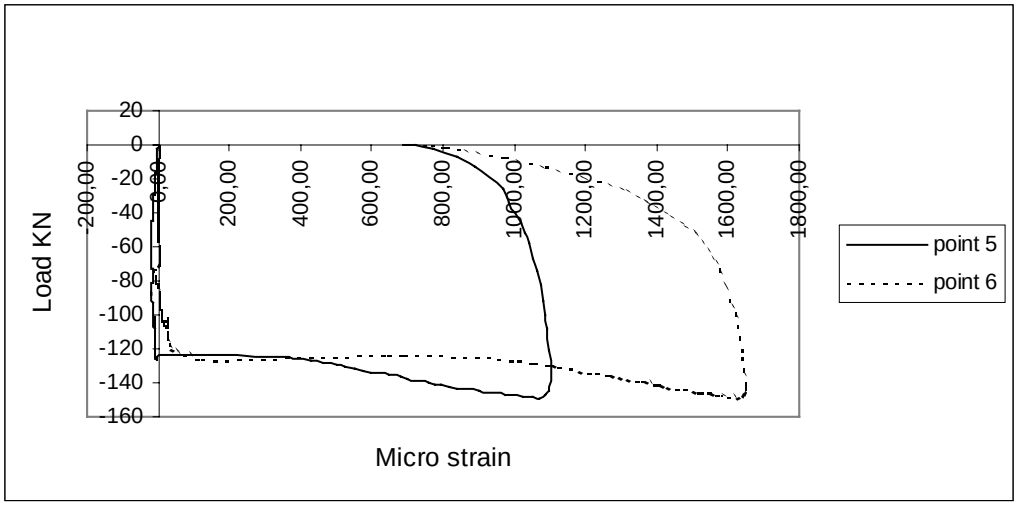

Strain in reinforcement.
Figure 2.36

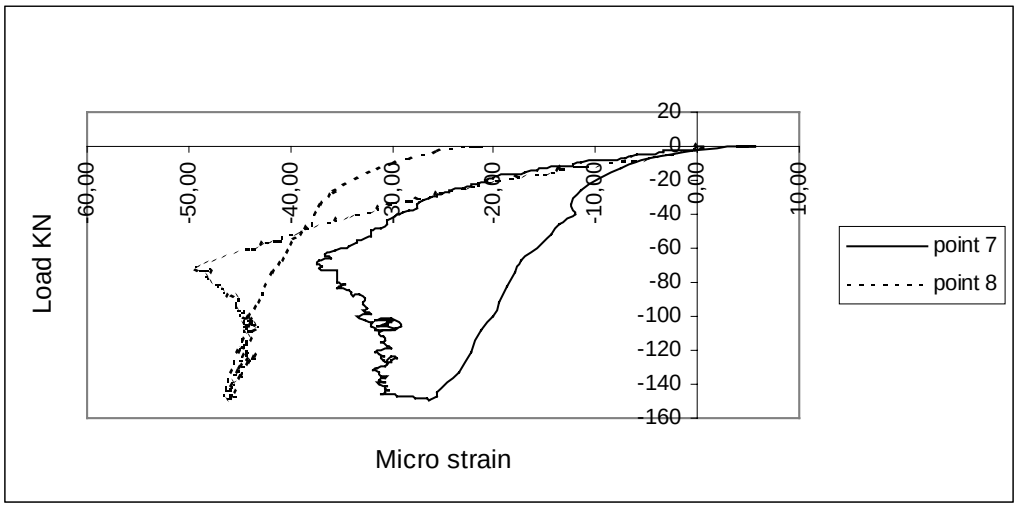

Strain in reinforcement.
Figure 2.37

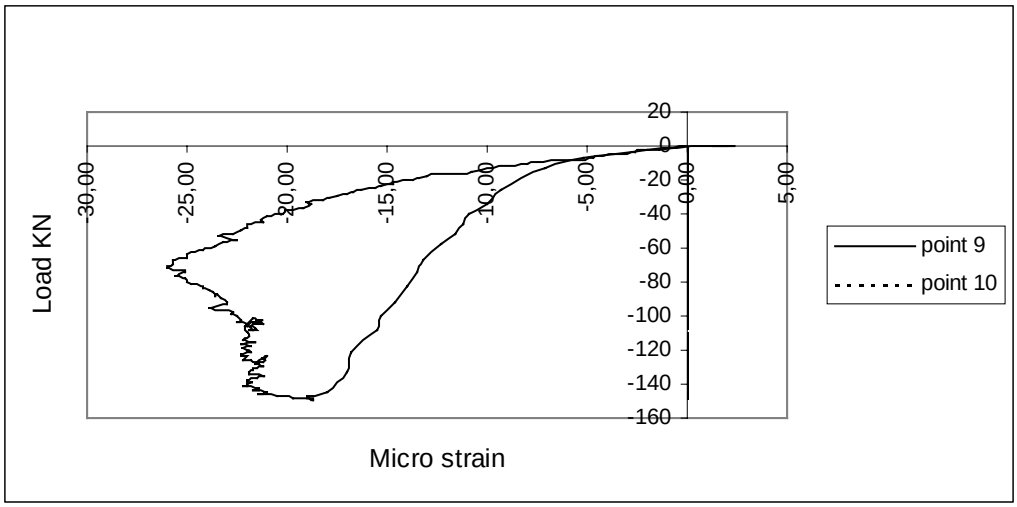

Strain in reinforcement.
Figure 2.38

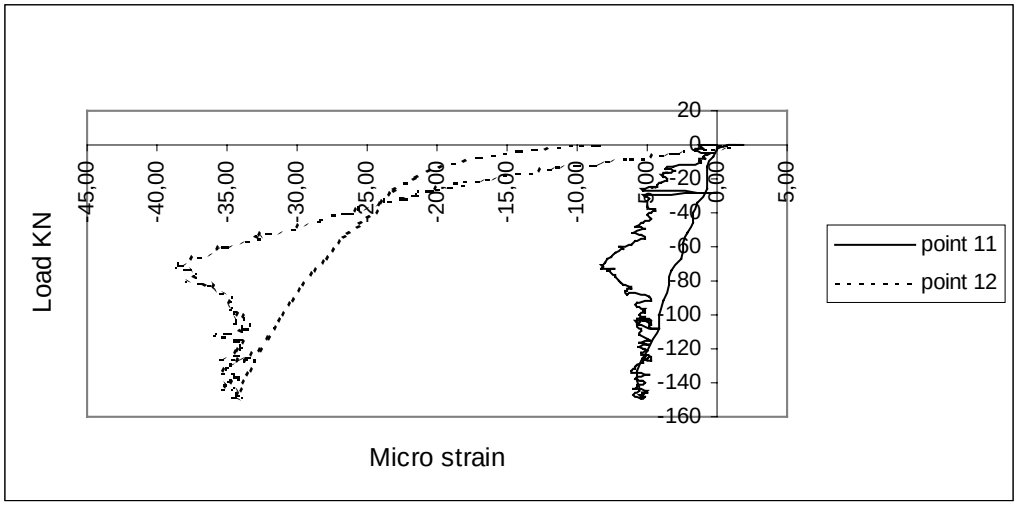

Strain in reinforcement.
Figure 2.39

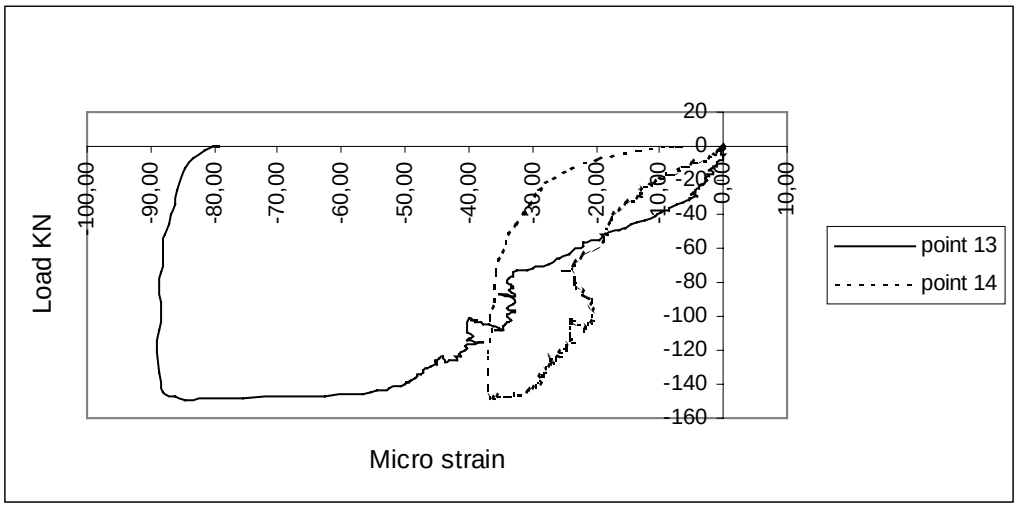

Strain in reinforcement.
Figure 2.40

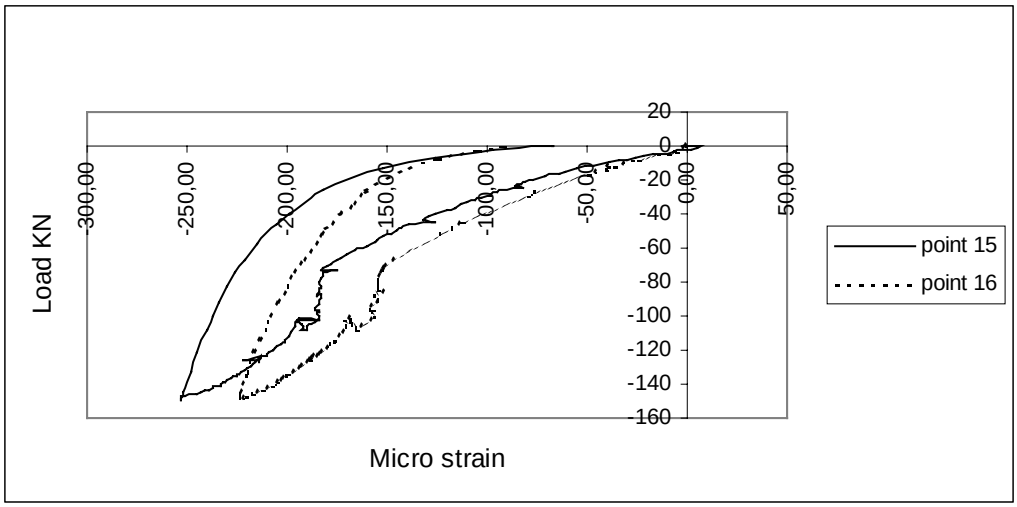

Strain in reinforcement.
Figure 2.41

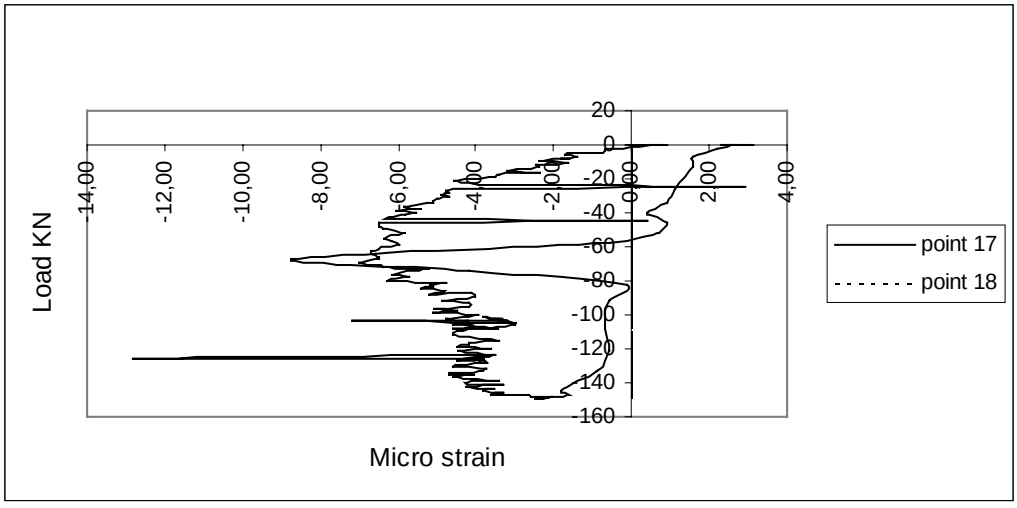

Strain in concrete.
Figure 2.42

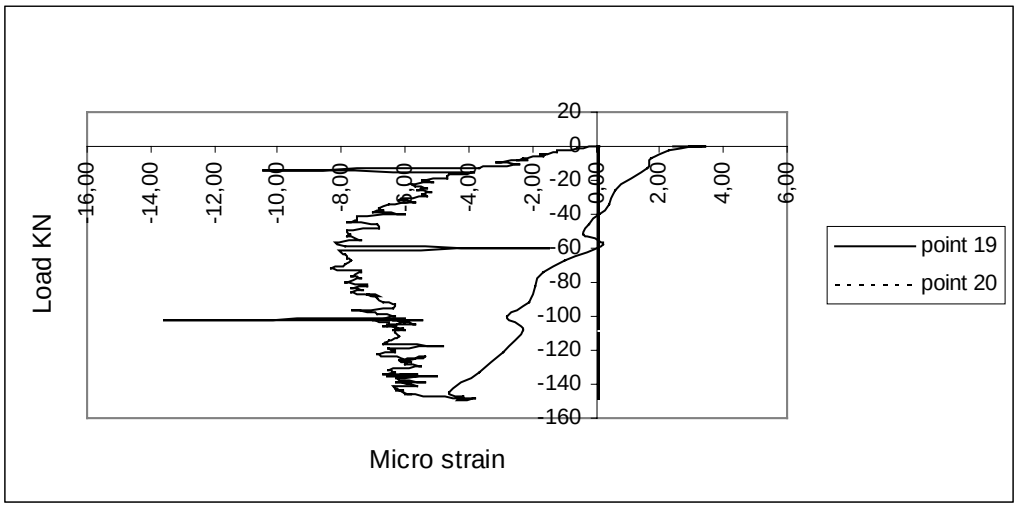

Strain in concrete.
Figure 2.43

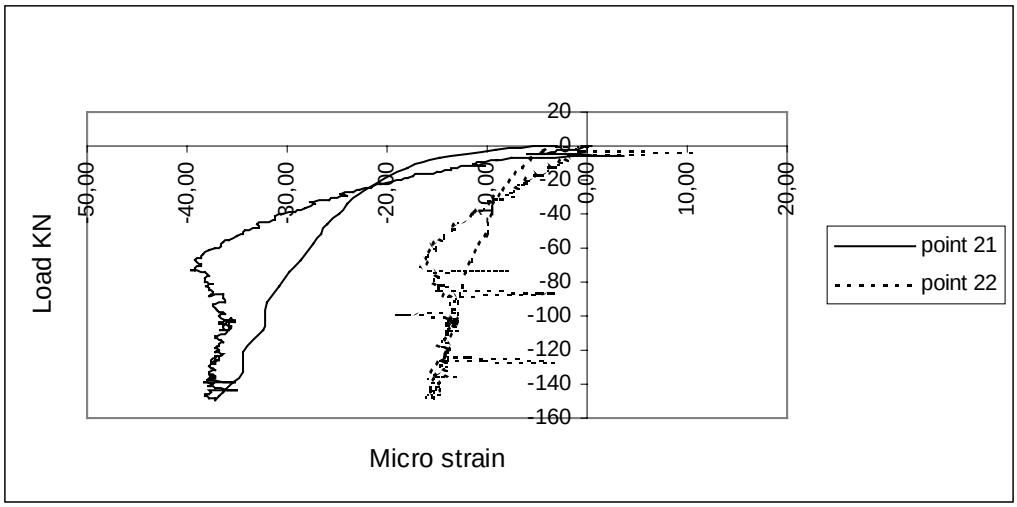

Strain in concrete.
Figure 2.44

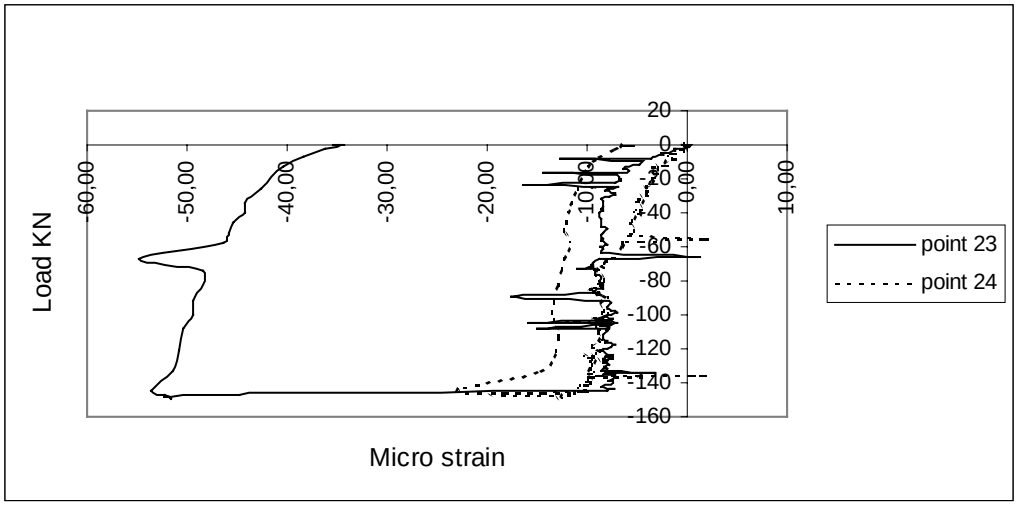

Strain in concrete.
Figure 2.45

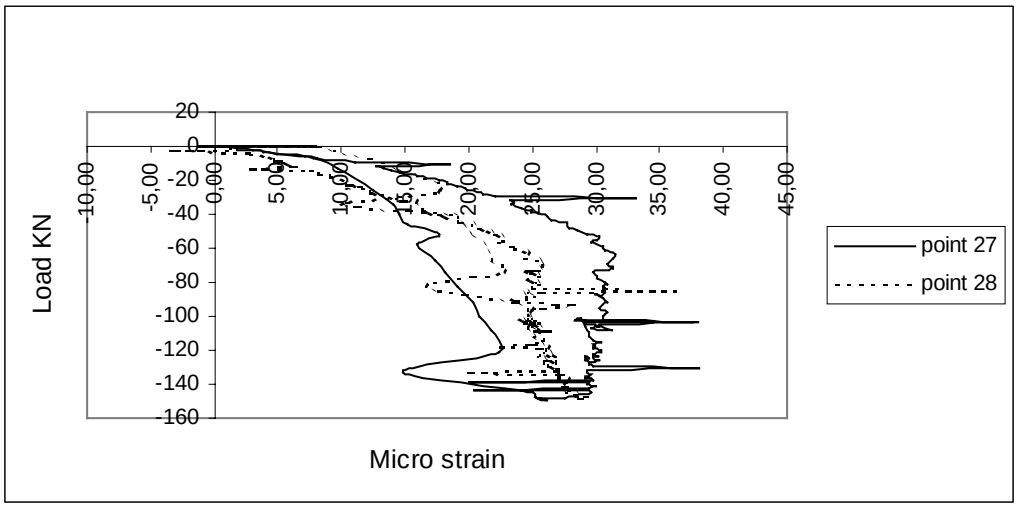

Strain in concrete.
Figure 2.46

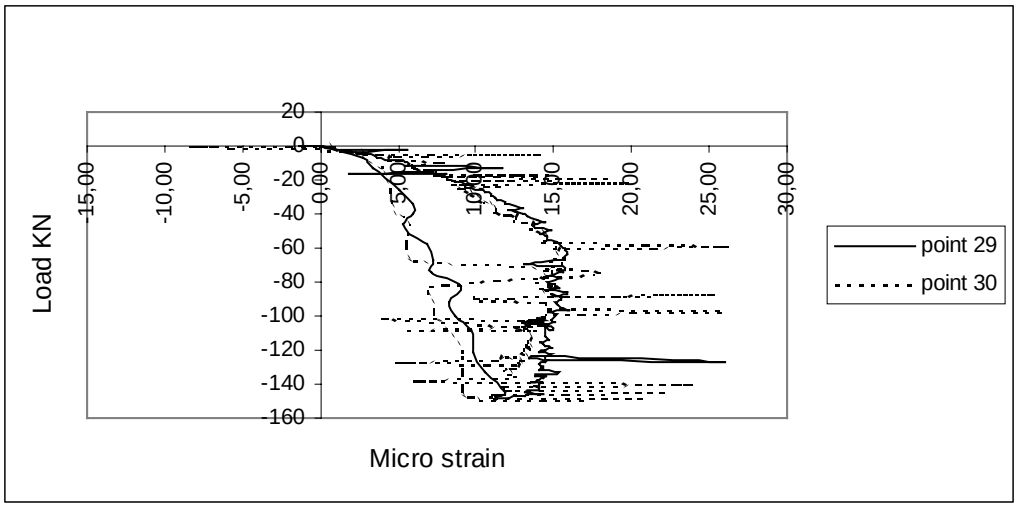

Strain in concrete.
Figure 2.47

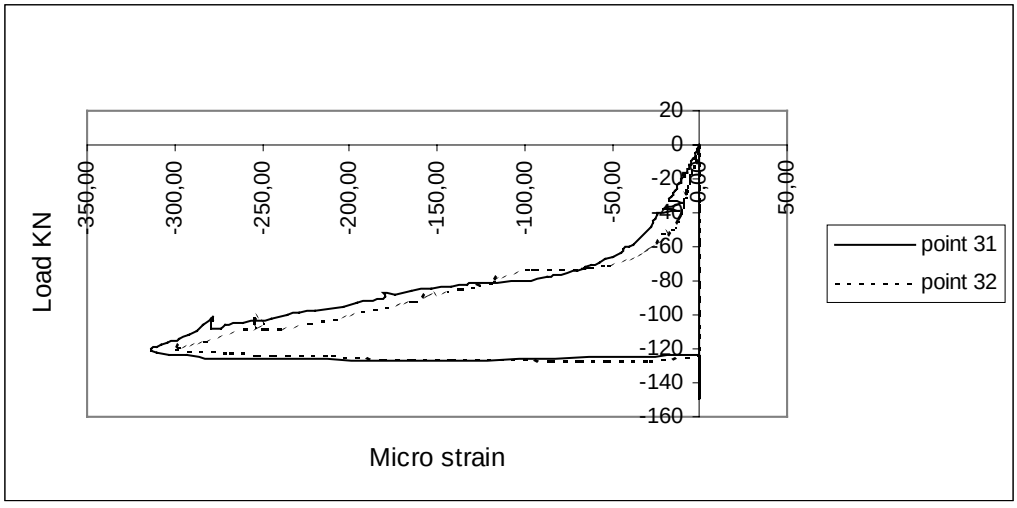

Strain in concrete.
Figure 2.48

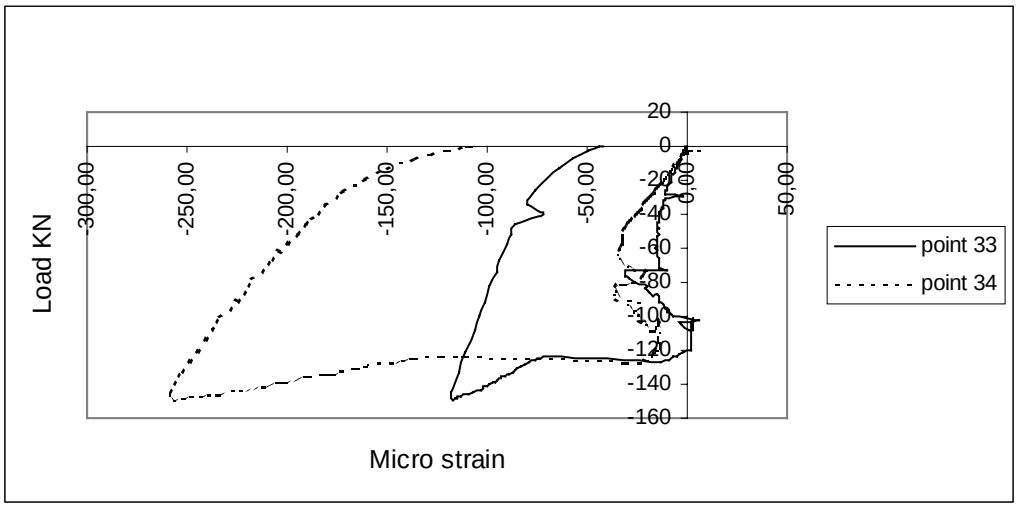

Strain in concrete.
Figure 2.49

In figure 2.50 – 2.58 the development of strain at the top and bottom surface of concrete for specimen S2 with load in the middle is listed. Strain in specimen S2 with load at the edge is listed in figure 2.59 – 2.67 and S2 with load in the corner is listed in figure 2.68 – 2.76.

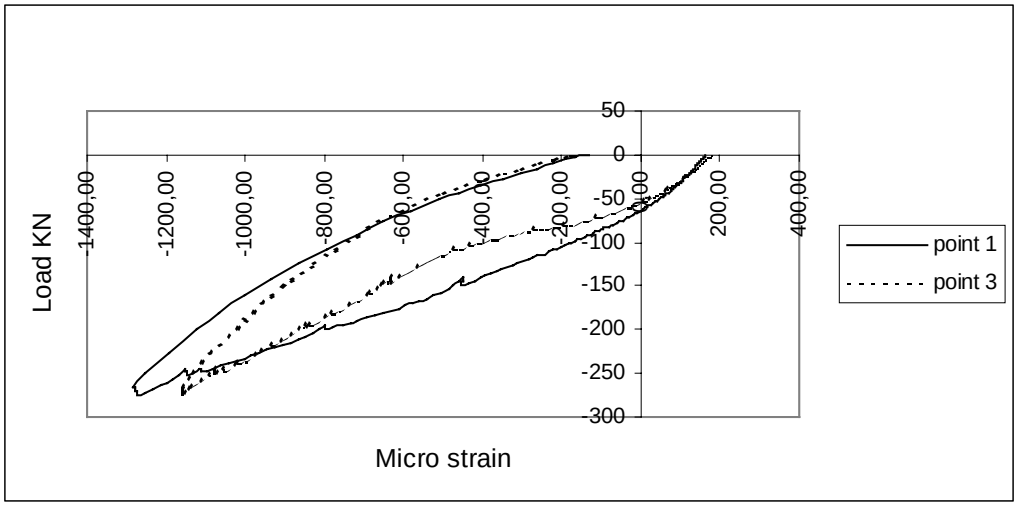

Strain in concrete.
Figure 2.50

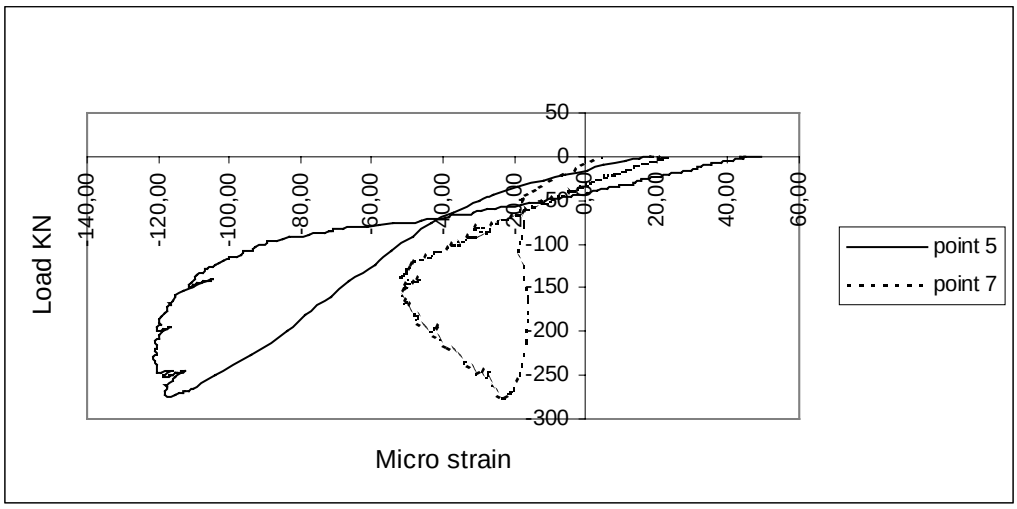

Strain in concrete.
Figure 2.51

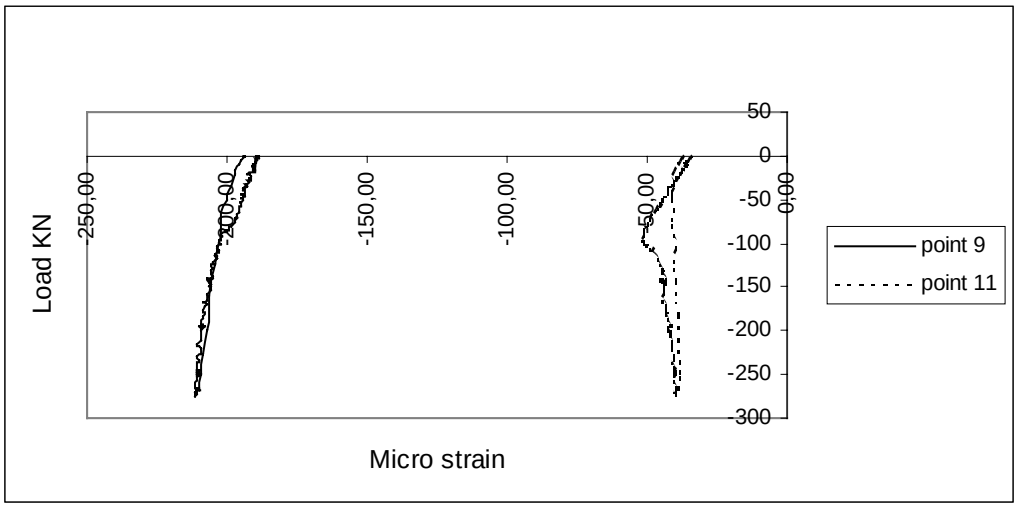

Strain in concrete.
Figure 2.52

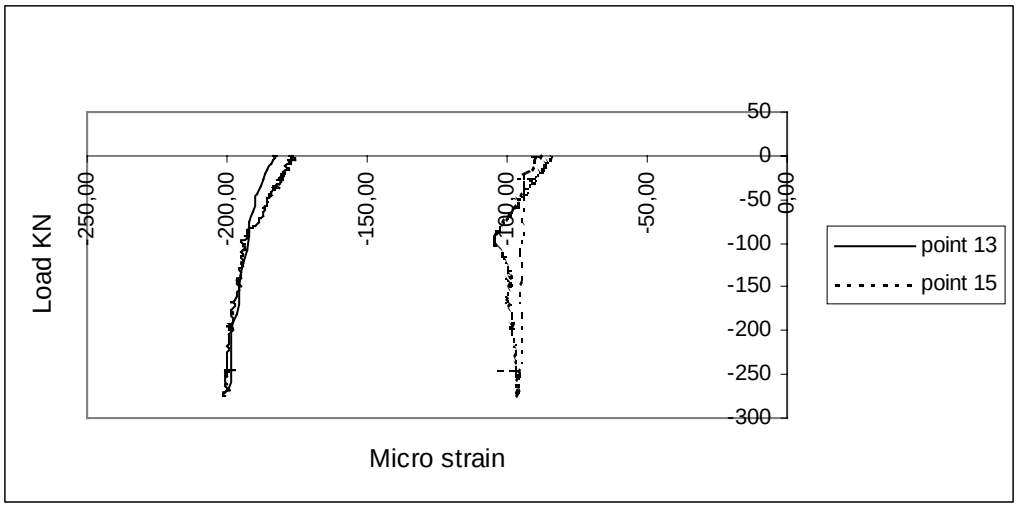

Strain in concrete.
Figure 2.53

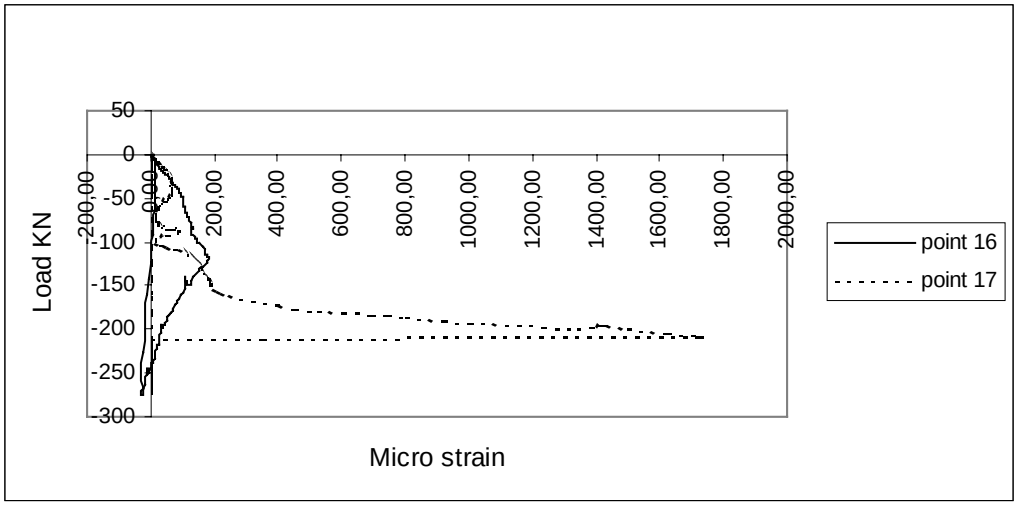

Strain in concrete.
Figure 2.54

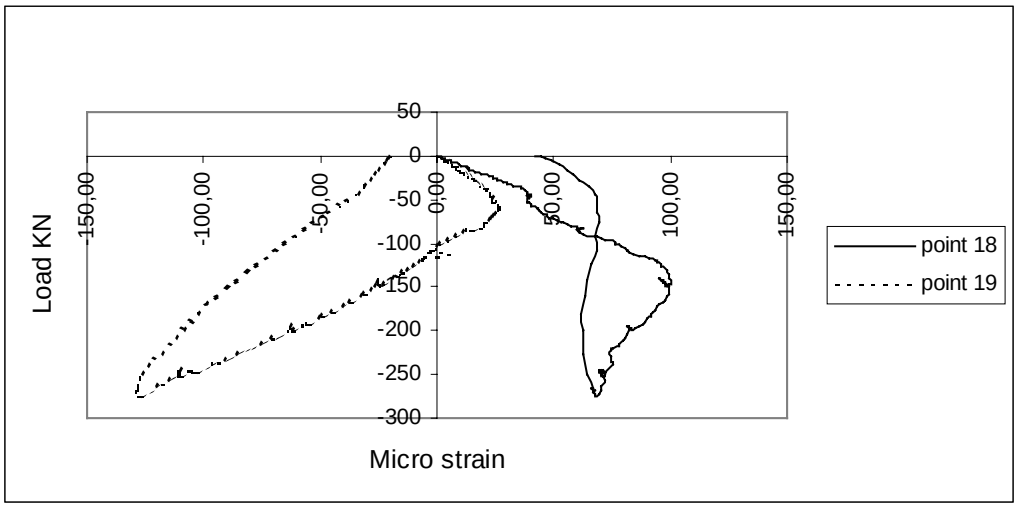

Strain in concrete.
Figure 2.55

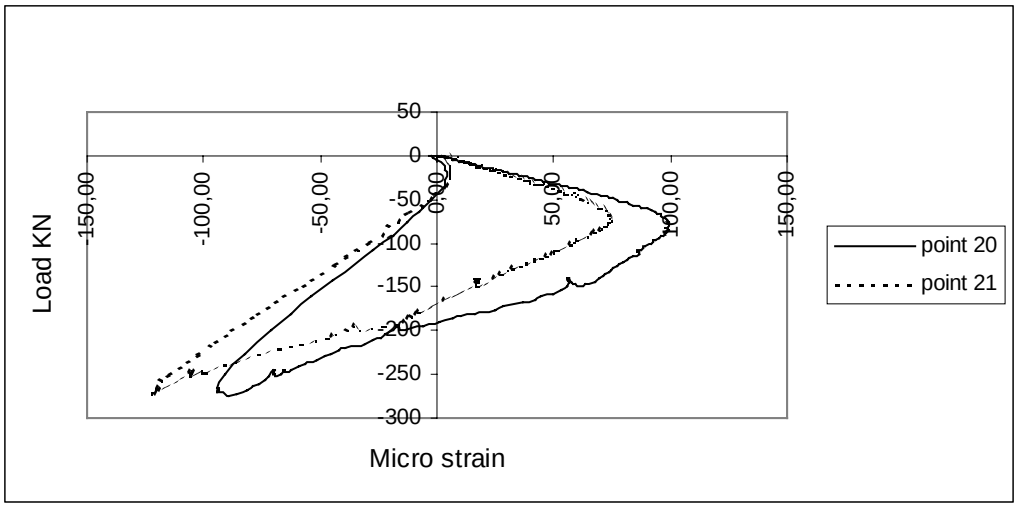

Strain in concrete.
Figure 2.56

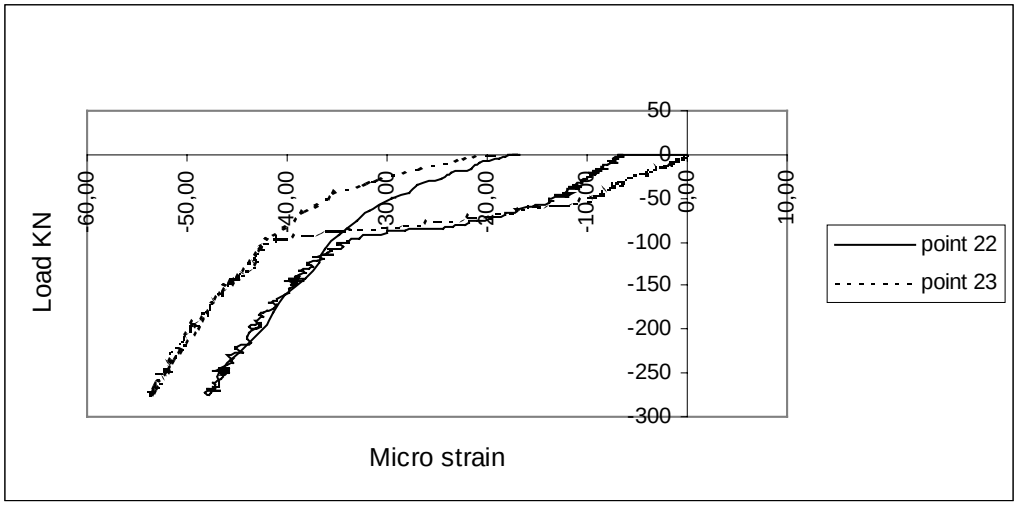

Strain in concrete.
Figure 2.57

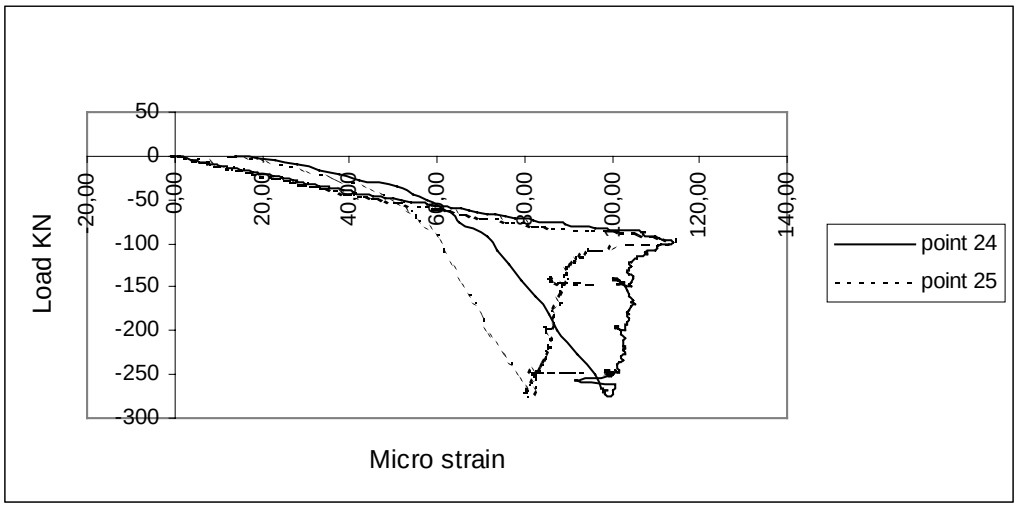

Strain in concrete.
Figure 2.58

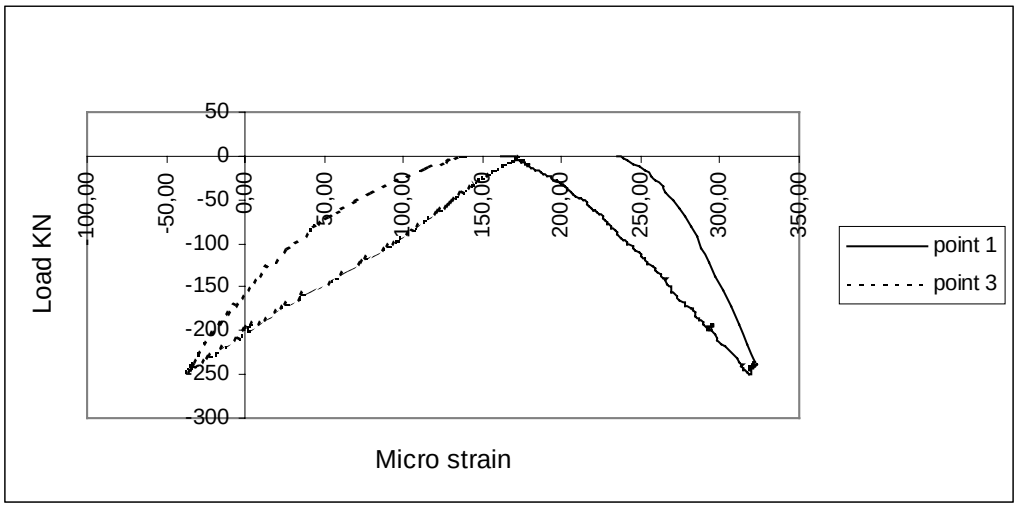

Strain in concrete.
Figure 2.59

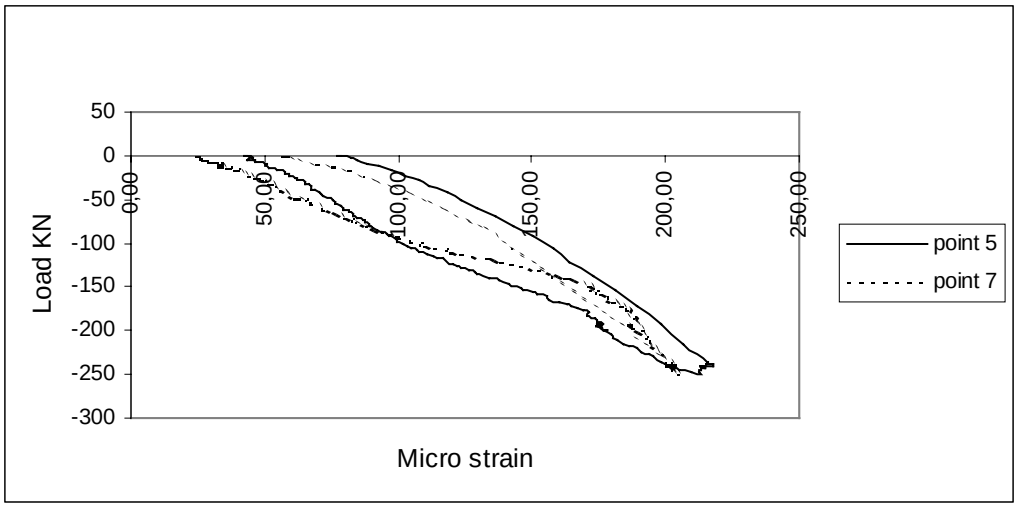

Strain in concrete.
Figure 2.60

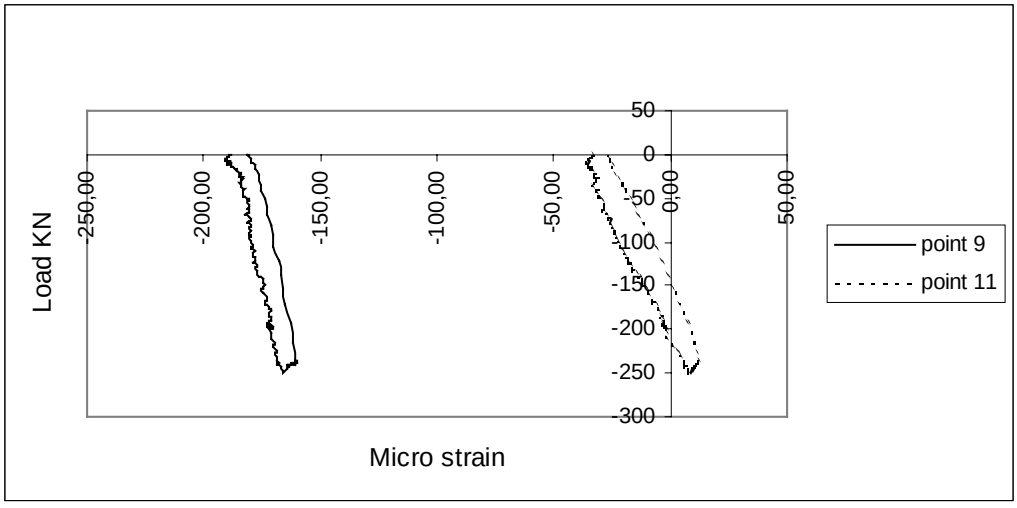

Strain in concrete.
Figure 2.61

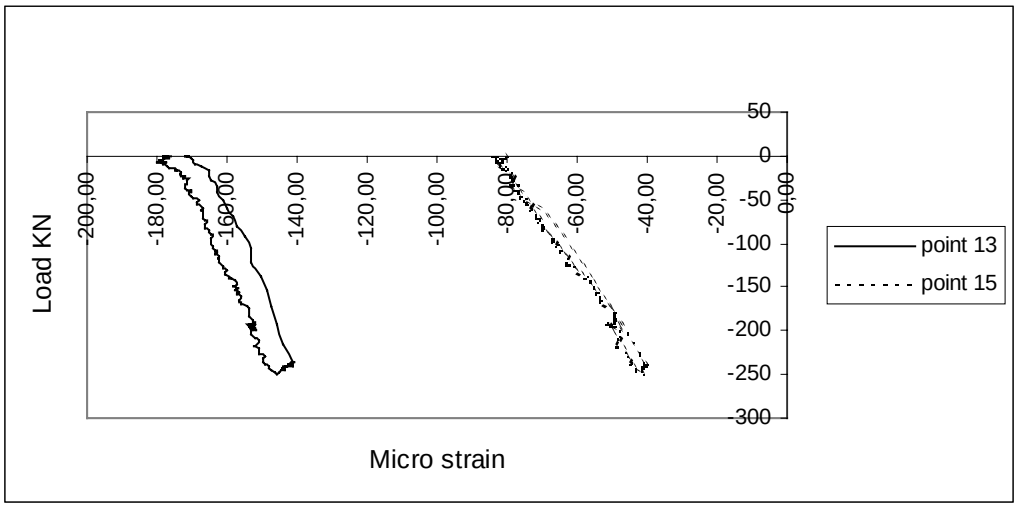

Strain in concrete.
Figure 2.62

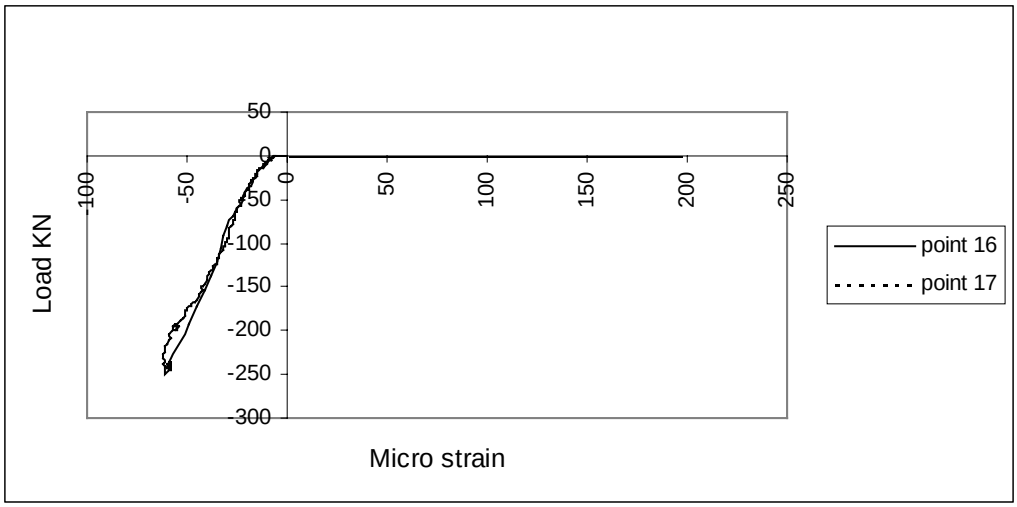

Strain in concrete.
Figure 2.63

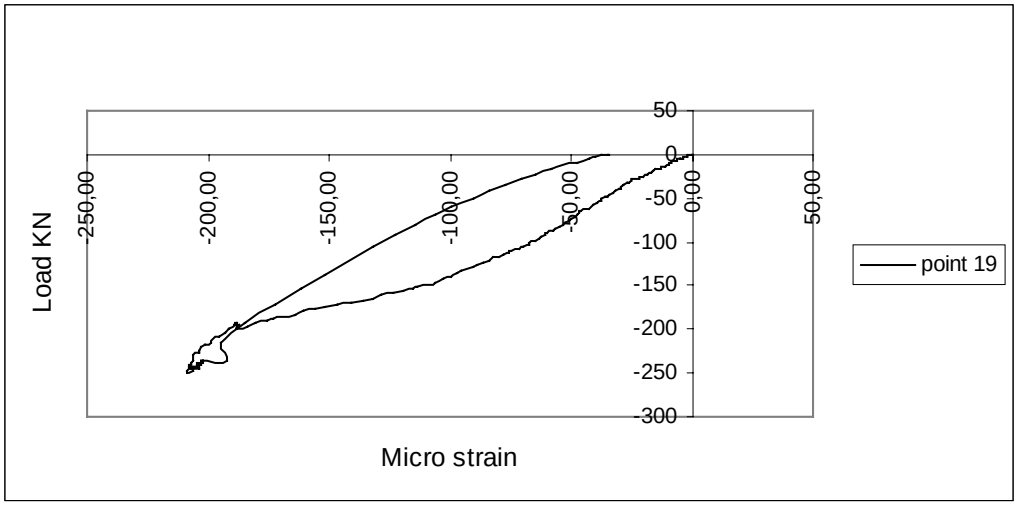

Strain in concrete.
Figure 2.64

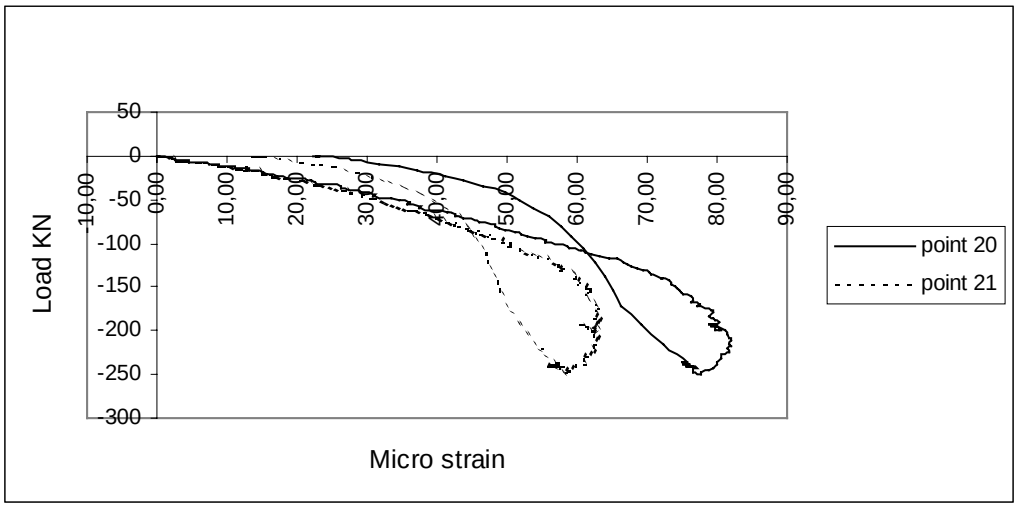

Strain in concrete.
Figure 2.65

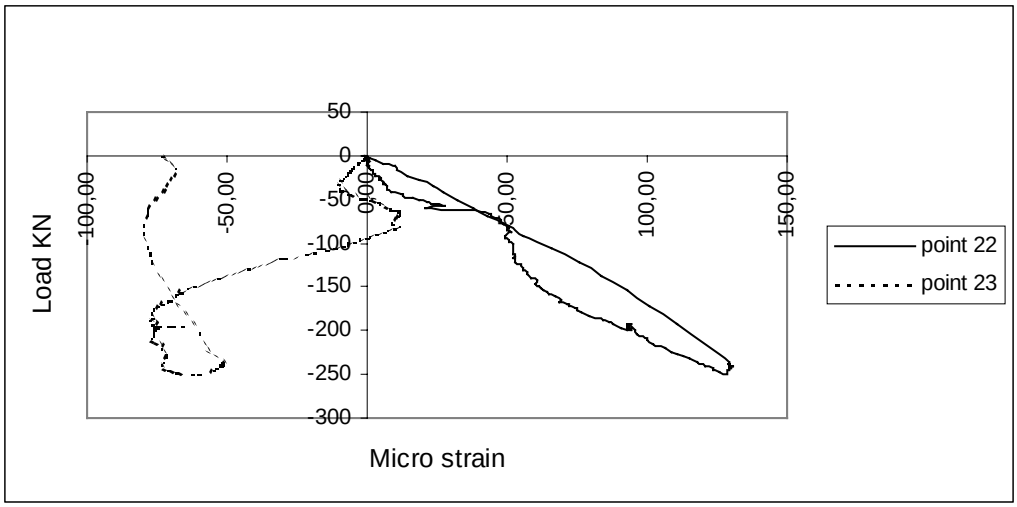

Strain in concrete.
Figure 2.66

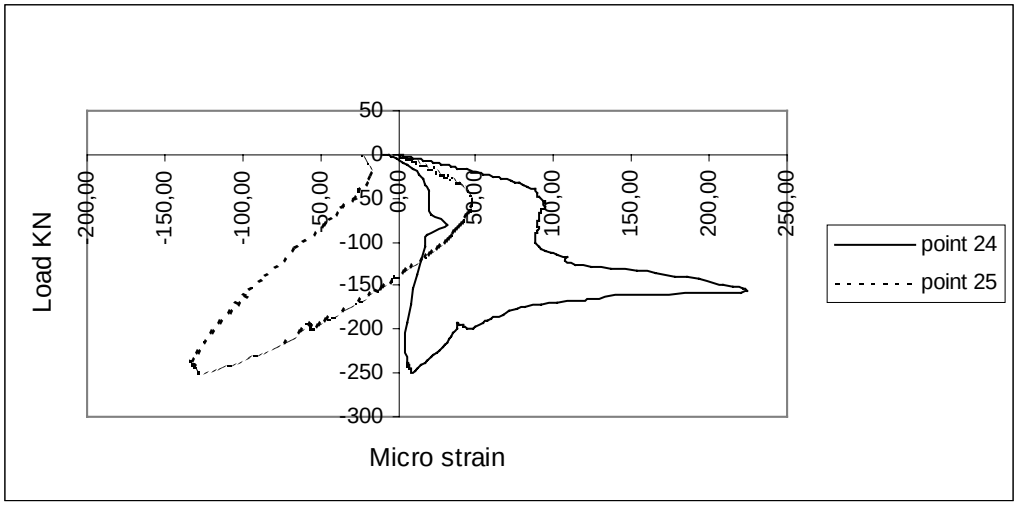

Strain in concrete.
Figure 2.67

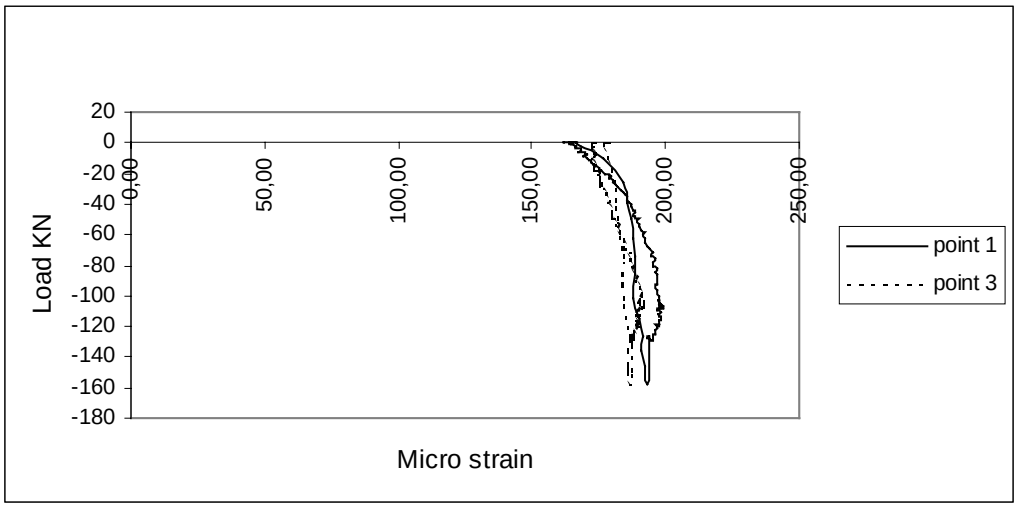

Strain in concrete.
Figure 2.68

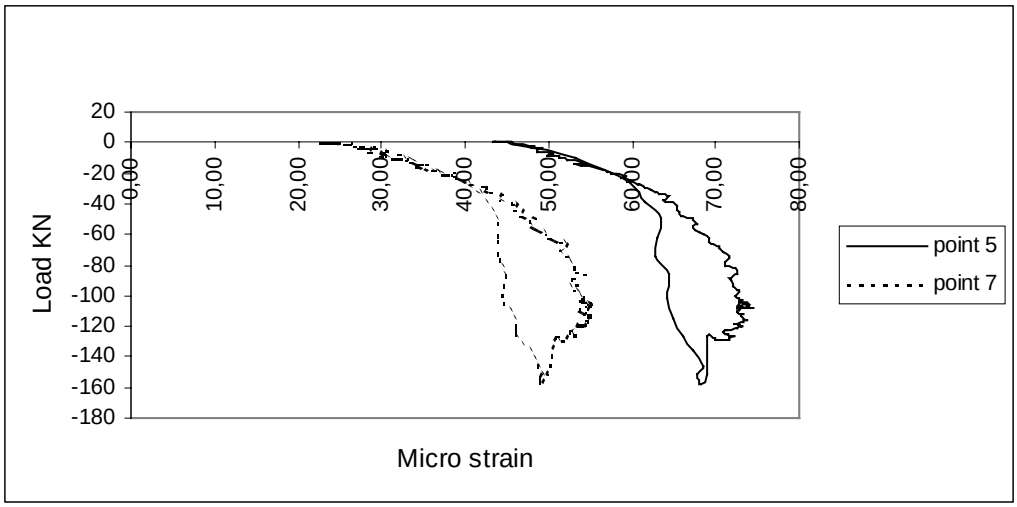

Strain in concrete.
Figure 2.69

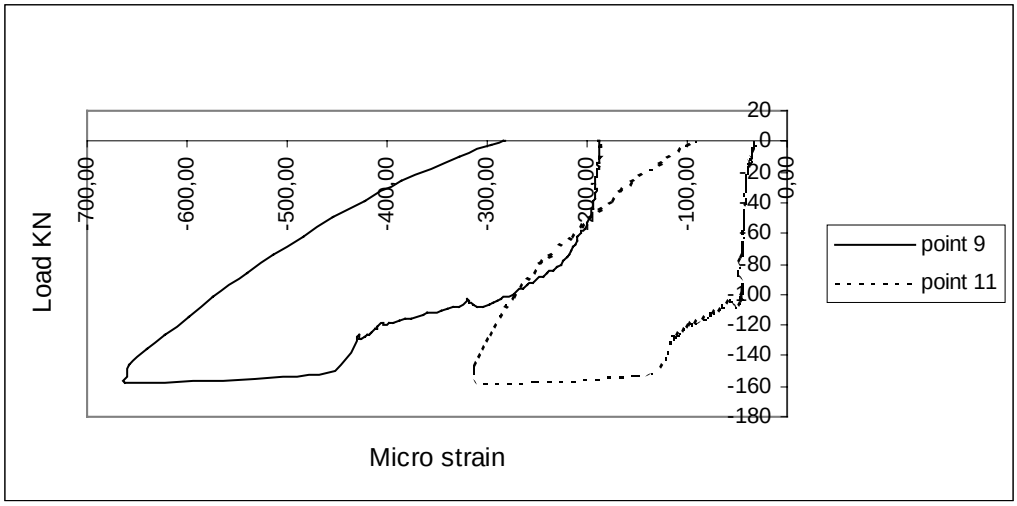

Strain in concrete.
Figure 2.70

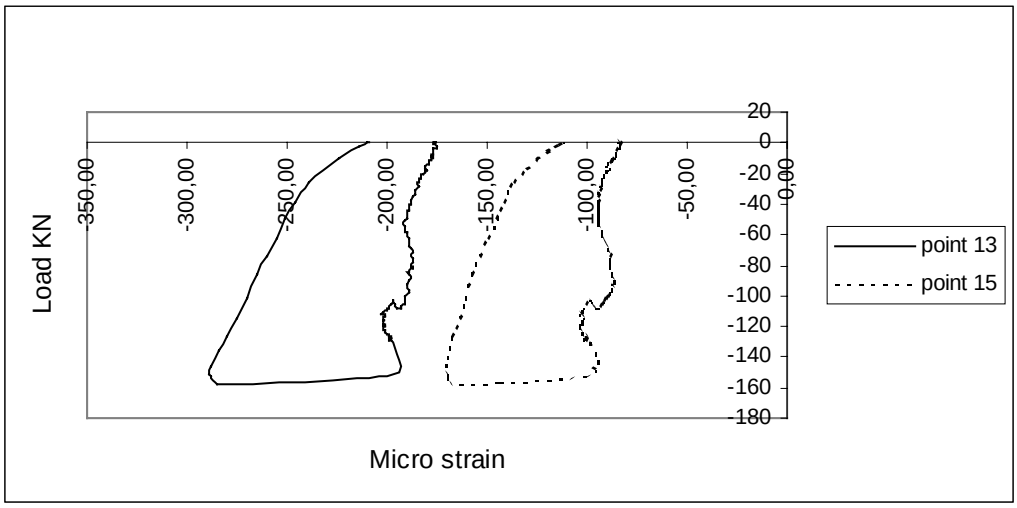

Strain in concrete.
Figure 2.71

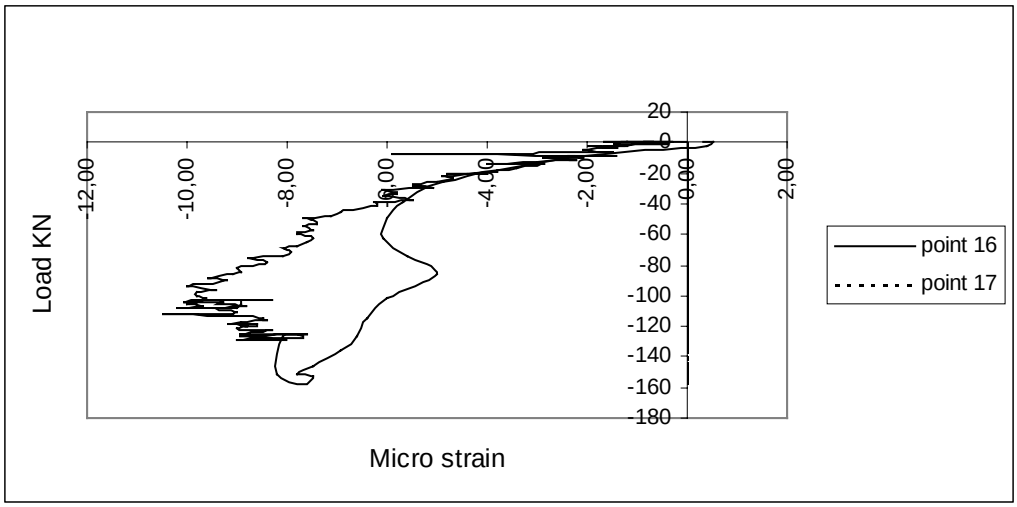

Strain in concrete.
Figure 2.72

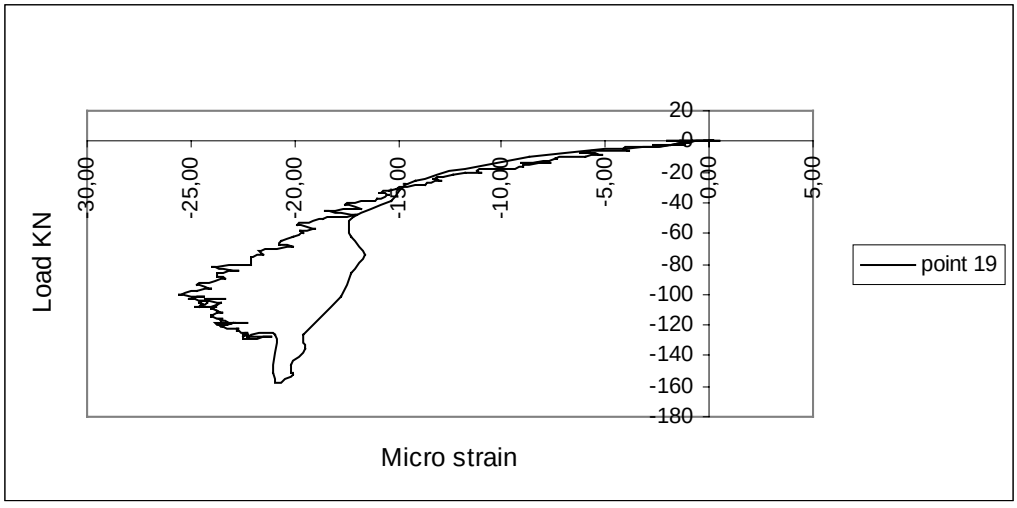

Strain in concrete.
Figure 2.73

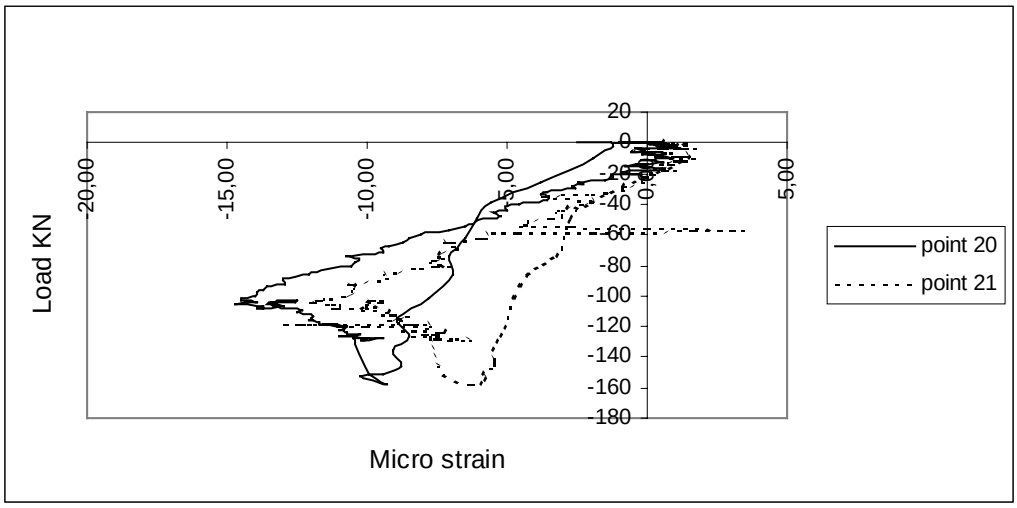

Strain in concrete.
Figure 2.74

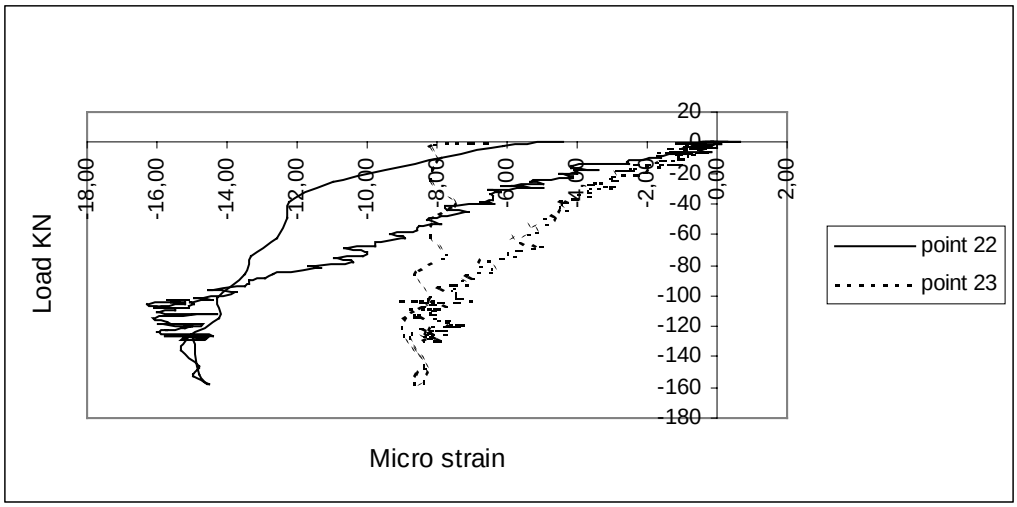

Strain in concrete.
Figure 2.75

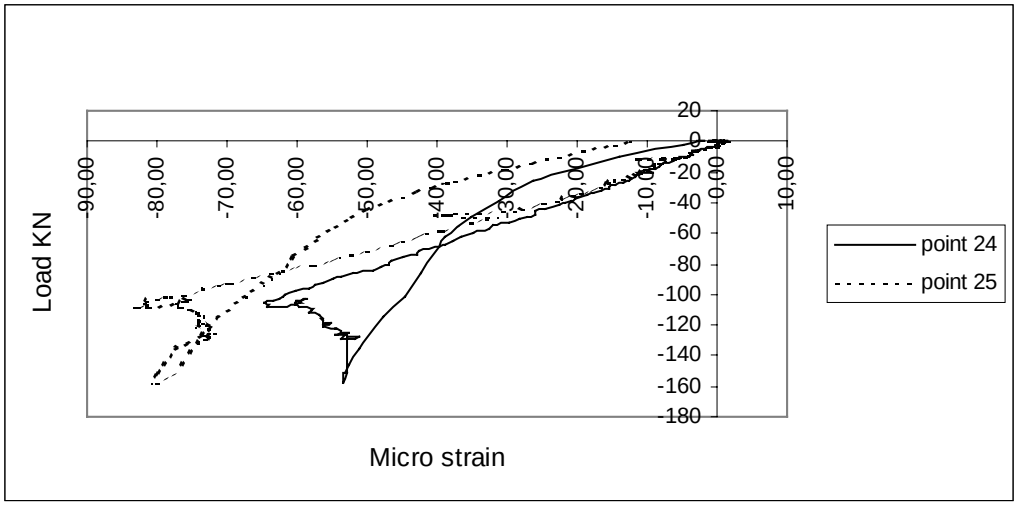

Strain in concrete.
Figure 2.76

In figure 2.77– 2.85 the development of strain at the top and bottom surface of concrete for specimen S3 with load in the middle is listed. Strain in specimen S3 with load at the edge is listed in figure 2.86 – 2.94 and S3 with load in the corner is listed in figure 2.95 – 2.103.

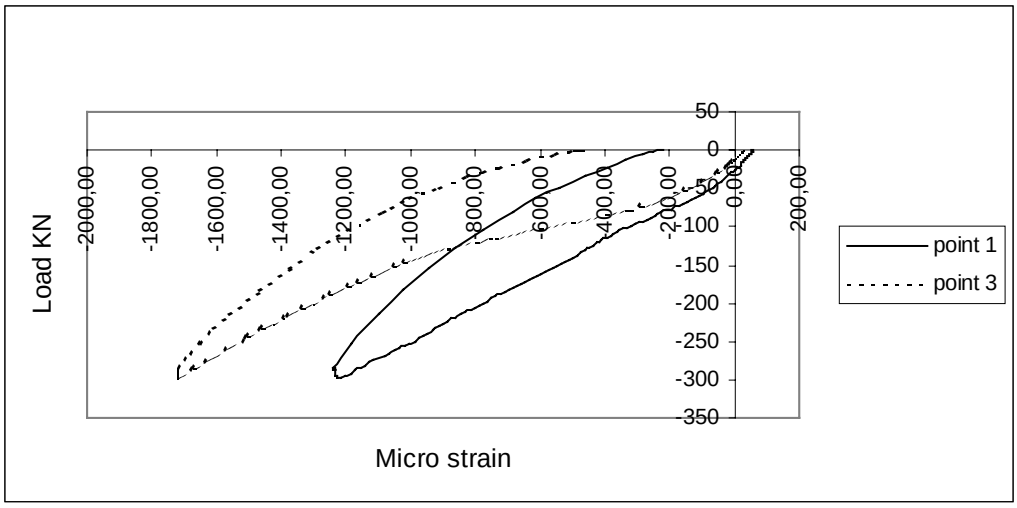

Strain in concrete.
Figure 2.77

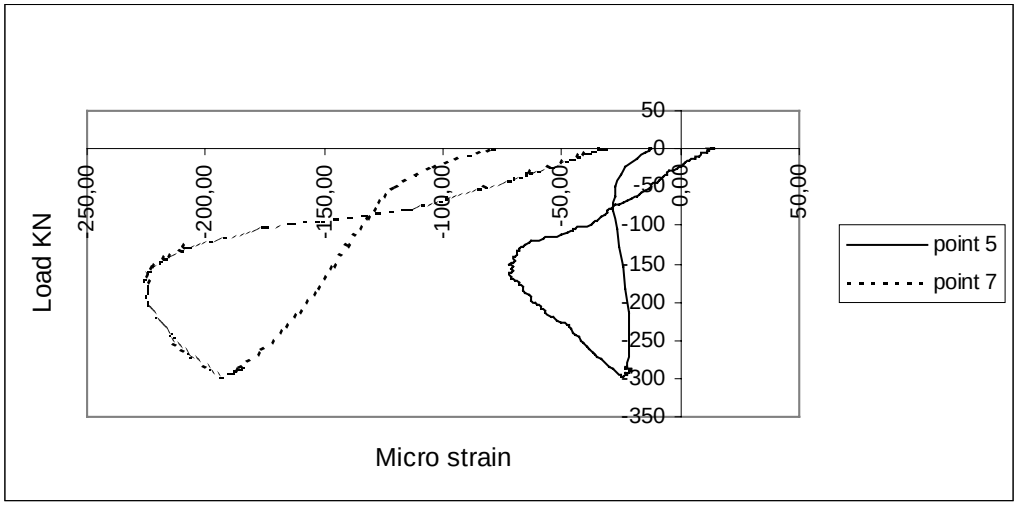

Strain in concrete.
Figure 2.78

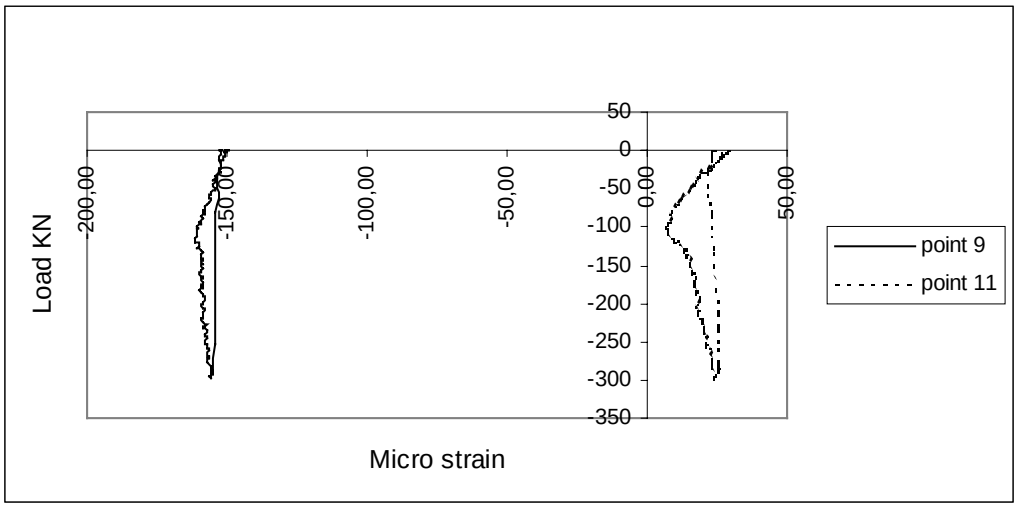

Strain in concrete.
Figure 2.79

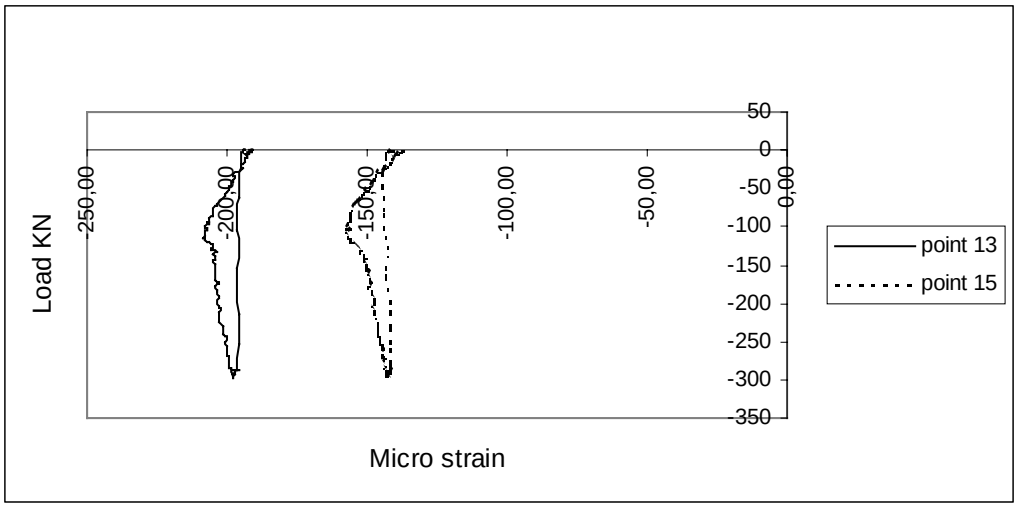

Strain in concrete.
Figure 2.80

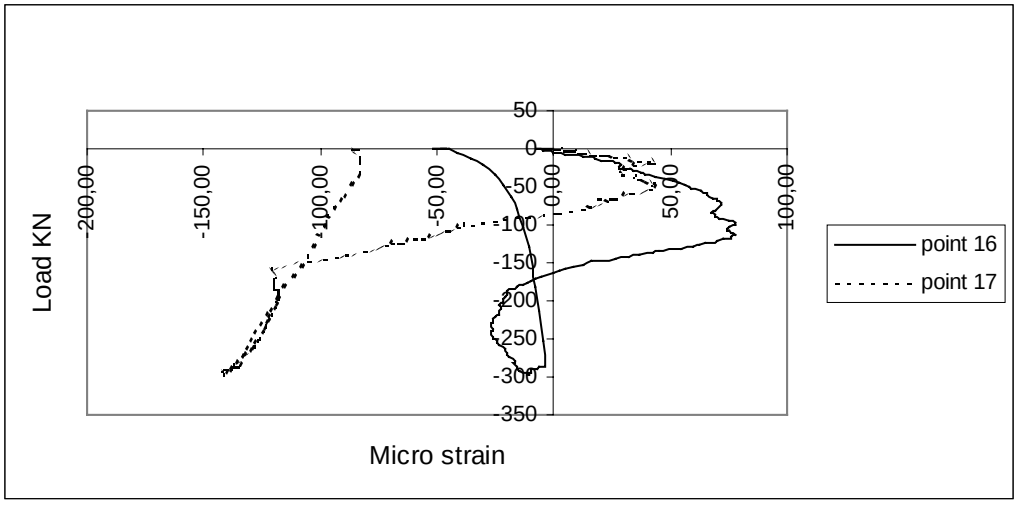

Strain in concrete.
Figure 2.81

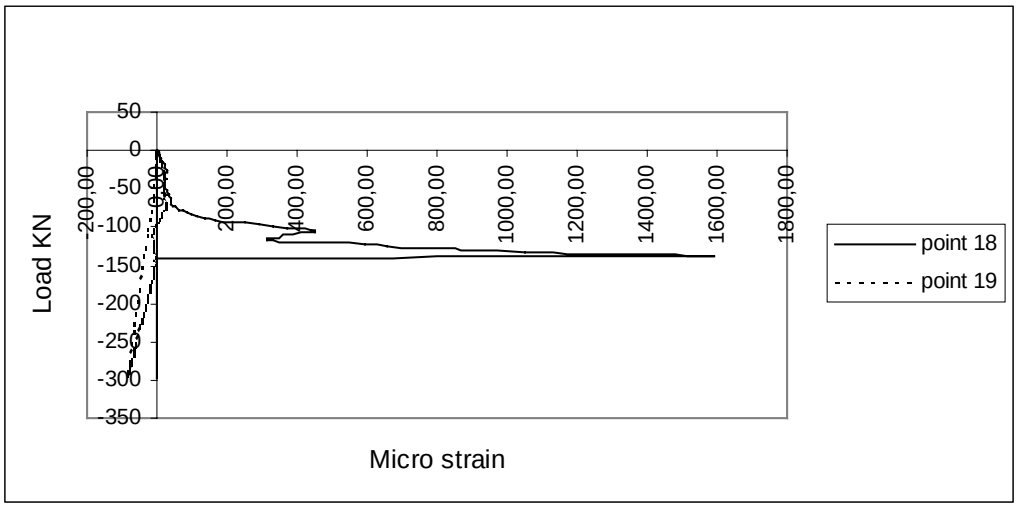

Strain in concrete.
Figure 2.82

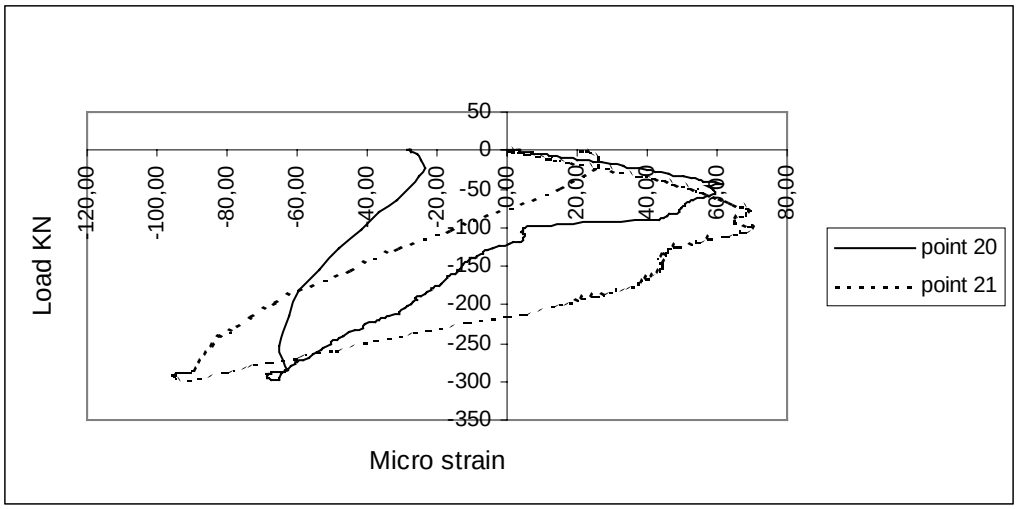

Strain in concrete.
Figure 2.83

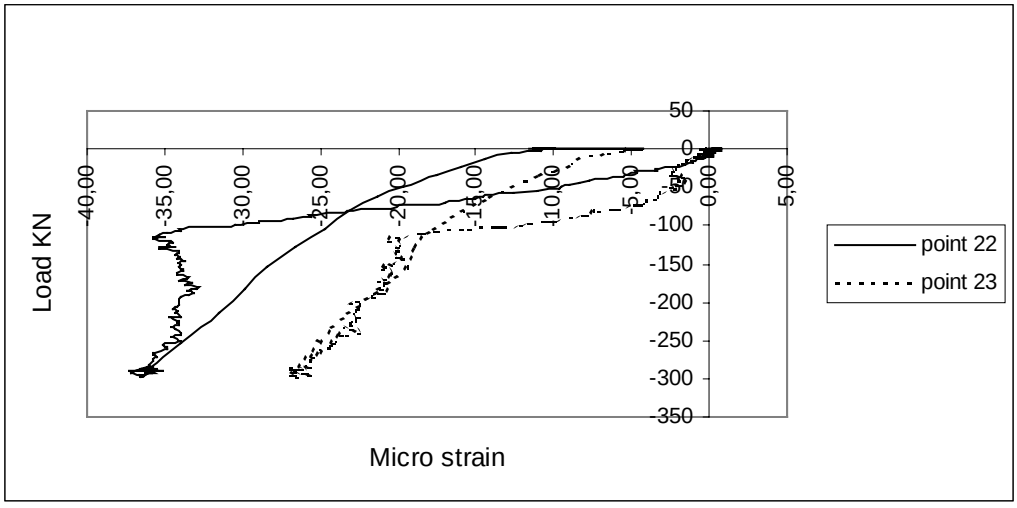

Strain in concrete.
Figure 2.84

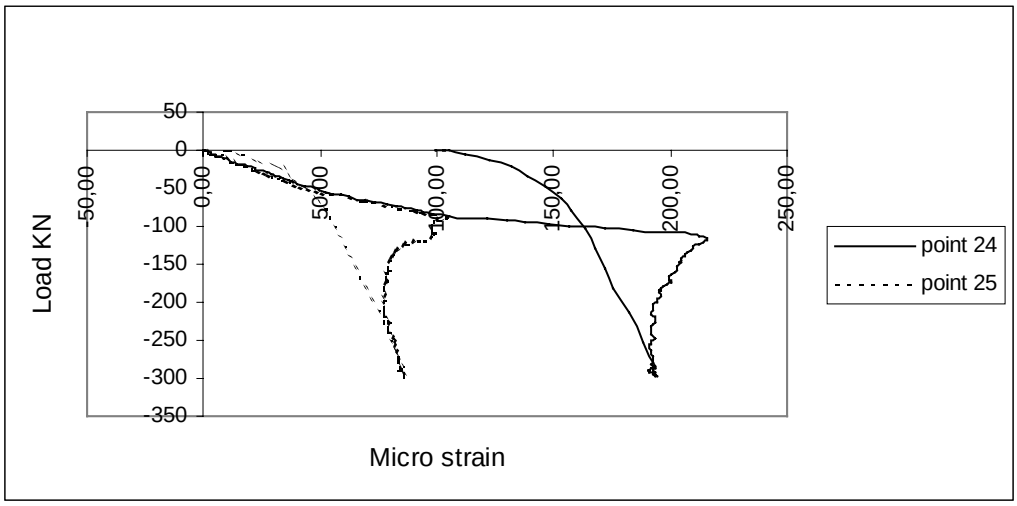

Strain in concrete.
Figure 2.85

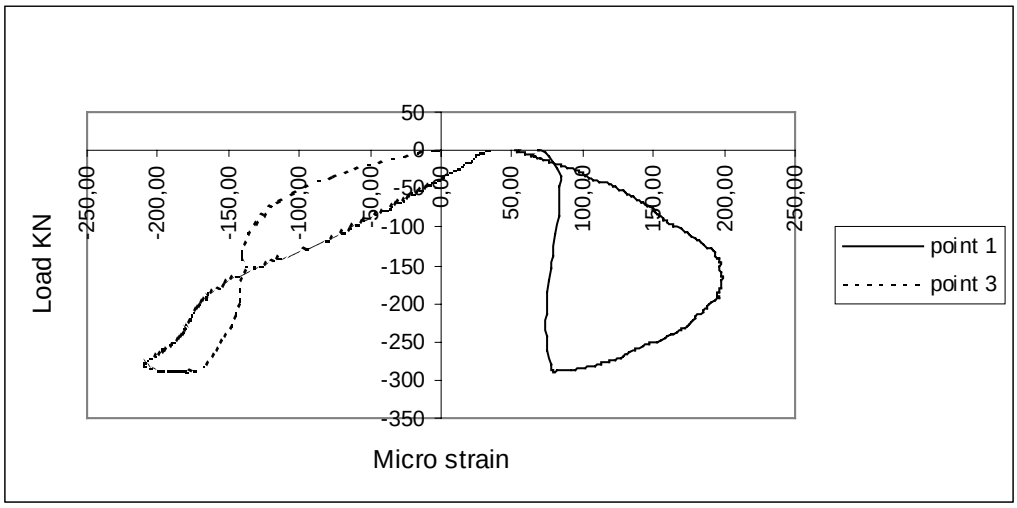

Strain in concrete.
Figure 2.86

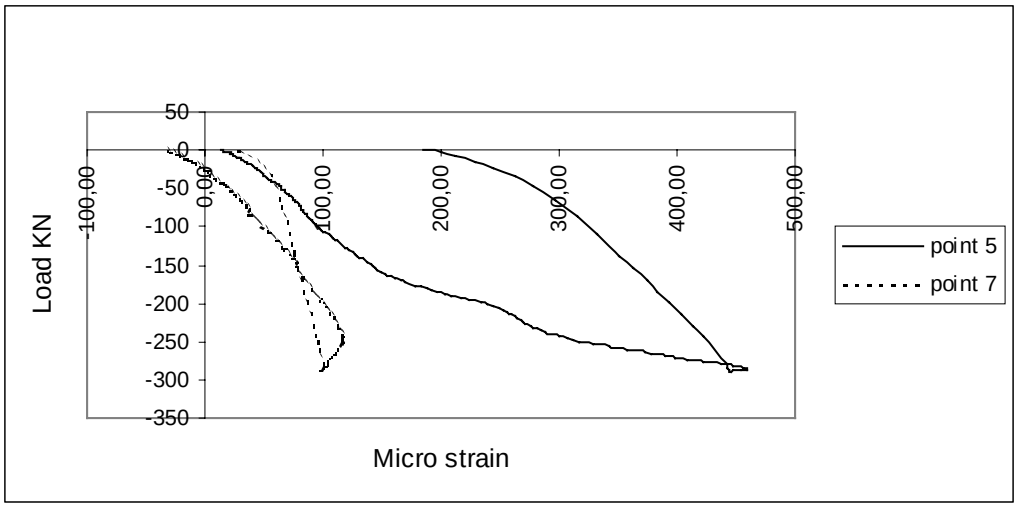

Strain in concrete.
Figure 2.87

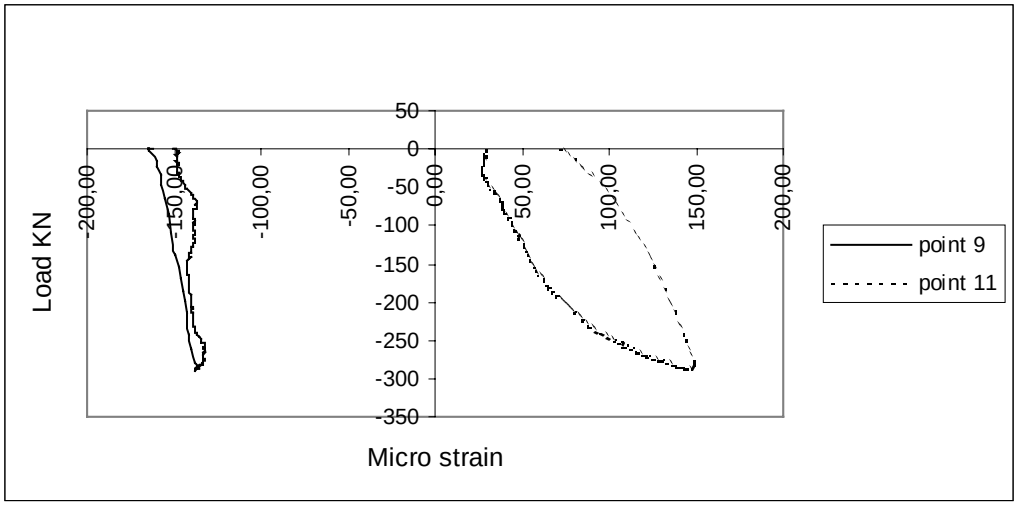

Strain in concrete.
Figure 2.88

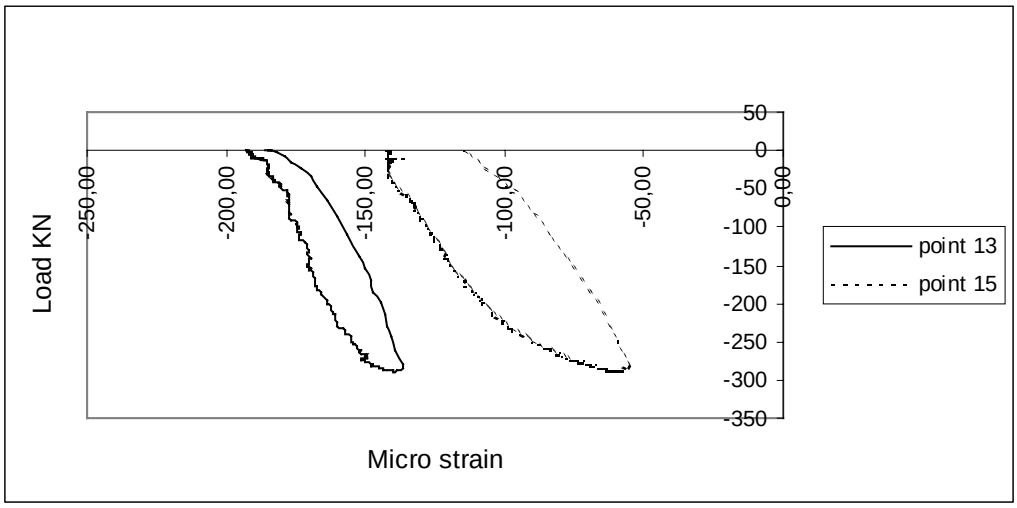

Strain in concrete.
Figure 2.89

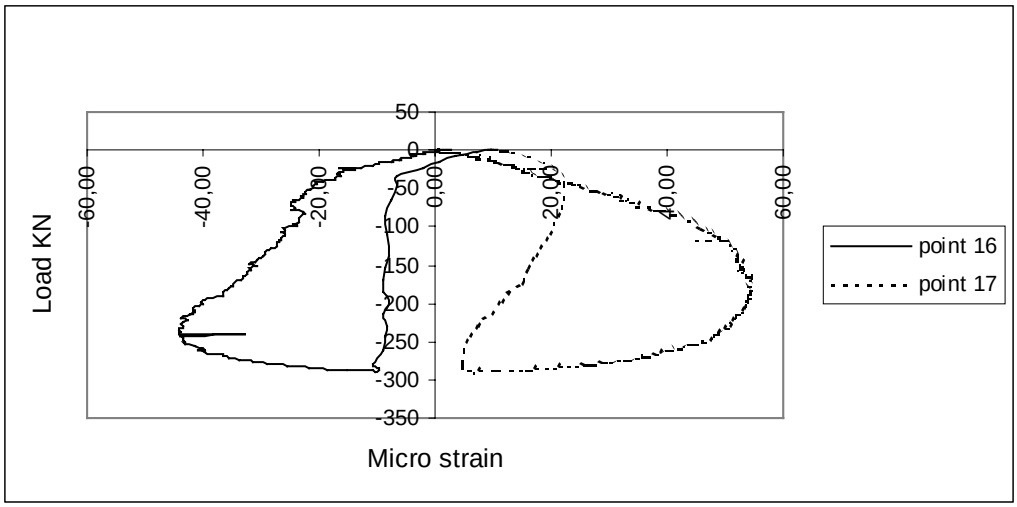

Strain in concrete.
Figure 2.90

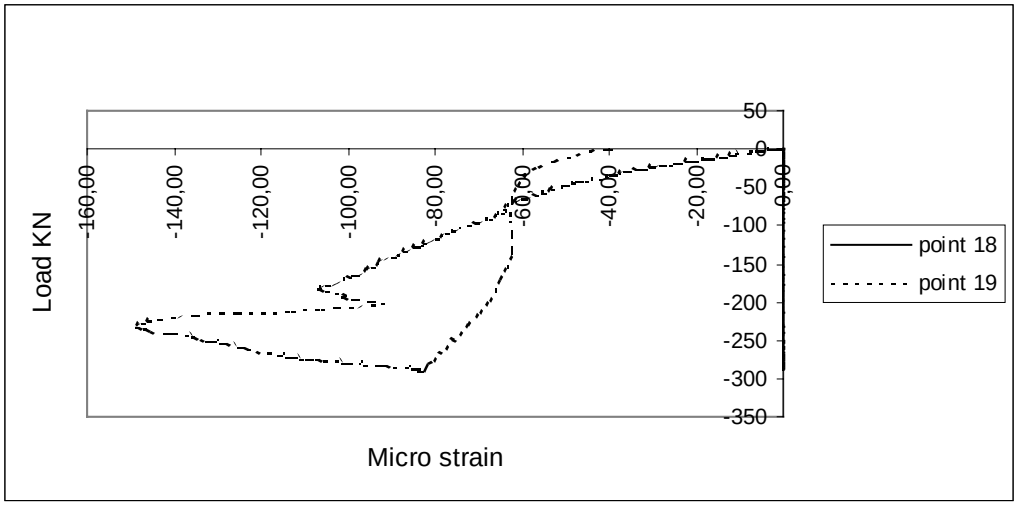

Strain in concrete.
Figure 2.91

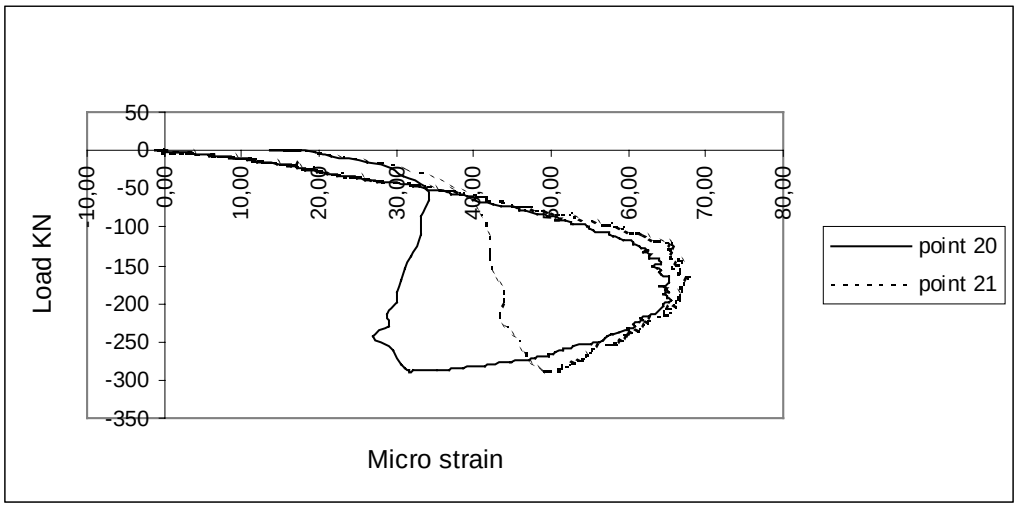

Strain in concrete.
Figure 2.92

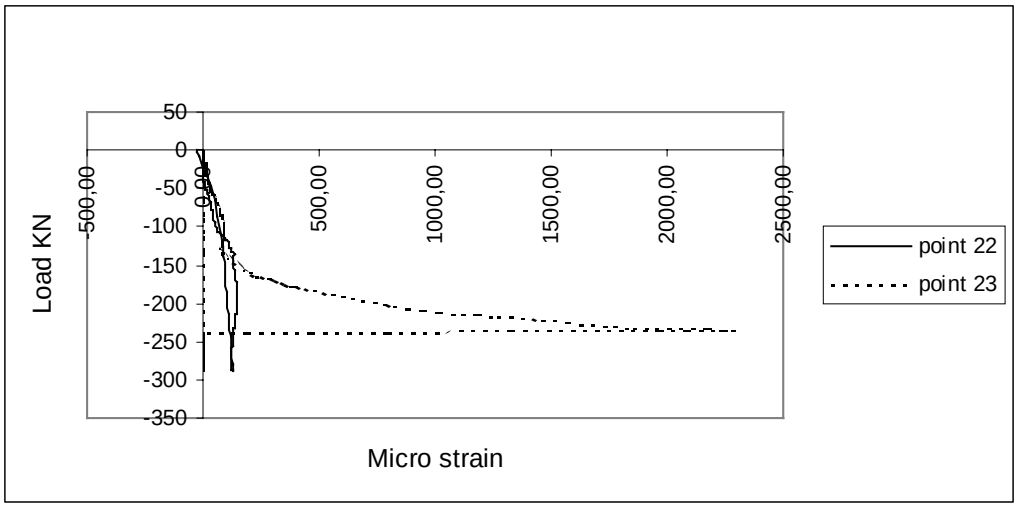

Strain in concrete.
Figure 2.93

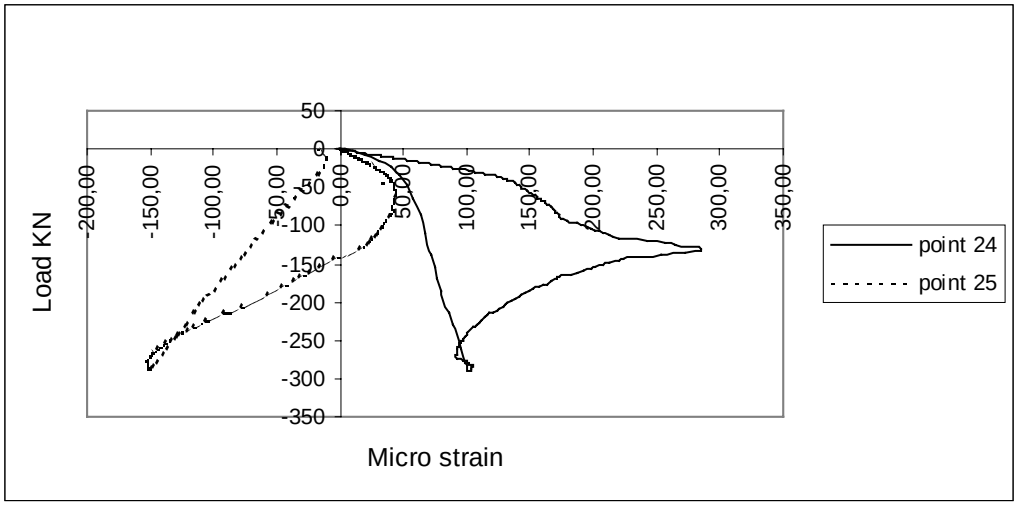

Strain in concrete.
Figure 2.94

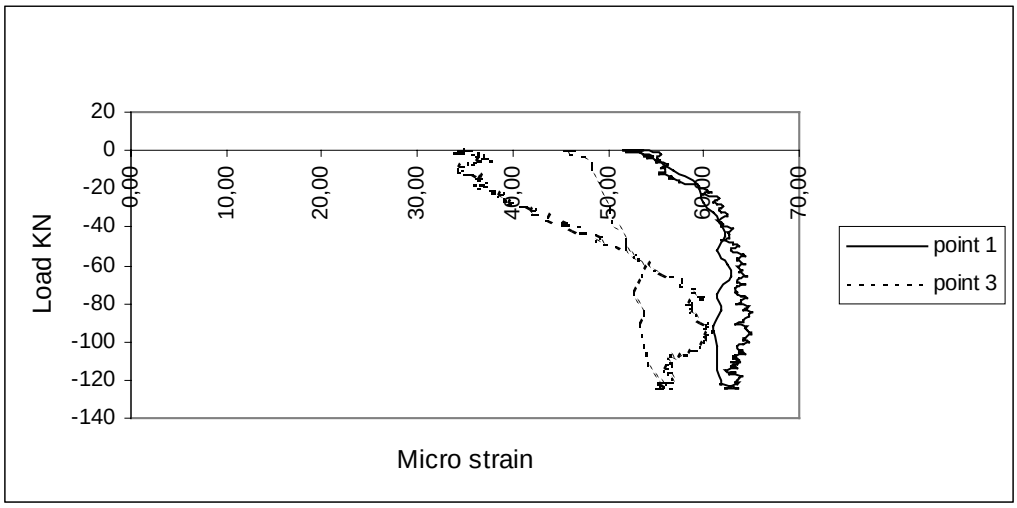

Strain in concrete.
Figure 2.95

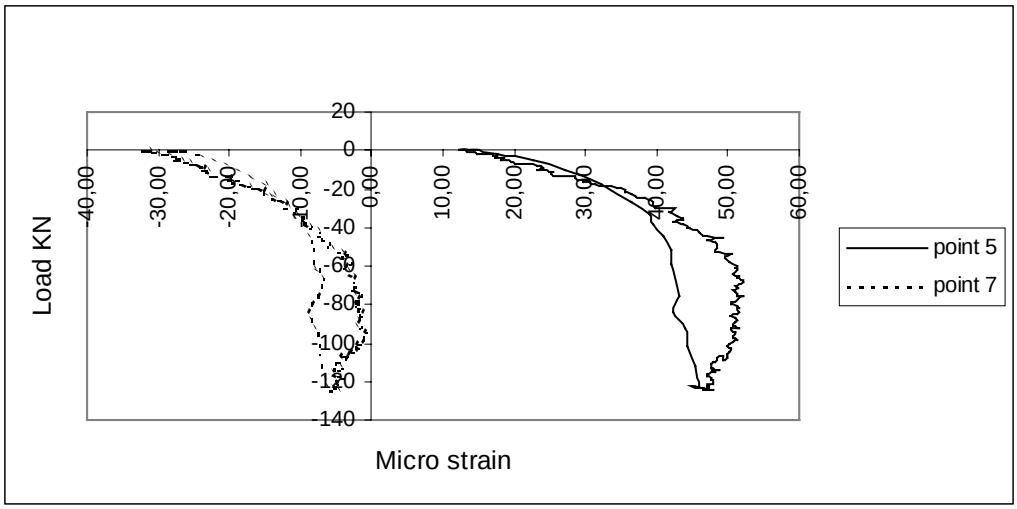

Strain in concrete.
Figure 2.96

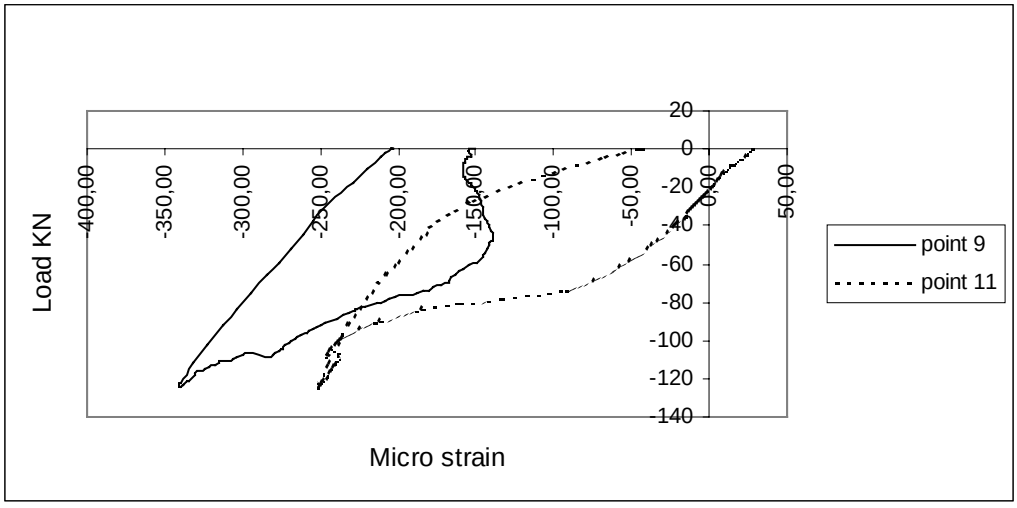

Strain in concrete.
Figure 2.97

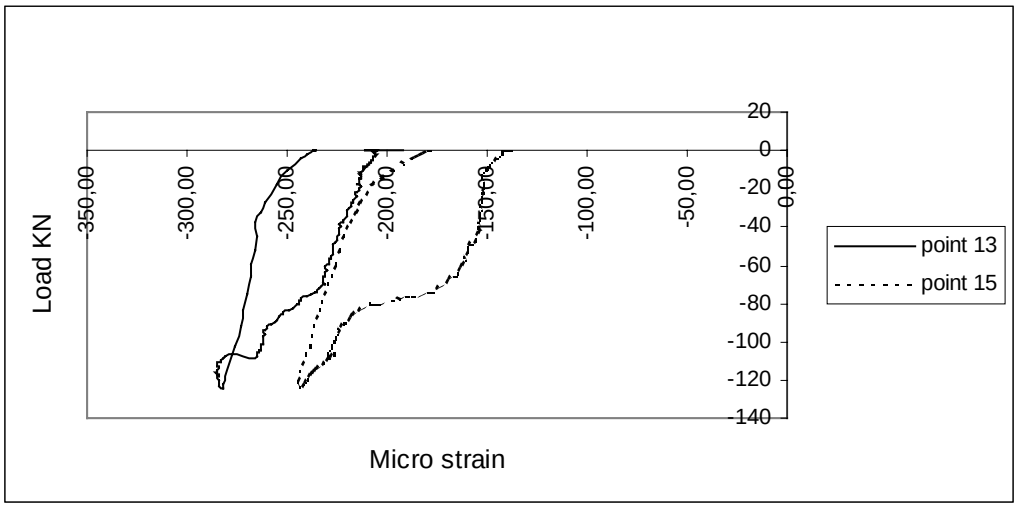

Strain in concrete.
Figure 2.98

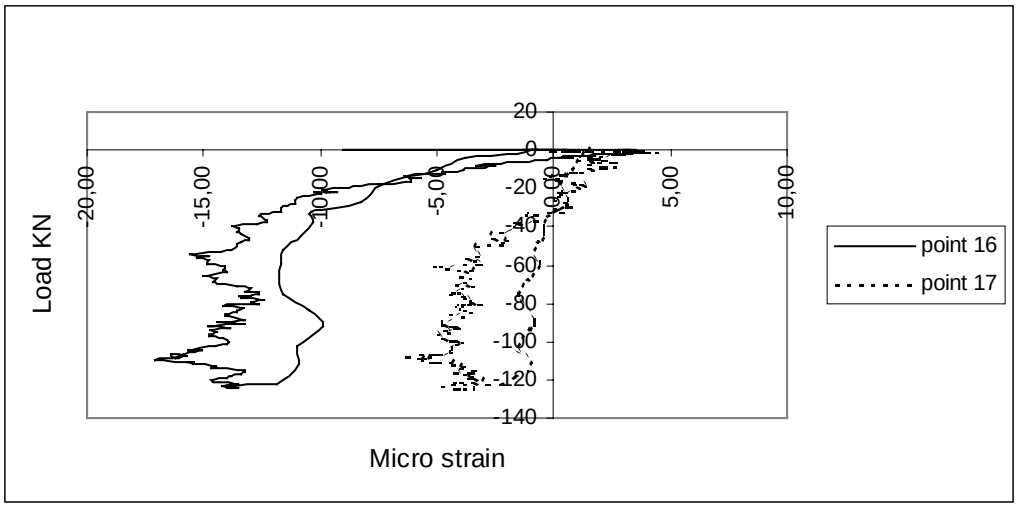

Strain in concrete.
Figure 2.99

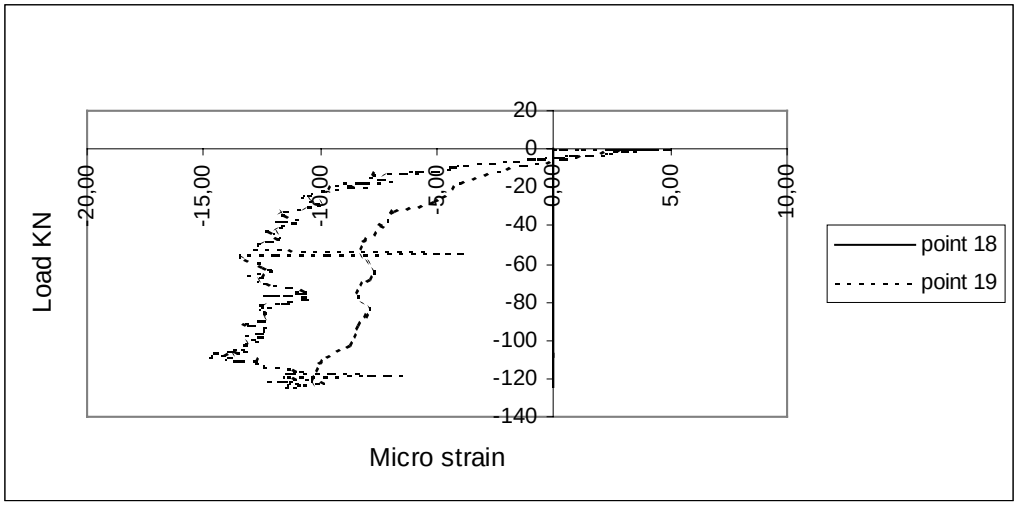

Strain in concrete.
Figure 2.100

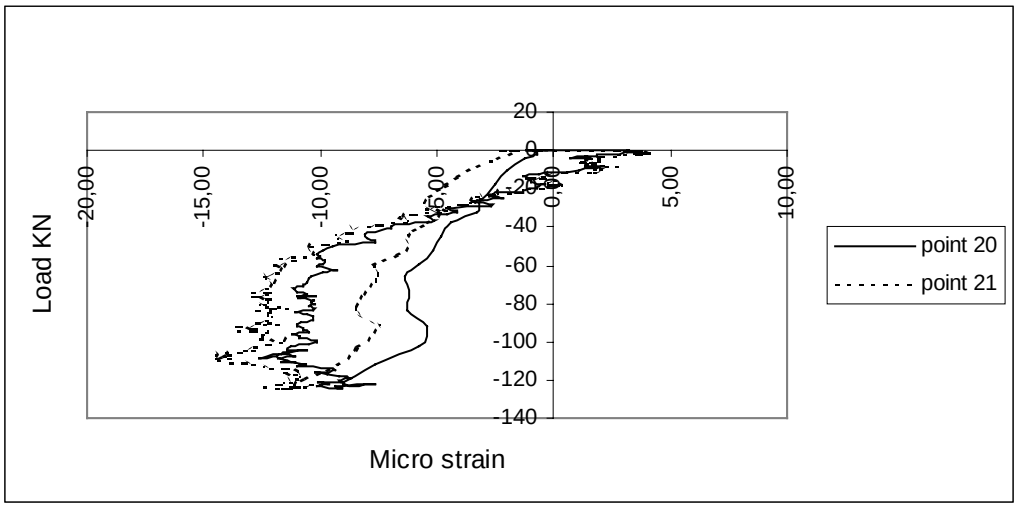

Strain in concrete.
Figure 2.101

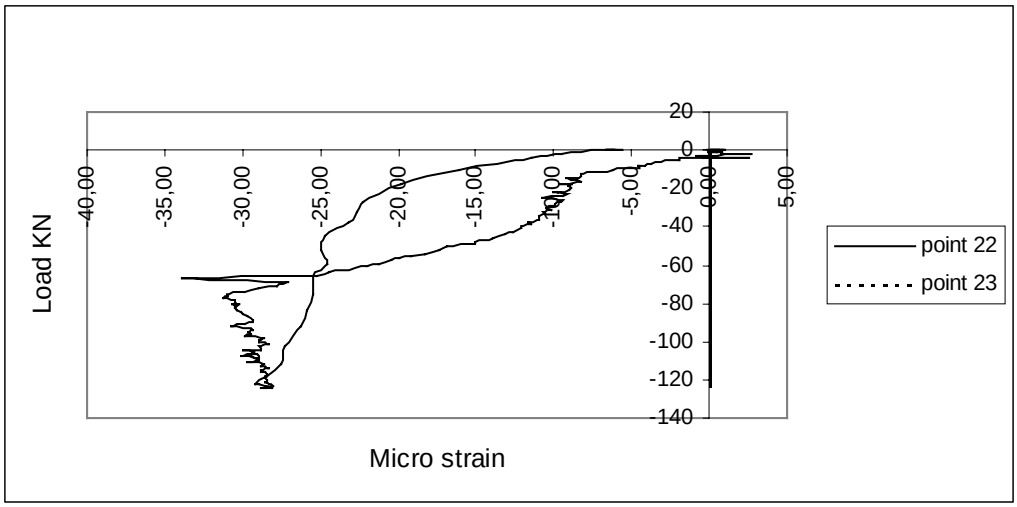

Strain in concrete.
Figure 2.102

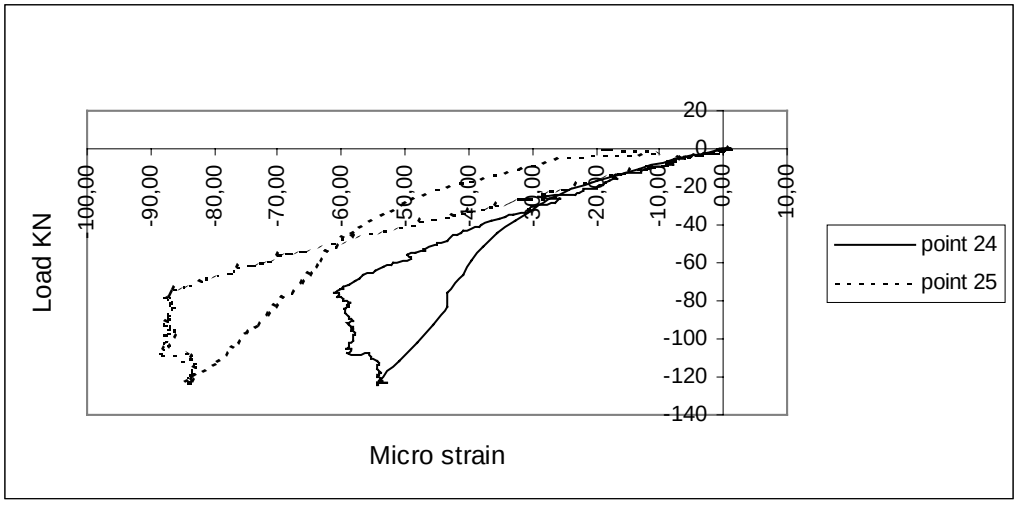

Strain in concrete.
Figure 2.103

B.3 Data used in FEM analysis.

In this chapter data used in FEM analysis with “DIANA” are listed for prestressed specimen S3.

```
Slabs on ground
:tendons c/c 930 mm
'COORDINATES'
   1    .000000E+00    .000000E+00    .000000E+00
   2   1.000000E+02    .000000E+00    .000000E+00
   3   3.000000E+02    .000000E+00    .000000E+00
.
.
 577   3.800000E+03   4.000000E+03    .000000E+00
 578   4.000000E+03   4.000000E+03    .000000E+00
'DIRECTIONS'
   1   1.00000E+00    .00000E+00    .00000E+00
   2    .00000E+00   1.00000E+00    .00000E+00
   3    .00000E+00    .00000E+00   1.00000E+00
'ELEMENTS'
CONNECT
   1 Q20SH  1 2 19 18
   2 Q20SH  2 3 20 19
.
.
.
 255 Q20SH  270 271 288 287
 256 Q20SH  271 272 289 288
 257 Q24IF  290 291 308 307 1 2 19 18
 258 Q24IF  291 292 309 308 2 3 20 19
.
.
.
 511 Q24IF  559 560 577 576 270 271 288 287
 512 Q24IF  560 561 578 577 271 272 289 288
MATERI
 / 1-256 / 1
 / 257-512 / 2
GEOMET
 / 1-256 / 1
 / 257-512 / 2
DATA
/ 1-256 / 1
/ 257-512 / 2
'MATERIALS'
:
:concrete
 1    YOUNG 25000
      POISON 0.2
      DENSIT 3.348979E-19
      YIELD   VMISES
```

```
      YLDVAL  27.5
      CRACK   1
      CRKVAL  2.5
      TAUCRI  1
      BETA    0.2
      TENSIO  1
      TENVAL  0.00125
:
:sub-base
 2    DSTIF  0.03  0.015
      SIGDIS -100000. -3333333. 0. 0. 0. 10000000.
:
:tendons
 3    YOUNG 196000
      POISON 0.2
      DENSIT 0
      YIELD  VMISES
      YLDVAL 1860
      NOBOND
'REINFO'
LOCATI
: tendons
  1    GRID
       PLANE -1. -1. 8.  4001. -1. 8.  4001. 4001. 8.  -
1. 4001. 8.
  2    GRID
       PLANE -1. -1. -8.  4001. -1. -8.  4001. 4001. -8.
-1. 4001. -8.
MATERI
  / 1-2 / 3
GEOMET
 / 1 / 3
 / 2 / 4
'DATA'
 1   NGAUS 2 2 7
 2   NGAUS 2 2
'GEOMETRY'
:
:concrete
 1   THICK 150
:
:sub-base
 2   THICK 500
     FLAT
:
:tendons in  x-dir c/c 930 mm =>0,1075 mm2/mm
 3   THICK 0.1075  0.
     XAXIS 1. 0. 0.
:tendons in  y-dir c/c 930 mm =>0,1075 mm2/mm
 4   THICK 0.  0.1075
     XAXIS 1. 0. 0.
```

```
:
'SUPPORTS'
 / 1 290 / TR 1
 / 1 17 290 306 / TR 2
 / 290-578 / TR 3
:
'LOADS'
CASE 1
WEIGHT
: gravity = 9.81 m/sec2
 3   -73231258.E6
CASE 2
REINFO
 / 1 /
      PRESTR 1200.  0.
CASE 3
REINFO
 / 2 /
      PRESTR  0.  1200.
CASE 4
ELEMEN
 / 18 /
     FACE
     FORCE -2.5
     DIRECT  3
'END'
```

B.4 Calculating of slabs on ground with different tendon distance.

In the next pages, some copies from calculating of slabs on ground by excel are shown. The results of this calculation are “Effective prestress” and “ Distance between tendons”.

URN:NBN:no-2318

Design of prestressed concrete slabs on ground

y=mx+b

Indata

Maximum allowable concrete tensile stress:	2,40	N/mm^2	Subgrade friction stress :	-0,02	N/mm^2
Coefficient of subgrade friction :	5,00E-01		Stress due to temperature differential :	-0,9775	N/mm^2
Concrete density :	24	KN/m^3	Coefficient depending of h and a :	226	mm
Tendon length :	4000	mm	Stress due to consentrated load :	-2,74	N/mm^2
Concrete modulus of elasticity :	23000	N/mm^2	Modulus of rupture :	4,42	N/mm^2
Coefficient of termal expansion :	8,50E-06		Stress ratio SR :	0,54	
Temperature differential :	8	^{o}C	Stressing force after 10 % loss :	150300	N
Poisson's ratio :	0,2		b =	-0,84	N/mm^2
Load :	73	KN	x =	3,71	N/mm^2
Slab thickness :	150	mm	m =	0,64806	
Modulus of subgrade reaction :	0,03	N/mm^3	y =	1,56	N/mm^2
Load area with radius :	230	mm	Effective prestress :	1,59	N/mm^2
Concrete compressive strength :	35	N/mm^2	Distance between tendons :	632	mm
Tendon area :	100	mm^2			

Alternative

c/c tendon :	630	mm	y =	1,56648
			x =	3,72055
			f_L =	-2,74305
			Crack load :	73 KN

Design of prestressed concrete slabs on ground

y=mx+b

Indata

Maximum allowable concrete tensile stress:	2,40	N/mm^2	Subgrade friction stress :	-0,02	N/mm^2
Coefficient of subgrade friction :	5,00E-01		Stress due to temperature differential :	-0,9775	N/mm^2
Concrete density :	24	KN/m^3	Coefficient depending of h and a :	226	mm
Tendon length :	4000	mm	Stress due to consentrated load :	-2,74	N/mm^2
Concrete modulus of elasticity :	23000	N/mm^2	Modulus of rupture :	4,42	N/mm^2
Coefficient of termal expansion :	8,50E-06		Stress ratio SR :	0,54	
Temperature differential :	8	^{o}C	Stressing force after 10 % loss :	150300	N
Poisson's ratio :	0,2		b =	-0,84	N/mm^2
Load :	73	KN	x =	3,71	N/mm^2
Slab thickness :	150	mm	m =	0,64806	
Modulus of subgrade reaction :	0,03	N/mm^3	y =	1,56	N/mm^2
Load area with radius :	230	mm	Effective prestress :	1,59	N/mm^2
Concrete compressive strength :	35	N/mm^2	Distance between tendons :	632	mm
Tendon area :	100	mm^2			

Alternative

c/c tendon :	930	mm	y = 1,05342
			x = 2,92887
			f_L = -1,95137
			Crack load : 52 KN